Mechanisms of biogenic formaldehyde generation in wood

Guigui Wan

Dissertation submitted to the faculty of the Virginia Polytechnic Institute and State University in partial fulfillment of the requirements for the degree of

Doctor of Philosophy

In

Macromolecular Science and Engineering

Charles E. Frazier, Chairman

Scott H. Renneckar

Maren Roman

Barry Goodell

Alan R. Esker

Dec 9, 2016

Blacksburg, Virginia

Keywords: wood, biogenic formaldehyde, heat, acid, lignin, extractives

Mechanisms of biogenic formaldehyde generation in wood

Guigui Wan

Abstract

This work addresses biogenic formaldehyde (CH_2O) generated by wood during the manufacture of non-structural wood-based composites, from which CH_2O emissions are regulated. The target for regulation has been anthropogenic CH_2O released from hydrolytically unstable amino resins like urea-formaldehyde. However, current regulations (the Formaldehyde Standards for Composite Wood Products Act, signed into law in 2010 and implemented in 2016) restrict allowable emissions to such low levels that biogenic CH_2O may affect regulation compliance. The industry has met the latest regulations with new amino resin technologies. Nevertheless persistent anecdotal reports suggest that biogenic CH_2O complicates regulation compliance. This work represents an industry/university cooperation to seek a more thorough understanding of biogenic CH_2O, to begin documentation of biogenic CH_2O levels in wood, and to study the conditions and chemical mechanisms of its formation.

Efforts began by establishing CH_2O analysis using the fluorimetric acetylacetone determination. A custom 12-liter chamber with controlled temperature and relative humidity, and "ultrapure" nitrogen (N_2) ventilation was created to measure CH_2O emissions from flakes sampled from four Virginia pine (*Pinus virginiana*) trees. Emissions from never-heated specimens varied significantly among the four trees, ranging from 0.02 – 0.19 μg CH_2O/m^3g dry wood. Heating (200°C, 1 hour), followed by chamber equilibration, resulted in significantly increased emissions on the order of 50%. Sequential heating, followed by chamber equilibration (in other words, heat/equilibrate/measure emission/repeat), resulted in declining emissions suggesting that a finite chemical source of CH_2O was being depleted by the sequential heat treatment. Flake specimens were stored in the open laboratory, and over 2-3 months laboratory storage, initially high emitting specimens gradually emitted less CH_2O, and initially low emitters gradually emitted more CH_2O. Concerns over laboratory contamination were perhaps allayed when background levels of laboratory CH_2O were determined to be

similar to the background levels in the ultrapure N_2 used to ventilate the chamber. Measurement of emissions was abandoned, and thereafter a simple water extraction technique (~ 94% CH_2O recovery) was used to measure the CH_2O content of never-heated and heated wood specimens, where the difference was identified as CH_2O generated due to heating.

Increment cores from living Virginia pine (*Pinus virginiana*), yellow-poplar (*Liriodendron tulipifera*), and radiata pine (*Pinus radiata*) trees were used to measure CH_2O content and CH_2O generation due to heating (200°C, 10 min). Significant variations within and between trees of the same species were observed. Tissue types (juvenile/mature, heartwood/sapwood) sometimes correlated to higher CH_2O contents and greater heat-generation potential; but sometimes not depending upon species. Heating increased CH_2O levels 3-60 fold. Heating with high moisture levels caused greater CH_2O generation than for dry specimens. This moisture effect and a separate serendipitous observation suggested that CH_2O generation is acid catalyzed. Radiata pine generated extraordinarily high CH_2O levels when heated, far exceeding the other two species. It was suggested that pine extractives might catalyze CH_2O generation, perhaps in lignin.

Pinus virginiana wood was heated (200°C, 10 or 60 min) while dry or after aqueous/acid or base pretreatment in order to reveal mechanisms of formaldehyde (CH_2O) generation. Among wood structural polymers, lignin was the overwhelming source of biogenic CH_2O, consistent with prior reports. The effects of wood extractives are mentioned below. The selection of acid catalyst strongly affected CH_2O generation as predicted in the acidolysis literature of lignin model compounds and isolated lignins. Lignin methoxyl cleavage was also observed, but was considered an unlikely source of thermochemical CH_2O. Alkaline pretreatments suppressed CH_2O generation. Regarding wood-based composite manufacture, the implications are that lignin reactions can be manipulated during hot-pressing. Potential benefits include reduced product emissions, and/or novel crosslinking strategies using biogenic CH_2O.

Heat generation of CH_2O in Virginia pine and radiata pine was substantially reduced by extractives removal, but there was no such effect in yellow-poplar wood. Results suggested that

pine extractives promote CH_2O generation by catalyzing or otherwise promoting C2 cleavage (acidolysis) in lignin. Thioacidolysis demonstrated that pine lignin reactions were strongly dependent upon the presence or absence of the extractives. When present, pine extractives seemed to promote C2 cleavage (CH_2O generation), but otherwise reduced the overall extent of lignin degradation. When pine extractives were removed, lignin suffered substantial degradation, but apparently less C2 cleavage since CH_2O generation was reduced. In contrast, thioacidolysis showed that yellow-poplar extractives appeared to promote lignin degradation, but extractives removal had no detectable impact on CH_2O generation. Implications exist for biorefinery research because it was shown that lignin reactions can be strongly affected by wood extractives.

Two dimensional, proton-carbon, correlation NMR spectroscopy (2D NMR), and solvent submersion dynamic mechanical analysis (DMA) was used to investigate wood changes caused by heating in the presence or absence of external acid catalysis. 2D NMR was relatively insensitive to fine lignin changes that were detected using thioacidolysis. 2D NMR was effective for observing lignin changes under more extreme heating conditions, and evidence was found for lignin crosslinking reactions that probably occurred through substitution into lignin aromatic rings. DMA showed that most heating conditions caused an increase in the lignin glass transition temperature (Tg), consistent with heat-induced lignin crosslinking. Under one experimental condition of wood heating, DMA showed a reduction in the lignin glass transition temperature (Tg). This suggested that lignin cleavage without subsequent repolymerization might be promoted by carefully controlled conditions, and this has implications for biorefinery research where lignin repolymerization can be problematic.

Finally, this work strongly supported the hypothesis that lignin generates CH_2O through well-known acidolysis pathways where CH_2O is borne from the lignin gamma-methylol group. Therefore, it was predicted that upon heating corn (*Zea mays L.*) stalk should generate less CH_2O than wood because corn stalk lignins exhibit a high degree of coumaric acid esterfication at the gamma-methylol group. This hypothesis was perhaps verified- it was found that in 4 out of 6 experimental heating conditions that corn stalk generated significantly less CH_2O than Virginia pine.

Acknowledgement

It has been a few years since I started my Ph.D study. Completing this degree is not an easy task at all. Many unexpected obstacles have been overcome before reaching to this step. However, it is surely the most rewarding experience I ever had, not only because of the academic achievements, but more importantly, because of the people I have met and worked with during this amazing journey.

Thank you very much, Dr. Frazier. I certainly couldn't make it this far without your support, encouragement, and criticism. This project had a rough start, but your passion and enthusiasm to pursue the unknowns inspired me to immerse myself into this exploration, and finally enjoy the challenges. It is truly my honor to work with you, and you are the best mentor I ever have in my life.

Also I need to take a moment to thank my committee members, Dr. Maren Roman, Dr. Alan Esker, Dr. Barry Goodell and Dr. Scott Renneckar. For all these years, your insightful comments and suggestions not only helped me to improve this project, but also provided new thoughts and perspectives on the future work.

I am grateful to have the opportunity to work with my wonderful lab colleagues, Dr. Ann Norris, Mohammad Tasooji, Christa Stables, Cole Burch, Kyle Mirabile and Chuck Wang. You helped me not only academically, but also personally. Your friendship will be cherished in my heart. No matter where you are going to be in the future, I wish you all a happiest life forever.

Thank you very much, Linda Caudill. Thanks for all your hard work to run the WBC center (Wood-Based Composites Center). My privileged experience with the industrial members in the center offered me a different perspective to look into things and helped me to transit into the next stage of my life.

I also owe many thanks to Rick Caudill, David Jones, Brooks Saville Jr, Dr. Mehdi Ashraf-Khorassani, and Dr. N. Murthy Shanaiah. Thanks very much for your time and effort to assist me with my research.

Also for all my friends at Blacksburg, your company made this journey enjoyable and I am so lucky to have you all in my life.

All of these wouldn't be possible without the support from my family, especially from my parents. Your unconditional love always motivates me to become a better self. Guiqiong and Guimin, thank you for being around with our parents while I am away. Thank you, Chengshuai for being a loving and supportive boyfriend. These past three years with you went by so fast, and I wish we have many more three years ahead.

Table of Contents

Abstract.....II

Acknowledgement..... V

Chapter 1 Introduction.....1

1.1. Motivation..... 1

1.2. Literature Review..... 2

1.2.1. Formaldehyde 2

1.2.2. Wood cell wall components and relation to CH_2O emission or generation..... 6

1.2.3. Heat treatment of wood 15

1.2.4. Analytical methods 16

1.2.5. References 24

Chapter 2 Method for measuring formaldehyde emission of wood using a micro chamber.....40

Attribution 40

2.1. Abstract..... 40

2.2. Introduction 41

2.3. Materials and methods..... 43

2.4. Results and discussions..... 46

2.5. Conclusions 53

2.6. References 53

Chapter 3 Biogenic formaldehyde: Content and heat generation in the wood of three tree species 57

Attribution 57

3.1. Abstract..... 57

3.2. Introduction 58

3.3. Materials and methods..... 59

3.4. Results and discussions 61
3.5. Conclusions 73
3.6. References 74

Chapter 4 Formaldehyde in pine wood forms as predicted by lignin acidolysis .77

4.1. Abstract 77
4.2. Introduction 77
4.3. Materials and Methods 79
4.4. Results and discussions 81
4.5. Conclusions 88
4.6. References 89

Chapter 5 Pine extractives control lignin reactions and the formation of biogenic formaldehyde 94

5.1. Abstract 94
5.2. Introduction 94
5.3. Materials and methods 96
5.4. Results and discussions 98
5.5. Conclusions 106
5.6. References 107

Chapter 6 Evidence of in situ lignin crosslinking and repolymerization 110

6.1. Abstract 110
6.2. Introduction 111
6.3. Materials and methods 113
6.4. Results and discussions 116
6.5. Conclusions 126
6.6. References 126

Chapter 7 The effect of lignin esterification on biogenic formaldehyde generation 131

7.1. Abstract 131
7.2. Introduction 131
7.3. Materials and methods 132
7.4. Results and discussions 134
7.5. Conclusions 140
7.6. References 140

Chapter 8 Conclusions and future work 144

Appendix A Rheological analysis of switchgrass stem 148

Attribution 148
A.1. Abstract 148
A.2. Introduction 149
A.3. Materials and methods 150
A.4. Results and discussions 153
A.5. Conclusions 164
A.6 References 165

Appendix B Biogenic formaldehyde generation potential from three wood species 167

Appendix C Rheology of heated Virginia pine wood 171

Appendix D NMR spectra for synthesized lignin model compounds 178

List of Figures

Figure 1.1. Condensation reaction among formaldehyde, acetylacetone (AcAc) and ammonium to form a fluorescent compound, diacetyldihydrolutidine (DDL). [14] 3

Figure 1.2. Reaction between formaldehyde and 2,4-dinitrophenylhydrazine (DNPH) to form 2,4-dinitrophenylhydrazone. [15-17]..... 3

Figure 1.3. Cellulose structure with cellobiose unit as the repeating unit. 7

Figure 1.4. Lignin monomers, coniferyl alcohol (G), sinapyl alcohol (S), and p-coumaryl alcohol (H). [55]..... 9

Figure 1.5. G-unit lignin dimers depicting the most common intermonomer linkages in lignin. [56, 57] 9

Figure 1.6. Simplified representation of a softwood lignin segment, adapted from Ralph. [58] 10

Figure 1.7. Formaldehyde generation mechanism from lignin β-O-4 structure under acidic condition. [72]..... 11

Figure 1.8. Formaldehyde generation mechanism from lignin β-5 structure under acidic condition. [80]..... 12

Figure 1.9. Formaldehyde generation mechanisms from lignin β-O-4 and β-5 structures under basic condition. [81, 82] 12

Figure 1.10. Example of resin acids and fatty acids. [90] 14

Figure 1.11. Acidolysis reaction scheme for lignin. [72-79] 18

Figure 1.12. Lignin β-O-4 thioacidolysis reaction scheme. [137] 19

Figure 1.13. Structures of dimeric products recovered from thioacidolysis followed by desulphration. [146] 19

Figure 1.14. Selective ether cleavage by the DFRC method. [139] 21

Figure 1.15. Short acquisition time (17 min) experiment on aspen cell walls in DMSO-d6/pyridine-d5 (4:1, v:v) using a 750 MHz cryoprobe-equipped NMR. The spectrum is adequate for many purposes-chemometrics, and S/G ratio estimation, for example. [161]..... 24

Figure 2.1. Hantzsch reaction, formaldehyde reacted with acetylacetone and ammonium into diacetyldihydrolutidine (DDL), which can be detected and quantified using fluorometer. [10] 42

Figure 2.2. Left: a custom aluminum flake tray with 110 flakes loaded in the slots. Right: gas emissions chamber (center), with the controlled temperature circulator (left), and the RH generator (right). 44

Figure 2.3. Left: one example curve for the fluorimeter calibration. Right: curve slopes for multiple calibrations in an 8-month period. Time elapsed between two calibrations was roughly 4 weeks. A new light source was installed just before the # 7 calibration. 46

Figure 2.4. Background CH_2O from nitrogen tanks, number of measurements for each tank n $\geqslant$ 3..... 47

Figure 2.5. Formaldehyde emissions from never-heated Virginia pines, FB1, FB2, NC1 and NC2. Error bars = ± 1 standard deviation. Numbers above columns are number of measurements. 49

Figure 2.6. Formaldehyde emissions from FB1 (control, never-heated) flakes, and sequentially heated FB1 flakes at 120°C for 1 hour and 2 hours. Error bar = $\pm$ 1 standard deviation. Numbers above columns are number of measurements..... 49

Figure 2.7. Formaldehyde emissions from FB1 control (never-heated) flakes, heated FB1 flakes after sequential heating at 200°C up to 6 hours. Error bar = $\pm$ 1 standard deviation. Numbers above columns are number of measurements..... 50

Figure 2.8. The effect of NH_4Cl pretreatment on CH_2O emissions from heated NC2 wood flakes (200°C, 1 h). Error bar = $\pm$ 1 standard deviation. Numbers above columns are number of measurements..... 51

Figure 2.9. Formaldehyde emissions from wood flakes. Among each set of measurement, loaded flake tray sat in open laboratory at room temperature. Error bar = ± 1 standard deviation. Numbers above columns are number of measurements. X axis represents the experimental date. 52

Figure 2.10. CH_2O content (Y axis, unit: µg CH_2O in 1L air) of laboratory air over 4 month period. X axis represents the experimental date. Within each day, only one measurement was taken. 52

Figure 3.1. Typical within core, and between core, variability in CH_2O content, and in CH_2O generation, among cores from the same tree (Virginia pine tree 3, juvenile tissue), under different drying and thermal treatments as indicated. Note ordinate scales vary. 63

Figure 3.2. Average CH_2O content in Never-dried/Never-heated Virginia pine, trees 3-8, for juvenile (J) and mature wood (M). Each column averaged over 1-3 cores with 2-4 measurements per core; numbers above columns indicate total number of measurements. *Tree 8 was diseased. Error bars = ± 1 standard deviation. 64

Figure 3.3. Demonstration of heating effects on CH_2O generation potential from average CH_2O contents of Never-dried/Never-heated and Never-dried/Heated specimens in juvenile (J) and mature wood (M). Each column averaged over 1-5 cores with 2-4 measurements per core; numbers above columns indicate total number of measurements. *Tree 8 was diseased. Error bars = ± 1 standard deviation. 65

Figure 3.4. Average CH_2O content (Never-dried/Never-heated) and CH_2O generation potential (Never-dried/Heated) in yellow-poplar, trees 1-5. Each column averaged over 15 total measurements where heartwood (H) and sapwood (S) specimens were respectively randomized among 4-8 cores from the same tree. Error bars = ± 1 standard deviation..... 66

Figure 3.5. Average CH_2O content (Never-dried/Never-heated) and CH_2O generation potential (Never-dried/heated) for Virginia pine trees 3-8 (1-3 cores per tree, 2-4 measurements per core) and yellow-poplar trees 1-5 (6-8 cores per tree with respective tissue types randomized among cores from the same tree, 3 measurements per tree.

Numbers above columns indicate total number of measurements. Error bars = ± 1 standard deviation. 66

Figure 3.6. Effect of drying agent (P_2O_5 vs. molecular sieves) on CH_2O content and CH_2O generation in Virginia pine. Never-dried specimens: trees 3-7; P_2O_5 dried specimens: trees 1-4; molecular sieves dried specimens: trees 5-7; 1-5 cores per tree. Numbers above columns indicate total number of measurements. Error bars = ± 1 standard deviation. 67

Figure 3.7. Effect of drying (with molecular sieves) on the CH_2O content in Never-heated Virginia pine (trees 5-8) and yellow-poplar (trees 1-5). Numbers above columns indicate total number of measurements from 4-5 trees, 1-8 cores per tree. Error bars = ± 1 standard deviation. 68

Figure 3.8. Effect of moisture content on heat generation of CH_2O: Virginia pine (trees 5-7, 1-5 cores per tree, 2-4 measurements per core) vs. yellow-poplar (trees 1-5, 6-8 cores, 3 measurements per tree). Numbers above columns represent number of measurements. Error bars = ± 1 standard deviation. 69

Figure 3.9. Effect of disease state on CH_2O content and generation from molecular sieves dried Virginia pines, trees 5 and 6 healthy, and tree 8 diseased. Numbers above columns represent number of measurements; each column averaged over 1-5 cores, 3-4 measurements per core. Error bars = ± 1 standard deviation. 70

Figure 3.10. Species effect on CH_2O content and generation from molecular sieves dried specimens. Numbers above columns indicate number of measurements. Virginia pine: trees 5-7, 1-5 cores per tree, 2-4 measurements per core. Yellow-poplar: trees 1-5, specimens randomized among 6-8 cores, 3 measurements per tree. Radiata pine: 2 trees, specimens randomized among 4 cores, 3 measurements per tree. Error bars = ± 1 standard deviation. 72

Figure 4.1. Pathways for the acid-catalyzed cleavage of lignin β-aryl ether linkages. [26-31] 79

Figure 4.2. CH_2O generation from 200°C, 10 min heating and aqueous/acid pretreatment (tree 1) and aqueous/alkaline pretreatment (tree 2 mature tissue; * blue). DBSA = dodecylbenzenesulfonic acid. Error bars = ±1 standard deviation; n ⩾ 3..... 87

Figure 4.3. CH_2O generation (log scale) from 200˚C, 10 min heating of tree 1 specimens with aqueous/acid pretreatment including acid ammonium salts. Error bars = ± 1 standard deviation; n ⩾ 9. 87

Figure 5.1. Lignin acidolysis pathways; only C2 cleavage produces CH_2O. 95

Figure 5.2. The effect of extractives removal (Soxhlet) on CH_2O generation due to heating (200°C 10 min). The number of trees represented is the same as in Table 5.1, except for extracted Virginia pine, which is 2 trees. Number of measurements for each tree/tissue type, n ⩾ 3. Error bars = ± 1 standard deviation. 99

Figure 5.3. Effect of extraction method (Soxhlet or room temperature extraction) on CH_2O generation during heating (200˚C 10 min) from Virginia pine (tree 1) flakes. Number of measurements n ⩾ 3. Error bar = ± 1 standard deviation..... 101

Figure 5.4. CH_2O content and heat generation (200°C, 10 min) total extracts, acid extracts, and neutral extracts obtained from Soxhlet and room temperature (RT) extraction. Number of measurements n ⩾ 3. Error bar = ± 1 standard deviation. 101

Figure 5.5. CH_2O content and heat generation (200°C, 10 min) from unextracted whole-wood, extracted wood, total extract, and reconstituted Virginia pine flakes. Number of measurement n ⩾ 3. Error bars = ± 1 standard deviation..... 102

Figure 5.6. CH_2O generation in reconstituted pine flakes, where unit contributions of the total extract (red) and extracted wood (blue) are presented, as calculated from the wood/extract composition and the CH_2O activity (g CH_2O generated/g dry mass) of the total extract and extracted wood. Initial CH_2O levels (Never-heated levels, Figure 5.4) were subtracted. Dash line indicates CH_2O generation of the extracted pine..... 103

Figure 6.1. Lignin reaction pathways under acid-catalyzed thermal treatment. A: C3 cleavage, B: C2 cleavage, C: repolymerization of homovanillin to form stilbene, D: lignin crosslinking

reaction, competing with A and B because these three reactions share the same intermediate, benzyl carbocation, E: demethoxylation, lignin methoxyl cleaved to form methanol, potentially with a very reactive catechol structure. 112

Figure 6.2. Stilbene and possible Hibbert's ketones observed from Virginia pine specimen after heat treatment at 200°C for 60 min with acid pretreatment (A60). 116

Figure 6.3. HSQC spectra for yellow-poplar (sapwood tissue), changes in the aliphatic and aromatic structures. a: Control, no heating; b: E/H10; c: H10; d: A10, e: E/H60; f: H60; g: A60. Aliphatic region: 90-45 ppm, 5.8-2.8 ppm; aromatic region: 140-95 ppm, 8-6 ppm. Chemical shifts of analyzed structures obtained from [29-31, 36] 122

Figure 6.4. HSQC spectra for Virginia pine (tree 2 mature tissue), changes in the aliphatic and aromatic structures. a: Control, no heating; b: E/H10; c: H10; d: A10, e: E/H60; f: H60; g: A60. Aliphatic region: 90-45 ppm, 5.8-2.8 ppm; aromatic region: 140-95 ppm, 8-6 ppm. Chemical shifts of analyzed structures obtained from [29-31, 36] 123

Figure 6.5. CH_2O generation (200°C, 10-120 min) from Virginia pine tree 2 mature tissue, under water, acid and base pretreated condition. Number of measurements n $\geqslant$ 3. Error bars = $\pm$ 1 standard deviation. 124

Figure 6.6. HSQC spectra for Virginia pine (tree 2 mature tissue), changes in the aliphatic and aromatic structures. a: Control, no heating; b: H10; c: H60; d: B10, e: B60; f: A10; g: A60. Aliphatic region: 90-45 ppm, 5.8-2.8 ppm; aromatic region: 140-95 ppm, 8-6 ppm. Chemical shifts of analyzed structures obtained from [29-31, 36] 125

Figure 7.1. CH_2O is generated from γ-methylol of lignin propane side chain through C2 cleavage degradation. Virginia pine lignin: γ-methylol of lignin propane side chain is free without acid esterification. Corn stalk lignin: extensive esterification at γ position by p-coumaric acid. 136

Figure 7.2. DFRC reaction scheme for formation of analyzable ester conjugates and acylated β-aryl ether units in corn stalk lignin. Compounds 1 (p-coumarate ester (G) and p-coumarate ester (S)) derived from esterified lignin unit, and model compounds synthesized for

quantification purposes. Compounds 2 (H, G, and S) originated from non-esterified lignin unit. 137

Figure A.1. Stem color phenotype in 4CL-7 + (top) and 4CL-7 – (bottom) specimens. The presence of the transgene correlated with brown stem color, while transgene absence correlated with green stem color. 151

Figure A.2. Specimen clamping system assembled without the surrounding solvent-submersion hardware. 152

Figure A.3. Example frequency sweep data at temperature extremes for a specimen (4LC-7 40 +) immersed in ethylene glycol; oscillation stress = 50,000 Pa. 154

Figure A.4. Typical stress sweep data used to establish the LVR limit at the analytical temperature extremes, (specimen: 4LC-7 5 +; 0.5 Hz). Arrows indicate the maximum stress used in the linear stress/strain fit; stresses above this level result in correlation coefficients (R^2) below 0.99995. 155

Figure A.5. Average storage moduli of all switchgrass specimens at 25˚C and 120˚C. Obtained from stress sweep experiments; number of observations, n = 5-6; error bars = ± 1 standard deviation. 156

Figure A.6. Example of first heating scan (red trace) and first cooling scan (black trace) of a switchgrass specimen (10 -) immersed in ethylene glycol. 159

Figure A.7. Examples of good (left) and poor (right) first cool tan δ curves, and the non-linear fitting used to improve precision in the Tg (temperature at tan δ maxima) determination. 159

Figure A.8. Comparison of first cool scans for 40 + (red trace) and 18 - (black trace) specimens; number of measurements, n = 3. Error bars = ± 1 standard deviation. 160

Figure A.9. Example of storage modulus, loss modulus, and tan δ master curves for 40 + (red) and 18 - (black) specimens. 162

Figure A.10. Shift factor log a_T against 1/T (K^{-1}) for 18 – (n = 4) and 40 + (n = 6), n is number of measurements, slope is the activation energy Ea. 18 – : 310.7 ± 14.9 kJ/mol, 40 + : 261.3 ± 15.1 kJ/mol. 162

Figure A.11. Initial cooling (before isothermal frequency scans, black trace) and final cooling ramp (after isothermal frequency scans, red trace) overlay for 18 -. 163

Figure A.12. Examples of % strain response for unidirectional continuous shear stress on specimen 40 + and 18 -. 163

Figure B.1. Acid-catalyzed (HCl or H_2SO_4) CH_2O generation from Virginia pine (tree 1 flakes), heated at 200°C from 10 min up to 120 min. Number of measurements n ≥ 3. Y axis is in log scale……167

Figure B.2. Acid-catalyzed (HCl, HBr, and HI) CH_2O generation from Virginia pine (tree 1 flakes), heated at 200°C from 10 min up to 120 min. Number of measurements n ≥ 3. Y axis is in log scale……168

Figure B.3. Acid-catalyzed (tosyl acid and dodecylbenzene sulfonic acids) CH_2O generation from Virginia pine (tree 1 flakes), heated at 200°C from 10 min up to 120 min. Number of measurements n ≥ 3. Y axis is in log scale……168

Figure B.4. Formaldehyde generation potential from three wood species, heated at 200°C from 10 min up to 120 min without catalysts. Number of measurements n ≥ 3. Y axis in log scale……169

Figure B.5. Formaldehyde generation potential from three wood species, heated at 200°C from 10 min up to 120 min, catalyzed by TsOH (tosyl acid). Number of measurements n = 3. Y axis in log scale……169

Figure B.6. Formaldehyde generation potential from three wood species, heated at 200°C from 10 min up to 120 min, catalyzed by NaOH (sodium hydroxide). Number of measurements n = 3. Y axis in log scale……170

Figure B.7. Formaldehyde generation potential from radiata pine, heated at 200°C from 10 min up to 120 min, catalyzed by NaOH (sodium hydroxide) or TsOH (tosyl acid). Number of measurements n = 3. Y axis in log scale……170

Figure C.1. Example curve of first cooling for XL grain oriented specimen (H/C60)……173

Figure C.2. Example of TTS (Time-Temperature Superposition) master curves for XL grain oriented specimens……176

Figure C.3. Shift factors (TTS) for XL-grain oriented specimens……177

Figure C.4. Tg (glass transition temperature) and Ea (activation energy associated with Tg) summary for XL-grain oriented specimens……177

Figure D.1. ^{1}HNMR spectrum for p-coumarate ester (G) derived from esterified lignin unit after the DFRC (Derivatization Followed by Reductive Cleavage) reaction……178

Figure D.2. ^{13}CNMR spectrum for p-coumarate ester (G) derived from esterified lignin unit after DFRC reaction……178

Figure D.3. ^{1}HNMR spectrum for p-coumarate ester (S) derived from esterified lignin unit after DFRC reaction……179

Figure D.4. ^{13}CNMR spectrum for p-coumarate ester (S) derived from esterified lignin unit after DFRC reaction……179

Figure D.5. ^{1}HNMR (left) and ^{13}CNMR (right) spectra for purified homovanillin……180

Figure D.6. Model compound (HA-THIO) of homovanillin after thioacidolysis……180

Figure D.7. ^{1}HNMR (left) and ^{13}CNMR (right) spectra for purified HA-THIO……180

List of Tables

Table 1.1. Formaldehyde release from cotton linter, starch and glucose after heat treatments at 40°C, 100°C, and 150°C for 3 hours, measured by the Flask method. [42]..... 7

Table 1.2. Formaldehyde release from pure galactose, arabinose, xylose after heat treatments at 40°C, 100°C, and 150°C for 3 hours, measured by the Flask method. [42]..... 8

Table 1.3. Classification of organic extractives in woods. [89] 13

Table 2.1. Averaged background and flake emissions measurements using fritted tipped and open tipped impingers over 3 measurements. Standard deviations in parentheses. 48

Table 3.1. Tree specimen information: Species, range of age, etc. Moisture content (MC%) at harvest and extractives content (EC%) are based on dry wood mass. MC% and EC% for yellow-poplar and radiata pine were averaged over all trees listed. MC% for Virginia pine was averaged over trees 1-6, and EC% was averaged over trees 5 and 6. Standard deviations in parentheses. 61

Table 4.1. CH_2O generated in dry, tree 1 specimens due to heating (200°C, 60 min), and the corresponding compositional analysis and thioacidolysis yield of experimental and control specimens. Standard deviations in parentheses ($n \geqslant 3$). 82

Table 4.2. CH_2O generated in tree 2 specimens due to 200°C heating (10 or 60 min) under various conditions, and the corresponding compositional analysis, methoxyl content, and thioacidolysis yield of experimental and control specimens. Standard deviations in parentheses ($n \geqslant 2$). 84

Table 4.3. CH_2O generation from isolated cellulose, xylan, and tree 2 mature tissue due to 200°C, 10 min heating with H_2O and acid (TsOH) pretreatment, and initial levels in unheated controls. Standard deviations in parentheses; n = 3. 85

Table 5.1. Specimen information for increment cores used in this study where the extractives content (EC%) was determined through Sohxlet extraction and reported as a

percentage based upon dry wood mass. Standard deviations in parentheses. EC% for Virginia pine was averaged over two trees. [5] 99

Table 5.2. CH_2O generation in yellow-poplar (sapwood) and Virginia pine (tree 2, mature tissue) during heating (200˚C, 10 or 60 min), and the corresponding thioacidolysis yield. Number of observations, n ⩾ 2 for thioacidolysis, and n ⩾ 3 for CH_2O measurements. Standard deviations in parentheses. 105

Table 6.1. The extractives effect on lignin degradation and CH_2O generation for yellow-poplar (sapwood tissue) and Virginia pine (tree 2, mature tissue) under heat treatments at 200˚C, 10, 20 or 60 min. Number of measurements n ⩾ 2 for thioacidolysis, n ⩾ 3 for CH_2O measurements, n = 2 for methoxyl content, n = 1 for HSQC. HSQC calculation based on internal standard methoxyl content. Control: no heating. Standard deviations in parentheses. 116

Table 6.2. Glass transition temperature (Tg), activation energy associated with glass transition (Ea) of XL-grained Virginia pine tree 1 after various heat treatments (200˚C), number of repetitions n ⩾ 2. Standard deviations in parentheses..... 120

Table 7.1. Sugar, lignin and ash contents (based on initial dry mass) for extracted never-heated Virginia pine and corn stalk, number of measurements n ⩾ 2. Standard deviations in parentheses. 135

Table 7.2. DFRC product yield for corn stalk. H, G, S monomers derived from non-esterified lignin β-O-4. p-coumarate ester (S) obtained from ether-linked esterified lignin unit. %p-coumarate ester based on total DFRC product yield. Number of measurements n = 3. Standard deviations in parentheses. 138

Table 7.3. CH_2O content and generation (200˚C 10 min) from unextracted and extracted Virginia pine and corn stalk specimens. Number of measurements n ⩾ 3. Initial CH_2O content from never-heated control specimens subtracted. Standard deviations in parentheses. CH_2O reported based on Klason lignin content of never-heated specimens (Table 7.1). 138

Table A.1. Probability values (p-values) from the intragroup comparison of average storage moduli at the experimental temperature extremes (25˚C and 120˚C) using the nonparametric Wilcoxon method; number of measurements n = 5-6. 156

Table A.2. Probability values (p-values) from the intergroup comparison of average storage moduli at the experimental temperature extremes (25˚C and 120˚C) using the nonparametric Wilcoxon method; number of measurements n = 5-6. 157

Table A.3. Average glass transition temperature (Tg), tan δ maxima, and width of the tan δ signal at half maximum (Width) for 4CL-7 specimens; Number of measurements n = 3, standard deviations in parentheses..... 160

Table A.4. Activation energy (Ea) calculated for 40 + (n = 6) and 18 – (n = 4) according to the equation above. n = number of measurements, standard deviations in parentheses. 161

Table A.5. Ultimate strength comparison between 18 - and 40 +. Number of measurements n = 4, standard deviations in parentheses..... 164

Table C.1. Summary of storage modulus (G'), glass transition temperature (Tg), max tan delta, activation energy associated with glass transition (Ea) for rectangular specimens with three grain orientations after various heat treatments. Number of measurements n ≥ 2 for stress sweeps and temperature ramps, number of measurements n ≥ 1 for Time-Temperature Superposition (TTS), standard deviations in parentheses……174

Chapter 1 Introduction

1.1. Motivation

In 1985, the U.S. Housing and Urban Development Agency enacted the first U.S. legislation limiting formaldehyde emissions from composite wood products for interior applications. [1] The industry complied with voluntary product standards that dramatically reduced indoor formaldehyde exposure from composite wood products. In 2004, the International Agency for Research on Cancer reclassified formaldehyde from "probably carcinogenic to humans" to "carcinogenic to humans." This prompted the California Air Resources Board (CARB) to approve (2007) an airborne toxic control measure to further reduce formaldehyde emissions from nonstructural composite wood products, such as particleboard and medium density fiberboard. Events culminated when in July 2010, President Obama signed into law Senate Bill 1660 establishing the Formaldehyde Standards for Composite Wood Products Act. This extended the CARB standard to all 50 states, and the U.S. Environmental Protection Agency (EPA) was charged to implement the regulation by January 1, 2013. While the EPA delayed implementation, U.S. industry-wide compliance was effectively reached in 2012. Finally, on December 12, 2016, EPA published (in the Federal Register) the long awaited rule to reduce formaldehyde emissions from nonstructural wood composites produced domestically and imported into the U.S. (essentially equivalent to the CARB phase II action of 2012). The new allowable emission levels vary by product, but the limits (not to be exceeded) are in the range of 50 to 100 ppb. Consequently, average emissions must be substantially lower thereby effecting the most rigorous standard in the world. Intended to reduce emissions from the adhesive binder, these regulations are complicated by significant and variable native-wood emissions (biogenic formaldehyde). For example, Mayer and Boehme demonstrated that solid wood emits formaldehyde at from 5 to 50% of the new limits, [2, 3] depending upon tree species and wood moisture content. Heretofore native emissions have received little attention, so they are poorly documented and not well understood.

In 2010, a National Science Foundation, Industry/University Cooperative Research Center called the Wood-based Composites Center (WBC) was established at Virginia Tech. At

that time, the WBC industry members pooled funding and initiated research to begin documentation of biogenic formaldehyde levels in wood, and to study the conditions and chemical mechanisms of its formation. Since the fall of 2011, this dissertation represents most of the WBC's biogenic formaldehyde research, and it sets the stage for further studies.

1.2. Literature Review

1.2.1. Formaldehyde

Formaldehyde is a colorless, flammable gas at room temperature. It is one among a large group of chemicals called volatile organic compounds (VOCs) that are subject to regulation in the wood-based composites industry. As the simplest, smallest aldehyde, it is highly reactive; and this is why it is incredibly useful and potentially toxic. At high vapor pressures, formaldehyde is readily detectable from its distinct, pungent odor that is typically accompanied by a burning sensation to the eyes, nose and lungs.

Formaldehyde is an important substance for many chemical and technical applications. It is manufactured as a liquid (formalin) or a solid (paraformaldehyde, and the NH_3 adduct hexamethylenetetramine). It is perhaps best known for the synthesis of wood adhesives, such as urea-formaldehyde (UF) and phenol-formaldehyde (PF) resins. [4] It is the hydrolytic instability of UF resins, not PF resins, that leads to the formaldehyde emissions targeted in U.S. and global regulations.

Formaldehyde (CH_2O) is mostly found in the air, outdoors and indoors. [5, 6] It can be released into air from materials and products made with CH_2O, and also from automobile exhaust [7], cigarettes [8], burning wood [9, 10], kerosene [10] and natural gas [11].

<u>Analytical quantification methods</u>

There are a variety of quantitative analyses for CH_2O in biological and environmental samples, and in commercial products. For analysis in gas form, CH_2O is typically trapped in water-filled impingers attached to vacuum/pressure-activated gas lines, whereafter derivatives are formed to aid quantitation by numerous analytical methods. In 1943, Goldman and Yagoda

drew formaldehyde-containing air through impingers loaded with sodium bisulfite solution to form nonvolatile sodium formaldehyde-bisulfite compounds, which can be titrated with aqueous iodine. [12] In 1956, West and Sen developed the now widely used chromotropic acid determination, where in the presence of concentrated sulfuric acid, a deep purple-violet colored compound forms that is quantified colorimetrically (580 nm). [13] Nash [14] developed a formaldehyde determination by means of the Hantzsch reaction using 2,4-pentanedione (acetylacetone or AcAc), Figure 1.1. The product diacetyldihydrolutidine (DDL) is fluorescent and can be quantified by fluorimetry or colorimetry. The chromotropic acid and the AcAc colorimetric determinations are highly specific, but not perfectly free of interferences.

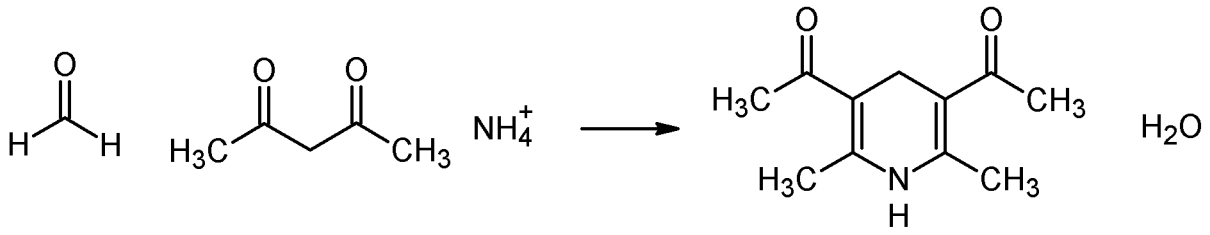

Figure 1.1. Condensation reaction among formaldehyde, acetylacetone (AcAc) and ammonium to form a fluorescent compound, diacetyldihydrolutidine (DDL). [14]

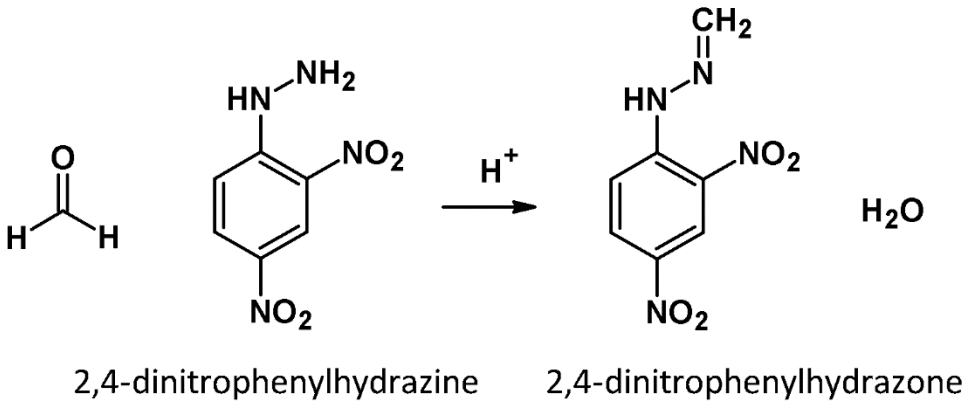

Figure 1.2. Reaction between formaldehyde and 2,4-dinitrophenylhydrazine (DNPH) to form 2,4-dinitrophenylhydrazone. [15-17]

Analytical interference is avoided by the 2,4-dinitrophenylhydrazine (DNPH) method which employs chromatographic separation, typically liquid chromatography, Figure 1.2. [15,

18] The DNPH method is widely considered as the best, balancing sensitivity and accuracy with relative ease and expense.

However, in this work the fluorimetric AcAc determination was selected due to advice from colleagues at the Fraunhofer, Wilhelm-Klauditz-Institut for Wood Research in Braunschweig, Germany. They showed that the chromatographic DNPH and fluorimetric AcAc methods are essentially equivalent. [19] The fluorimetric AcAc method is highly sensitive, [20] simpler, less costly, and very highly selective because, among the aldehydes, only the CH_2O adduct exhibits significant fluorescence. [21]

Emission from wood-based composites and wood

Historically, composite wood products have not been the sole source of CH_2O in home interiors; UF-based insulation is notable. [22] However, UF-bonded composite wood products occur in a variety of forms, and are remanufactured into many consumer products that have significantly contributed to indoor CH_2O exposure. [23-27] Consequently, numerous standard methods are used to measure CH_2O emissions from composite wood products, as established by different countries around the world. [28] The methods vary in scale and methodology, but most require carefully controlled temperature, relative humidity, specimen preconditioning, loading (specimen mass/unit volume of analytical chamber), and sometimes prescribed ventilation rates. Large environmental chambers are used in the United States (ASTM E1333-2002), Europe (EN 717-1) and Asia to sample full size composite specimens on the order of 2.5 m in dimension. The principal benefit of such large scale sampling is to accommodate emissions variations occurring in smaller specimens sampled from a single composite panel. Large chamber methods are costly and time consuming, therefore requiring considerable infrastructure. [29] Large and smaller scale chamber methods prescribe ventilation where the air exiting the chamber is passed through water-filled impingers that collect CH_2O for subsequent quantification. While certification requirements often demand these ventilated chamber methods, there are a number of smaller scale methods used for quality control screening, and which may be correlated to ventilated chambers. Desiccator methods are common as for ASTM D5582, and Japanese standard JIS A1460 and JAS 233, where a prescribed

number of small specimens are placed into a desiccator (~10 liter volume) with a vessel of water that absorbs emitted CH_2O. The CH_2O released from the test pieces at fixed temperature, relative humidity and time is absorbed by the water and determined photometrically. [30] Dramatically different is the perforator method (EN 120), which is widely used in Europe. It is believed to measure a very important board emission characteristic, which is free, extractable CH_2O content. Small specimens are boiled in toluene, which condenses and passes through a water solution that strips CH_2O from the toluene. [31] The flask method measures CH_2O release from small specimens over water in a closed container at a constant temperature. The flask method is simple and effective for screening purposes and also particularly suitable for teaching and demonstration purposes. [28]

There are generally three CH_2O emission sources from wood-based composites manufactured with UF resins: 1) free CH_2O not incorporated into the thermoset network (the "sol" fraction), 2) hydrolysis CH_2O from degradation of the thermoset network, and 3) natural, biogenic CH_2O from wood. The first and third sources dominate emissions out of the hot-press, whereafter they decline as a function of temperature, relative humidity, product form, etc. to a pseudo-steady-state emission caused by network hydrolysis. Notably, this hydrolytic instability and consequential CH_2O emission still has not caused widespread replacement of this highly effective and inexpensive resin. [32, 33] Much research has been devoted to reducing synthetic (anthropogenic) CH_2O emission from the resins, principally by reducing the F/U mole ratio and modifying the formulation, [34-37] and adding CH_2O scavengers. [36, 38] Alternative "no-added-formaldehyde" (NAF) resins, such as those based upon soybean flour, have captured only minor portions of this vast market. [39-41] Arguably these alternatives have played a substantial and contentious role in the regulatory process.

A few studies have been conducted on biogenic CH_2O levels in wood, conditions promoting its formation, and the likely chemical sources within wood. [2, 30, 42-44] While greater detail will appear later, the salient points are summarized as follows:

1) Biogenic CH_2O emissions increase due to wood heating at temperatures as low as 40°C, but particularly at temperatures around 140°C.

2) CH_2O emission is tree species and moisture content dependent, and sometimes tissue type dependent (i.e. juvenile vs. mature tissue).
3) All organic wood components are capable of forming CH_2O when heated, but per unit mass, lignin appears to be most productive.

For this work, it will be helpful to define three type of biogenic CH_2O: content, generated (generation), and emitted (emission). Biogenic CH_2O **content** is that which is present naturally in wood, before or after heat treatment, and which is considered **free** CH_2O (easily removed using room temperature water extraction). [45] This includes CH_2O and methylene glycol adsorbed onto/dissolved into the woody matrix, and also formaldehyde hemiacetals (hemiformals). Acetals (formals) are not easily removed and are not considered free forms of CH_2O. [45, 46] The easily removed free CH_2O can all be **emitted** into the atmosphere (capable of gaseous **emission)**, particularly at high wood moisture levels; but CH_2O emits much more slowly as declining moisture levels promote formation of hemiformals. [45, 46] **Generated** CH_2O, and CH_2O **generation** refers to that which is formed due to heating, minus the CH_2O **content** prior to heating. However, sometimes in this work the existing CH_2O content was very low, and without serious consequence CH_2O reported as **generated** included the prior existing content.

1.2.2. Wood cell wall components and relation to CH_2O emission or generation

The chemical composition of wood is complex. The main components of wood are cellulose, hemicelluloses, lignin, and an array of low molecular weight compounds known as extractives. All of these organic wood components can contribute to CH_2O generation and emission. [42]

Cellulose

Cellulose is generally regarded as the most abundant biopolymer on Earth. It has an extremely wide distribution, ranging from plants, to microorganisms, and even animals. [47] Cellulose is the main component of wood, which comprises 40-50% of the dry mass.

Cellulose can be characterized as a linear high molecular weight polymer built up from D-glucopyranose units. Anhydroglucose units are linked by β-(1→4) glucosidic linkages, and the repeating unit is cellobiose, as shown in Figure 1.3.

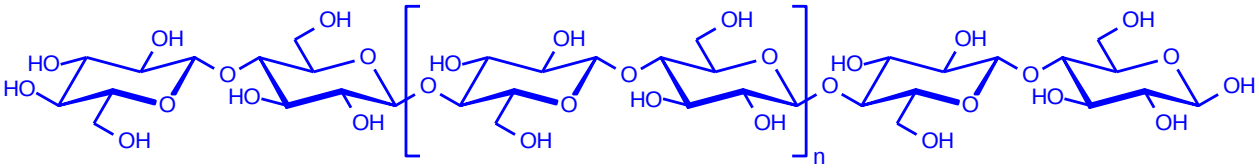

Figure 1.3. Cellulose structure with cellobiose unit as the repeating unit.

Schafer, M. and Roffael, E. measured the amount of CH_2O released from cotton linters, starch, and glucose after heat treatments at 40°C, 100°C, and 150°C for 3 hours using the flask method, Table 1.1. [42]

Table 1.1. Formaldehyde release from cotton linter, starch and glucose after heat treatments at 40°C, 100°C, and 150°C for 3 hours, measured by the Flask method. [42]

Samples	**CH_2O (μg/g sample)**		
	40°C	**100°C**	**150°C**
Cotton linter	1.0	2.1	5.1
Starch	N.D	0.6	0.8
Glucose	N.D	2.0	4.1

Hemicelluloses

In addition to cellulose, a variety of hemicelluloses, are present in wood, and other plant tissues. Unlike cellulose, the hemicelluloses are heteropolysacchrides that may contain a variety of sugar units, principally D-glucose, D-xylose, D-mannose, L-arabinose, D-galactose, and 4-O-methyl-D-glucuronic acid. [48] Compared to cellulose, hemicelluloses have shorter chains (degree of polymerization < 200) often with monosaccharide branches. [48] Typically, wood composes 20-35% hemicellulose by dry mass. [48] The simplest hemicellulose nomenclature refers to the principal backbone sugars. For instance, glucuronoxylans have backbones

composed of xylose and are simply referred to as xylans. Galactoglucomannans have backbones made from glucose and mannose, and are simply referred to as glucomannans.

Softwoods and hardwoods both contain xylans and glucomannans, but in different ratios and with different degrees of branching and acetylation.[49] In hardwoods, the xylans predominate, and are typically highly acetylated. Glucomannans predominate in softwoods, with no branching and no acetylation. Hardwoods usually contain more acetyl groups than softwoods. For example, in paper birch (hardwood) there are 6 or 7 acetyl groups substituted on every 10 xylose units. [50] The O-acetyl groups in hemicelluloses play an important role in thermal stability. [51] Hemicelluloses experience deacetylation to form acetic acid under heat treatments. And the acetic acid is believed to promote more degradation not only in polysaccharides [52, 53] but also in lignin [54], and this probably impacts CH_2O generation during heat treatments.

Schafer, M. and Roffael, E. measured the amount of formaldehyde release from pure galactose, arabinose, and xylose after heat treatments at 40°C, 100°C, and 150°C for 3 hours using flask method, as shown in Table 1.2. [42]

Table 1.2. Formaldehyde release from pure galactose, arabinose, xylose after heat treatments at 40°C, 100°C, and 150°C for 3 hours, measured by the Flask method. [42]

Sample	**CH_2O (µg/g sample)**		
	40°C	**100°C**	**150°C**
Galactose	N.D	1.1	4.7
Arabinose	0.2	1.7	11.9
Xylose	N.D	1.7	12.7

Lignin

Lignin is the second abundant polymeric organic substance in the plant world next to cellulose. It is a complex polymer resulting from coupling of 4-hydroxyphenylpropanoids, principally coniferyl (G), sinapyl (S) and p-coumaryl (H) alcohols, Figure 1.4. [55] The most

common linkages among these basic lignin monomer units include β-O-4, β-5, and β-β, Figure 1.5. [56, 57] Among these linkages, β-O-4 is the most frequent. Functional groups that influence the lignin reactivity include methoxyl, phenolic hydroxyl, aliphatic hydroxyl, benzyl alcohol, noncyclic benzyl ether and carbonyl groups. The lignin polymer is formed by combinatorial-like phenolic coupling reactions, via radicals generated by peroxidase-H_2O_2, under simple chemical control where monolignols react endwise with the growing polymer. [58] Figure 1.6 depicts a simplified structure for softwood lignin. [58]

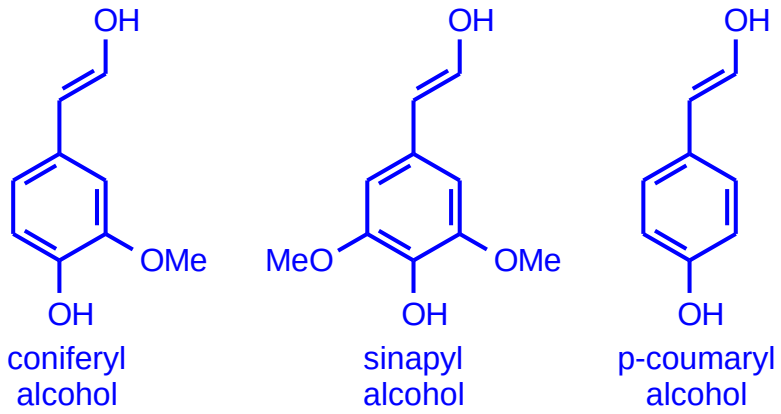

Figure 1.4. Lignin monomers, coniferyl alcohol (G), sinapyl alcohol (S), and p-coumaryl alcohol (H). [55]

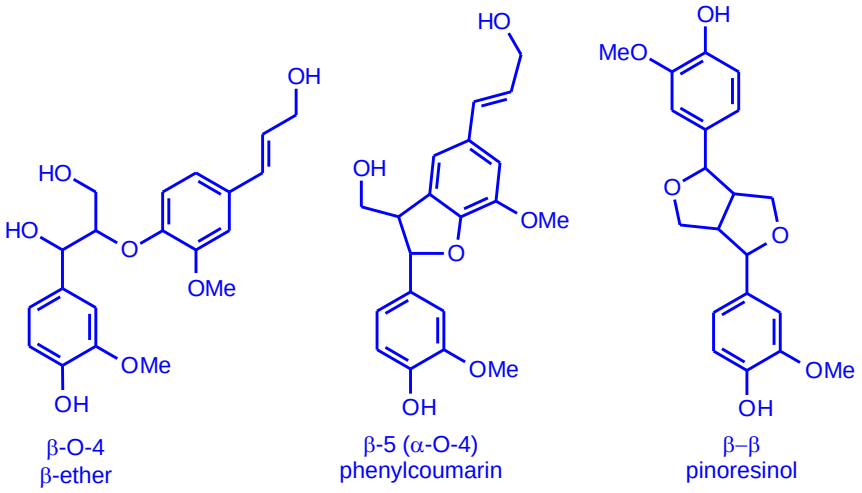

Figure 1.5. G-unit lignin dimers depicting the most common intermonomer linkages in lignin. [56, 57]

Lignin bonds with cellulose microfibrils, and crosslinks with other cell wall components, thereby stiffening and fortifying secondary cell walls within xylem tissues. [59-61] Lignin made it possible for plants to adapt to dry-land conditions, resisting ultraviolet radiation, macro- and microbiological competition, and growing to sometimes enormous dimensions. [62] On the other hand, the evolutionary success of lignin restricts access to cellulose via enzymatic hydrolysis [63] and pulping [64-66], and results in the recalcitrance that is the principal barrier to lignocellulosic biorefineries.

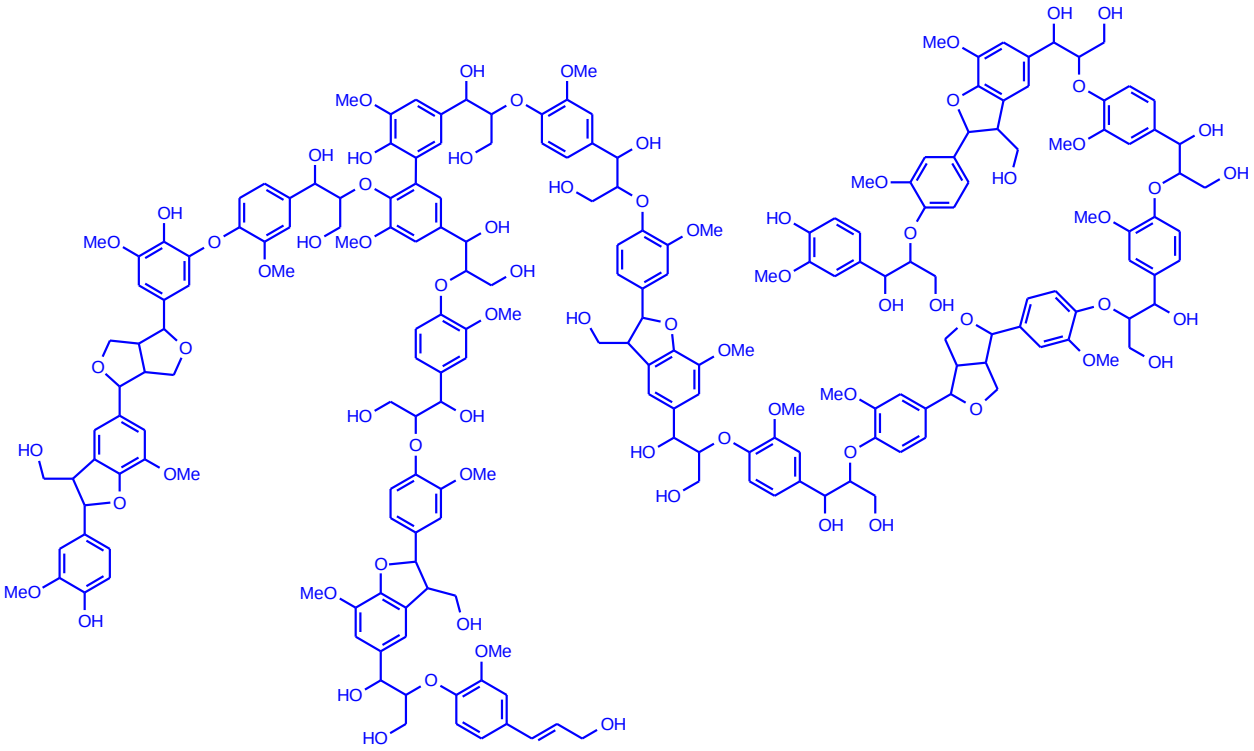

Figure 1.6. Simplified representation of a softwood lignin segment, adapted from Ralph. [58]

Unlike cellulose or hemicelluloses, lignin exhibits significant variation among different plant species, and different parts of the same plant, all of which also vary under changing growth conditions. [67-70] Typically, woods contain 20-40% lignin by dry mass, whereas aquatic and herbaceous angiosperms as well as many monocotyledons are less lignified. [70] Lignins can be divided into two major groups: guaiacyl lignins (G lignins) and guaiacyl-syringyl lignins (G-S lignins). G lignins are principally composed by coniferyl alcohol while G-S lignins contain a varying composition of guaiacyl and syringyl units, and small amount of p-coumaryl (H) units.

Most lignins in softwoods are G lignins, while hardwoods have G-S lignins. [71] For grass lignins, all three monomers are present with much higher amount of H units than in tree lignins. [71]

All organic wood components are capable of generating CH_2O, but lignin appears to be the major source. [42] According to Schäfer and Roffael, upon heating lignin seems to have a higher CH_2O emission potential than the polysaccharides. [42] Due to the acidic nature of most woods, in situ lignin thermochemistry might be described by the classic lignin acidolysis literature. [72-79] Extensive acidolysis studies on lignin model compounds and isolated lignins indicate that β-O-4 and β-5 bonds are capable of generating CH_2O through similar reaction mechanisms, while β-β linkages cannot, Figure 1.7 and Figure 1.8. [72, 73, 80]

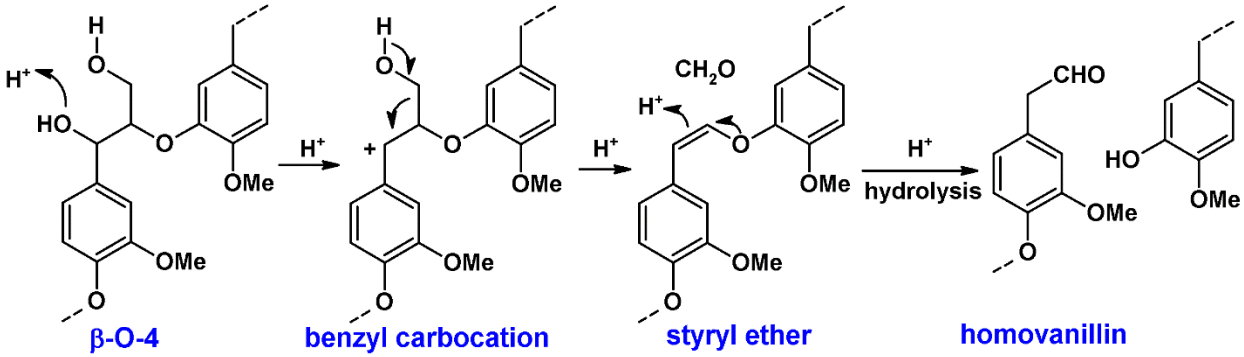

Figure 1.7. Formaldehyde generation mechanism from lignin β-O-4 structure under acidic condition. [72]

Lignin β-O-4 and β-5 structures containing free phenolic groups (lignin chain ends) are also capable of generating CH_2O under base-catalyzed conditions, Figure 1.9. [81, 82] In comparison, acid-catalyzed CH_2O generation (as depicted in Figures 1.7 and 1.8) could occur all along the length of the lignin chain.

Under certain conditions, lignin can also react with formaldehyde. Studies of the formation of formaldehyde from lignin during acidolysis suggested that the liberated formaldehyde was partly consumed by substituting into aromatic rings to form diphenylmethane structures. [74] For spruce Björkman lignins, the yield of formaldehyde through acidolysis decreased with increasing lignin concentration in the reaction mixture. A

plausible explanation was that formaldehyde liberated was consumed by reaction with lignin. [72]

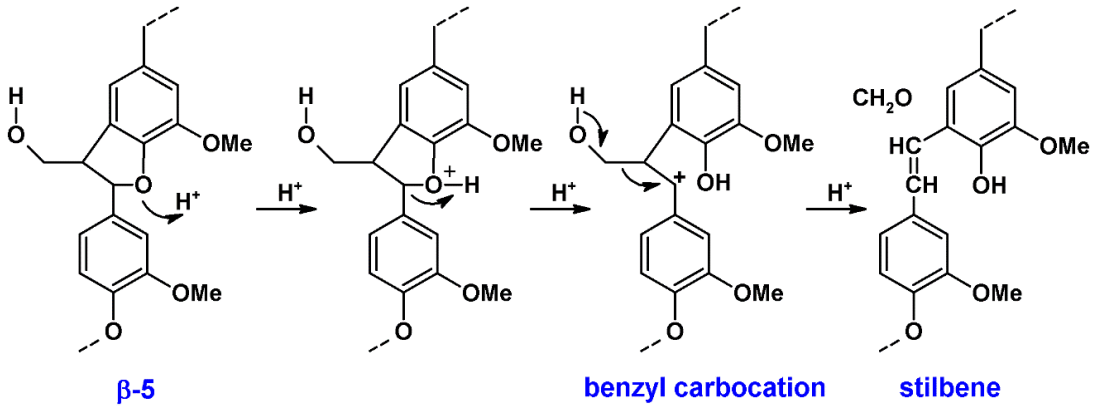

Figure 1.8. Formaldehyde generation mechanism from lignin β-5 structure under acidic condition. [80]

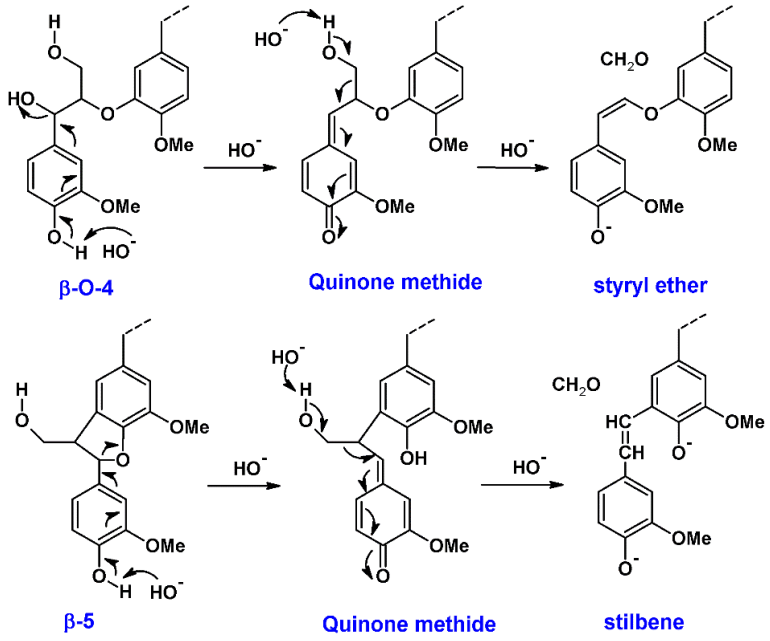

Figure 1.9. Formaldehyde generation mechanisms from lignin β-O-4 and β-5 structures under basic condition. [81, 82]

During Kraft pulping or under thermal treatment, it is known that lignin undergoes extensive condensation to form highly stable carbon-carbon linkages; and this might include the diphenylmethane structures mentioned above. [83] This was suggested on the basis of

model compound experiments and structural analysis of the residual lignin in Kraft pulp by the nuclear exchange degradation technique. [84] 13C NMR and 31P NMR spectra of Kraft lignins also proved the existence of diphenylmethane moieties of the 5-CH_2-5 type. [85-87] However, the use of the more diagnostic 2D NMR (HMQC: Heteronuclear Multiple Quantum Coherence) techniques in lignin structural investigations did not detect 5-CH_2-5 moieties. [88]

Extractives

Table 1.3. Classification of organic extractives in woods. [89]

Aliphatic and alicyclic compounds	Phenolic compounds	Other compounds
	Simple phenols	Sugars
Terpenes and terpenoids	Stilbenes	Cyclitols
	Lignans	Tropolones
	Isoflavones	Amino acids
Esters of fatty acids	Condensed tannins	Alkaloids
Fatty acids and alcohols	Flavonoids	Coumarins
Alkanes	Hydrolyzable tannins	Quinones

Wood also contains a broad variety of nonstructural compounds that can be extracted from wood using polar and non-polar solvents. Extractives include resin acids, fats, waxes, terpenes, phenolic compounds, certain carboxyhydrates and some inorganic salts. [90, 91] Table 1.3 [89] summarizes a typical classification of organic extractives in woods.

Among these extractives, some are neutral, while others are weakly acidic, which partially contribute to the weak acidity of most woods. Additionally, acetyl groups and uronic acid residues linked to polyoses are also responsible for the wood acidity of many species. [92] Acidic extractives including resin acids and fatty acids, have a pKa around 4-5, which is the same range of wood acidity. Figure 1.10 lists several examples of resin acids and fatty acids. Abietic acid, neoabietic acid and levopimaric acid are common resin acids. [90] They all have the same

skeleton, three fused rings with the empirical formula $C_{19}H_{29}COOH$. [90] As for the fatty acids, they are carboxylic acids with a long aliphatic tail (chain), either saturated (i.e. palmitic acid) or unsaturated (i.e. oleic acid). [90]

Extractives usually constitute less than 10% of the dry weight of normal wood of species that grow in temperate climates, while tropical woods may have as much as 20%. [93] Extractives species and contents vary dramatically depending on plant species. Even for the same species, they can differ as a function of growing conditions. Also extractives from different sampling sites within the same tree can exhibit huge differences. [94] Most of the extractives are located in the ray tracheid and vessel, and phenolic compounds are accumulated in the heartwood. [90]

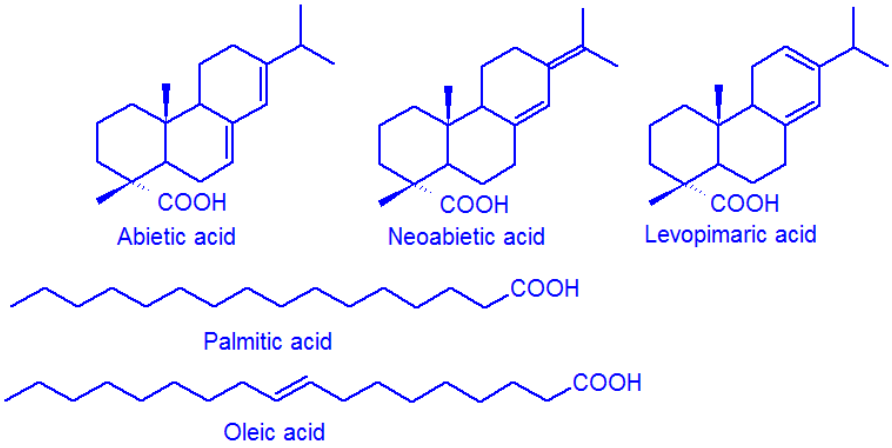

Figure 1.10. Example of resin acids and fatty acids. [90]

The existence of extractives often influences the reproducibility and accuracy of various analyses, such as the compositional analysis. To exclude the effect from extractives, extraction is performed before further analysis. There are many extraction standards, which typically involve different solvent systems, temperatures and pressures. [95] Extraction solvent systems may contain just one solvent, or a combination of several solvents. [96] Also, the criteria for selecting solvent systems relate to the experimental objective, and the biomass type. There is no single solvent system, which is good for every aspect. Dichloromethane is relatively nonpolar and is able to extract fats, resins, oils, sterols, and terpenes; ethanol/benzene is more polar and extracts most of the ether-solubles plus most of the organic materials insoluble in water; hot

water extracts some inorganic salts and low molecular weight polysaccharides including gums and starches. [90, 97-99]

The content of extractives decreases during storage of the wood specimens, and free lipophilic fats, fatty and resin acids, and sterols decrease enormously. [100, 101] Researchers found that with increasing storage time, the spruce and pine wood particles emit less formaldehyde than non-stored wood. [30] Correlation between these two observations may be made.

Due to their complexity, extractives may play multiple roles regarding CH_2O generation in wood. They might participate in lignin catalysis, [102] or upon heating might directly generate CH_2O; [42] or the extractives might reduce emissions by reacting with (scavenging) CH_2O. [103-108] Schäfer and Roffael used the flask method to measure CH_2O release from unextracted and extracted woods at different temperatures. The results revealed extracted chips released significantly lower amounts of formaldehyde comparing to unextracted chips. [42] Furthermore, saturated fatty acids generated only minute quantities, whereas abietic acid (resin acid) released much higher amounts of formaldehyde. Schäfer and Roffael also found pine formed more formaldehyde than spruce, which may due to the catalytic effect from extractives in pine, especially higher amount of resin acids, [42, 94] as will be discussed in later chapters.

1.2.3. Heat treatment of wood

Wood is an incredibly versatile material, that has and continues to provide critical societal value. However, due to its hygroscopic nature, wood has some undesirable properties, such as poor resistance against biological attack, and water swelling/shrinkage. [109] These disadvantages limit the outdoor use of wood, and a variety of strategies have been studied to overcome these problems. Most common have been chemical treatments, and these typically involve chemicals and chemical emissions that present other technical and societal concerns. [110-112] In recent years, wood thermal treatments that reduce hydrophilicity have been identified as a possible alternative to traditional chemical treatments. [113-115] These heat treatments occur in the range of 160°C to 260°C, often under anaerobic conditions. [116] These

treatments thermally degrade wood and reduce its equilibrium moisture content, [117] and some of the degradative reactions are generally related to biogenic CH_2O generation.

Wood heat treatments generally improve dimensional stability, durability, and resistance to biodegradation. [113] However depending upon the treatment severity, stiffness and strength are compromised, particularly strength. [113, 117] Extensive studies have been conducted to investigate mass loss, surface chemistry, color change, and chemical transformation. [118, 119] Hemicelluloses are subject to degradation, [120, 121] and this is accompanied by the formation of volatiles, including acetic acid, that may catalyze further degradation in polysaccharides and lignin. [52-54] Wood thermal treatments may impact cellulose crystallinity, [83, 122], and of course the matrix within which the cellulose fibrils occur. [123-125] Consequently, lignin degradation occurs, [78, 79, 126], and this includes demethoxylation which could lead to crosslinking within lignin and with the polysaccharides. [83, 126-129]

Under relatively mild heating conditions (~25°C – 200°C) it has often been reported that hemicelluloses are the least thermally stable polymers in wood, and that lignin is substantially more stable. [117, 127, 130-135] According to Ramiah, M. V [136], the decomposition temperature was found to increase from 117°C to 170°C in the order of hemicelluloses<lignin<cellulose. However, these conclusions were based upon the determination of acid insoluble lignin (Klason lignin), which is a crude analysis that does not reveal subtle changes in lignin structure. Preferred methods for assessing the thermal stability of in situ lignin are the lignin monomer analyses such as thioacidolysis [137, 138], and Derivatization Followed by Reductive Cleavage (DFRC) [139]. For example, thioacidolysis shows that lignin β-aryl ether bonds undergo substantial cleavage and repolymerization at heating conditions that effect little or no change in the hemicelluloses. [127, 140, 141]

1.2.4. Analytical methods

Compositional analyses

There are lots of different methods for compositional analysis, varying in biomass particle size, sample amount, acid concentration, hydrolysis temperature, or sugar detection

methods. [142, 143] In this project, the standard NREL procedure: Determination of Structural Carbohydrates and Lignin in Biomass (NREL/TP-510-42618) was used for compositional analysis. Soxhlet extraction is performed to remove extractives: 1) a single 95% ethanol extraction is enough for wood specimens, including softwoods and hardwoods; 2) an extra water extraction step is needed before the sequential 95% ethanol extraction for biomass, like corn stover, having significant amounts of water soluble materials. Afterwards 72% sulfuric acid is used to hydrolyze the dry extractives-free biomass powder (~40˚C), followed by a second acid hydrolysis at lower acid concentration (4%) and higher temperature (120°C). Acid insoluble lignin is filtered and measured gravimetrically after being oven dried at 105°C for at least 4 hours, while the soluble lignin content is measured using UV-Vis spectroscopy. After the two-step acid hydrolysis, polysaccharides are hydrolyzed into sugar monomers, which can be quantified using High Performance Liquid Chromatography (HPLC) or Ion Chromatography (IC). [144]

Acidolysis

Acidolysis is a common method to analyze uncondensed lignin β-O-4 linkages by looking into the degraded monomeric products. [72-79] Efforts also devoted to look into low-molecular weight lignin acidolysis products, and structural elements including β-5, β-β, β-1, glyceraldehyde-2-aryl ether, 2-aryl ether, 2-aryloxypropiophenone, cinnamaldehyde, cinnamic acid, benzaldehyde, benzoic acid, and quinonoid types were identified too. [74] Comparing to thioacidolysis, the yield of this method is lower probably due to incomplete ether linkage cleavage, but the obvious advantage is that this method does not involve smelly chemicals and the reaction conditions are milder and simpler. [145] The acidolysis reaction condition is quite simple, which involves sample refluxing in 82% dioxane aqueous solution with 0.2 M HCl as catalyst for 4 h. Based on extensive acidolysis literature studies on lignin model compounds and isolated lignin samples, the reaction scheme of lignin β-O-4 units in acidolysis is shown in Figure 1.11. [72-79] There are two well-established pathways, C2 cleavage and C3 cleavage, and C3 cleavage is the dominant pathway in lignin β-O-4 acidolysis. C2 cleavage produces CH_2O, a phenylacetaldehyde derivative, and a free phenol; whereas C3 cleavage produces the Hibbert's ketones and a free phenol.

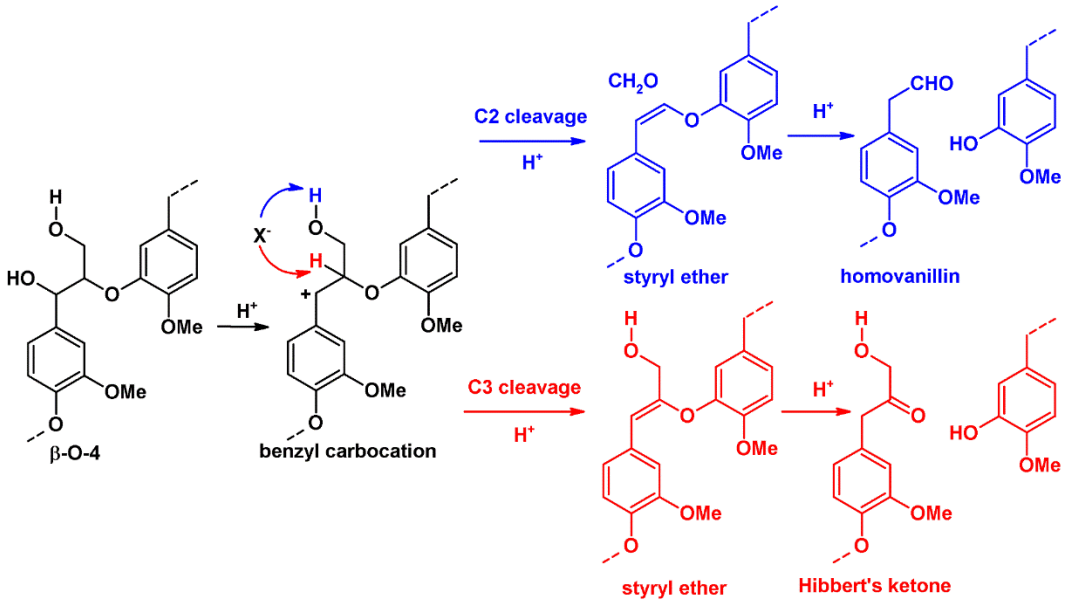

Figure 1.11. Acidolysis reaction scheme for lignin. [72-79]

Like most woods, Virginia pine is naturally acidic and in situ lignin thermochemistry might be described by the classic lignin acidolysis literature. Based on acidolysis studies on lignin models and isolated lignins, the relative occurrence of these pathways depends upon the nature of the acid catalyst. [75, 76] This suggests that CH_2O formation in whole wood could be manipulated by the selection of external acid catalyst, as will be discussed in later chapters.

<u>Thioacidolysis and desulfuration reaction</u>

Thioacidolysis has been proven to be an extremely useful tool for characterizing and identifying structural components in lignin. [137] Lapierre et al [137] investigated this reaction with appropriate lignin model compounds and isolated lignins, Figure 1.12. The first step of the reaction takes place at the benzyl alcohol or benzyl ether group. Reaction of C_β cleaves the ether bond with participation of the thioethyl group previously introduced at C_α. And final products are threo and erythro isomers regardless of the stereochemistry of the initial structure after the final substitution at C_γ position. [137]

To obtain more structural information about lignin structures, dimeric products after thioacidolysis require further examination, which reflect the various types of condensed linkages, such as β-5, β-1, and 5-5 et al. However, the dimers derived from direct thioacidolysis

are extensively thioethylated at the phenylpropane side chains, resulting in low volatility and complexity in multiple diastereoisomeric forms. For this purpose, Lapierre et al. added one reaction step after thioacidolysis, which is called desulphuration over Raney Nickel. [146] This added step is capable of increasing the volatility and reducing the number of diastereoisomers in a reproducible fashion. The dimers obtained after desulphuration are shown in Figure 1.13. [146] Even some minor linkages patterns can be characterized and quantified, such as diphenyl ether, the phenylisochroman, and the tetrahydrofuran structures. [146]

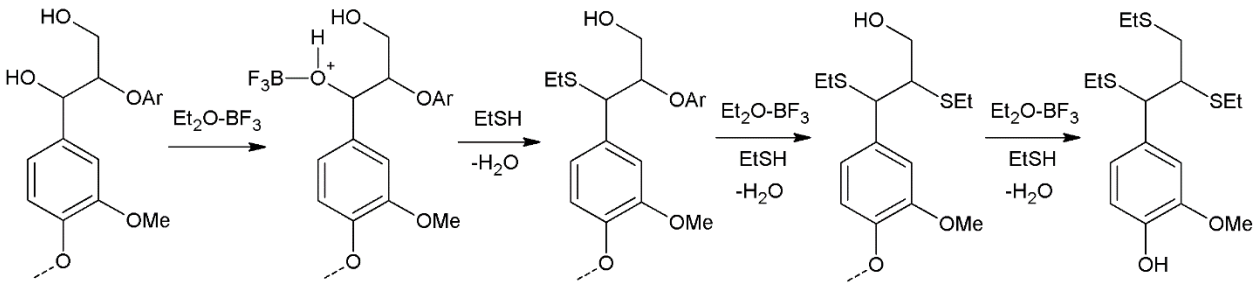

Figure 1.12. Lignin β-O-4 thioacidolysis reaction scheme. [137]

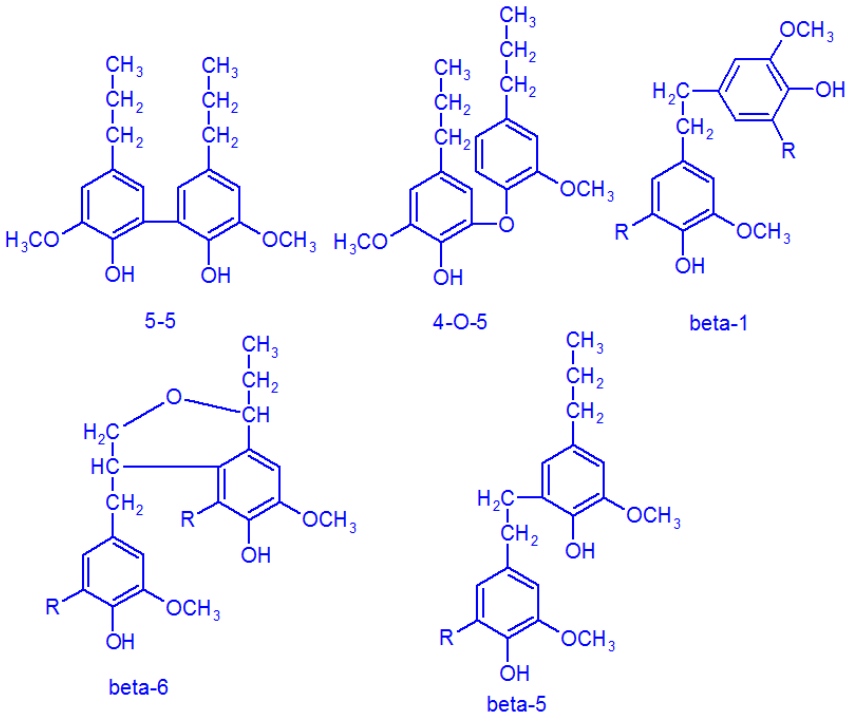

Figure 1.13. Structures of dimeric products recovered from thioacidolysis followed by desulphration. [146]

Derivatization followed by reductive cleavage (DFRC)

Thioacidolysis is extremely useful for analyzing ether-linked lignin structures. However, one of the reagents, ethanolthiol, has an unbearable smell. The threshold for human detection is as low as one part in 2.8 billion parts of air. [147] So many researchers are reluctant to use this method.

Lu and Ralph [139] developed a new method for selective and efficient cleavage of arylglycerol-β-aryl (β-O-4) ether linkages in lignin. This method was described and applied to several lignin β-ether models, isolated lignin and wood samples. [148] The term "DFRC" is abbreviation for Derivatization Followed by Reductive Cleavage, which indicates it is a two step reaction, shown in Figure 1.14. [139] The first step is cell wall solubilization and derivatization with acetyl bromide, while the second step is the reductive cleavage of resulting β-bromo ethers by zinc dust. [139] The primary lignin-derived monomers released are essentially 4-acetoxycinnamyl acetate (p-hydroxycinnamyl peracetate, **H**), 4-acetoxy-3-methoxycinnamyl acetate (coniferyl peracerate, **G**), and 4-acetoxy-3,5-dimethoxycinnamyl acetate (sinapyl peracerate, **S**). The final products can be identified by GC, GC/MS and NMR.

Compared to thioacidolysis, one disadvantage of DFRC is the lower monomer yield, which may due to incomplete cleavage on lignin ether linkages. [149]

However, DFRC also has several advantages over thioacidolysis. The reaction temperature for DFRC is milder, which is 50°C or even at room temperature. Thioacidolysis reagents need to be refreshed on a daily basis, which adds more effort to this method while the DFRC reagent mixture can be stored in the refrigerater for months. DFRC reaction does not use any chemicals with extremely unpleasant smell as thioacidolysis does. Another advantage of DFRC raises up when it comes to analyze grass lignins. Grass lignins are partially esterified with p-coumaric acid at γ-position of lignin propane side chain. This naturally occurring ester remains totally intact after DFRC degradation, whereas 40% of the original ester linkages were hydrolyzed in thioacidolysis, which makes the final result biased. [150] DFRC also can be easily modified to identify new features such as naturally occurring acetates using propionate

reagents (propionyl bromide/propionic acid/propionic anhydride) to replace all acetate analogues. [148]

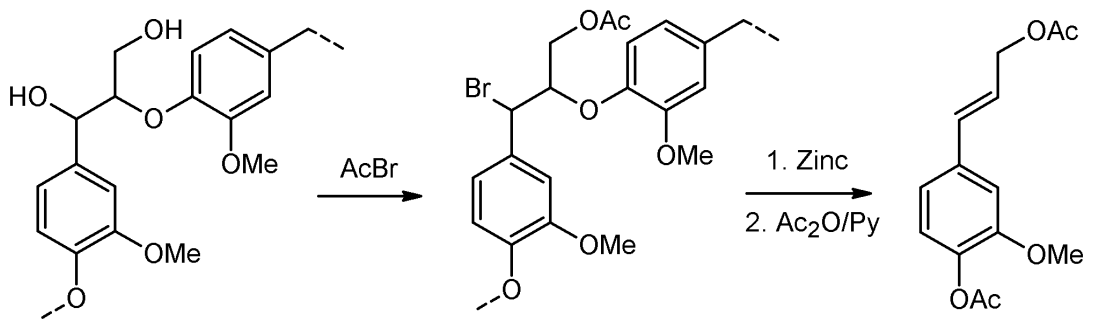

Figure 1.14. Selective ether cleavage by the DFRC method. [139]

<u>Biomass rheology and viscoelasticity</u>

Rheology is the study of deformation and flow in materials, both liquids and solids. Carefully measured deformations reveal insights about molecular structures, hierarchical organizations, and aspects of material processings. Dynamic mechanical analysis (DMA) is one common rheological methodology. It involves application of an oscillating stress or strain, and the resulting strain or stress is measured. The DMA response in polymeric materials is viscoelastic; it is simultaneously elastic like a spring, and also viscous like the flowing water.

The viscous response of a lignocellulosic material is not macroscopic liquid flow, but rather localized flow as when two polymeric segments rub and slip past one another when mechanical energy is dissipated. When carefully conducted, the DMA of viscoelastic lignocelluloses may be used to reveal insights about the structure and organization of cellulose, hemicelluloses, and lignin. Most of this type of research has been devoted to wood, with examples such as [123, 151-154]. Given the variety of polymers and the complexity of their organization in lignocellulose, it is interesting to note that lignocellulose exhibits only one major thermo-mechanical softening transition above sub-ambient temperature, a glass-to-rubber transition attributed to lignin. [155, 156] Relaxation of amorphous cellulose and hemicelluloses in water-swollen wood occurs at sub-ambient temperature. [124, 125] The in situ lignin glass transition is quite sensitive to moisture levels, meaning that moisture control is a very practical experimental concern. [123, 152, 157]. Similar to water, ethylene glycol saturated wood

specimens behave similarly under heat treatment, but within a wider temperature range due to higher boiling point of the solvent.

Rheological properties of other biomasses type, such as switchgrass were investigated by Chowdhury et al [152]. The thermo-rheological response of switchgrass stem is quite similar to that of wood, and tissue maturity effects are easily detected in switchgrass. In Appendix A, two groups of transgenic switchgrass plants were subjected to solvent-submersion tensile-torsion DMA tests for measuring rheological properties, including glass transition temperature (Tg) or activation energy associated with Tg (Ea).

Nuclear Magnetic Resonance (NMR)

NMR is a physical phenomenon in which nuclei in a magnetic field absorb and re-emit electromagnetic radiation. The radiation is at a specific frequency which depends on the strength of the magnetic field and the magnetic properties of the isotope of the atoms. The most commonly studied nuclei are ^{1}H and ^{13}C. It is a powerful non-selective, non-destructive analytical tool that enables one to ascertain molecular structure including relative configuration, relative and absolute concentrations, and even intermolecular interactions of an analyte.

NMR is a relatively new analytical technique for analyzing chemical structure of wood, or isolated wood components, which enables non-destructive interpretation of the structures. Absolute quantification remains elusive, but NMR provides unparalleled structural information on the complex polymers of the cell walls, and it is valid to provide comparative assessment. [158]

The whole NMR process seems complex and takes longer time than common wet chemistry methods, such as compositional analysis, thioacidolysis and DFRC. It involves the following steps [158]: simple cell wall isolation (or extraction), which is commonly required for all other analysis; fine grinding, so called ball-milling to minimize the sample particle size; swelling and dissolution in a solvent mixture; NMR acquisition and interpretation, usually takes hours to days depending on instrumentation and acquisition parameters setting.

The NMR techniques in lignin and whole cell wall research have been improved over the past decades, as reviewed in [158-162]. More recently, by utilizing the resolution and dispersion of high-resolution and high field 2D and 3D NMR, considerable structural information is available without the need to isolate fractions. Two dimensional NMR, such as HSQC (Heteronuclear Single Quantum Coherence) in which more than a single NMR parameter is presented in a spectrum, has been widely used to elegantly elucidate aspects of lignin structure and bonding. One example of HSQC spectra on whole wood tissue is shown in Figure 1.15. [161]

There are typically two types of cell wall samples, acetylated cell walls and native cell walls for 2D NMR. Acetylated cell wall samples can be dissolved in solvents, therefore yields better NMR signals comparing to gel-like native cell wall sample, but at the expense of losing natural acetylation information from native cell walls. Two dimensional NMRs in principle, quantifiable by measuring contour volume integrals, but gel samples are particularly challenging but doable because of their rapid relaxation. But the reproducibility has been very good when the same materials are taken through the full grinding, dissolution/swelling and NMR procedures, even when samples are run many months apart. [158]

2D NMR has been widely used with lots of other analytical methods, such as pyrolysis, DFRC, and thioacidolysis. [158, 163, 164] The structural information obtained from 2D NMR includes [158, 163]: intramolecular lignin linkages, such as β-O-4, β-5, β-β, and dibenzodioxocins et al., and their relative proportion; various lignin endgroups, including cinnamyl alcohol endgoups and cinnamyl aldehyde endgroups; lignin aromatic units (G, H, and S) composition and S/G ratio; natural acetylation, p-coumarate and ferulates and their linkages to lignin or carbohydrates. 2D NMR also was conducted on residual lignin from kraft pulp of pine and eucalyptus to investigate the condensed lignin linkages, including diarylmethane moieties and β-β, β-5 structures. Diarylmethane moieties were believed to exist in kraft lignin due to condensation reaction between formaldehyde and lignin, but failed to be detected in all literatures using 2D NMR techniques. [164]

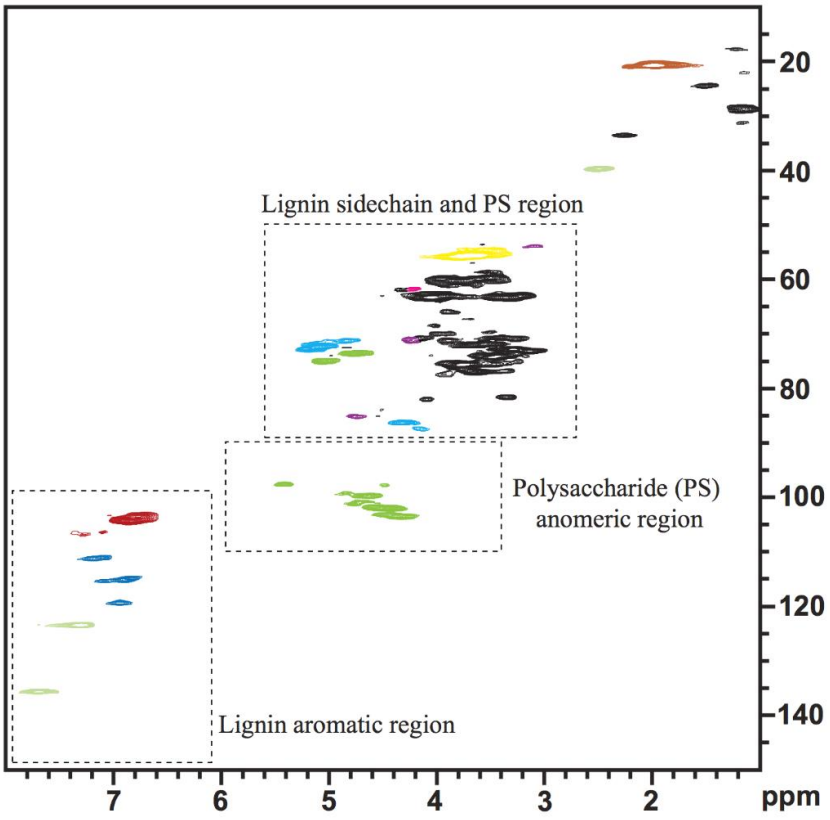

Figure 1.15. Short acquisition time (17 min) experiment on aspen cell walls in DMSO-d6/pyridine-d5 (4:1, v:v) using a 750 MHz cryoprobe-equipped NMR. The spectrum is adequate for many purposes-chemometrics, and S/G ratio estimation, for example. [161]

The biggest challenge for 2D NMR quantification is to choose the proper internal standard. Among many have been done, lignin aromatics signal is the most commonly used, such as the C2 or C5 signals in aromatic rings. [165-167]

Later on, HSQC was used to investigate structural changes of in situ lignin after various heat treatments in this project. Lignin methoxyl group content was attempted to be used as internal standard for quantification.

1.2.5. References

1. Ruffing, T.C., W.P. Shi, N.R. Brown, and P.M. Smith, *Review of United States and International Formaldehyde Emission Regulations for Interior Wood Composite Panels.* Wood and Fiber Science, 2011. **43**(1): p. 21-31.

2. Meyer, B. and C. Boehme, *Formaldehyde emission from solid wood.* Forest Products Journal, 1997. **47**(5): p. 45-48.
3. Agency, E.P., *Formaldehyde emission standards for composite wood products (RIN 2070-AJ44)*. 2016.
4. Pizzi, A., *Recent developments in eco-efficient bio-based adhesives for wood bonding: opportunities and issues.* Journal of Adhesion Science and Technology, 2006. **20**(8): p. 829-846.
5. Salthammer, T., S. Mentese, and R. Marutzky, *Formaldehyde in the indoor environment.* Chem Rev, 2010. **110**(4): p. 2536-72.
6. Zhang, J.F., Q.C. He, and P.J. Lioy, *Characteristics of Aldehydes - Concentrations, Sources, and Exposures for Indoor and Outdoor Residential Microenvironments.* Environmental Science & Technology, 1994. **28**(1): p. 146-152.
7. Lipari, F. and S.J. Swarin, *Determination of formaldehyde and other aldehydes in automobile exhaust with an improved 2, 4-dinitrophenylhydrazine method.* Journal of Chromatography A, 1982. **247**(2): p. 297-306.
8. Girman, J.R., M.G. Apte, G.W. Traynor, J.R. Allen, and C.D. Hollowell, *Pollutant emission rates from indoor combustion appliances and sidestream cigarette smoke.* Environment International, 1982. **8**(1): p. 213-221.
9. Lipari, F., J.M. Dasch, and W.F. Scruggs, *Aldehyde emissions from wood-burning fireplaces.* Environ Sci Technol, 1984. **18**(5): p. 326-30.
10. Kim Oanh, N.T., L.H. Nghiem, and Y.L. Phyu, *Emission of polycyclic aromatic hydrocarbons, toxicity, and mutagenicity from domestic cooking using sawdust briquettes, wood, and kerosene.* Environmental science & technology, 2002. **36**(5): p. 833-839.
11. Corrêa, S.M. and G. Arbilla, *Formaldehyde and acetaldehyde associated with the use of natural gas as a fuel for light vehicles.* Atmospheric Environment, 2005. **39**(25): p. 4513-4518.
12. Goldman, F. and H. Yagoda, *Collection and estimation of traces of formaldehyde in air.* Industrial & Engineering Chemistry Analytical Edition, 1943. **15**(6): p. 377-378.

13. West, P.W. and B. Sen, *Spectrophotometric determination of traces of formaldehyde.* Fresenius' Zeitschrift für analytische Chemie 1956. **153**(3): p. 177-183.

14. Nash, T., *The colorimetric estimation of formaldehyde by means of the Hantzsch reaction.* Biochem J, 1953. **55**(3): p. 416-21.

15. A. Nageswari, K. V. S. R. Krishna Reddy, and K. Mukkanti, *Low-Level Quantitation of Formaldehyde in Drug Substance by HPLC–UV.* Chromatographia, 2012. **75**: p. 275-280.

16. Maboudou, P., D. Mathieu, H. Bachelet, J.F. Wiart, and M. Lhermitte, *Detection of oxidative stress. Interest of GC-MS for malondialdehyde and formaldehyde monitoring.* Biomed Chromatogr, 2002. **16**(3): p. 199-202.

17. del Barrio, M.A., J. Hu, P. Zhou, and N. Cauchon, *Simultaneous determination of formic acid and formaldehyde in pharmaceutical excipients using headspace GC/MS.* Journal of Pharmaceutical and Biomedical Analysis, 2006. **41**(3): p. 738-743.

18. Risner, C.H. and P. Martin, *Quantitation of formaldehyde, acetaldehyde, and acetone in sidestream cigarette smoke by high-performance liquid chromatography.* J Chromatogr Sci, 1994. **32**(3): p. 76-82.

19. Salthammer, T. and S. Mentese, *Comparison of analytical techniques for the determination of aldehydes in test chambers.* Chemosphere, 2008. **73**(8): p. 1351-6.

20. Belman, S., *The fluorimetric determination of formaldehyde.* Analytica Chimica Acta, 1963. **29**: p. 120-126.

21. Vairavamurthy, A., J.M. Roberts, and L. Newman, *Methods for determination of low molecular weight carbonyl compounds in the atmosphere: a review.* Atmospheric Environment. Part A. General Topics, 1992. **26**(11): p. 1965-1993.

22. *An update on formaldehyde, Publication 725, Revision 012013.*, U.S.C.P.S. Commission., Editor. 2013.

23. Ayrilmis N., Buyuksari U., Avci E., and K. E., *Utilization of pine (Pinus pinea L.) cone in manufacture of wood based composite.* Forest Ecology and Management, 2009. **259**: p. 65-70.

24. Kim, S., J.A. Kim, H.J. Kim, and S.D. Kim, *Determination of formaldehyde and TVOC emission factor from wood-based composites by small chamber method.* Polymer Testing, 2006. **25**(5): p. 605-614.

25. Guler, C. and U. Buyuksari, *Effect of Production Parameters on the Physical and Mechanical Properties of Particleboards Made from Peanut (Arachis Hypogaea L.) Hull.* Bioresources, 2011. **6**(4): p. 5027-5036.

26. Moubarik, A., A. Allal, A. Pizzi, F. Charrier, and B. Charrier, *Characterization of a formaldehyde-free cornstarch-tannin wood adhesive for interior plywood.* European Journal of Wood and Wood Products, 2010. **68**(4): p. 427-433.

27. Mao, A., E. Hassan, and M.G. Kim, *The Effects of Adding Melamine at Different Resin Synthesis Points of Low Mole Ratio Urea-Melamine-Formaldehyde (UMF) Resins.* Bioresources, 2013. **8**(4): p. 5733-5748.

28. Risholm-Sundman, M., A. Larsen, E. Vestin, and A. Weibull, *Formaldehyde emission-comparison of different standard methods.* Atmospheric Environment, 2007. **41**(15): p. 3193-3202.

29. Que, Z.L., F.B. Wang, L.F. Ma, and F. Takeshi, *Evaluation of formaldehyde emission from particleboard using the large chamber and desiccator method at various loading ratios.* Journal of Forestry Research, 2013. **24**(1): p. 137-142.

30. Salem, M.Z.M. and M. Bohm, *Understanding of Formaldehyde Emissions from Solid Wood: An Overview.* Bioresources, 2013. **8**(3): p. 4775-4790.

31. E. Roffael, B. Johnsson, and B. Engstrom, *On the measurement of formaldehyde release from low-emission wood-based panels using the perforator method.* Journal of the International Academy of Wood Science, 2010. **44**(3): p. 369-377.

32. Pizzi, A. and K.L. Mittal, *Urea-formaldehyde adhesives*, in *Handbook of Adhesive Technology,*. 2003. p. 635-652.

33. Pizzi, A. and K.L. Mittal, *Wood adhesives*. 2011: CRC Press.

34. B., S. and H. P. *Formaldehyde emission from particleboard and other building materials*. in *Proceedings of the 12th International Particleboard Symposium*. 1978. Washington State University: Pullman, WA.

35. Meyer, B., W.E. Johns, and J.K. Woo, *Formaldehyde Release from Sulfur-Modified Urea-Formaldehyde Resin Systems.* Forest Products Journal, 1980. **30**(3): p. 24-31.

36. Tohmura, S.I., A. Inoue, and S.H. Sahari, *Influence of the melamine content in melamine-urea-formaldehyde resins on formaldehyde emission and cured resin structure.* Journal of wood science, 2001. **47**(6): p. 451-457.

37. Que, Z.L., T. Furuno, S. Katoh, and Y. Nishino, *Effects of urea-formaldehyde resin mole ratio on the properties of particleboard.* Building and Environment, 2007. **42**(3): p. 1257-1263.

38. Hematabadi, H., R. Behrooz, A. Shakibi, and M. Arabi, *The reduction of indoor air formaldehyde from wood based composites using urea treatment for building materials.* Construction and Building Materials, 2012. **28**(1): p. 743-746.

39. Sellers, T., *Wood adhesive innovations and applications in North America.* Forest Products Journal, 2001. **51**(6): p. 12-22.

40. Yang, I., M.L. Kuo, D.J. Myers, and A.B. Pu, *Comparison of protein-based adhesive resins for wood composites.* Journal of Wood Science, 2006. **52**(6): p. 503-508.

41. Lin, Q.J., N.R. Chen, L.P. Bian, and M.Z. Fan, *Development and mechanism characterization of high performance soy-based bio-adhesives.* International Journal of Adhesion and Adhesives, 2012. **34**: p. 11-16.

42. Schafer, M. and E. Roffael, *On the formaldehyde release of wood.* Holz Als Roh-Und Werkstoff, 2000. **58**(4): p. 259-264.

43. Martinez, E. and M.I. Belanche, *Influence of veneer wood species on plywood formaldehyde emission and content.* Holz Als Roh-Und Werkstoff, 2000. **58**(1-2): p. 31-34.

44. Bohm, M., M.Z.M. Salem, and J. Srba, *Formaldehyde emission monitoring from a variety of solid wood, plywood, blockboard and flooring products manufactured for building and furnishing materials.* Journal of Hazardous Materials, 2012. **221**: p. 68-79.

45. Tasooji, M. and C.E. Frazier, *Simple Milligram-Scale Extraction of Formaldehyde from Wood.* ACS Sustainable Chemistry & Engineering, 2016. **4**(9): p. 5041-5045.

46. Myers, G.E., *Mechanisms of formaldehyde release from bonded wood products.* In ACS Symposium series-American Chemical Society (USA), 1986.

47. Stone, B., *Cellulose: structure and distribution*, in *Encyclopedia of life sciences*. 2005, John Wiley & Sons, Ltd.

48. Scheller, H.V. and P. Ulvskov, *Hemicelluloses.* Annual Review of Plant Biology, Vol 61, 2010. **61**: p. 263-289.

49. Fengel, D. and G. Wegener, *Wood: chemistry, ultrastructure, reactions*. 1983: Walter de Gruyter.

50. Bouveng, H.O., P.J. Garegg, and B. Lindberg, *Position of the O-Acetyl Groups in Birch Xylan.* Acta Chemica Scandinavica, 1960. **14**(3): p. 742-748.

51. Shimizu, K., F. Teratani, M. Hashi, and K. Miyazaki, *Effect of the thermal treatment on wood hemicelluloses.* Mokuzai Gakkaishi, 1972. **18**(2): p. 79-84.

52. Theander, O. and D.A. Nelson, *Aqueous, High-Temperature Transformation of Carbohydrates Relative to Utilization of Biomass.* Advances in Carbohydrate Chemistry and Biochemistry, 1988. **46**: p. 273-326.

53. Roos, A.A., T. Persson, H. Krawczyk, G. Zacchi, and H. Stalbrand, *Extraction of water-soluble hemicelluloses from barley husks.* Bioresource Technology, 2009. **100**(2): p. 763-769.

54. Lai, Y.Z., *Chemical degradation In: Wood and Cellulosic Chemistry*, ed. D.N.S. Hon and N. Shiraishi. 1991, New York: Marcel Dekker, Inc.

55. Lewis, N.G. and E. Yamamoto, *Lignin - Occurrence, Biogenesis and Biodegradation.* Annual Review of Plant Physiology and Plant Molecular Biology, 1990. **41**: p. 455-496.

56. Adler, E., *Lignin Chemistry - Past, Present and Future.* Wood Science and Technology, 1977. **11**(3): p. 169-218.

57. Boerjan, W., J. Ralph, and M. Baucher, *Lignin biosynthesis.* Annual Review of Plant Biology, 2003. **54**: p. 519-546.

58. Ralph, J., K. Lundquist, G. Brunow, F. Lu, H. Kim, P.F. Schatz, J.M. Marita, R.D. Hatfield, S.A. Ralph, J.H. Christiansen, and W. Boerjan, *Lignins: natural polymers from oxidative*

coupling of 4-hydroxyphenyl-propanoids. Phytochemistry Reviews, 2004. **3**(1-2): p. 29-60.

59. Lawoko, M., G. Henriksson, and G. Gellerstedt, *Structural differences between the lignin-carbohydrate complexes present in wood and in chemical pulps.* Biomacromolecules, 2005. **6**(6): p. 3467-3473.
60. Buranov, A.U. and G. Mazza, *Lignin in straw of herbaceous crops.* Industrial Crops and Products, 2008. **28**(3): p. 237-259.
61. Koshijima, T. and T. Watanabe, *Association between lignin and carbohydrates in wood and other plant tissues*. 2013: Springer Science & Business Media.
62. Weng, J.K. and C. Chapple, *The origin and evolution of lignin biosynthesis.* New Phytologist, 2010. **187**(2): p. 273-285.
63. Grabber, J.H., *How do lignin composition, structure, and cross-linking affect degradability? A review of cell wall model studies.* Crop Science, 2005. **45**(3): p. 820-831.
64. Baucher, M., C. Halpin, M. Petit-Conil, and W. Boerjan, *Lignin: Genetic engineering and impact on pulping.* Critical Reviews in Biochemistry and Molecular Biology, 2003. **38**(4): p. 305-350.
65. Chakar, F.S. and A.J. Ragauskas, *Review of current and future softwood kraft lignin process chemistry.* Industrial Crops and Products, 2004. **20**(2): p. 131-141.
66. Ohgren, K., R. Bura, J. Saddler, and G. Zacchi, *Effect of hemicellulose and lignin removal on enzymatic hydrolysis of steam pretreated corn stover.* Bioresource Technology, 2007. **98**(13): p. 2503-2510.
67. Rencoret, J., G. Marques, A. Gutierrez, D. Ibarra, J. Li, G. Gellerstedt, J.I. Santos, J. Jimenez-Barbero, A.T. Martinez, and J.C. del Rio, *Structural characterization of milled wood lignins from different eucalypt species.* Holzforschung, 2008. **62**(5): p. 514-526.
68. Sun, J.X., X.F. Sun, R.C. Sun, P. Fowler, and M.S. Baird, *Inhomogeneities in the chemical structure of sugarcane bagasse lignin.* J Agric Food Chem, 2003. **51**(23): p. 6719-25.
69. Onnerud, H. and G. Gellerstedt, *Inhomogeneities in the chemical structure of spruce lignin.* Holzforschung, 2003. **57**(2): p. 165-170.

70. Sarkanen, K.V. and C.H. Ludwig, *Lignins: occurrence, formation, structure and reactions*. 1971, New York: Wiley Interscience.

71. Nimz, H.H., D. Robert, O. Faix, and M. Nemr, *Carbon-13 NMR spectra of lignins, 8. Structural differences between lignins of hardwoods, softwoods, grasses and compression wood.* Holzforschung-International Journal of the Biology, Chemistry, Physics and Technology of Wood, 1981. **35**(1): p. 16-26.

72. Lundquist, K. and L. Ericsson, *Acid degradation of lignin III formation of formaldehyde.* Acta Chemica Scandinavica, 1970. **24**: p. 3681-3686.

73. Lundquist, K. and R. Lundgren, *Acid Degradation of Lignin .7. Cleavage of Ether Bonds.* Acta Chemica Scandinavica, 1972. **26**(5): p. 2005-&.

74. Lundquist, K., *Low-molecular weight lignin hydrolysis products.* Applied Polymer Symposia, 1976. **28**: p. 1393-1407.

75. Yasuda, S., K. Adachi, N. Terashima, and K. Ota, *Chemical Structures of Sulfuric-Acid Lignin .8. Reactions of 1,2-Diaryl-1,3-Propanediol and Pinoresinol with Sulfuric-Acid.* Mokuzai Gakkaishi, 1985. **31**(2): p. 125-131.

76. Karlsson, O., K. Lundquist, S. Meuller, and K. Westlid, *On the Acidolytic Cleavage of Arylglycerol Beta-Aryl Ethers.* Acta Chemica Scandinavica Series B-Organic Chemistry and Biochemistry, 1988. **42**(1): p. 48-51.

77. Imai, T., T. Yokoyama, and Y. Matsumoto, *Revisiting the mechanism of beta-O-4 bond cleavage during acidolysis of lignin IV: dependence of acidolysis reaction on the type of acid.* Journal of Wood Science, 2011. **57**(3): p. 219-225.

78. Sturgeon, M.R., S. Kim, K. Lawrence, R.S. Paton, S.C. Chmely, M. Nimlos, T.D. Foust, and G.T. Beckham, *A Mechanistic Investigation of Acid-Catalyzed Cleavage of Aryl-Ether Linkages: Implications for Lignin Depolymerization in Acidic Environments.* Acs Sustainable Chemistry & Engineering, 2014. **2**(3): p. 472-485.

79. Lahive, C.W., P.J. Deuss, C.S. Lancefield, Z.H. Sun, D.B. Cordes, C.M. Young, F. Tran, A.M.Z. Slawin, J.G. de Vries, P.C.J. Kamer, N.J. Westwood, and K. Barta, *Advanced Model Compounds for Understanding Acid-Catalyzed Lignin Depolymerization: Identification of*

Renewable Aromatics and a Lignin-Derived Solvent. Journal of the American Chemical Society, 2016. **138**(28): p. 8900-8911.

80. Lundquist, K. and K. Hedlund, *Acid Degradation of Lignin .5. Degradation Products Related to Phenylcoumaran Type of Structure.* Acta Chemica Scandinavica, 1971. **25**(6): p. 2199-+.

81. Ekman, K.H., *Formaldehyde obtained by alkaline hydrolysis of wood and lignin.* Tappi, 1965. **48**: p. 398.

82. Santos, R.B., P.W. Hart, H. Jameel, and H.M. Chang, *Wood Based Lignin Reactions Important to the Biorefinery and Pulp and Paper Industries.* Bioresources, 2013. **8**(1): p. 1456-1477.

83. Wikberg, H., *Advanced solid state NMR spectroscopic techniques in the study of thermally modified wood*. 2005: Hanne Wikberg.

84. Chiang, V.L. and M. Funaoka, *The formation and quantity of diphenylmethane type structures in residual lignin during kraft delignification of Douglas-fir.* Holzforschung, 1988. **42**: p. 385-391.

85. Ahvazi, B.C., G. Pageau, and D.S. Argyropoulos, *On the formation of diphenylmethane structures in lignin under kraft, EMCC®, and soda pulping conditions.* Canadian journal of chemistry, 1998. **76**(5): p. 506-512.

86. Gellerstedt, G. and D. Robert, *Quantitative 13C NMR analysis of kraft lignins.* Acta Chem. Scand. B, 1987. **41**(7): p. 541-546.

87. Brosse, N., R. El Hage, M. Chaouch, M. Pétrissans, S. Dumarçay, and P. Gérardin, *Investigation of the chemical modifications of beech wood lignin during heat treatment.* Polymer Degradation and Stability, 2010. **95**(9): p. 1721-1726.

88. Balakshin, M.Y., E.A. Capanema, C.L. Chen, and H.S. Gracz, *Elucidation of the structures of residual and dissolved pine kraft lignins using an HMQC NMR technique.* Journal of agricultural and food chemistry, 2003. **51**(21): p. 6116-6127.

89. Alén, R., *Structure and chemical composition of wood*, in *Forest products chemistry*, P. Stenius, Editor. 2000, Fapet Oy.

90. W.E.Hillis, *Distribution, properties and formation of some wood extractives.* Wood science and technology, 1971. **5**: p. 272-289.

91. Stanley, R.G., *Extractives of wood, bark and needles of the Southern pines: a review.* For. Prod. J, 1959. **19**(11): p. 50-56.

92. Ucar, G. and M.B. Ucar, *The Estimation of Acidic Behavior of Wood by Treatment with Aqueous Na2HPO4 Solution.* Journal of Analytical Methods in Chemistry, 2012.

93. Pettersen, R.C., *The chemical composition of wood*, in *The chemical composition of wood*, R. Rowell, Editor. 1984. p. 68-74.

94. Fengel. D. and W. G., *Extractives*, in *Wood chemistry, ultrastructure, reactions*. 1983, Kessel Verlag: Remagen. p. 182.

95. Demirbas, A., *Chemicals from Forest Products by Efficient Extraction Methods.* Fuel Science & Technology International, 1994. **12**(3): p. 417-431.

96. Maldas, D.C. and D.P. Kamdem, *Wettability of extracted southern pine.* Forest Products Journal, 1999. **49**(11-12): p. 91-93.

97. Burnes, T.A., R.A. Blanchette, and R.L. Farrell, *Bacterial biodegradation of extractives and patterns of bordered pit membrane attack in pine wood.* Applied and Environmental Microbiology, 2000. **66**(12): p. 5201-5205.

98. Shebani, A.N., A.J. van Reenen, and M. Meincken, *The effect of wood extractives on the thermal stability of different wood species.* Thermochimica Acta, 2008. **471**(1-2): p. 43-50.

99. W.E.Hillis, *Wood extractives and their significance to the pulp and paper industries*. 2014: Academic Press.

100. Silverio, F.O., L.C.A. Barbosa, C.R.A. Maltha, P.H. Fidencio, M.P. Cruz, D.P. Veloso, and A.F. Milanez, *Effect of storage time on the composition and content of wood extractives in Eucalyptus cultivated in Brazil.* Bioresource Technology, 2008. **99**(11): p. 4878-4886.

101. Gutierrez, A., J.C. del Rio, F.J. Gonzalez-Vila, and J. Romero, *Variation in the composition of wood extractives from Eucalyptus globulus during seasoning.* Journal of Wood Chemistry and Technology, 1998. **18**(4): p. 439-446.

102. Tasooji, M., G. Wan, G. Lewis, H. Wise, and C.E. Frazier, *Biogenic formaldehyde: Content and heat generation in the wood of three tree species.* **Chapter 3** in this dissertation.

103. Kalisch, J.H., *Alkali-formaldehyde pretreatment of coniferous woods in sulphite pulping.* Pulp Pap Mag Can, 1969. **21**: p. 55-68.

104. Lelis, R., E. Roffael, and G. Becker, *Zum Verhalten von Splint-und Kernholz der Kiefer bei der Verleimung mit Diisocyanat-Klebstoffen (PMDI).* Holz Zentralblatt, 1992. **134**: p. 2204-2210.

105. H., S. and R. E, *Untersuchungen der Schälfurnier-Eignung von in Deutschland erwachsenem Douglasienholz.* Holz Roh Werkst, 1993. **51**: p. 167-176.

106. Dix, B. and E. Roffael, *Einfluß der Verkernung und des Baumalters auf die Eigenschaften von Spanplatten aus Kiefernholz (Pinus sylvestris) Teil 1: Kernholz und seine Eigenschaften.* Holz als Roh-und Werkstoff, 1997. **55**(1): p. 25-33.

107. Buyuksari, U., N. Ayrilmis, E. Avci, and E. Koc, *Evaluation of the physical, mechanical properties and formaldehyde emission of particleboard manufactured from waste stone pine (Pinus pinea L.) cones.* Bioresource Technology, 2010. **101**(1): p. 255-259.

108. Hoong, Y.B., M.T. Paridah, Y.F. Loh, M.P. Koh, C.A. Luqman, and A. Zaidon, *Acacia mangium Tannin as Formaldehyde Scavenger for Low Molecular Weight Phenol-Formaldehyde Resin in Bonding Tropical Plywood.* Journal of Adhesion Science and Technology, 2010. **24**(8-10): p. 1653-1664.

109. Hon, D.N.S., *Chemical modification of lignocellulosic materials*. 1995: CRC Press.

110. Rowell, R.M. *Chemical modification of wood: Advantages and disadvantages*. 1975. American Wood-Preservers' Association.

111. Nicholas, D.D., *Wood deterioration and its prevention by preservative treatments: Degradation and Protection of Wood*. Vol. 1. 1982: Syracuse University Press.

112. Warner, J.E. and K.R. Solomon, *Acidity as a Factor in Leaching of Copper, Chromium and Arsenic from Cca-Treated Dimension Lumber.* Environmental Toxicology and Chemistry, 1990. **9**(11): p. 1331-1337.

113. Tjeerdsma, B.F., M. Boonstra, A. Pizzi, P. Tekely, and H. Militz, *Characterisation of thermally modified wood: molecular reasons for wood performance improvement.* Holz als Roh-und Werkstoff, 1998. **56**(3): p. 149-153.

114. Weiland, J.J. and R. Guyonnet, *Study of chemical modifications and fungi degradation of thermally modified wood using DRIFT spectroscopy.* Holz Als Roh-Und Werkstoff, 2003. **61**(3): p. 216-220.

115. Mazela, B., R. Zakrzewski, W. Grześkowiak, G. Cofta, and M. Bartkowiak, *Resistance of thermally modified wood to basidiomycetes.* Electronic Journal of Polish Agricultural Universities, 2004. **7**(1): p. 1505-0297.

116. Militz, H. *Heat treatment of wood: European processes and their background*. in *Enhancing the durability of lumber and engineered wood products*. 2002. Kissimmee, FL. Madison, WI: Forest products society.

117. Kocaefe, D., S. Poncsak, and Y. Boluk, *Effect of thermal treatment on the chemical composition and mechanical properties of birch and aspen.* BioResources, 2008. **3**(2): p. 517-537.

118. Hakkou, M., M. Petrissans, A. Zoulalian, and P. Gerardin, *Investigation of wood wettability changes during heat treatment on the basis of chemical analysis.* Polymer Degradation and Stability, 2005. **89**(1): p. 1-5.

119. Rodrigo Marques de Oliveira, A.B., Almir Sales, Débora Gonçalves, *Wettability, shrinkage and color changes of Araucaria angustifolia after heating treatment.* Materials Research, 2010. **13**(3): p. 351-354.

120. F. C. Beall and H. W. Eickner, *Thermal degradation of wood components: a review of the literature*. 1970: Ft. Belvoir Defence Technical Information Center.

121. Singh, A., K. Das, and D. Sharma, *Integrated process for production of xylose, furfural, and glucose from bagasse by two-step acid hydrolysis.* Ind. Eng. Chem. Prod. Dev., 1984. **23**: p. 257-262.

122. Rowell, R., S. Lange, J. McSweeny, and M. Davis. *Modification of wood fiber using steam*. in *The 6th Pacific Tim Bio-based composites symposium. Workshop on the chemical modification of cellulosics*. 2002. Portland, Oregon, USA.

123. Salmén, L., *Viscoelastic properties of in situ lignin under water-saturated conditions.* Journal of Materials science, 1984. **19**(9): p. 3090-3096.

124. Furuta, Y., Y. Obata, and K. Kanayama, *Thermal-softening properties of water-swollen wood: The relaxation process due to water soluble polysaccharides.* Journal of Materials Science, 2001. **36**(4): p. 887-890.

125. Furuta, Y., M. Nakajima, E. Nakanii, and M. Ohkoshi, *The Effects of Lignin and Hemicellulose on Thermal-Softening Properties of Water-Swollen Wood.* Mokuzai Gakkaishi, 2010. **56**(3): p. 132-138.

126. Kim, J.Y., H. Hwang, S. Oh, Y.S. Kim, U.J. Kim, and J.W. Choi, *Investigation of structural modification and thermal characteristics of lignin after heat treatment.* International Journal of Biological Macromolecules, 2014. **66**: p. 57-65.

127. Windeisen, E., C. Strobel, and G. Wegener, *Chemical changes during the production of thermo-treated beech wood.* Wood Science and Technology, 2007. **41**(6): p. 523-536.

128. Wikberg, H. and S.L. Maunu, *Characterisation of thermally modified hard-and softwoods by 13 C CPMAS NMR.* Carbohydrate Polymers, 2004. **58**(4): p. 461-466.

129. Boonstra, M.J. and B. Tjeerdsma, *Chemical analysis of heat treated softwoods.* Holz Als Roh-Und Werkstoff, 2006. **64**(3): p. 204-211.

130. Kollmann, F. and D. Fengel., *Changes in the chemical composition of wood by thermal treatment.* Howl als Roh- und Werkstoff 1965. **23**(12): p. 461-468.

131. Fengel, D. and G. Wegener., *Wood: chemistry, ultrastructure, reactions*. 1984: Walter de Gruyter.

132. LeVan, S., R.J. Ross, and J.E. Winandy, *Effects of fire retardant chemicals on the bending properties of wood at elevated temperatures*. 1990, Madison, WI, USA: US Department of Agriculture, Forest Service, Forest Products Laboratory.

133. Mburu, F., S. Dumarcay, F. Huber, M. Petrissans, and P. Gerardin, *Evaluation of thermally modified Grevillea robusta heartwood as an alternative to shortage of wood resource in Kenya: Characterisation of physicochemical properties and improvement of bio-resistance.* Bioresource Technology, 2007. **98**(18): p. 3478-3486.

134. Esteves, B.M. and H.M. Pereira, *Wood Modification by Heat Treatment: A Review.* Bioresources, 2009. **4**(1): p. 370-404.

135. Gonzalez-Pena, M.M., S.F. Curling, and M.D.C. Hale, *On the effect of heat on the chemical composition and dimensions of thermally-modified wood.* Polymer Degradation and Stability, 2009. **94**(12): p. 2184-2193.

136. Ramiah, M.V., *Thermogravimetric and differential thermal analysis of cellulose, hemicellulose, and lignin.* J. Appl. Polym. Sci, 1970. **14**: p. 1323-1337.

137. Lapierre, C., B. Monties, and C. Rolando, *Thioacidolysis of Lignin - Comparison with Acidolysis.* Journal of Wood Chemistry and Technology, 1985. **5**(2): p. 277-292.

138. Rolando, C., B. Monties, and C. Lapierre, *Thioacidolysis*, in *Methods in lignin chemistry*. 1992, Springer Berlin Heidelberg. p. 334-349.

139. Lu, F.C. and J. Ralph, *Derivatization followed by reductive cleavage (DFRC method), a new method for lignin analysis: Protocol for analysis of DFRC monomers.* Journal of Agricultural and Food Chemistry, 1997. **45**(7): p. 2590-2592.

140. Assor, C., V. Placet, B. Chabbert, A. Habrant, C. Lapierre, B. Pollet, and P. Perre, *Concomitant Changes in Viscoelastic Properties and Amorphous Polymers during the Hydrothermal Treatment of Hardwood and Softwood.* Journal of Agricultural and Food Chemistry, 2009. **57**(15): p. 6830-6837.

141. Brosse, N., R. El Hage, M. Chaouch, M. Petrissans, S. Dumarcay, and P. Gerardin, *Investigation of the chemical modifications of beech wood lignin during heat treatment.* Polymer Degradation and Stability, 2010. **95**(9): p. 1721-1726.

142. Sherrard, E.C. and E.E. Harris, *Factors influencing properties of isolated wood lignin.* Ind. Eng. Chem, 1932. **24**(1): p. 103-106.

143. Ritter, G.J., R.L. Mitchell, and R.M. Seborg, *Some factors that influence the conversion of cellulosic materials to sugar.* J. Am. Chem. Soc, 1933. **55**(7): p. 2989-2991.

144. (NREL), N.R.E.L., *Determination of structural carbohydrates and lignin in biomass*. 2007.

145. Lapierre, C., B. Monties, C. Rolando, and L.D. Chirale, *Thioacidolysis of lignin: comparison with acidolysis.* Journal of wood chemistry and technology, 1985. **5**(2): p. 277-292.

146. Lapierre, C., B. Pollet, B. Monties, and C. Rolando, *Thioacidolysis of spruce lignin: GC-MS analysis of the main dimers recovered after Raney nickel desulphuration.* Holzforschung-International Journal of the Biology, Chemistry, Physics and Technology of Wood, 1991. **45**(1): p. 61-68.

147. *Ethanethiol*. Available from: http://en.wikipedia.org/wiki/Ethanethiol#Odor.

148. Lu, F. and J. Ralph, *The DFRC Method for Lignin Analysis. 2. Monomers from Isolated Lignins.* J Agric Food Chem, 1998. **46**(2): p. 547-552.

149. Holtman, K.M., H.M. Chang, H. Jameel, and J.F. Kadla, *Elucidation of lignin structure through degradative methods: Comparison of modified DFRC and thioacidolysis.* Journal of Agricultural and Food Chemistry, 2003. **51**(12): p. 3535-3540.

150. Lu, F.C. and J. Ralph, *Detection and determination of p-coumaroylated units in lignins.* Journal of Agricultural and Food Chemistry, 1999. **47**(5): p. 1988-1992.

151. Placet, V., J. Passard, and P. Perré, *Viscoelastic properties of green wood across the grain measured by harmonic tests in the range 0-95C : hardwood vs. softwood and normal wood vs. reaction wood.* Holzforschung, 2007. **61**(5): p. 548-557.

152. Chowdhury, S., J. Fabiyi, and C.E. Frazier, *Advancing the dynamic mechanical analysis of biomass: comparison of tensile-torsion and compressive-torsion wood DMA.* Holzforschung, 2010. **64**(6): p. 747-756.

153. Chowdhury, S. and C.E. Frazier, *Compressive-torsion DMA of yellow-poplar wood in organic media.* Holzforschung, 2013. **67**(2): p. 161-168.

154. Chowdhury, S. and C.E. Frazier, *Thermorheological complexity and fragility in plasticized lignocellulose.* Biomacromolecules, 2013. **14**(4): p. 1166-73.

155. Olsson, A.M. and L. Salmén, *The effect of lignin composition on the viscoelastic properties of wood.* Nordic Pulp and Paper Research Journal, 1997. **12**(3): p. 140-144.

156. Stelte, W., C. Clemons, J.K. Holm, J. Ahrenfeldt, U.B. Henriksen, and A.R. Sanadi, *Fuel pellets from wheat straw: The effect of lignin glass transition and surface waxes on pelletizing properties.* BioEnergy Research, 2012. **5**(2): p. 450-458.

157. Kelley, S.S., T.G. Rials, and W.G. Glasser, *Relaxation Behavior of the Amorphous Components of Wood.* Journal of Materials Science, 1987. **22**(2): p. 617-624.

158. Mansfield, S.D., H. Kim, F. Lu, and J. Ralph, *Whole plant cell wall characterization using solution-state 2D NMR.* Nat Protoc, 2012. **7**(9): p. 1579-89.

159. Ralph, J., J.M. Marita, R. S.A., R.D. Hatfield, L. F., E. RM., P. J., S. Quideau, R.F. Helm, and J.H. Grabber, *Solution-state NMR of lignins*, in *Advances in lignocellulosics characterization*, D.S. Argyropoulos, Editor. 1999, TAPPI Press: Atlanta, GA. p. 55-108.

160. Kim, H., J. Ralph, T. Akiyama, and Chicago, *Solution-state 2D NMR of ball-milled plant cell wall gels in DMSO-d 6.* BioEnergy Research, 2008. **1**(1): p. 56-66.

161. Kim, H. and J. Ralph, *Solution-state 2D NMR of ball-milled plant cell wall gels in DMSO-d6/pyridine-d5.* Organic & biomolecular chemistry, 2010. **8**(3): p. 576-591.

162. Yelle, D.J., J. Ralph, and C.R. Frihart, *Characterization of nonderivatized plant cell walls using high-resolution solution-state NMR spectroscopy.* Magnetic Resonance in Chemistry, 2008. **46**(6): p. 508-517.

163. Del Río, J.C., J. Rencoret, P. Prinsen, A.T. Martínez, J. Ralph, and A. Gutiérrez, *Structural characterization of wheat straw lignin as revealed by analytical pyrolysis, 2D-NMR, and reductive cleavage methods.* Journal of agricultural and food chemistry, 2012. **60**(23): p. 5922-5935.

164. Capanema, E.A., M.Y. Balakshin, C.L. Chen, J.S. Gratzl, and H. Gracz, *Structural analysis of residual and technical lignins by 1H-13C correlation 2D NMR-spectroscopy.* Holzforschung, 2001. **55**(5): p. 302-308.

165. Sette, M., H. Lange, and C. Crestini, *Quantitative HSQC Analyses of Lignin: A Practical Comparison.* Comput Struct Biotechnol J, 2013. **6**: p. e201303016.

166. Heikkinen, H., T. Elder, H. Maaheimo, S. Rovio, J. Rahikainen, K. Kruus, and T. Tamminen, *Impact of steam explosion on the wheat straw lignin structure studied by solution-state nuclear magnetic resonance and density functional methods.* J Agric Food Chem, 2014. **62**(43): p. 10437-44.

167. Yuan, T.Q., S.N. Sun, F. Xu, and R.C. Sun, *Characterization of lignin structures and lignin–carbohydrate complex (LCC) linkages by quantitative 13C and 2D HSQC NMR spectroscopy.* Journal of agricultural and food chemistry, 2011. **59**(19): p. 10604-0614.

Chapter 2 Method for measuring formaldehyde emission of wood using a micro chamber

Guigui Wan, Christa Stables, and Charles E. Frazier

Macromolecular Science & Engineering, Sustainable Biomaterials

Virginia Tech, Blacksburg VA 24061, U.S.A

Attribution

For the work described here the formaldehyde emissions chamber and associated hardware was established by Christa Stables. Formaldehyde emissions measurements on wood were conducted by Guigui Wan. Heather Wise did the lab air measurements.

2.1. Abstract

A 12 liter micro chamber was established for measuring formaldehyde (CH_2O) emissions from 4 Virginia pine trees, FB1, FB2, NC1 and NC2. FB1 emitted the highest amount of CH_2O among the trees studied, possibly due to the different storage conditions. Emissions from the trees FB2, NC1 and NC2 were also significantly different although they had similar preparation history, indicating natural variation in CH_2O emission. Heat treatment at 200°C (or 120°C) for 1 h increased CH_2O emission, but sequential heating (up to 6 hours) decreased it. Ammonium chloride (NH_4Cl) pretreatment led to higher emission compared to specimens without pretreatment but experienced the same heat treatment (200°C, 1 h), which contradicted to the CH_2O generation from NH_4Cl pretreated flakes (200°C, 10 min). Flakes with low emission rate tended to have higher emissions after being stored in the open laboratory for a period of time, and flakes with high initial emission rate had lower emissions. Monitoring CH_2O content in the laboratory environment over a 4 month period indicated that air contained a small amount of CH_2O, even lower than CH_2O content in the ultrapure N_2 carrier gas used in the emissions chamber.

2.2. Introduction

There are numerous standard methods used to measure formaldehyde emissions from wood-based composites, as established by different countries around the world. [1] The methods vary in scale and methodology, but most require carefully controlled temperature, relative humidity, sample preconditioning before testing, chamber loading (specimen mass/unit volume), and sometimes prescribed ventilation rates. Large environmental chambers are used in the United States (ASTM E1333-2002), Europe (EN717-1) and Asia to sample full size composite specimens on the order of 2.5 m in dimension. The principal benefit of such large scale sampling is to accommodate emissions variations that are observed in smaller specimens sampled from a single composite panel. Large chamber methods are costly and time consuming, therefore requiring considerable infrastructure. [2] Large and smaller scale chambers prescribe chamber ventilation where the air exiting the chamber is passed through water-filled impingers that collect formaldehyde for subsequent quantification. While certification requirements often demand these ventilated chamber methods, there are a number of smaller scale methods used for quality control screening and which may be correlated to ventilated chambers. Desiccator methods are common as for ASTM D5582, and Japanese standard JIS A 1460 and JAS 233, where a prescribed number of small specimens are placed into a desiccator (~10 liter volume) with a vessel of water that absorbs emitted formaldehyde. The formaldehyde released from the test pieces at fixed temperature, relative humidity and time is absorbed by the water and determined photometrically. [3] Dramatically different is the perforator method (EN 120), which is widely used in Europe. It is believed to measure a very important board emission characteristic, which is free, extractable formaldehyde content. Small specimens are boiled in toluene, which condenses and passes through a water solution that strips the formaldehyde from the toluene. [4] Alternatively, the flask method measures formaldehyde release from small specimens over water in a closed container at a constant temperature. The flask method is simple and effective for screening purposes and also particularly suitable for teaching and demonstration purposes. [1]

There are a variety of analytical methods used to quantify formaldehyde, but only the most common techniques are mentioned here. Formaldehyde analysis using colorimetry has evolved extensively since Bonnet studied the characteristic color reactions between formaldehyde and certain alkaloids more than 100 years ago. [5] Later on, Hanzlik and Collins reacted a series of standard formaldehyde solutions with phloroglucinol to form a gradation of colors from pink to deep red, which can be used for color matching developed from samples with unknown formaldehyde concentration. [6, 7] In 1937, Eegriwe first employed chromotropic acid for detecting formaldehyde. [8] During the 1940s and 1950s, the emergence of well-developed chromatography instrumentation greatly improved the accuracy and detection limits of formaldehyde quantitation. Chromatographic formaldehyde determinations are free from interference since all the reaction products are resolved, typically using liquid chromatography. Here the most common analytical reagent is 2,4-dinitrophenylhydrazine (DNPH). The DNPH formaldehyde determination is widely considered to be the most reliable and authoritative. However, a non-chromatographic method using 2,4-pentanedione (acetyl acetone, AcAc) has been shown as equivalent to DNPH methods. [9]

First described by Nash, [10] the AcAc method employs the Hantzsch reaction as shown in Figure 2.1. The reaction product is diacetyldihydrolutidine (DDL), which is fluorescent; and the fluorometric detection of DDL is about 10 times more sensitive than the corresponding colorimetric (UV) determination. [11] The Hantzsch reaction is highly specific to formaldehyde. [12] More importantly the formaldehyde reaction product, DDL, is strongly fluorescent whereas the Hantzsch reaction with other aldehydes gives rise to weakly or non-fluorescent products. [12]

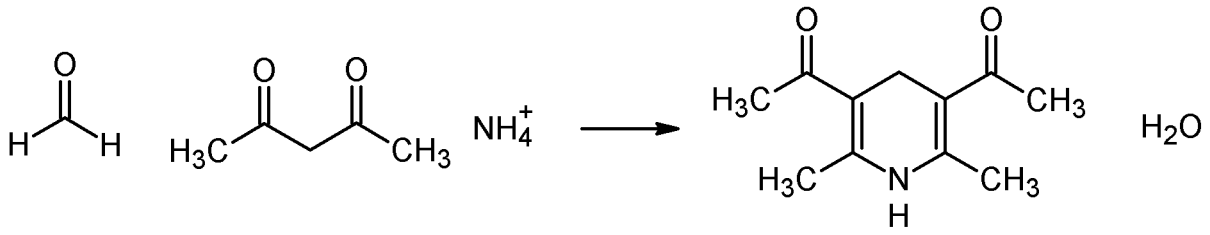

Figure 2.1. Hantzsch reaction, formaldehyde reacted with acetylacetone and ammonium into diacetyldihydrolutidine (DDL), which can be detected and quantified using fluorometer. [10]

The objective of this work was to measure natural biogenic formaldehyde that forms within, and is emitted from, wood. The desire was to measure biogenic formaldehyde emissions under pseudo-equilibrium conditions in a ventilated chamber. Since standardized ventilated chambers are quite expensive, a cheaper and simpler custom chamber was devised using a 12 liter jacketed glass reactor. The principal experimental variables were variations among different trees within one tree species, and also the effects of wood heating.

2.3. Materials and methods

Four 70-80 year old Virginia pine (*Pinus virginiana*) trees were harvested from the Blacksburg, VA area. Two trees, named FB1 and FB2, came from Virginia Tech's Fishburn Forest, a 1,300 acre teaching and demonstration forest adjacent to campus. Tree NC1 and NC2, were harvested from a region (~4 ha) near Blacksburg, VA, the Nellie's Cave area. Stem sections (~15 cm thick) were cut from locations that were ~1.2 m above ground. Except FB1, fresh sections of FB2 NC1 and NC2 were immediately processed in flakes (80×80×80-100 mm, tan.×long.×rad.) by slicing the tangential face using a rotary flaker with the thin dimension in the radial direction. The first 20 years of juvenile tissue was excluded. Flakes were stored in the open laboratory at room temperature. The first emission measurement for these three trees was taken within 1-2 weeks after harvest. For FB1, tree stems were frozen for ~16 months, then thawed, air dried, and immersed into distilled water for 3 days, then flakes were prepared as above. The first measurement for FB1 was taken ~20 months after harvest. Within each tree, flakes were randomized and placed into a custom aluminum rack (Figure 2.2 (left), 46x7.5x7.5 cm, length×width×depth) with 110 slots, dry mass of loaded flakes ranging from 130 g to 150 g. Only FB1 contained significant amounts of compression wood.

Specimen pretreatment and heat treatment

Prior to heating, flakes were subjected to pretreatments: 1) control, no treatment, 2) dipped in 10 mM acid (NH_4Cl) for 1 sec, and air dried. Flakes were loaded into flake tray and heated at 200°C or 120°C for 1 h, then subjected to sequential heating up to 6 hours. Specimens were identified with respect tree name, pretreatments, heating temperature and

heating time, i.e. NC2 200°C-1h, FB1 200°C-6h or NC2 Acid/200°C-1h. Specimens with no heat treatments were referred as NC1, NC2, FB1 and FB2.

Gas Emission Chamber

CH_2O emissions chamber (Figure 2.2, (right)) was composed of a 12 liter glass chamber (58 cm in height) and a three-neck glass cap with ground joints. Fixed to the chamber lid was a small fan, pointed downwards into the chamber body, that ensured turbulent flow within the chamber. The chamber temperature was set at 25°C, controlled by a water-circulating jacket around the outside chamber wall with aid of a thermo-couple. Ultra-high purity nitrogen (N_2, purity > 99.999%) was adjusted to 1000 ml/min through a purge rotameter and blew into a relative humidity generator (VTI RH200), then directed into the chamber to generate a 50% relative humidity environment. N_2 carried out CH_2O from the chamber and bubbled into two impingers (25 ml) containing 20 ml water, front and back for 1 hour. After 1 hour gas sampling, the water volume in each impinger was measured and denoted as V_{front} and V_{back}. Impingers are available with standard nozzles (open tip) or special nozzles (fritted tip, 170 to 200 μm glass frit).

Figure 2.2. Left: a custom aluminum flake tray with 110 flakes loaded in the slots. Right: gas emissions chamber (center), with the controlled temperature circulator (left), and the RH generator (right).

Background CH_2O measurement was taken after ~24 hours equilibrium, while emission from wood flakes started after at least 48 hours equilibrium in the well-conditioned chamber. For heat treatment, loaded flake tray was heated in oven, then cooled to room temperature for

~30 min, and immediately inserted into chamber and equilibrated for at least 48 hours before emission measurements.

The chamber was thoroughly cleaned and dried under two general circumstances: 1) switching to a new N_2 tank; 2) switching to new flake specimens. Background formaldehyde was measured from each gas tank (without specimens), and subtracted from actual measurements of wood flakes.

Calibration and CH_2O measurement

A CH_2O batch solution was made by diluting standard 37wt% formaldehyde solution (0.5 ml) with HPLC water into 1 L flask, standardized to determine exact concentration, then further diluted into a series of CH_2O solutions. These CH_2O solutions (4 ml) was mixed with 4 ml AcAc solution (150 g ammonium acetate, 2 ml acetyl acetone and 3 ml acetic acid), and reacted in 60°C water bath for 10 min, and finally subjected to fluorimeter measurement at 35°C. Fluorimeter setting: excitation wavelength at 410 nm, emission scan from 470 nm to 530 nm, emission and excitation slits at 10 nm and scan speed 200 nm/min. The emission intensity from 505 nm to 515 nm was averaged and used to generate the calibration curve with plotting CH_2O in μg as X axis and intensity as Y axis. Calibration was done on monthly basis to ensure experimental accuracy. AcAc solution was stored in amber bottle at 10°C, and refreshed on monthly basis.

For CH_2O samples in front and back impingers, 4 ml CH_2O solution was mixed with 4 ml AcAc solution and repeated the above step. Fluorescence intensity was referred as $Intensity_{front}$ and $Intensity_{back}$, and CH_2O emission was calculated in μg/L according to following equation:

$$CH2O\ emission = \frac{\frac{Intensity_{front}}{Slope(\mu g^{-1})} \times \frac{V_{front}(ml)}{4ml} + \frac{Intensity_{back}}{Slope\ (\mu g^{-1})} \times \frac{V_{back}(ml)}{4ml}}{1000ml/min \times 60min}$$

With known dry flake mass (g), CH_2O emission in μg/L can be converted into μg/m^3 g.

CH_2O in open lab environment was collected by pumping the air through two sequentially set front and back water-containing impingers at ~1000 ml/min air flow rate for 60 min. And CH_2O content was quantified as described above in μg/L.

2.4. Results and discussions

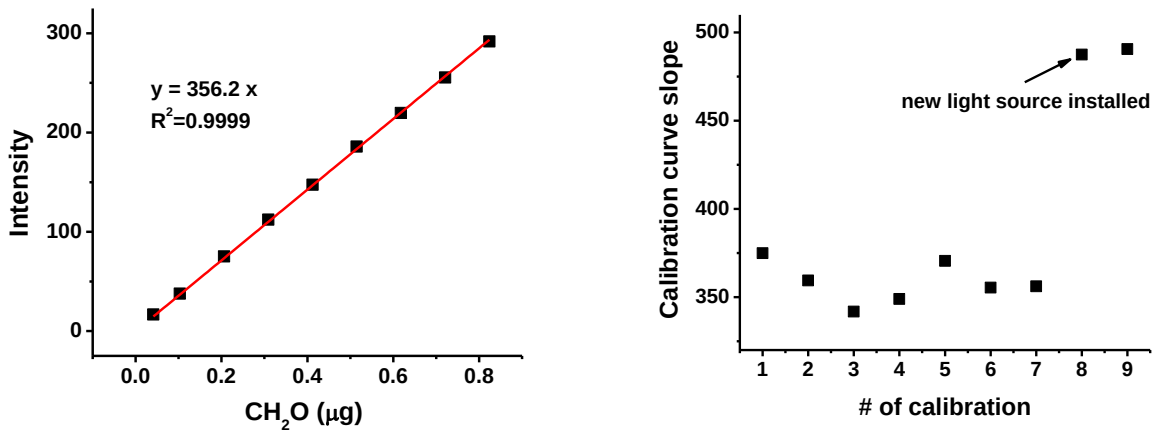

Figure 2.3. Left: one example curve for the fluorimeter calibration. Right: curve slopes for multiple calibrations in an 8-month period. Time elapsed between two calibrations was roughly 4 weeks. A new light source was installed just before the # 8 calibration.

Figure 2.3 demonstrated an example curve for fluorimeter calibration (left), and also curve slopes for multiple calibrations in an 8-month period (right). Time elapsed between two calibrations was roughly 4 weeks. Calculations for testing wood specimens were based on the most up-to-date calibration. Variation between two calibrations ranged from 4% to 6%, which may due to: 1) instrument sensitivity fluctuation, i.e. light source; 2) operational variation from the experimenter. By increasing the frequency for instrument calibration may compensate the intensity fluctuation from the instrument itself, but it does not affect operational variation from the experimenter. So we made an arbitrary decision to conduct instrument calibration on a monthly basis, and the 4% to 6% variation was accepted. Under the following circumstances, the instrument calibration must be repeated to ensure the analytical accuracy: 1) instrument maintenance or repair; 2) variation between two sequential calibrations is more than 6%; 3) any noticeable signal abnormality. For example, in Figure 2.3 (right), due to the replacement of

a new light source, the instrument calibration was conducted. This replacement was reflected by a sudden increase of calibration curve slope. In other word, the light source replacement led to the increase of instrument sensitivity.

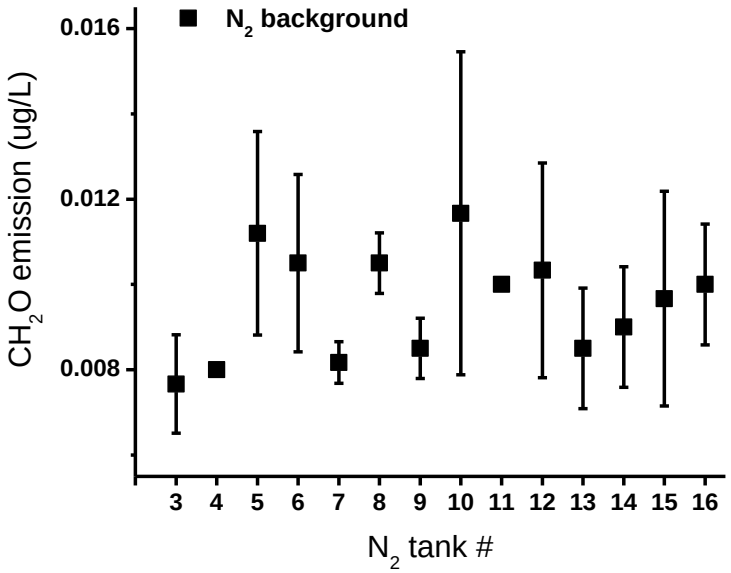

Figure 2.4. Background CH_2O from nitrogen tanks, number of measurements for each tank n ≥ 3.

As for carrier gas, house air was used initially, but abandoned because of significant CH_2O contamination. Ultra-pure N_2 was used instead. And tank-specific background CH_2O content was monitored and shown in Figure 2.4. Clearly, carrier gas contained CH_2O, but in a relatively consistent manner. All the flake emission measurements below were corrected by tank-specific CH_2O background.

Water-containing impingers were used to absorb the gaseous CH_2O. Impingers with different tip types may have different absorbance efficiency. Tables 2.1 summarized the emissions measurement for both tank background and FB1 flake using impingers with different tip types, fritted tip and open tip. No significant difference was observed for FB1, but tip type appeared to have some impact on background measurements, therefore following CH_2O emission measurements were all conducted using impingers with fritted tips.

Figure 2.5 summarizes the CH_2O emissions from never-heated Virginia pine, FB1, FB2, NC1 and NC2. Among all four trees, FB1 emitted the highest CH_2O. This may due to the ~16 month storage in freezer or substantial amount of compression wood it contained. To make a valid comparison, FB2, NC1 and NC2 were chosen. Clearly, even within the same species, CH_2O emissions varied significantly among different trees. Specimen equilibrated in chamber for at least 48 hours before first measurements, and the following 3-6 measurements occurred within 1-3 days.

Table 2.1. Averaged background and flake emissions measurements using fritted tipped and open tipped impingers over 3 measurements. Standard deviations in parentheses.

CH_2O (μg/L)	Fritted tip	Open tip
Background (tank 2)	0.012 (0.001)	0.010 (0.001)
FB1 (tank 3)	0.037 (0.002)	0.038 (0)

It has been well known that heat treatments promote biogenic CH_2O generation, [13-17] and it possibly leads to a higher emission. Figure 2.6 and Figure 2.7 featured how sequential heating (120°C and 200°C) affected CH_2O emission from FB1. After first 1 hour heating, CH_2O emission increased significantly, probably because part of the heat-generated CH_2O remained in the wood, released into chamber later and increased the emission. However, the sequential 1 hour heating (2 hour and more) led to decreased CH_2O emission.

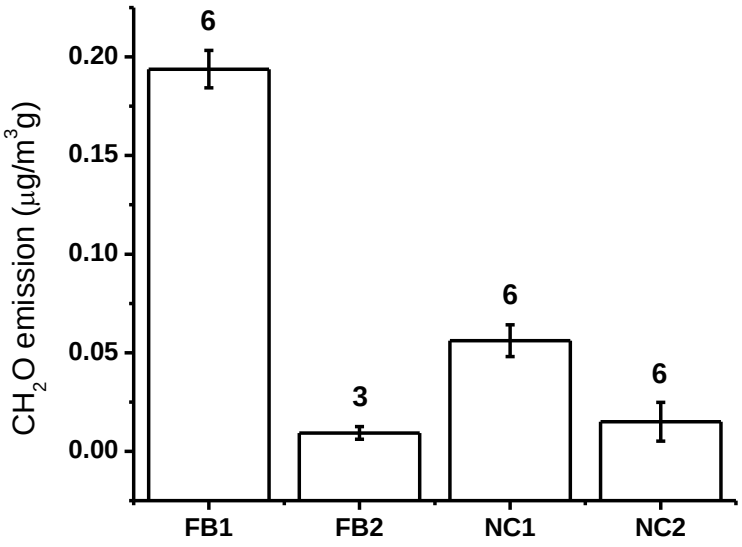

Figure 2.5. Formaldehyde emissions from never-heated Virginia pines, FB1, FB2, NC1 and NC2. Error bars = ± 1 standard deviation. Numbers above columns are number of measurements.

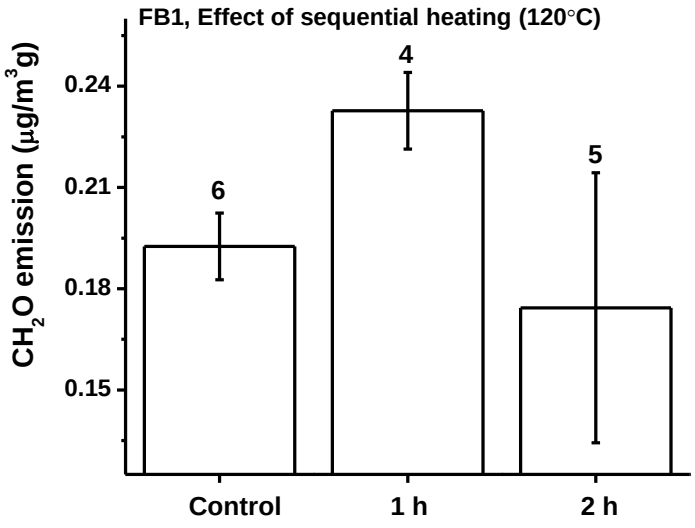

Figure 2.6. Formaldehyde emissions from FB1 (control, never-heated) flakes, and sequentially heated FB1 flakes at 120°C for 1 hour and 2 hours. Error bar = ± 1 standard deviation. Numbers above columns are number of measurements.

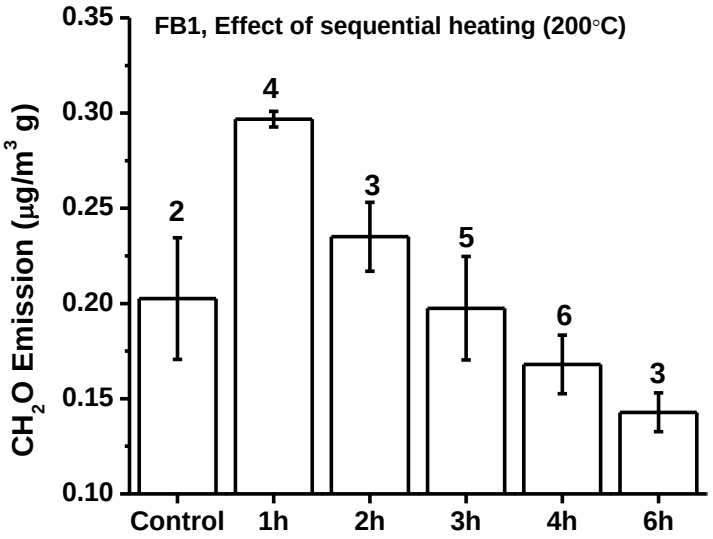

Figure 2.7. Formaldehyde emissions from FB1 control (never-heated) flakes, heated FB1 flakes after sequential heating at 200°C up to 6 hours. Error bar = ± 1 standard deviation. Numbers above columns are number of measurements.

Ammonium salts (NH_4Cl or $(NH_4)_2SO_4$) are used to catalyze urea-formaldehyde resins where the CH_2O/NH_3 reaction releases strong acids, HCl or H_2SO_4 that catalyzes resin cure. [18] It has been known that strong acid can catalyze in situ lignin degradation and result in higher CH_2O generation from wood. [19-24] Our previous study revealed that NH_4Cl pretreatment didn't lead to higher CH_2O generation once heated at 200°C for 10 min, which probably due to the scavenging effect of ammonium. [25] And the scavenging product, hexamethylenetetramine is very stable under AcAc reaction condition (60°C, 10 min), meaning no decomposition into CH_2O and interference with the measurement. [10] Figure 2.8 revealed that NH_4Cl pretreatment increased CH_2O emission from wood flakes compared to specimens with no pretreatment but experienced the same heat treatment (200°C for 60 min). CH_2O emission can not be reflected simply by CH_2O generation. Emission is a much more complex phenomenon. Moreover emission was measured at 50% relative humidity, while CH_2O generation was quantified in a water saturation condition. This different testing environment

may possibly influence CH_2O release from wood, [26] leading to the opposite trend on CH_2O emission observed in Figure 2.8.

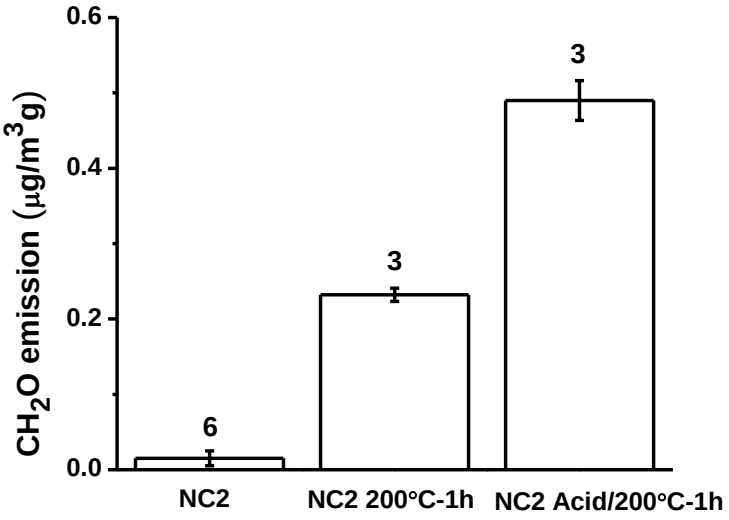

Figure 2.8. The effect of NH_4Cl pretreatment on CH_2O emissions from heated NC2 wood flakes (200°C, 1 h). Error bar = ± 1 standard deviation. Numbers above columns are number of measurements.

Figure 2.9 summarizes formaldehyde emissions from treated flakes before and after being stored in lab for a period of time. Clearly, high emitters declined over time, i.e. FB1, and NC2 200°C-1h. On the contrary, emission from low emitters increased, i.e. FB2. This possibly can be explained by the complicated formaldehyde equilibrium between wood flakes and atmosphere. For specimen containing low formaldehyde, it tends to absorb atmospheric formaldehyde into the matrix. Once placed into the chamber again, it emits more formaldehyde. On the other hand, for specimen containing higher formaldehyde initially, it tends to emit formaldehyde into the atmosphere, which possibly results in lower formaldehyde emission once placed back into the chamber. This hypothesis brings up concern over sample storage in open lab and possible environmental contamination. And CH_2O content in laboratory environment was monitored through 4 month period, Figure 2.10. Room temperature ranged from 20°C to 26.7°C while relative humidity of laboratory environments varied from 60% to 80%.

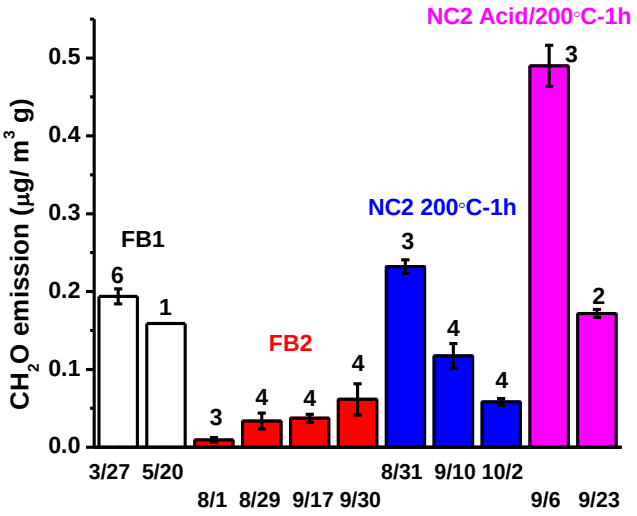

Figure 2.9. Formaldehyde emissions from wood flakes. Among each set of measurement, loaded flake tray sat in open laboratory at room temperature. Error bar = ± 1 standard deviation. Numbers above columns are number of measurements. X axis represents the experimental date.

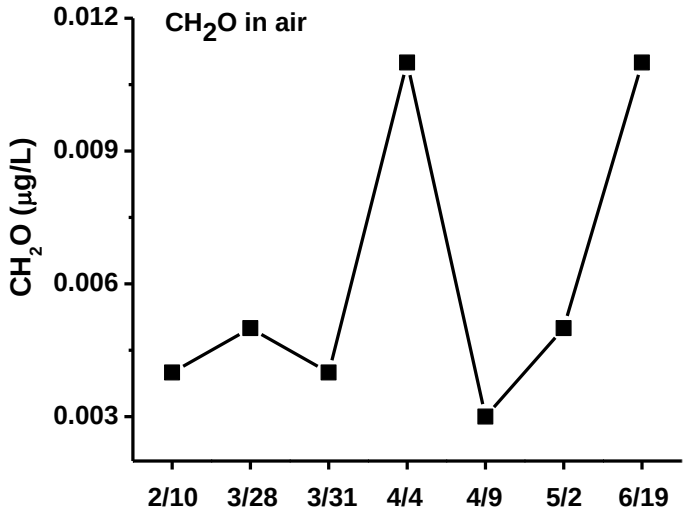

Figure 2.10. CH_2O content (Y axis, unit: μg CH_2O in 1L air) of laboratory air over 4 month period. X axis represents the experimental date. Within each day, only one measurement was taken.

Figure 2.10, CH_2O in laboratory environment ranged from 0.0015 to 0.003 µg/L air, which was even lower than CH_2O background measured from N_2 tank, 0.0075 - 0.012 µg/L. In this regard, CH_2O in lab environment is possibly not a concern for specimen contamination during storage. However, storing in open lab environment could be complicated due to other lab activities. So the ideal environment for specimen storage would be in a closed environment with no background CH_2O or any other interferences.

2.5. Conclusions

Four Virginia pine trees, FB1, FB2, NC1 and NC2 were subjected to CH_2O emissions measurements using a custom 12 liters micro chamber. Among 4 trees studies, FB1 emitted the highest amount of CH_2O, but probably due to different storage condition. Emission variation also existed among the other tree trees, FB2, NC1 and NC2 even they had similar preparation history. Heat treatment at 200°C (or 120°C) for 1 h increased the emissions, but sequential heating (up to 6 hours) decreased that emissions continuously. Ammonium chloride pretreatment led to higher emission from wood flakes compared to flakes without pretreatment but experienced the same heat treatment (200°C 1 h). Flakes with low emission rate tended to increase emission after being stored in open laboratory for a period of time, and flakes with high initial emission rate did the opposite. CH_2O content in laboratory environment ranged from 0.0015 to 0.003 µg/L, which was even lower than CH_2O background measured from N_2 tank, 0.0075-0.012 µg/L.

2.6. References

1. Risholm-Sundman, M., A. Larsen, E. Vestin, and A. Weibull, *Formaldehyde emission-comparison of different standard methods.* Atmospheric Environment, 2007. **41**(15): p. 3193-3202.
2. Que, Z.L., F.B. Wang, L.F. Ma, and F. Takeshi, *Evaluation of formaldehyde emission from particleboard using the large chamber and desiccator method at various loading ratios.* Journal of Forestry Research, 2013. **24**(1): p. 137-142.

3. Salem, M.Z.M. and M. Bohm, *Understanding of Formaldehyde Emissions from Solid Wood: An Overview.* Bioresources, 2013. **8**(3): p. 4775-4790.

4. E. Roffael, B. Johnsson, and B. Engstrom, *On the measurement of formaldehyde release from low-emission wood-based panels using the perforator method.* Journal of the International Academy of Wood Science, 2010. **44**(3): p. 369-377.

5. Bonnet, F., *A colorimetric method for the detection and estimation of formaldehyde.* Journal of the American Chemical Society, 1905. **27**(5): p. 601-605.

6. Hanzlik, P.J. and R.J. Collins, *Hexamethylenamin - The liberation of formaldehyd and the antiseptic efficiency under different chemical and biological conditions.* Archives of Internal Medicine, 1913. **12**(5): p. 578-612.

7. Collins, R.J. and P.J. Hanzlick, *A colorimetric method for the estimation of free formaldehyde and hexamethylenamine.* Journal of Biological Chemistry, 1916. **25**(2): p. 231-237.

8. Eegriwe, E., *Reaktionen und Reagenzien zum Nachweis organischer Verbindungen* Journal of Analytical Chemistry, 1937. **110**(1): p. 22-25.

9. Salthammer, T. and S. Mentese, *Comparison of analytical techniques for the determination of aldehydes in test chambers.* Chemosphere, 2008. **73**(8): p. 1351-6.

10. Nash, T., *The colorimetric estimation of formaldehyde by means of the Hantzsch reaction.* Biochem J, 1953. **55**(3): p. 416-21.

11. Belman, S., *The fluorimetric determination of formaldehyde.* Analytica Chimica Acta, 1963. **29**: p. 120-126.

12. Vairavamurthy, A., J.M. Roberts, and L. Newman, *Methods for determination of low molecular weight carbonyl compounds in the atmosphere: a review.* Atmospheric Environment. Part A. General Topics, 1992. **26**(11): p. 1965-1993.

13. Meyer, B. and C. Boehme, *Formaldehyde emission from solid wood.* For. Prod. J, 1997. **47**(5): p. 45.

14. Martinez, E. and M.I. Belanche, *Influence of veneer wood species on plywood formaldehyde emission and content.* Holz Als Roh-Und Werkstoff, 2000. **58**(1-2): p. 31-34.

15. Schafer, M. and E. Roffael, *On the formaldehyde release of wood.* Holz Als Roh-Und Werkstoff, 2000. **58**(4): p. 259-264.

16. Tasooji, M. and C.E. Frazier, *Simple Milligram-Scale Extraction of Formaldehyde from Wood.* ACS Sustainable Chemistry & Engineering, 2016. **4**(9): p. 5041-5045.

17. Tasooji, M., G. Wan, G. Lewis, H. Wise, and C.E. Frazier, *Biogenic formaldehyde: Content and heat generation in the wood of three tree species.* **Chapter 3** in this dissertation.

18. Stefke, B. and M. Dunky, *Catalytic influence of wood on the hardening behavior of formaldehyde-based resin adhesives used for wood-based panels.* Journal of Adhesion Science and Technology, 2006. **20**(8): p. 761-785.

19. Lundquist, K. and L. Ericsson, *Acid degradation of lignin III formation of formaldehyde.* Acta Chemica Scandinavica, 1970. **24**: p. 3681-3686.

20. Lundquist, K. and R. Lundgren, *Acid Degradation of Lignin .7. Cleavage of Ether Bonds.* Acta Chemica Scandinavica, 1972. **26**(5): p. 2005-&.

21. Lundquist, K., *Low-molecular weight lignin hydrolysis products.* Applied Polymer Symposia, 1976. **28**: p. 1393-1407.

22. Imai, T., T. Yokoyama, and Y. Matsumoto, *Revisiting the mechanism of beta-O-4 bond cleavage during acidolysis of lignin IV: dependence of acidolysis reaction on the type of acid.* Journal of Wood Science, 2011. **57**(3): p. 219-225.

23. Sturgeon, M.R., S. Kim, K. Lawrence, R.S. Paton, S.C. Chmely, M. Nimlos, T.D. Foust, and G.T. Beckham, *A Mechanistic Investigation of Acid-Catalyzed Cleavage of Aryl-Ether Linkages: Implications for Lignin Depolymerization in Acidic Environments.* Acs Sustainable Chemistry & Engineering, 2014. **2**(3): p. 472-485.

24. Lahive, C.W., P.J. Deuss, C.S. Lancefield, Z.H. Sun, D.B. Cordes, C.M. Young, F. Tran, A.M.Z. Slawin, J.G. de Vries, P.C.J. Kamer, N.J. Westwood, and K. Barta, *Advanced Model Compounds for Understanding Acid-Catalyzed Lignin Depolymerization: Identification of Renewable Aromatics and a Lignin-Derived Solvent.* Journal of the American Chemical Society, 2016. **138**(28): p. 8900-8911.

25. Wan, G. and C.E. Frazier, *Formaldehyde in pine wood forms as predicted by lignin acidolysis.* **Chapter 4** in this dissertation.

26. Myers, G.E., *Mechanisms of formaldehyde release from bonded wood products.* In ACS Symposium series-American Chemical Society (USA), 1986.

Chapter 3 Biogenic formaldehyde: Content and heat generation in the wood of three tree species

Mohammad Tasooji, Guigui Wan, George Lewis, Heather Wise, and Charles E. Frazier

Macromolecular Science & Engineering, Sustainable Biomaterials

Virginia Tech, Blacksburg VA 24061, U.S.A

Attribution

For the work described here formaldehyde measurements for Virginia pine was accomplished by Mohammad Tasooji and Heather Wise. George Lewis and Guigui Wan completed yellow-poplar measurements, and radiate pine was tested by Guigui Wan. Extractives and moisture content were determined by George Lewis and Guigui Wan.

3.1. Abstract

Global trends in allowable formaldehyde (CH_2O) emissions from nonstructural wood-based composites require a renewed consideration of biogenic CH_2O from wood. Increment cores from living Virginia pine (*Pinus virginiana*), yellow-poplar (*Liriodendron tulipifera*), and radiata pine (*Pinus radiata*) trees were used to measure CH_2O and CH_2O generation due to heating (200°C, 10 min). Significant variations within and between trees of the same species were observed. Tissue types (juvenile/mature, heartwood/sapwood) sometimes correlated to higher CH_2O contents and greater heat-generation potential; but sometimes not depending upon species. Heating increased CH_2O levels 3-60 fold. Heating with high moisture levels caused greater CH_2O generation than for dry (never-heated) specimens. This moisture effect and a separate serendipitous observation suggested that CH_2O generation is acid catalyzed. Radiata pine generated extraordinarily high CH_2O levels when heated, far exceeding the other species. It was suggested that pine extractives might catalyze CH_2O generation, perhaps in lignin. Regarding wood-based composites, findings suggested that compliance with emissions regulations may be complicated by CH_2O generated in the hot-press. If we could reveal the

precise mechanisms of CH_2O biogenesis in wood, we could perhaps manipulate these mechanisms for beneficial purposes.

3.2. Introduction

This work addresses biogenic formaldehyde (CH_2O) generated by wood during the manufacture of non-structural wood-based composites, from which CH_2O emissions are regulated. Global trends have shown steady reductions in allowable formaldehyde emissions from these consumer products. The target for regulation has been anthropogenic CH_2O released from hydrolytically unstable amino resins like urea-formaldehyde. However, current regulations restrict allowable emissions to such low levels that biogenic formaldehyde may affect regulation compliance. It is well known that wood contains biogenic formaldehyde and that heating generates much greater quantities. [1-6] Our industry interactions indicate that the latest emissions regulations have been met with new amino resin technologies. Nevertheless, there are persistent anecdotal reports of complications attributed to biogenic CH_2O. As part of an industry/university cooperation, we seek a more thorough accounting of all CH_2O sources in wood-based composites, both anthropogenic and biogenic. Biogenic CH_2O from wood has been documented for at least 39 years, but relatively little data is available, and none addresses CH_2O levels in living trees. [4, 7, 8] Our goal was to thoroughly document the occurrence of biogenic CH_2O in the living tree, and simulate its generation as occurring in composite manufacture. In this work industrial drying is omitted and emphasis is placed on hot-press simulation using 10 minute, 200°C treatments. In order to conduct large scale, nondestructive sampling of living trees, a simple milligram-scale water extraction was developed and shown to recover ~94% of the extractable CH_2O. [9] Specimen heat treatments and CH_2O determinations are conveniently conducted in a single glass vessel, so all biogenic CH_2O is retained and quantified. For our purposes this new procedure is preferable to the well-known perforator method that exposes 100g specimens to boiling toluene. [10] Since wood possesses abundant hydroxyl groups, CH_2O exists in a complex equilibrium that includes sorbed CH_2O and/or methylene glycol, covalently bonded hemiformal (hemiacetal), and covalently bonded formal (acetal). [9, 11, 12] Among these compounds, all except formal are “free” forms that are readily

extractable with water at room temperature. The free CH_2O that is readily extractable is capable of gaseous emission from the woody matrix. [9, 11] However the rate of emission is strongly dependent upon the wood moisture content. Dry wood tends to retain CH_2O and water saturated wood rapidly releases it [11], suggesting that hemiformals play a key role in wood/CH_2O equilibria.

With plans for additional tree species, the three included in this study were Virginia pine, yellow-poplar, and radiata pine. While commercially insignificant, Virginia pine (*Pinus virginiana*) was studied because of its availability and similarity to the commercially important southern pines. Yellow-poplar (*Liriodendron tulipifera*) is commercially important in the eastern United States, and radiata pine (*Pinus radiata*) is commercially valued on a global scale. Ultimately, the desire is to determine how biogenic CH_2O affects emissions from composite products.

3.3. Materials and methods

Virginia pine (*Pinus virginiana*) trees from a wooded region (~4 ha) east of Blacksburg, VA, U.S.A. (Nellies Cave area), were sampled as follows: increment cores (5 mm dia.) sampled at ~1.4m above ground, from 8 trees, 6-8 cores per tree from a 100 cm^2 area; sealed in plastic straws (trees 1-6) or Pyrex glass tubes (trees 7-8), and subsequently razor cut into ~1 mm thick disks; juvenile (first 10-15 rings from pith) and mature (last 40-70 rings to bark) tissue was isolated and stored frozen (-18°C for trees 1-6, and -80°C for trees 7-8). Among the 8 Virginia pines, all appeared healthy except tree 8 which had large sections of dead branches in the crown.

Yellow-poplar (*Liriodendron tulipifera*) trees were generally isolated specimens growing on the Virginia Tech campus and sampled as follows: increment cores (5 mm dia.) sampled ~1.4 m above ground from 5 healthy trees, 4-8 cores per tree from a 100 cm^2 area, sealed in Pyrex glass tubes, and razor cut into ~1 mm thick disks; heartwood and sapwood were separated based on the color difference. Within each tree, all heartwood and sapwood sections were randomized respectively, and separately stored at -80°C.

Radiata pine (*Pinus radiata*) trees were sampled from a commercial plantation in Chile. Tree 1 was sampled from a stock having 587 trees/ha (silvicultural management pruned and thinned), at UTM coordinate location 18 H, 664859.83 m E, 5913603.16 m S. Tree 2 was sampled from a stock having 933 trees/ha, at UTM coordinate location 18 H, 664847.41 m E, 5913502.29 m S. Sampling occurred as follows: increment cores (10 mm diameter) were sampled at 1.2-1.6 m above ground in a vertical line with 8 cm separation, 6 cores per tree, vacuum dried at 17°C for one week, sealed in plastic tubes, shipped from Chile, and received four days later. Upon arrival, juvenile (first 10 rings from pith) and mature (last 9-18 rings) tissue was separated, and cut into ~1mm thick disks. Within each tree, all juvenile and mature sections were randomized respectively, and separately stored at -80°C.

Extractives content was measured using 95% ethanol extraction according to standard method NREL/TP-510-42910: Determination of Extractives in Biomass.

Specimen preparation

Specimens are identified with respect to drying history (Never-dried; Dried) and thermal treatment (Never-heated; Heated). Never-dried specimens: freshly cut disks were sealed and placed in a second container (purged with N_2) and stored as described above. Prior to use, cold-storage sample vials were warmed in a water bath at room temperature for 20-30 min. Dried specimens: wood disks were placed in a desiccator and dried by cycling between vacuum (0.15 mm Hg) and dry N_2 gas, three times; stored over P_2O_5 or molecular sieves and N_2 for at least 48 hours until reaching constant weight. Heated specimens: 200°C, 10 min as detailed below; Never-Heated specimens: no heat exposure. Within each tree, 1-3 cores were used for Never-dried measurements while another 3-5 cores were used for Dried measurements. Within each core, 2-4 CH_2O measurements were conducted.

CH_2O measurements

The CH_2O determination was described in a previous publication [9]: wood samples (Never-heated: 30-60 mg, Heated: 5-10 mg, dry mass) were sealed in a 50 ml serum bottle. All samples were subjected to either heat treatment (200°C, 10 min) or no heating. After cooling to

room temperature, HPLC water (15 ml or 20 ml) was charged via syringe, and the specimen/bottle set at room temperature for 1 hour with occasional shaking. After 1 hour, 4 ml of the CH_2O solution was sampled and analyzed by fluorimetric acetylacetone detection. Prior to CH_2O measurement, wood specimen moisture content was measured and used to normalize CH_2O mass, reported in µg/g dry wood. Simple pairwise statistical comparisons were conducted, but normality of the data sets was not verified.

3.4. Results and discussions

Sample information summary

Table 3.1 shows the number of trees studied, range in age, moisture content, and extractives content.

Table 3.1. Tree specimen information: Species, range of age, etc. Moisture content (MC%) at harvest and extractives content (EC%) are based on dry wood mass. MC% and EC% for yellow-poplar and radiata pine were averaged over all trees listed. MC% for Virginia pine was averaged over trees 1-6, and EC% was averaged over trees 5 and 6. Standard deviations in parentheses.

Species	**Virginia pine**		**Yellow-poplar**		**Radiata pine**	
Age (years)	60-85		30-40		19-28	
# of trees	8		5		2	
Tissue type	Mature	Juvenile	Sapwood	Heartwood	Mature	Juvenile
MC%	81.7 (11.4)	29.3 (12.4)	72.5 (0.8)	128.3 (10.9)	~130*	~40*
EC%	3.5 (1.0)	7.3 (0.5)	3.4 (1.1)	4.3 (0.9)	1.1 (0.2)	2.3 (0.6)

*MC% not available, but estimated by collaborators according to prior experience.

CH_2O content and CH_2O generation potential in Never-dried specimens

Specimens are discussed with respect to drying history (Never-dried; Dried) and thermal treatment (Never-heated; Heated). One notable observation was the variability within individual cores, and between cores within the same tree as related to CH_2O content and CH_2O generation potential. Virginia pine tree 3 (juvenile tissue) was randomly selected to demonstrate this point, Figure 3.1. In some cases there was significant variability within individual cores, but on average no significant difference between cores (i.e. Never-dried/Never-heated, cores 1-3). In other cases, there was little variability within individual cores, with or without significant differences between cores, on average. The variations shown here were representative for juvenile and mature tissue in all Virginia pines trees analyzed, where the specific patterns of variation seemed random. In other words, the CH_2O content and the CH_2O generation potential were non-uniform within the tissues studied. Since sub-sample groupings were based upon tissue maturity (cm-scale), the heterogeneity within and between cores could be related to anatomical variations that were perhaps not randomized during tree core sectioning (mm-scale). For instance, the occurrence of resin canals (epithelial parenchyma) could be expected to vary among tree core sections. Whereas earlywood/latewood effects (if they occur) would be expected to undergo randomization with perhaps no detectable impact. Consequently, the within and between core variability observed here may be associated with the heterogeneous distribution of wood extractives associated with resin canals. If wood extractives play a role in biogenic CH_2O generation, then the extractives must be considered as a potential source and/or they might interact with wood to suppress or promote CH_2O. For instance, condensed tannins are formaldehyde scavengers, and have been used in resin formulations to lower CH_2O emission from the commercial products. [2, 13-15] Likewise, evidence presented later suggests that CH_2O generation is acid catalyzed and so acidic wood extractives will likely play a catalytic role.

Figure 3.2 shows tissue maturity effects in Never-dried/Never-heated Virginia pine for trees 3-8. CH_2O levels ranged from about 1-5 µg/g of dry wood, comparable to the findings of Meyer and Boehme [1] and also by Weigl et al. [4] when using the perforator (boiling toluene) extraction on pine specimens. Recall that tree 8 was diseased, but its CH_2O content was not unusual. Among trees 3-7, it appeared as if tissue maturity effects were effectively random;

there was no significant effect in tree 4, and in trees 3, 5, 6, and 7 tissue maturity effects were seen but with no sensible pattern. Using *Pinus sylvestris*, Weigl et al. found that juvenile wood contained less CH_2O than mature wood. Similarly, Dix and Raffael [16] showed that particleboard made with *Pinus sylvestris* heartwood generally emitted less CH_2O than when using the corresponding sapwood (although juvenile wood was not explicitly identified).

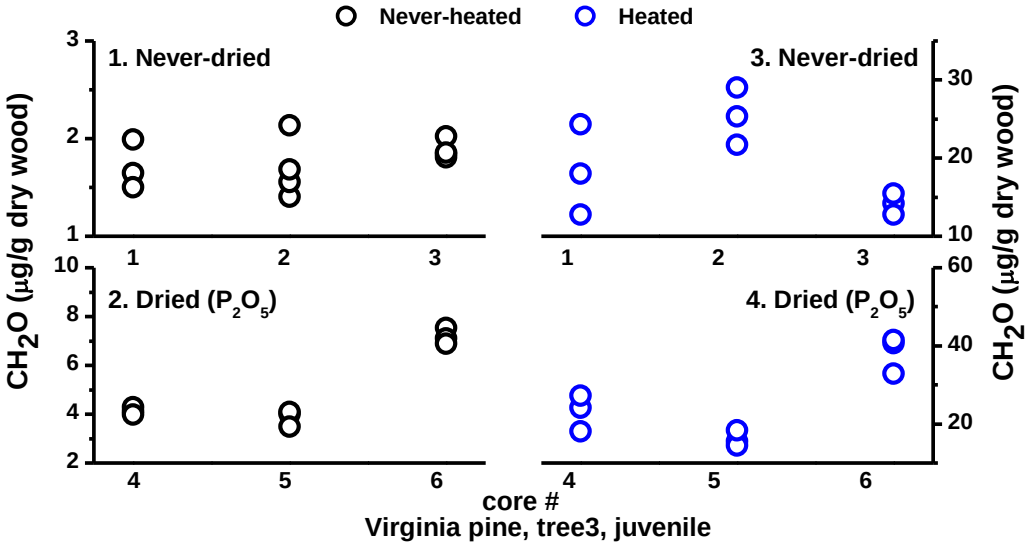

Figure 3.1. Typical within core, and between core, variability in CH_2O content, and in CH_2O generation, among cores from the same tree (Virginia pine tree 3, juvenile tissue), under different drying and thermal treatments as indicated. Note ordinate scales vary.

When comparing Never-dried/Never-heated to Never-dried/Heated specimens, Figure 3.3 demonstrates the well-known impact of heating [17-19] on biogenic CH_2O generation, and in this case tissue maturity effects became clear. Heating increased the CH_2O content by a factor of 9-34 in juvenile wood, and by a factor of 7-61 in mature wood. Upon heating, the mature tissue always exhibited a higher CH_2O content, and the generation potential (factor increase) was greater in mature tissue for trees 3, 4, 7, and 8. The true CH_2O generation potential requires correction for levels found in Never-dried/Never-heated specimens; but that was not applied to Figure 3.3, and the correction had little impact on the factor increase. Mature Virginia pine contained less extractives and more water than juvenile wood (Table 3.1). For trees 3, 4, 7, and 8, perhaps the greater moisture content in the mature tissue explains the

greater CH_2O generation potential, but both tissue types were likely above the fiber saturation point. Again, the variability within and between trees was notable, and the diseased tree 8 appeared normal in comparison to the healthy trees. If the behavior shown in Figure 3.3 is applicable to commercially significant southern pines like *Pinus taeda*, it is apparent that CH_2O generation during composite hot-pressing could be highly variable. The potential impact on panel emissions seems obvious, but the precise relationship between biogenic CH_2O generation and actual product emissions is currently unknown (discussed later).

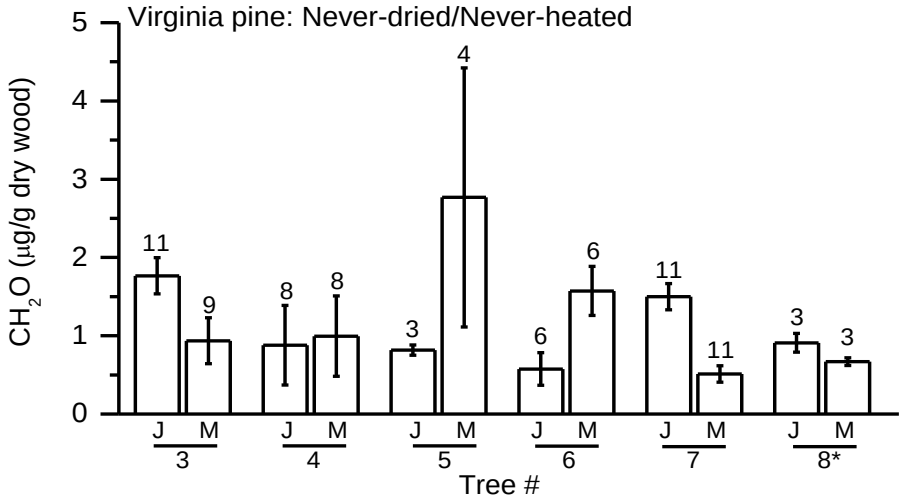

Figure 3.2. Average CH_2O content in Never-dried/Never-heated Virginia pine, trees 3-8, for juvenile (J) and mature wood (M). Each column averaged over 1-3 cores with 2-4 measurements per core; numbers above columns indicate total number of measurements. *Tree 8 was diseased. Error bars = ± 1 standard deviation.

As in Virginia pine trees, yellow-poplar trees exhibited a similar degree of variability within and between trees, Figure 3.4. However in Never-dried/Never-heated yellow-poplar the heartwood always exhibited a higher CH_2O content than sapwood. The extractives content in the respective tissues was about the same, but the composition is known to differ; and the heartwood had higher moisture, Table 3.1. Upon heating the CH_2O generation potential was greater for the sapwood (increasing by a factor of 10-19), whereas in heartwood the CH_2O content increased by a factor of 3-5. The lower CH_2O generation potential of yellow-poplar

heartwood might be due to CH_2O reaction with aporphine alkaloids (phenolic and nonphenolic) that occur in the heartwood at levels of about 1% whereas only trace quantities appear in the sapwood. [20, 21]

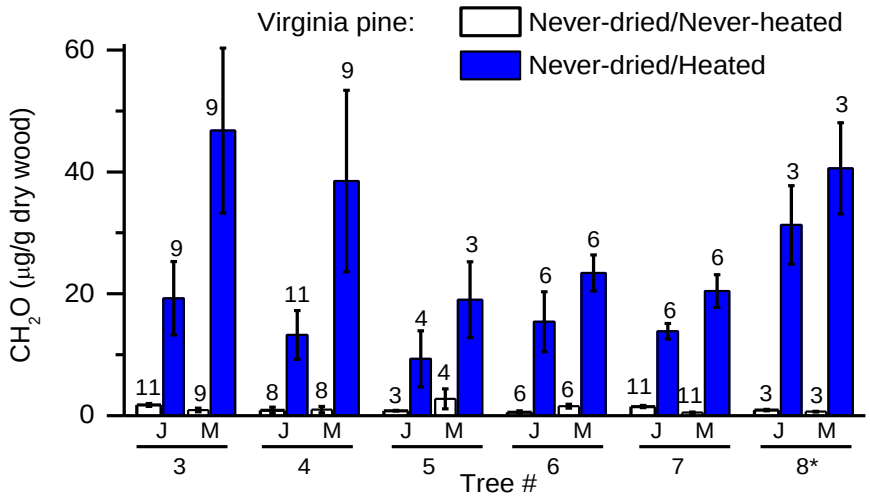

Figure 3.3. Demonstration of heating effects on CH_2O generation potential from average CH_2O contents of Never-dried/Never-heated and Never-dried/Heated specimens in juvenile (J) and mature wood (M). Each column averaged over 1-5 cores with 2-4 measurements per core; numbers above columns indicate total number of measurements. *Tree 8 was diseased. Error bars = ± 1 standard deviation.

A general species comparison was conducted by pooling all yellow-poplar data and comparing it to Virginia pine data pooled over trees 3-8 (tree 8 being diseased), Figure 3.5. Considering Never-dried/Never-heated specimens, it was determined that living yellow-poplar trees contained more CH_2O than living Virginia pine. This suggests that CH_2O emissions in the drying stage might be greater when processing yellow-poplar as compared to southern pine. Yellow-poplar wood appeared to generate more CH_2O when heated (Never-dried/Heated). CH_2O generated in yellow-poplar heartwood was significantly greater than that generated in Virginia pine juvenile wood ($p << 0.01$); but when comparing yellow-poplar sapwood to Virginia pine mature wood the difference was less significant ($p = 0.11$).

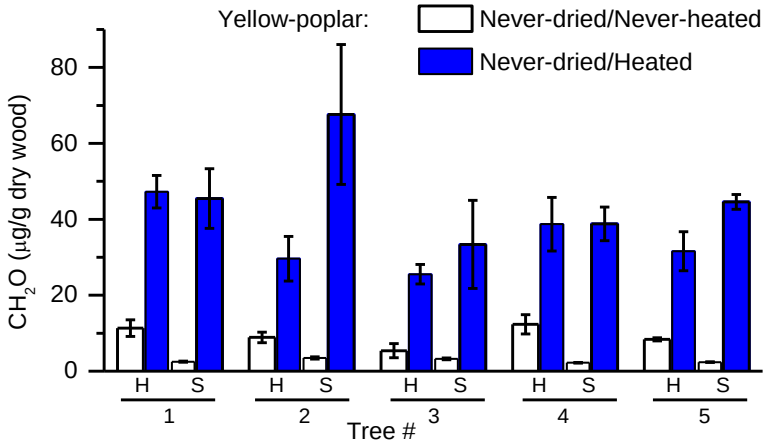

Figure 3.4. Average CH_2O content (Never-dried/Never-heated) and CH_2O generation potential (Never-dried/Heated) in yellow-poplar, trees 1-5. Each column averaged over 15 total measurements where heartwood (H) and sapwood (S) specimens were respectively randomized among 4-8 cores from the same tree. Error bars = ± 1 standard deviation.

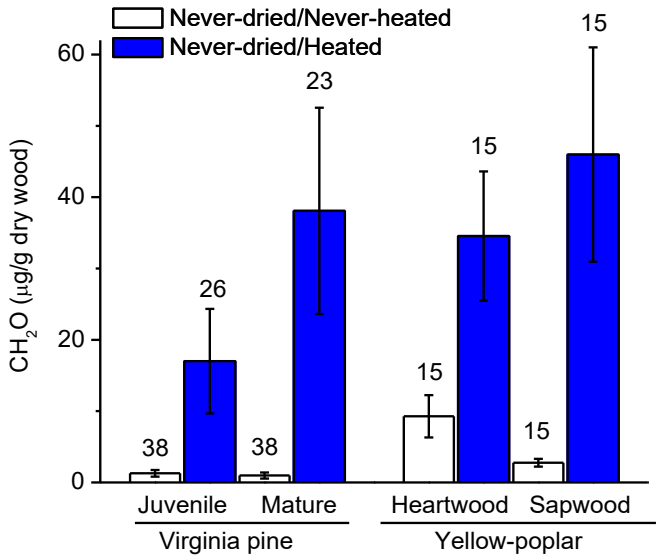

Figure 3.5. Average CH_2O content (Never-dried/Never-heated) and CH_2O generation potential (Never-dried/heated) for Virginia pine trees 3-8 (1-3 cores per tree, 2-4 measurements per core) and yellow-poplar trees 1-5 (6-8 cores per tree with respective tissue types randomized among cores from the same tree, 3 measurements per tree). Numbers above columns indicate total number of measurements. Error bars = ± 1 standard deviation.

Effect of drying agent: P_2O_5 vs. molecular sieves

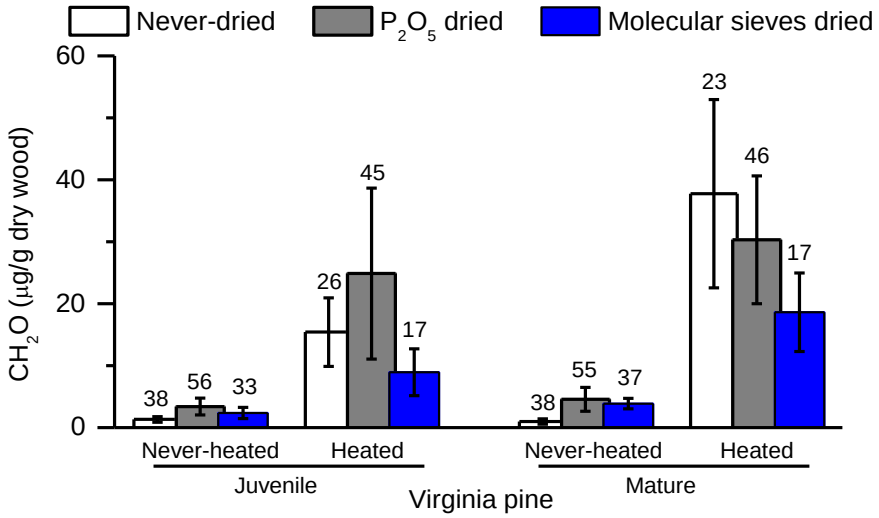

Figure 3.6. Effect of drying agent (P_2O_5 vs. molecular sieves) on CH_2O content and CH_2O generation in Virginia pine. Never-dried specimens: trees 3-7; P_2O_5 dried specimens: trees 1-4; molecular sieves dried specimens: trees 5-7; 1-5 cores per tree. Numbers above columns indicate total number of measurements. Error bars = ± 1 standard deviation.

While analyzing Virginia pine, it was observed that room temperature drying often increased the CH_2O content measured in wood. This was surprising given that no specimen heating occurred. Meyer and Boehme made similar observations after drying pine, spruce, and Douglas-fir at 30°C; drying resulted in increased CH_2O emission from solid wood (but drying substantially reduced emissions from solid oak). [1] When drying resulted in greater emissions, Meyer and Boehme suggested that CH_2O generation must have occurred even after their specimens were dried. This hypothesis cannot be refuted, but it seems questionable since over short periods elevated temperatures are required to form biogenic formaldehyde (data not shown). In any case, we became suspicious that room temperature drying in the presence of P_2O_5 might lead to catalytic effects from phosphoric acid contamination. Consequently, the effects of room temperature, vacuum drying in the presence of either P_2O_5 or molecular sieves was studied, Figure 3.6. In the absence of heating, on average it was found that drying always caused an increase in CH_2O content in juvenile and mature Virginia pine; but this increase was significantly less when drying with molecular sieves as compared to P_2O_5. This suggests that

phosphoric acid contamination could catalyze CH_2O formation. This assertion is supported when considering the effects of heating, where drying with molecular sieves resulted in less heat-generated CH_2O as compared to drying with P_2O_5. From this analysis we concluded that P_2O_5 should never be used to dry wood that is intended for chemical study. Furthermore the remaining discussion will only feature specimens dried with molecular sieves.

Species effects in drying

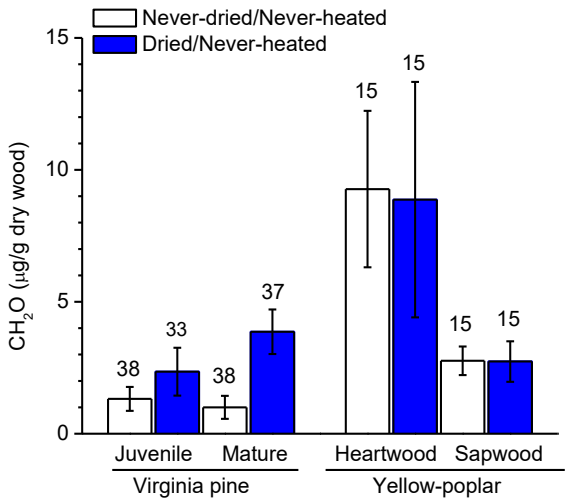

Figure 3.7. Effect of drying (with molecular sieves) on the CH_2O content in Never-heated Virginia pine (trees 5-8) and yellow-poplar (trees 1-5). Numbers above columns indicate total number of measurements from 4-5 trees, 1-8 cores per tree. Error bars = ± 1 standard deviation.

To further consider the effects of drying on CH_2O content in Never-heated specimens, Figure 3.7 compares Virginia pine to yellow-poplar. Unlike Virginia pine, it was found that drying caused no significant change in the CH_2O content of yellow-poplar wood. This result is similar to that of Meyer and Boehme, but only in that the behavior of softwoods and hardwood is very different. Meyer and Boehme found that drying caused a significant reduction of CH_2O content in oak. [1] Initial consideration might suggest that drying (without heating) would result in a CH_2O content reduction. However if hemiformals dominate the equilibria in wood, then CH_2O retention would increase as drying proceeds. Regarding the effects of drying on hardwoods, the discrepancy with Meyer and Boehme might be explained by the different drying conditions

employed. In this work vacuum drying to a moisture content of less than 1% [22] was employed, whereas Meyer and Boehme dried specimens to 7-9% moisture with air circulation. If these observations are explained by the moisture dependent hemiformal equilibrium, then one could conceive relatively simple methods to reduce CH_2O content in wood, where increasing moisture promotes CH_2O release. [11] Nevertheless it is perplexing to find that CH_2O content is higher in softwoods after drying. As Meyer and Boehme suggested, it is possible that biogenic CH_2O is generated during the course of drying and analysis; otherwise there must be an unknown mechanism that affects the CH_2O equilibrium in softwoods. If the latter case is true, then perhaps softwood extractives play a unique role.

When heated at 200°C for 10 minutes, wet wood generates significantly more CH_2O, Figure 3.8. Since it appears that acids catalyze CH_2O generation (Figure 3.6), it is reasonable to conclude that naturally occurring wood acids would be less active when wood is very dry. Furthermore, heating at higher moisture contents is expected to hydrolyze wood esters and release more acids that catalyze a corresponding increase in CH_2O generation.

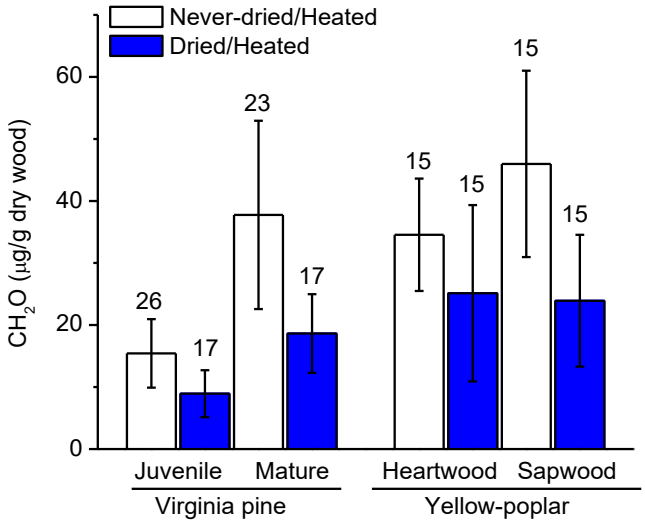

Figure 3.8. Effect of moisture content on heat generation of CH_2O: Virginia pine (trees 5-7, 1-5 cores per tree, 2-4 measurements per core) vs. yellow-poplar (trees 1-5, 6-8 cores, 3 measurements per tree). Numbers above columns represent number of measurements. Error bars = ± 1 standard deviation.

Recall that the diseased Virginia pine tree 8 did not exhibit unusual behavior when Never-dried/Never-heated (Figure 3.2) or Never-dried/Heated (Figure 3.3); CH_2O content and generation fell within range of the seven healthy trees. However for Dried/Heated specimens (dried with molecular sieves), tree 8 generated much more CH_2O than trees 5 and 6. Too little data is presented to reach a firm conclusion, but we could reasonably expect trees to exhibit disease-related changes in CH_2O generation due to changes in extractives composition [23]. However it is not clear why Virginia pine tree 8 would appear normal when Never-dried, but abnormal when Dried/Heated. Perhaps the reduced acid activity in the dried and diseased tree impedes CH_2O scavenging (reaction) by phenolic extractives, whereas scavenging mechanisms in healthy trees are different and less affected by reduced acid activity. This convoluted conjecture is feasible, but perhaps the more important message is that among all possible biological variables CH_2O equilibria in wood could be very complex.

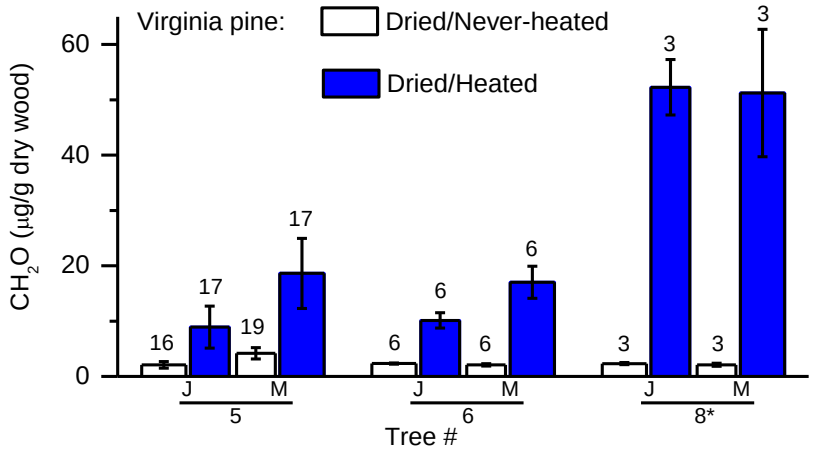

Figure 3.9. Effect of disease state on CH_2O content and generation from molecular sieves dried Virginia pines, trees 5 and 6 healthy, and tree 8 diseased. Numbers above columns represent number of measurements; each column averaged over 1-5 cores, 3-4 measurements per core. Error bars = ± 1 standard deviation.

Species effect: CH_2O content and generation

Recall from the experimental section that radiata pine specimens were received after drying, and the comparison to Virginia pine and yellow-poplar is shown in Figure 3.10. When

heated, the CH_2O content in dry radiata pine increased by a factor of 32-40, whereas the increases for Virginia pine and yellow-poplar were by factors of 4-5 and 3-9, respectively. We should expect higher CH_2O levels in radiata pine when heated at higher moisture contents, Figure 3.8. The extraordinary CH_2O generation in radiata pine suggests that compliance to emissions regulations could be troublesome for radiata-based composites, noting that all CH_2O determined in this work is capable of gaseous emission (moisture dependent emission). As mentioned, the precise relationship between biogenic CH_2O levels and actual composite emissions is currently unknown. However a direct relationship seems reasonable, as demonstrated by Birkeland et al. [5] who measured significant biogenic emissions from panels bonded with no-added CH_2O adhesives. Birkeland et al. [5] demonstrated that biogenic emissions dissipated 12-20 days after hot-pressing (storage at 50% relative humidity, 23°C). Consequently, special measures might be required to meet emissions regulations in radiata-based composites (verified to the authors from personal communication with industry representatives). Note that both pines exhibit tissue maturity effects. Mature wood in Virginia pine generates significantly more CH_2O than juvenile wood ($p << 0.01$), but the effect is less significant in radiata pine ($p = 0.07$).

Compared to Virginia pine, what could explain the extraordinary CH_2O generation in radiata pine? Among the structural wood polymers, the available literature indicates that lignin generates much more CH_2O than the polysaccharides [2], consistent with our findings to be published later. It seems unlikely that lignin effects would explain the differences observed in Virginia and radiata pine. Consequently, a plausible hypothesis could involve differences in the extractives. Three scenarios should be considered: 1) that extractives directly generate CH_2O, 2) that extractives scavenge (react with) CH_2O, or 3) that extractives catalyze CH_2O generation, perhaps in lignin. The first scenario is known to occur, and strong evidence exists for the second [2].

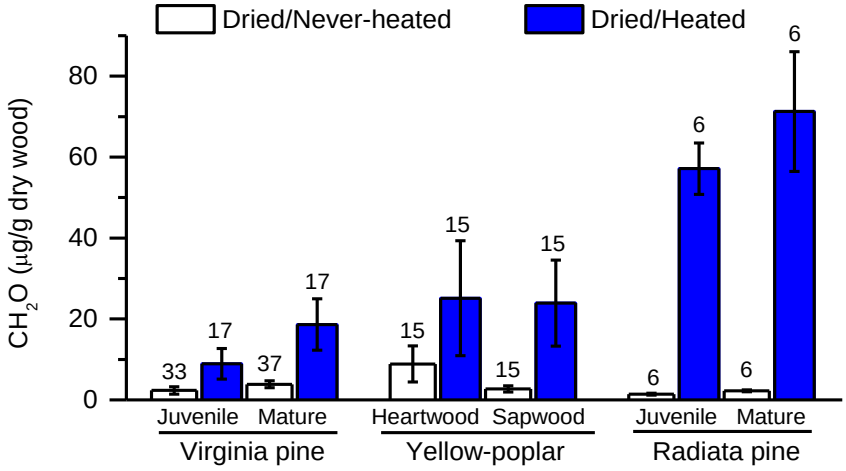

Figure 3.10. Species effect on CH_2O content and generation from molecular sieves dried specimens. Numbers above columns indicate number of measurements. Virginia pine: trees 5-7, 1-5 cores per tree, 2-4 measurements per core. Yellow-poplar: trees 1-5, specimens randomized among 6-8 cores, 3 measurements per tree. Radiata pine: 2 trees, specimens randomized among 4 cores, 3 measurements per tree. Error bars = ± 1 standard deviation.

Schäfer and Roffael [2] provided data that suggests a catalytic role for extractives, but they did not discuss it. When heated (150°C, 3h), unextracted pine generated CH_2O at 288 µg/g dry wood, and extracted pine generated 167 µg/g dry wood, a 42% reduction caused by extractives removal (4% extractives). Using pure specimens, they also demonstrated that pine fatty acids and the resin acid, abietic acid, directly generate CH_2O when heated similarly; but abietic acid was far more productive, generating CH_2O at 179 µg/g abietic acid. Using these numbers and assuming direct CH_2O generation by abietic acid, if this pine wood contained 4% extractives in the form of pure abietic acid, removal should cause only a 3% reduction in CH_2O generated by heating. In other words, Schäfer and Roffael's data suggests that pine extractives could be acting as catalysts, indirectly generating much more CH_2O than is directly generated from their thermal decomposition. The catalytic role of pine extractives in CH_2O generation by wood is a plausible hypothesis that must be verified. It is also plausible that every combination of scenarios 1, 2, and 3 mentioned above could affect CH_2O generation by wood (and implicit to scenario 1 is that lignocellulose could catalyze CH_2O generation by the extractives). Perhaps this

explains some of the findings in this work where influential parameters such as tissue type, moisture content, and disease state appeared to be highly complex and variable within and between tree species. Hopefully future studies will reveal the precise mechanisms of biogenic CH_2O generation. Perhaps we could manipulate those mechanisms to reduce CH_2O emissions in wood composites, or even use biogenic CH_2O to improve composite performance regardless of the adhesive technology.

3.5. Conclusions

As was well known, wood naturally contains CH_2O and it generates much more when heated at 200°C, 10 min. This study documented these effects in increment cores sampled from living trees, eight Virginia pine, five yellow-poplar, and two radiata pine trees. Significant variations within and between trees of the same species were observed as expected. Besides this normal variation, other influential parameters appeared to be complex and highly varied. For instance, tissue types (juvenile/mature, heartwood/sapwood) sometimes correlated to higher CH_2O contents and greater heat-generation potential; but sometimes not depending upon tree species. When heated, wet wood (near or above fiber saturation) generated more CH_2O than did dry wood, consistent with an acid catalyzed mechanism (and separate evidence for acid catalysis was found). Heating increased CH_2O levels anywhere from 3-60 times that in unheated wood, depending upon tissue type, moisture content, and species. CH_2O scavenging effects were perhaps detected in yellow-poplar heartwood. The diseased state of one Virginia pine tree did not correlate with unusual results when the wood was wet; but after drying there was evidence for greater heat-generation potential when compared to two healthy trees. Most remarkable was that radiata pine generated extraordinarily high CH_2O levels when heated, far exceeding that in Virginia pine and yellow-poplar. It was hypothesized that the remarkable behavior of radiata pine might be related to extractives effects. It was suggested that pine extractives might catalyze CH_2O generation, perhaps in lignin. Considering the manufacture of wood-based composites, the findings suggest that compliance with CH_2O emissions regulations can be complicated by biogenic CH_2O that is created in the hot-press. The precise relationship between biogenic CH_2O levels and actual composite emissions is currently unknown. However

it is known that all CH_2O measured here is capable of gaseous emission, and higher moisture levels promote emission. If we could reveal the precise mechanisms of CH_2O biogenesis in wood, we could perhaps manipulate these mechanisms for beneficial purposes.

Acknowledgements. This project was supported by the Wood-Based Composites center, a National Science Foundation Industry/University Cooperative Research Center (Award #1035009). Partial funding was also supplied by the Virginia Agricultural Experiment Station and the McIntire Stennis Program of the National Institute of Food and Agriculture, U.S. Department of Agriculture. Special thanks go to collaborators at Arauco for sampling, drying, and shipping radiata pine specimens.

3.6. References

1. Meyer, B. and C. Boehme, *Formaldehyde emission from solid wood.* For. Prod. J, 1997. **47**(5): p. 45.
2. Schafer, M. and E. Roffael, *On the formaldehyde release of wood.* Holz Als Roh-Und Werkstoff, 2000. **58**(4): p. 259-264.
3. Roffael, E., *Volatile organic compounds and formaldehyde in nature, wood and wood based panels.* Holz als Roh-und Werkstoff, 2006. **64**(2): p. 144-149.
4. Weigl, M., R. Wimmer, E. Sykacek, and M. Steinwender, *Wood-borne formaldehyde varying with species, wood grade, and cambial age.* For. Prod. J, 2009. **59**(1/2): p. 88.
5. Birkeland, M.J., L. Lorenz, J.M. Wescott, and C.R. Frihart, *Determination of native (wood derived) formaldehyde by the desiccator method in particleboards generated during panel production.* Holzforschung, 2010. **64**(4): p. 429-433.
6. Salem, M.Z.M. and M. Bohm, *Understanding of Formaldehyde Emissions from Solid Wood: An Overview.* Bioresources, 2013. **8**(3): p. 4775-4790.
7. Martinez, E. and M.I. Belanche, *Influence of veneer wood species on plywood formaldehyde emission and content.* Holz Als Roh-Und Werkstoff, 2000. **58**(1-2): p. 31-34.

8. Bohm, M., M.Z.M. Salem, and J. Srba, *Formaldehyde emission monitoring from a variety of solid wood, plywood, blockboard and flooring products manufactured for building and furnishing materials.* Journal of Hazardous Materials, 2012. **221**: p. 68-79.

9. Tasooji, M. and C.E. Frazier, *Simple milligram-scale extraction of formaldehyde from wood.* ACS Sustainable Chemistry & Engineering, 2016. **4**(9): p. 5041-5045.

10. ISO, *Wood-based panels -- Determination of formaldehyde release -- Part 5: Extraction method (called the perforator method)*. 2015.

11. Myers, G.E., *Mechanisms of Formaldehyde Release from Bonded Wood Products.* Acs Symposium Series, 1986. **316**: p. 87-106.

12. Aydin, I., G. Colakoglu, S. Colak, and C. Demirkir, *Effects of moisture content on formaldehyde emission and mechanical properties of plywood.* Building and Environment, 2006. **41**(10): p. 1311-1316.

13. Hashida, K., S. Ohara, and R. Makino, *Improvement of formaldehyde-scavenging ability of condensed tannins by ammonia treatment.* Holzforschung, 2006. **60**(2): p. 178-183.

14. Hoong, Y.B., M.T. Paridah, Y.F. Loh, H. Jalaluddin, and L.A. Chuah, *A new source of natural adhesive: Acacia mangium bark extracts co-polymerized with phenol-formaldehyde (PF) for bonding Mempisang (Annonaceae spp.) veneers.* International Journal of Adhesion and Adhesives, 2011. **31**(3): p. 164-167.

15. Navarrete, P., A. Pizzi, S. Tapin-Lingua, B. Benjelloun-Mlayah, H. Pasch, K. Rode, L. Delmotte, and S. Rigolet, *Low Formaldehyde Emitting Biobased Wood Adhesives Manufactured from Mixtures of Tannin and Glyoxylated Lignin.* Journal of Adhesion Science and Technology, 2012. **26**(10-11): p. 1667-1684.

16. Dix, B. and E. Roffael, *Influence of heartwood and the age of tree on the properties of particleboards from pine (Pinus sylvestris) .2. Physical-technical properties and formaldehyde release of particleboards made from sap- and heartwood of pine.* Holz Als Roh-Und Werkstoff, 1997. **55**(2): p. 103-109.

17. Marutzky, R. and E. Roffael, *Über die Abspaltung von Formaldehyd bei der thermischen Behandlung von Holzspänen. Teil I: Modell-Versuche.* Holzforschung-International Journal of the Biology, Chemistry, Physics and Technology of Wood, 1977. **31**(1): p. 8-12.

18. Jiang, T., D.J. Gardner, and M.G. Baumann, *Volatile organic compound emission arising from the hot-pressing of mixed-hardwood particleboard.* Forest products journal, 2002. **52**(11/12): p. 66.

19. McDonald, A.G., J.S. Gifford, D. Steward, P.H. Dare, S. Riley, and I. Simpson, *Air emission from timber drying: high temperature drying and re-drying of CCA treated timber.* Holz als Roh-und Werkstoff, 2004. **62**(4): p. 291-302.

20. Chen, C.L., H.M. Chang, and E.B. Cowling, *Chemistry of Liriodendron-Tulipifera L .1. Aporphine Alkaloids and Lignans in Heartwood of Liriodendron-Tulipifera.* Phytochemistry, 1976. **15**(4): p. 547-550.

21. Chen, C.L., H.M. Chang, E.B. Cowling, C.Y.H. Hsu, and R.P. Gates, *Aporphine Alkaloids and Lignans Formed in Response to Injury of Sapwood in Liriodendron-Tulipifera.* Phytochemistry, 1976. **15**(7): p. 1161-&.

22. Sun, N., S. Das, and C.E. Frazier, *Dynamic mechanical analysis of dry wood: Linear viscoelastic response region and effects of minor moisture changes.* Holzforschung, 2007. **61**(1): p. 28-33.

23. Szczepkowski, A., D. Nicewicz, and P. Koczoń, *The relationship between tree health and chemical composition of beech (Fagus sylvatica L.) and oak (Quercus robur L.) wood of Polish provenances.* Acta Scientiarum Polonorum, Silvarum Colendarum Ratio et Industria Lignaria, 2007. **6**(3): p. 77-88.

Chapter 4 Formaldehyde in pine wood forms as predicted by lignin acidolysis

Guigui Wan, and Charles E. Frazier

Macromolecular Science & Engineering, Sustainable Biomaterials

Virginia Tech, Blacksburg VA 24061, U.S.A

4.1. Abstract

Pinus virginiana wood was heated (200°C, 10 or 60 min) while dry or aqueous/acid or base pretreatment in order to reveal mechanisms of formaldehyde (CH_2O) generation. Among wood structural polymers, lignin was the overwhelming source of biogenic CH_2O, consistent with prior reports. The effects of wood extractives were ignored and reserved for a later report. The selection of acid catalyst strongly affected CH_2O generation as predicted in the acidolysis literature of lignin model compounds and isolated lignins. Lignin methoxyl cleavage was also observed, but was considered an unlikely source of thermochemical CH_2O. Regarding wood-based composite manufacture, the implications are that lignin reactions can be manipulated during hot-pressing. Potential benefits include reduced product emissions, and/or novel crosslinking strategies using biogenic CH_2O. Perhaps even lignin repolymerization could be promoted for benefit, in direct opposition to biorefinery strategies for lignin removal.

4.2. Introduction

Wood contains natural, biogenic formaldehyde (CH_2O), and heating generates much higher levels that vary according to wood moisture content, tissue type, and tree species [1-5]. Biogenic CH_2O levels can vary dramatically for reasons that are not understood. For instance, Tasooji et al. demonstrated that *Pinus radiata* generates 2-6 times more CH_2O than does *Liriodendron tulipifera* and *Pinus virginiana* when heated at 200°C (10 min). [5] Catalytic interactions involving wood extractives might explain species effects, but this and other hypotheses must be examined if we hope to control biogenic CH_2O. [5] CH_2O emissions from nonstructural wood-based composites have long been regulated, but the intended target was hydrolytically unstable amino resins. The authors' industry interactions indicate that the latest

emissions regulations have been met with new amino resin technologies. However, persistent anecdotal reports cite complications attributed to biogenic CH_2O. These concerns motivated an industry/university cooperation to reveal mechanisms of CH_2O generation in wood so that they could be manipulated for some benefit.

All organic wood components are capable of generating CH_2O, but lignin appears to be the major source [3, 6]. Wood extractives are not addressed here, but it is known that the extractives will directly generate CH_2O [3], or they may catalyze CH_2O generation [5], or they react with CH_2O such that emissions are reduced [7-12]. Excluding extractives, this is a study of Virginia pine (*Pinus virginiana*) to determine the CH_2O generation potential of its structural biopolymers. Specimens were heated at 200°C for 10 or 60 min, where the 10 min treatment simulates industrial hot-press conditions. Under relatively mild heating conditions (~25°C – 200°C) it has often been reported that hemicelluloses are the least thermally stable polymers in wood, and that lignin is substantially more stable. [13-19] However, these conclusions were based upon the determination of acid insoluble lignin (Klason lignin), which is a crude analysis that does not reveal subtle changes in lignin structure. Preferred methods for assessing the thermal stability of in situ lignin are the lignin monomer analyses such as thioacidolysis [20, 21], and derivatization followed by reductive cleavage (DFRC) [22]. For example, thioacidolysis shows that lignin β-aryl ether bonds undergo substantial cleavage and repolymerization at heating conditions that effect little or no change in the hemicelluloses. [23-25]

Like most woods, Virginia pine is naturally acidic and in situ lignin thermochemistry might be described by the classic lignin acidolysis literature. Extensive acidolysis studies on model compounds and isolated lignins indicate that β-aryl ether bonds are readily cleaved via a benzylic carbocation reacting in one of two pathways, C2 cleavage or C3 cleavage, Figure 4.1. [26-31] C2 cleavage produces CH_2O, a phenylacetaldehyde derivative, and a free phenol; whereas C3 cleavage produces the Hibbert's ketones and a free phenol. The relative occurrence of these pathways depends upon the nature of the acid catalyst. [32, 33] This suggests that CH_2O formation in whole wood could be manipulated by the selection of external acid catalyst. That prediction is confirmed here, where CH_2O generation in Virginia pine is studied under various heating conditions.

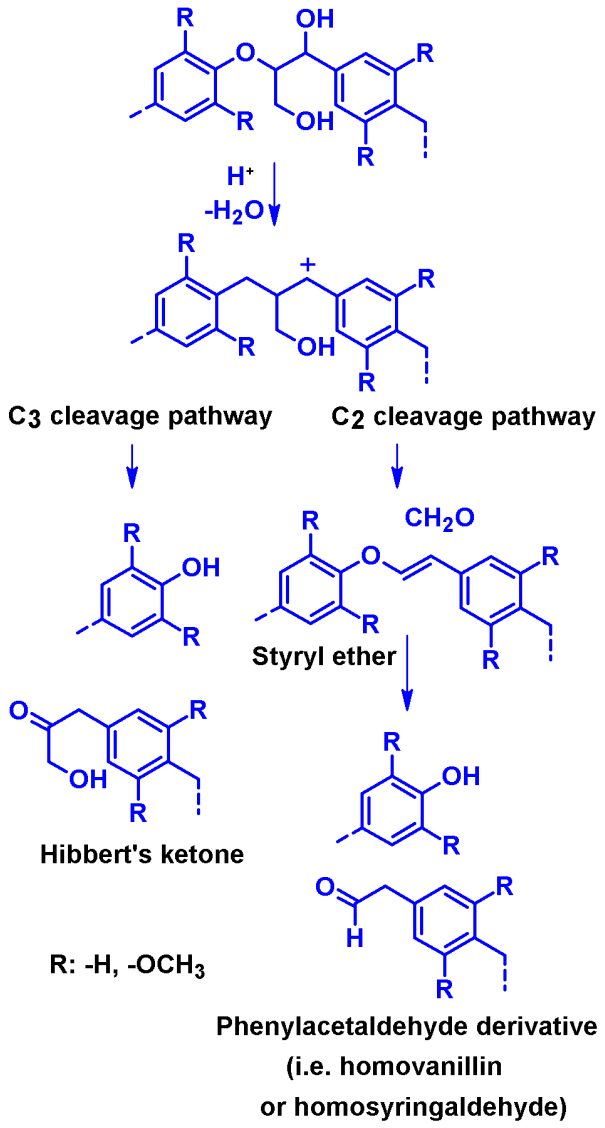

Figure 4.1. Pathways for the acid-catalyzed cleavage of lignin β-aryl ether linkages. [26-31]

4.3. Materials and Methods

Two healthy Virginia pine (*Pinus virginiana*) trees, 70-80 years old, were felled in a natural, wooded region (~4 ha) east of Blacksburg, VA, U.S.A., (Nellies Cave area). Stem sections (~15 cm thick) were cut from locations that were 1.0-1.3 m above ground.

Tree 1: fresh sections were air dried for 7 days, immersed in water for 3 days, debarked, and processed into flakes (70×100×0.5 mm, tan.×long.×rad.). The first 10 years of juvenile tissue was excluded. Flakes were stored in the open laboratory at room temperature for ~5 months.

Prior to aqueous pretreatment/heating, flakes were razor cut into smaller pieces (~0.5×0.5×0.5 mm).

Tree 2: fresh sections were processed into flakes as above, but immediately after felling with no water immersion, and no open-air storage; juvenile and mature tissues were combined and randomized. Specimens were stored at -80°C. Also obtained from tree 2 were six increment cores (5 mm dia) at ~1.4m above ground from a 100 cm^2 area; they were transported to the laboratory and razor cut into ~1mm thick disks; juvenile (first 10 rings from pith) and mature (last 60-70 rings) tissue was isolated and stored at -80°C. Sampling, processing, and storage of all tree 2 specimens was conducted as rapidly as possible in order to minimize atmospheric exposure; from harvest to final storage, 12 hrs elapsed. Prior to aqueous pretreatment/heating, specimens were razor cut into small pieces (~0.5×0.5×0.5 mm).

Specimen pretreatment/heating/CH_2O measurement

Specimens were dried by cycling between vacuum (0.15 mm Hg) and dry N_2, three times, and then stored with dry N_2/P_2O_5 (tree 1) or dry N_2/molecular sieves (tree 2) until reaching constant weight. Prior to heating, unextracted specimens were pretreated as follows: 1) Dry control, no treatment, 2) saturated in HPLC water, 3) saturated in 10 mmol acid, 4) saturated in 10 mmol NaOH. Saturated specimens were subsequently adjusted to 100% moisture content. Heat treatments were conducted in sealed 50 ml serum bottles for 10 or 60 min. [4] The CH_2O generated during heating remained sealed in the serum bottle and was determined as in [4]. Specimens were identified with respect pretreatments prior to heating (Dry; H_2O; Acid; Base) and heating time, i.e. Dry/10, Acid/60, etc.

Cellulose (Sigma-Aldrich, powder, cotton linters) and xylan (Sigma-Aldrich, beechwood, ≥90%, HPLC grade) were pretreated as above, subjected to heating and CH_2O determination as above, using 100 mg specimens.

Compositional analysis

Specimens were Soxhlet extracted (95% ethanol, 48 hours), ground, sieved to retain the >40 mesh fraction, vacuum dried, and subjected to duplicate compositional analysis as in

NREL/TP-510-42618: Determination of Structural Carbohydrates and Lignin in Biomass. Ion chromatography (IC, Metrohm) was used for sugar analysis.

Buffer Capacity

Unextracted tree 1: ground and sieved to retain the 20-80 mesh fraction, then vacuum dried over N_2/P_2O_5. Roughly 3 g powder suspended in 300 ml NaCl (1 mM) solution for 30 min with continuous stirring under N_2, then titrated with NaOH standard solution (25 mM) to reach pH = 10 for acidic buffering capacity; or titrated with HCl standard solution (25 mM) to reach pH = 3 for alkaline buffering capacity. Analyses conducted in triplicate. Duplicate analyses of unextracted tree 2 specimens (0.2 g mature tissue) were conducted similarly using particles >40 mesh, and titrated with standard solutions with concentration 20 mM in 100 ml saline. All buffering measurements were corrected using blanks (saline solution without wood).

Thioacidolysis

Unextracted tree 2 and tree 1 specimens (mature tissue) were subjected to heating as described above, and control specimens (no heating), were Soxhlet extracted (95% ethanol, 48 hours), air dried, ground and sieved to retain > 40 mesh fraction, then vacuum dried as above. Roughly 10 mg extracted wood powder reacted with 10 ml thioacidolysis reagent (dioxane:ethanthiol:BF_3 etherate=43.75:5:1.25, v:v:v) in a 20 ml screw-cap test tube (under dry N_2, 100°C, 4 hours) with continuous stirring, as described by Lapierre et al [20, 21].

Methoxyl Content Determination

Tree 2 specimens (mature tissue) were Soxhlet extracted (95% ethanol, 48 hours), ground and sieved to retain > 40 mesh fraction, and subjected to duplicate analysis as in ASTM D1166-84: standard test method for methoxyl groups in wood and related materials.

4.4. Results and discussions

When tree 1 specimens were heated at 200°C (60 min) in the dry state (no aqueous pretreatments), CH_2O generation correlated with major thermochemical changes in lignin and minor changes in the polysaccharides, Table 4.1. CH_2O generation was about 30 times greater

than previously reported for similar specimens heated at 200°C for only 10 min. [5] Among the sugars only minor to moderate reductions in xylose and arabinose were observed. Whereas thioacidolysis yields decreased dramatically, while the total (soluble + insoluble) lignin content increased slightly. This indicates substantial lignin cleavage and repolymerization and, as previously reported, demonstrates that Klason lignin analysis is inappropriate for judging thermal stability in lignocellulose [23-25]. As per the lignin acidolysis literature, it appears that CH_2O was generated through the C2 cleavage pathway, while the polysaccharides were largely resistant to heating. This interpretation is consistent with the prior analysis of isolated lignin, cellulose, and monosaccharides. [3] It is reemphasized that wood extractives are not addressed here, and the complex role played by the extractives will be reported later. In that regard, wood extractives from tree 1 were likely altered through air oxidation since tree 1 specimens were stored in the open-air for five months.

Table 4.1. CH_2O generated in dry, tree 1 specimens due to heating (200°C, 60 min), and the corresponding compositional analysis and thioacidolysis yield of experimental and control specimens. Standard deviations in parentheses (n ≥ 3).

Tree 1	**Compositional analysis (% dry wood mass)**						**Thioacidolysis yield**	**Measured CH_2O**
	glu	xyl	gal	ara	man	Total lignin	**(μmol/g wood)**	
Control	44.4 (0.5)	6.8 (0.0)	4.2 (0.2)	1.1 (0.1)	12.7 (0.0)	28.1 (0.0)	287.5 (13.4)	0.4 (0.1)
Dry/60	44.2 (1.1)	6.6 (0.1)	4.1 (0.1)	0.9 (0.0)	12.6 (0.2)	28.6 (0.1)	33.5 (4.2)	44.3 (6.3)

Tree 2 specimens were processed to minimize aging effects and subjected to a broader and more damaging array of thermal treatments- dry and wet conditions, with or without tosylic acid catalysis- where CH_2O generation was accompanied by thermochemical changes in both lignin and the polysaccharides, Table 4.2. As above, heating under dry conditions caused little or no sugar decomposition; whereas aqueous pretreatments caused significant sugar degradation that was more extensive under acid catalysis. As thermal treatments became more

extreme, CH_2O generation increased, yields of soluble and insoluble lignin increased, and the corresponding thioacidolysis yields decreased. However note that H_2O/10 specimens generated CH_2O with no detectable reduction in thioacidolysis yield. This might suggest that incipient CH_2O generation is dominated by reaction of β-5 linkages (not detected in thioacidolysis); but this is in contradiction to model compound studies [31], and the anomaly perhaps indicates a deficiency in thioacidolysis sensitivity. Note that lignin methoxyl groups were cleaved by aqueous treatments with and without external acid catalysis, and to an extent far exceeding CH_2O generation. The resulting methanol is not expected to form CH_2O thermochemically, but the corresponding lignin catechols are noteworthy for potentially significant reactions. The sugar decomposition noted in Table 4.2 raises the distinct possibility that polysaccharides contribute to CH_2O generation under more damaging heat treatments. If so, then monosaccharide decomposition did not lead to an equimolar production of CH_2O, consistent with the known propensity of monosaccharides to form furans and relatively little CH_2O. [34, 35]

Insight on the potential CH_2O generation by wood polysaccharides was obtained by subjecting isolated cellulose and xylan to 200°C, 10 min heating with water and acid pretreatment, Table 4.3. Note that all unheated control specimens contained CH_2O (particularly high in xylan) and the CH_2O yields were corrected for this initial content. Relative to simple water pretreatment (H_2O/10), acid catalysis increased CH_2O generation in xylan and cellulose 2-4 times; but acid catalysis in whole wood increased CH_2O generation seven fold. If CH_2O yields from isolated cellulose and xylan are downwardly weighted for their respective compositions in whole wood, their total contribution to CH_2O generation in whole tissue would range from 2-3%.

Schäfer and Roffael [3] conducted similar work using isolated cellulose and various pure monosaccharides; their findings suggested that the polysaccharides would contribute to much less than 1% of the total CH_2O generated in whole wood. Of course isolated polysaccharides and monosaccharides are probably poor models of in situ polysaccharide degradation. For instance, when isolated cellulose and xylan were heated in the dry state (i.e. Dry/10), the measured CH_2O yields (data not shown) far exceeded the corresponding polysaccharide

degradation noted in Table 4.2. The models for in situ polysaccharide used here, and elsewhere [3], are poor and incomplete.

Table 4.2. CH_2O generated in tree 2 specimens due to 200°C heating (10 or 60 min) under various conditions, and the corresponding compositional analysis, methoxyl content, and thioacidolysis yield of experimental and control specimens. Standard deviations in parentheses (n ≥ 2).

Tree 2	% Sugar					% Lignin		Methoxyl Content#	Thioacid. Yield	CH_2O
	based on dry wood mass									
	glu	xyl	gal	ara	man	Sol.	Insol.	µmol/g dry wood		
Control	42.8 (0.1)	6.1 (0.1)	2.6 (0.0)	1.4 (0.0)	14.9 (0.1)	2.4 (0.1)	26.0 (0.3)	1596.9 (148.4)	314.6 (5.2)	0.1 (0.1)
Dry/10	42.7 (0.1)	6.2 (0.6)	2.7 (0.3)	1.3 (0.0)	14.9 (0.0)	2.5 (0.1)	26.0 (0.1)	-	-	0.9 (0.2)
H_2O/10	41.3 (0.0)	4.5 (0.0)	1.9 (0.1)	0.7 (0.1)	13.4 (0.1)	3.6 (0.1)	27.2 (0.1)	1006.5 (48.4)	328.2 (14.9)	4.2 (1.4)
Acid/10*	40.2 (0.1)	4.0 (0.1)	1.5 (0.0)	0.6 (0.1)	12.7 (0.0)	3.8 (0.1)	28.0 (0.0)	1032.3 (32.3)	100.7 (18.2)	29.7 (4.6)
Dry/60	42.5 (1.1)	6.0 (0.1)	2.5 (0.1)	1.1 (0.0)	14.8 (0.2)	2.6 (0.0)	26.3 (0.0)	-	-	-
H_2O/60	39.8 (0.2)	3.5 (0.0)	1.4 (0.0)	0.5 (0.0)	9.9 (0.0)	4.5 (0.2)	31.8 (0.2)	874.3 (93.6)	152.5 (3.8)	42.0 (1.8)
Acid/60*	34.1 (0.1)	2.0 (0.0)	1.1 (0.0)	0.5 (0.0)	6.1 (0.0)	5.8 (0.1)	38.8 (0.0)	735.5 (51.6)	26.3 (7.0)	120.1 (31.7)

*10 mM tosylic acid; #Duplicate analysis

Nevertheless, when considering all observations, Tables 4.1-4.3, we suggest that polysaccharide degradation contributes to less than 5% of the total CH_2O generated in whole tissue; and during milder heating conditions it is probably much less than 1%. Other methods

are required to prove this hypothesis, and once again be reminded that effects from wood extractives are simply omitted here. A definitive picture of CH_2O generation and its origins in whole wood could feasibly be obtained through the analysis of carbon isotope ratios. Stable isotopes undergo increasing degrees of fractionation as metabolic pathways are further removed from carbon fixation. [36-38] Consequently, careful measurement of carbon isotope ratios in biogenic CH_2O should reveal the relative contributions of lignin, polysaccharide, and extractives.

Table 4.3. CH_2O generation from isolated cellulose, xylan, and tree 2 mature tissue due to 200°C, 10 min heating with H_2O and acid (TsOH) pretreatment, and initial levels in unheated controls. Standard deviations in parentheses; n = 3.

	Measured CH_2O		
	Cellulose	**Xylan**	**Tree 2**
	µmol/g dry sample		
Control*	0.1 (0.0)	1.0 (0.1)	0.1 (0.1)
H_2O/10	0.3 (0.1)	0.4 (0.2)	4.2 (1.4)
Acid/10	1.0 (0.2)	0.8 (0.1)	29.6 (4.6)

* Numbers for unheated controls specimens subtracted from those of heated specimens.

Among the structural polymers, lignin appears to be the overwhelming source of biogenic CH_2O in lignocellulose. Consequently we should anticipate the manipulation of CH_2O generation through the application of acid or alkaline pretreatments. Particularly in the case of acid treatments, since the lignin acidolysis literature indicates that C2 cleavage is promoted by acids having larger counterions. [32, 33] Largely this prediction appears to be true, as shown in Figure 4.2. Among the acid halides studied, HBr and HI were equally effective, and both were more active than HCl. Between the sulfonic acids, dodecylbenzenesulfonic acid (DBSA) had a much greater catalytic effect than tosylic acid, and tosylic acid was a little more effective than

HCl. Note that phenylacetaldehyde (homovanillin) endgroups (produced by C2 cleavage, Figure 4.1) were not detected by carbon-proton correlation NMR. This suggests that repolymerization occurred rapidly as Lahive et al. [31] found using model compounds.

Figure 4.2, sharply contrasted to acid pretreatment was that NaOH did not promote CH_2O generation; alkali slightly reduced it. This suggests that alkaline phenolic adhesives (resoles) might suppress biogenic CH_2O generation in wood composites. However, terminal phenolic β-aryl ether, and phenolic β-5 structures are a known source of CH_2O emission during alkaline pulping. [39, 40] The alkaline reaction is initiated by phenol ionization and quinone methide formation, whereafter a retro-aldol reaction releases CH_2O from the gamma sidechain position to form styryl ethers and stilbenes. In fact styryl ethers were detected during the cure of alkaline resol resins with pine wood. [41] Under this scenario alkaline treatment is expected to promote CH_2O generation, but perhaps at lower levels than acids that react along the entire chain length (However Sturgeon et al. [30] suggest that acidolysis will occur by "unzipping" initiated at phenolic endgroups). Since alkali slightly suppressed CH_2O generation (Figure 4.2), perhaps phenolic endgroups did not react and acidolysis was suppressed by neutralization of wood acids. In this regard note that the alkaline and acid buffering capacity of Virginia pine specimens (tree 1 and tree 2) was respectively 0.05-0.08 mM HCl and 0.03-0.05 mM NaOH, so the wood buffer capacity was easily exceeded by all acid and alkaline pretreatments used here. Consequently it is surprising that alkaline pretreatment did not promote CH_2O generation above that seen with neutral water pretreatment.

The findings here appear to confirm literature predictions that the lignin C2 cleavage pathway can be manipulated in solid wood. [32, 33] This is a satisfying testament to the great and continuing history of acidolysis research on lignin models and isolated lignins. The wood composites industry should aspire to reap benefit from this field, which is still growing through biorefinery research. For instance, lignin acidolysis studies reveal interesting strategies to manipulate the reactions depicted in and related to Figure 4.1, where the general goal is to improve delignification by preventing lignin repolymerization. [31, 42, 43, 44] In the context of wood composite manufacture, perhaps in situ lignin reactions could be manipulated for some

benefit. Perhaps the intentional promotion of crosslinking through lignin repolymerization and/or reactions of biogenic CH_2O could be useful.

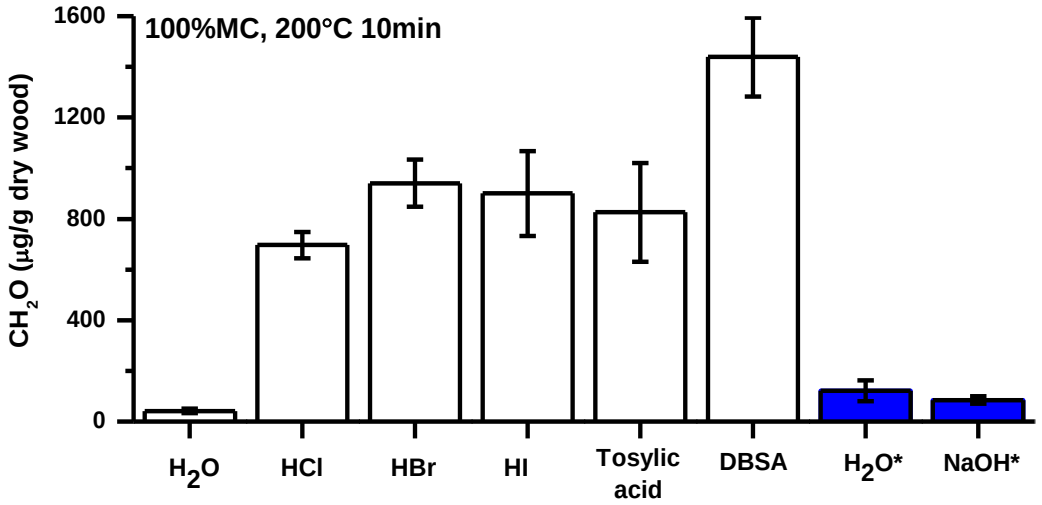

Figure 4.2. CH_2O generation from 200°C, 10 min heating and aqueous/acid pretreatment (tree 1) and aqueous/alkaline pretreatment (tree 2 mature tissue; * blue). DBSA = dodecylbenzenesulfonic acid. Error bars = ±1 standard deviation; n ≥ 3.

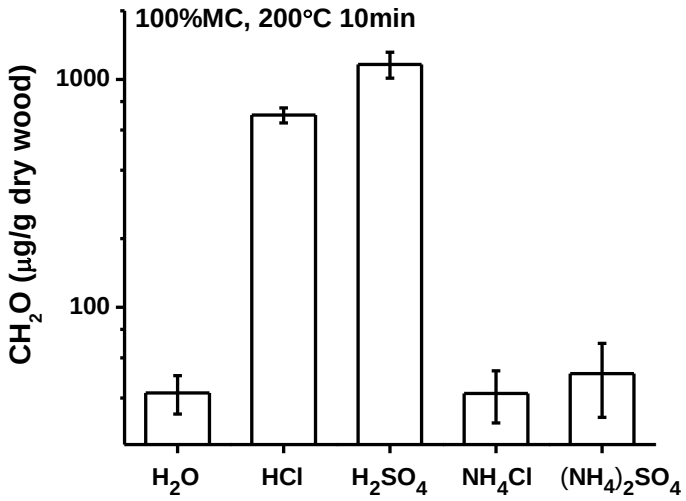

Figure 4.3. CH_2O generation (log scale) from 200°C, 10 min heating of tree 1 specimens with aqueous/acid pretreatment including acid ammonium salts. Error bars = ± 1 standard deviation; n ≥ 9.

In loose analogy to the latter case, it is probable that current industrial practice involves the reaction of biogenic CH_2O with the ammonium salts of amino resin catalysts. For instance, ammonium sulfate is used to catalyze urea-formaldehyde resins where the CH_2O/NH_3 reaction releases H_2SO_4 that catalyzes resin cure. [45] The concept is demonstrated in Figure 4.3 where it is seen that wood heat treatments with aqueous ammonium acid salts result in less detectable CH_2O. This CH_2O scavenging produces hexamethylenetetramine that reacts very slowly with the acetylacetone reagent used for CH_2O quantitation. [46] Nevertheless, the choice of ammonium acid salt still impacted the C2 cleavage pathway, where ammonium sulfate produced slightly more CH_2O than ammonium chloride did ($p = 0.18$). Finally, it is clear that the saturated wood conditions and acid concentrations used here do not reflect bondline conditions in wood composite manufacture. Nevertheless, the effects anticipated during industrial manufacture should reflect our findings. Furthermore, the free CH_2O (including hemiformals) dissolved in wood exists in a complex, moisture dependent equilibrium. [4] None have determined the precise relationship between gaseous emissions and the free CH_2O in wood, but a direct relationship appears very likely. [47, 48] Hopefully these findings can benefit the wood-based composites industry, and the sustainable use of timber resources.

4.5. Conclusions

Hot-press conditions used to manufacture wood-based composites cause the generation of natural, biogenic CH_2O from wood. In order to reveal mechanisms of CH_2O generation, Virginia pine specimens were subjected to heating under dry conditions and with aqueous/acid pretreatments. Among the wood structural polymers, it was demonstrated that lignin was the overwhelming source of biogenic CH_2O, consistent with prior reports. Well-established acidolysis studies of lignin model compounds and isolated lignins predict that in situ, whole wood, reactions will follow the C2 or C3 cleavage pathways depending upon the nature of the acid catalyst. Observations here seem to confirm that prediction, where acids with larger counterions promoted more CH_2O generation via the C2 pathway. Not addressed here are the complex effects wood extractives, the subject of a subsequent report. The findings suggest that

lignin reactions can be manipulated during composite manufacture to minimize CH_2O emissions from composite panels, promote other useful reactions, or both.

Acknowledgements. This project was supported by the Wood-Based Composites center, a National Science Foundation Industry/University Cooperative Research Center (Award #1035009). Partial funding was also supplied by the Virginia Agricultural Experiment Station and the McIntire Stennis Program of the National Institute of Food and Agriculture, U.S. Department of Agriculture.

4.6. References

1. Meyer, B. and C. Boehme, *Formaldehyde emission from solid wood.* For. Prod. J, 1997. **47**(5): p. 45.
2. Martinez, E. and M.I. Belanche, *Influence of veneer wood species on plywood formaldehyde emission and content.* Holz Als Roh-Und Werkstoff, 2000. **58**(1-2): p. 31-34.
3. Schafer, M. and E. Roffael, *On the formaldehyde release of wood.* Holz Als Roh-Und Werkstoff, 2000. **58**(4): p. 259-264.
4. Tasooji, M. and C.E. Frazier, *Simple milligram-scale extraction of formaldehyde from wood.* ACS Sustainable Chemistry & Engineering, 2016. **4**(9): p. 5041- 5045.
5. Tasooji, M., G. Wan, G. Lewis, H. Wise, and C.E. Frazier, *Biogenic formaldehyde: Content and heat generation in the wood of three tree species.* **Chapter 3** in this dissertation.
6. Tjeerdsma, B.F., M. Boonstra, A. Pizzi, P. Tekely, and H. Militz, *Characterisation of thermally modified wood: molecular reasons for wood performance improvement.* Holz Als Roh-Und Werkstoff, 1998. **56**(3): p. 149-153.
7. Kalisch, J.H., *Alkali-formaldehyde pretreatment of coniferous woods in sulphite pulping.* Pulp Pap Mag Can, 1969. **21**: p. 55-68.
8. Lelis, R., E. Roffael, and G. Becker, *Zum Verhalten von Splint-und Kernholz der Kiefer bei der Verleimung mit Diisocyanat-Klebstoffen (PMDI).* Holz Zentralblatt, 1992. **134**: p. 2204-2210.

9. H., S. and R. E, *Untersuchungen der Schälfurnier-Eignung von in Deutschland erwachsenem Douglasienholz.* Holz Roh Werkst, 1993. **51**: p. 167-176.

10. Dix, B. and E. Roffael, *Einfluß der Verkernung und des Baumalters auf die Eigenschaften von Spanplatten aus Kiefernholz (Pinus sylvestris) Teil 1: Kernholz und seine Eigenschaften.* Holz als Roh-und Werkstoff, 1997. **55**(1): p. 25-33.

11. Buyuksari, U., N. Ayrilmis, E. Avci, and E. Koc, *Evaluation of the physical, mechanical properties and formaldehyde emission of particleboard manufactured from waste stone pine (Pinus pinea L.) cones.* Bioresource Technology, 2010. **101**(1): p. 255-259.

12. Hoong, Y.B., M.T. Paridah, Y.F. Loh, M.P. Koh, C.A. Luqman, and A. Zaidon, *Acacia mangium Tannin as Formaldehyde Scavenger for Low Molecular Weight Phenol-Formaldehyde Resin in Bonding Tropical Plywood.* Journal of Adhesion Science and Technology, 2010. **24**(8-10): p. 1653-1664.

13. Kollmann, F. and D. Fengel., *Changes in the chemical composition of wood by thermal treatment.* Howl als Roh- und Werkstoff 1965. **23**(12): p. 461-468.

14. Fengel, D. and G. Wegener., *Wood: chemistry, ultrastructure, reactions*. 1984: Walter de Gruyter.

15. LeVan, S., R.J. Ross, and J.E. Winandy, *Effects of fire retardant chemicals on the bending properties of wood at elevated temperatures*. 1990, Madison, WI, USA: US Department of Agriculture, Forest Service, Forest Products Laboratory.

16. Mburu, F., S. Dumarcay, F. Huber, M. Petrissans, and P. Gerardin, *Evaluation of thermally modified Grevillea robusta heartwood as an alternative to shortage of wood resource in Kenya: Characterisation of physicochemical properties and improvement of bio-resistance.* Bioresource Technology, 2007. **98**(18): p. 3478-3486.

17. Kocaefe, D., S. Poncsak, and Y. Boluk, *Effect of Thermal Treatment on the Chemical Composition and Mechanical Properties of Birch and Aspen.* Bioresources, 2008. **3**(2): p. 517-537.

18. Esteves, B.M. and H.M. Pereira, *Wood Modification by Heat Treatment: A Review.* Bioresources, 2009. **4**(1): p. 370-404.

19. Gonzalez-Pena, M.M., S.F. Curling, and M.D.C. Hale, *On the effect of heat on the chemical composition and dimensions of thermally-modified wood.* Polymer Degradation and Stability, 2009. **94**(12): p. 2184-2193.

20. Lapierre, C., B. Monties, and C. Rolando, *Thioacidolysis of Lignin - Comparison with Acidolysis.* Journal of Wood Chemistry and Technology, 1985. **5**(2): p. 277-292.

21. Rolando, C., B. Monties, and C. Lapierre, *Thioacidolysis*, in *Methods in lignin chemistry*. 1992, Springer Berlin Heidelberg. p. 334-349.

22. Lu, F.C. and J. Ralph, *Derivatization followed by reductive cleavage (DFRC method), a new method for lignin analysis: Protocol for analysis of DFRC monomers.* Journal of Agricultural and Food Chemistry, 1997. **45**(7): p. 2590-2592.

23. Windeisen, E., C. Strobel, and G. Wegener, *Chemical changes during the production of thermo-treated beech wood.* Wood Science and Technology, 2007. **41**(6): p. 523-536.

24. Assor, C., V. Placet, B. Chabbert, A. Habrant, C. Lapierre, B. Pollet, and P. Perre, *Concomitant Changes in Viscoelastic Properties and Amorphous Polymers during the Hydrothermal Treatment of Hardwood and Softwood.* Journal of Agricultural and Food Chemistry, 2009. **57**(15): p. 6830-6837.

25. Brosse, N., R. El Hage, M. Chaouch, M. Petrissans, S. Dumarcay, and P. Gerardin, *Investigation of the chemical modifications of beech wood lignin during heat treatment.* Polymer Degradation and Stability, 2010. **95**(9): p. 1721-1726.

26. Lundquist, K. and L. Ericsson, *Acid degradation of lignin III formation of formaldehyde.* Acta Chemica Scandinavica, 1970. **24**: p. 3681-3686.

27. Lundquist, K. and R. Lundgren, *Acid Degradation of Lignin .7. Cleavage of Ether Bonds.* Acta Chemica Scandinavica, 1972. **26**(5): p. 2005-&.

28. Lundquist, K., *Low-molecular weight lignin hydrolysis products.* Applied Polymer Symposia, 1976. **28**: p. 1393-1407.

29. Imai, T., T. Yokoyama, and Y. Matsumoto, *Revisiting the mechanism of beta-O-4 bond cleavage during acidolysis of lignin IV: dependence of acidolysis reaction on the type of acid.* Journal of Wood Science, 2011. **57**(3): p. 219-225.

30. Sturgeon, M.R., S. Kim, K. Lawrence, R.S. Paton, S.C. Chmely, M. Nimlos, T.D. Foust, and G.T. Beckham, *A Mechanistic Investigation of Acid-Catalyzed Cleavage of Aryl-Ether Linkages: Implications for Lignin Depolymerization in Acidic Environments.* Acs Sustainable Chemistry & Engineering, 2014. **2**(3): p. 472-485.

31. Lahive, C.W., P.J. Deuss, C.S. Lancefield, Z.H. Sun, D.B. Cordes, C.M. Young, F. Tran, A.M.Z. Slawin, J.G. de Vries, P.C.J. Kamer, N.J. Westwood, and K. Barta, *Advanced Model Compounds for Understanding Acid-Catalyzed Lignin Depolymerization: Identification of Renewable Aromatics and a Lignin-Derived Solvent.* Journal of the American Chemical Society, 2016. **138**(28): p. 8900-8911.

32. Yasuda, S., K. Adachi, N. Terashima, and K. Ota, *Chemical Structures of Sulfuric-Acid Lignin .8. Reactions of 1,2-Diaryl-1,3-Propanediol and Pinoresinol with Sulfuric-Acid.* Mokuzai Gakkaishi, 1985. **31**(2): p. 125-131.

33. Karlsson, O., K. Lundquist, S. Meuller, and K. Westlid, *On the Acidolytic Cleavage of Arylglycerol Beta-Aryl Ethers.* Acta Chemica Scandinavica Series B-Organic Chemistry and Biochemistry, 1988. **42**(1): p. 48-51.

34. Van Dam, H.E., A.P.G. Kieboom, and H. Van Bekkum, *The conversion of fructose and glucose in acidic media: formation of hydroxymethylfurfural.* Starch-Stärke, 1986. **38**(3): p. 95-101.

35. Antal, M.J., T. Leesomboon, W.S. Mok, and G.N. Richards, *Mechanism of formation of 2-furaldehyde from D-xylose.* Carbohydrate Research, 1991. **217**: p. 71-85.

36. Loader, N.J., I. Robertson, and D. McCarroll, *Comparison of stable carbon isotope ratios in the whole wood, cellulose and lignin of oak tree-rings.* Palaeogeography, Palaeoclimatology, Palaeoecology, 2003. **196**(3): p. 395-407.

37. Harlow, B.A., J.D. Marshall, and A.P. Robinson, *A multi-species comparison of delta13C from whole wood, extractive-free wood and holocellulose.* Tree Physiol, 2006. **26**(6): p. 767-74.

38. Taylor, A.M., J.R. Brooks, B. Lachenbruch, J.J. Morrell, and S. Voelker, *Correlation of carbon isotope ratios in the cellulose and wood extractives of Douglas-fir.* Dendrochronologia, 2008. **26**(2): p. 125-131.

39. Balakshin, M.Y., E.A. Capanema, C.L. Chen, and H.S. Gracz, *Elucidation of the structures of residual and dissolved pine kraft lignins using an HMQC NMR technique.* Journal of agricultural and food chemistry, 2003. **51**(21): p. 6116-6127.

40. Dimmel, D.R. and G.G. Gellerstedt, *Chemistry of alkaline pulping*, in *Lignin and Ligans: Advances in Chemistry*, C. Heitner, D.R. Himmel, and J.A. Schmidt, Editors. 2010, Taylor & Francis: Boca Raton, FL. p. 349-391.

41. Yelle, D.J. and J. Ralph, *Characterizing phenol-formaldehyde adhesive cure chemistry within the wood cell wall* International Journal of Adhesion and Adhesives, 2016. **70**(26-36).

42. Li, J. and G. Gellerstedt, *Improved lignin properties and reactivity by modifications in the autohydrolysis process of aspen wood.* Industrial Crops and Products, 2008. **27**(2): p. 175-181.

43. Toledano, A., L. Serrano, and J. Labidi, *Improving base catalyzed lignin depolymerization by avoiding lignin repolymerization.* Fuel, 2014. **116**: p. 617-624.

44. Shuai L., Amiri M. T., Questell-Santiago Y. M., Heroguel F., Li Y., Kim H., Meilan R., Chapple C., Ralph J., Luterbacher J. S., *Formaldehyde stabilization facilitates lignin monomer production during biomass depolymerization.* Science, 2016. **354**(6310): p. 329-333.

45. Stefke, B. and M. Dunky, *Catalytic influence of wood on the hardening behavior of formaldehyde-based resin adhesives used for wood-based panels.* Journal of Adhesion Science and Technology, 2006. **20**(8): p. 761-785.

46. Nash, T., *The Colorimetric Estimation of Formaldehyde by Means of the Hantzsch Reaction.* Biochemical Journal, 1953. **55**(3): p. 416-421.

47. Myers, G.E., *Mechanisms of formaldehyde release from bonded wood products.* In ACS Symposium series-American Chemical Society (USA), 1986.

48. Birkeland, M.J., L. Lorenz, J.M. Wescott, and C.R. Frihart, *Determination of native (wood derived) formaldehyde by the desiccator method in particleboards generated during panel production.* Holzforschung, 2010. **64**(4): p. 429-433.

Chapter 5 Pine extractives control lignin reactions and the formation of biogenic formaldehyde

Guigui Wan, and Charles E. Frazier

Macromolecular Science & Engineering, Sustainable Biomaterials

Virginia Tech, Blacksburg VA 24061, U.S.A

5.1. Abstract

Wood contains natural, biogenic formaldehyde (CH_2O), and heating generates much more. Heat generation of CH_2O in Virginia pine and radiata pine was substantially reduced by extractives removal, but there was no such effect in yellow-poplar wood. Results suggested that pine extractives promote CH_2O generation by catalyzing or otherwise promoting C2 cleavage (acidolysis) in lignin. Thioacidolysis demonstrated that pine lignin reactions were strongly dependent upon the presence or absence of the extractives. When present, pine extractives seemed to promote C2 cleavage (CH_2O generation), but otherwise reduced the overall extent of lignin degradation. When pine extractives were removed, lignin suffered substantial degradation, but apparently less C2 cleavage since CH_2O generation was reduced. In contrast, thioacidolysis showed that yellow-poplar extractives appeared to promote lignin degradation, but extractives removal had no detectable impact on CH_2O generation. Implications exist for biorefinery research because it was shown that lignin reactions can be strongly affected by wood extractives. Hopefully these findings will lead to new strategies for manipulating lignin reactions during the manufacture of wood-based composites.

5.2. Introduction

Wood contains natural, biogenic formaldehyde (CH_2O), and heating generates much higher levels that vary according to moisture content, tissue type, and tree species. [1-5] This has implications for the regulation of CH_2O emissions from nonstructural wood-based composites, where global trends have shown steady reductions in allowable emissions. These long-standing regulations have targeted hydrolytically unstable amino resins, but the latest

regulations restrict allowable emissions to such low levels that biogenic CH_2O might impact regulation compliance. While current emissions regulations have been met with new amino resin technologies, persistent anecdotal reports cite complications attributed to biogenic CH_2O. These concerns motivated an industry/university cooperation to reveal mechanisms of CH_2O generation in wood so that they could be manipulated for some benefit. All organic wood components are capable of generating CH_2O, but lignin is the major source. [3, 6, 7] Recent evidence suggests that lignin generates CH_2O through the well-known lignin acidolysis pathways, Figure 5.1. [7] Lignin β-aryl ether bonds are readily cleaved via a benzylic carbocation acting in one of two pathways, C2 or C3 cleavage, where the former pathway generates CH_2O. [8-15] In other words, acidolysis studies using model compounds and isolated lignins predict that CH_2O generation in solid wood can be manipulated by the selection of external acid catalyst, and this was confirmed. [7]

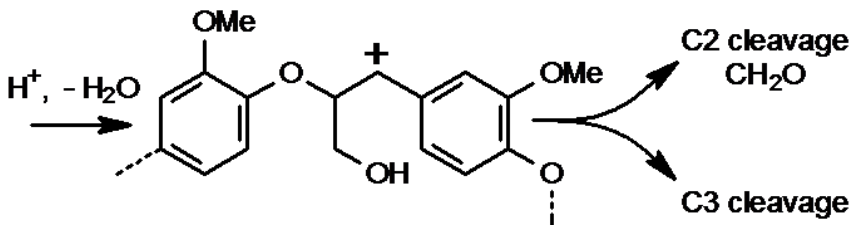

Figure 5.1. Lignin acidolysis pathways; only C2 cleavage produces CH_2O.

However, that previous report ignored the influence of wood extractives, which themselves might participate in lignin catalysis, [5] or upon heating might directly generate CH_2O; [3]or the extractives might reduce emissions by reacting with (scavenging) CH_2O. [16-21] Schäfer and Roffael [3] provided data that suggested a catalytic role of wood extractives in CH_2O generation; but the discussion of that possibility appeared elsewhere. [5] In the present study, wood from three tree species (*Pinus virginiana, Liriodendron tulipifera,* and *Pinus radiata*) was studied with respect to the impact of extractives removal on CH_2O generation during heating (200°C, 10 min). The effects of extractives reconstitution (putting the extractives back into *Pinus virginiana* wood) were studied. Furthermore, lignin transformations in *Pinus virginiana* and *Liriodendron tulipifera* were studied using thioacidolysis as a function of extractives removal and the corresponding heat-generation of CH_2O.

5.3. Materials and methods

Increment cores from Virginia pine, yellow-poplar, and radiata pine trees were sampled, razor cut into 1 mm thick sections, and stored as described in a previous publication. [5] Additionally, two healthy Virginia pine trees, 70-80 years old, were felled in a natural, wooded region east of Blacksburg, VA, U.S.A., (Nellies Cave area). Stem sections (~15 cm thick) were cut from locations that were 1.0-1.3 m above ground. Processing and storage details specific to these two Virginia pines are as follows.

Tree 1: fresh sections were air dried for 7 days, immersed in water for 3 days, debarked, and processed into flakes (~70×100×0.5 mm, tan.×long.×rad.). The first 10 years of juvenile tissue was excluded. Flakes were stored in the open laboratory at room temperature for ~5 months. Prior to solvent extraction or specimen heating, flakes were razor cut into smaller pieces (~0.5×0.5×0.5 mm).

Tree 2: fresh sections were processed into flakes as above, but immediately after felling with no water immersion, and no open-air storage; juvenile and mature tissues were combined and randomized. Specimens were stored at -80°C. Also obtained from tree 2 were six increment cores (5 mm dia) at ~1.4 m above ground from a 100 cm^2 area; they were transported to the laboratory and razor cut into ~1 mm thick disks; juvenile (first 10 rings from pith) and mature (last 60-70 rings) tissue was isolated and stored at -80°C. Sampling, processing, and storage of all tree 2 specimens was conducted as rapidly as possible in order to minimize atmospheric exposure; from harvest to final storage, 12 hrs elapsed. Prior to solvent extraction or specimen heating, flakes were razor cut into small pieces (~0.5×0.5×0.5 mm).

Specimen solvent extraction

Specimens were dried by cycling between vacuum (0.15 mm Hg) and dry N_2, three times, and then stored with dry N_2/P_2O_5 (Virginia pine tree 1) or dry N_2/molecular sieves (Virginia pine tree 2) until reaching constant weight, whereafter solvent extraction occurred in one of two ways. Soxhlet extraction: ~10 g of wood flakes, 95% ethanol, 200 ml/48 hours reflux. Room temperature (RT) extraction: ~50 g wood flakes, 95% ethanol, 1000 ml/48 hours followed by

fresh 1000 ml/24 hours, all at room temperature under high purity N_2 with continuous mechanical stirring, and with the extraction flask wrapped in foil to prevent light exposure. After extraction, wood specimens were air dried, and then vacuum dried as described above.

Extractives isolation/fractionation

Extractives solutions from above were rotary evaporated (room temperature, 2.7 KPa; 20 mm Hg), then vacuum dried (room temperature, 0.02 kPa; 0.15 mm Hg) to yield the whole raw extract (total extract). A portion of the total extract (5 g) was dissolved into alkaline ethanol (50 mL, 2M KOH in 95% ethanol); 50 mL water was added, and the mixture was partitioned against CH_2Cl_2 (3 x 50 mL). The combined organic phase was washed with water (3 x 50 mL), dried with $MgSO_4$, and concentrated as above to obtain the neutral fraction. The alkaline ethanol solution was acidified to pH ≤ 3 with HCl (37wt%) and partitioned against CH_2Cl_2 (3 x 50 mL); the combined organic phase was washed with water (3 x 50 mL), dried with $MgSO_4$, and concentrated as above to obtain the acid fraction. Total recoveries from this fractionation ranged from 91-93%, and extract samples were stored in closed vials under N_2 at -10°C.

Extractives reconstitution into wood

Portions from the isolated extractives (total extract) where dissolved into 95% ethanol and subjected to serial dilution to provide 3 solutions covering a range of concentrations. Reconstitution occurred by dipping dry, extracted pine flakes into these solutions (1 sec), removing from solution and placed on petri dish, air dried and then vacuum dry as described above.

CH_2O measurement

The CH_2O generation of wood specimens (~ 10 mg), and isolated extract specimens (~50 mg), was determined by heating (200°C, 10 or 60 min) within sealed 50 ml serum bottles that retain volatiles and allow CH_2O quantitation as previously described. [22] Control specimens (wood specimens: 20 mg, and isolated extract specimens: 100 mg) were subjected CH_2O quantitation but never heated.

Thioacidolysis

Thioacidolysis was conducted on Virginia pine (tree 2, mature tissue) and yellow-poplar (sapwood tissue) specimens as a function of extractives removal, and heating (200°C, 10 or 60 min). Wood specimens were ground and sieved to retain the >40 mesh fraction, vacuum dried as above, then subjected to thioacidolysis. [7, 23, 24] Specimens were identified by heating time (10 or 60 min) with respect the sequence of extraction (E) and heating (H). For instance, specimen H10/E, was first heated (10 min), then extracted and analyzed by thioacidolysis; whereas specimen E/H60 was first extracted, then dried, heated (60 min) and analyzed by thioacidolysis. Consequently, all thioacidolysis reactions were conducted on extractives free tissue.

5.4. Results and discussions

Increment cores were sampled from healthy, living Virginia pine, radiata pine, and yellow-poplar trees, Table 5.1. From these increment cores, wood specimens were heated (200°C, 10 min) in sealed containers that retain volatiles and allow for simple CH_2O extraction and quantitation. [4] The effects of extractives removal on CH_2O generation are shown in Figure 5.2. Tree species and tissue type effects are seen, as described previously. [5] For both Virginia pine and radiata pine specimens, extractives removal significantly reduced CH_2O generation, and the effects were dramatic in mature wood. Schäfer and Roffael produced similar findings when removing extractives from spruce and pine wood (species not reported). [3] In contrast, CH_2O generation in yellow-poplar wood was not significantly changed by solvent extraction, Figure 5.2. Consequently, pine extractives contribute to CH_2O generation, either directly by thermal degradation, or indirectly perhaps by catalyzing lignin, or possibly by both mechanisms. Southern pine extractives mostly feature fatty acids and resin acids, whereas yellow-poplar extractives are mostly sesquiterpenes, lignans, and tannins. [25-28]

Table 5.1. Specimen information for increment cores used in this study where the extractives content (EC%) was determined through Sohxlet extraction and reported as a percentage based upon dry wood mass. Standard deviations in parentheses. EC% for Virginia pine was averaged over two trees. [5]

Species	**Virginia pine**		**Yellow-poplar**		**Radiata pine**	
Age (years)	60-85		30-40		19-28	
# of trees	5		5		2	
Tissue type	Mature	Juvenile	Sapwood	Heartwood	Mature	Juvenile
EC%	3.5 (1.0)	7.3 (0.5)	3.4 (1.1)	4.3 (0.9)	1.1 (0.2)	2.3 (0.6)

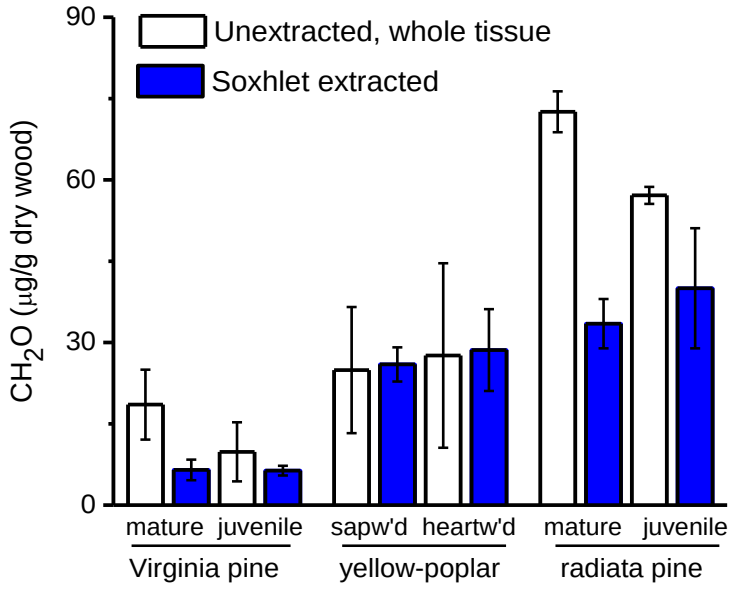

Figure 5.2. The effect of extractives removal (Soxhlet) on CH_2O generation due to heating (200°C 10 min). The number of trees represented is the same as in Table 5.1, except for extracted Virginia pine, which is 2 trees. Number of measurements for each tree/tissue type, n ≥ 3. Error bars = ± 1 standard deviation.

Given the role pine extractives play in CH_2O generation, flakes from Virginia pine tree 1 (aged in the open lab for 5 months) were subjected to two extraction techniques, either standard Soxhlet extraction or simple room temperature (RT) extraction. Both extraction methods were equally effective at removing existing CH_2O (never-heated specimens), but the resulting CH_2O generation was strongly dependent on the extraction technique, Figure 5.3. Extraction yields were 7.4% and 5.6% for Soxhlet and RT extraction respectively; so a 30% reduction in RT extraction efficiency resulted in much greater CH_2O generation, more than three times greater than from Soxhlet extraction. The substantial CH_2O generation resulting from RT extraction seems disproportionate to a 30% reduction in extraction efficiency. This might indicate that mild specimen heating during Soxhlet extraction altered the wood such that CH_2O generation was reduced. Consequently, one wonders if Soxhlet extraction should be excluded from lignin structural analysis. Likewise, Soxhlet extraction is expected to degrade the pine extract as shown in Figure 5.4, which compares the CH_2O generation of the isolated extracts. Soxhlet extraction yielded 75% acid and 25% neutral fractions, where the former generated the most CH_2O per unit mass of Soxhlet extract. In contrast, RT extraction yielded 65% acids and 35% neutrals, and the CH_2O generation from the neutral fraction far exceeded that observed in any extract, regardless of extraction technique. Regarding the RT extract, it seems that compounds in the acid and neutral fractions counteract each other in the total extract, because both the acid and neutral fractions exceeded the CH_2O generation of the total extract. Such interactions among pine extractives will severely complicate the identification of compound-specific effects on CH_2O generation, and no attempts were made to identify any extractive compounds in this study. The complexities revealed in Figure 5.3 are probably further complicated by air oxidation of extractives since Virginia pine tree 1 specimens were stored in the open lab for 5 months.

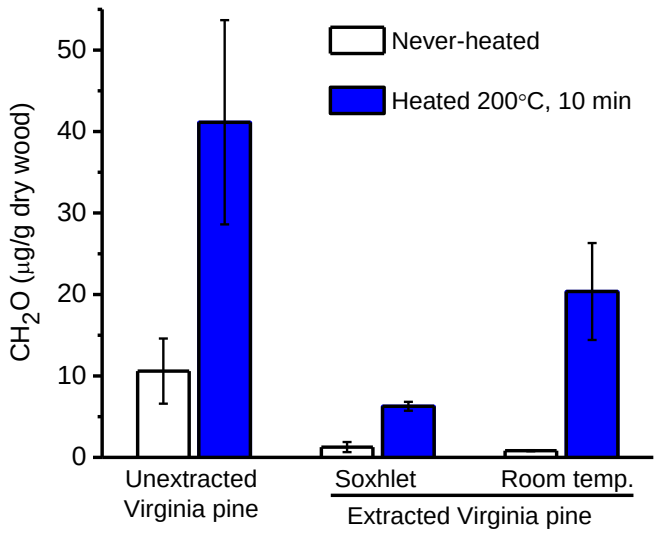

Figure 5.3. Effect of extraction method (Soxhlet or room temperature extraction) on CH_2O generation during heating (200°C 10 min) from Virginia pine (tree 1) flakes. Number of measurements n ≥ 3. Error bar = ± 1 standard deviation.

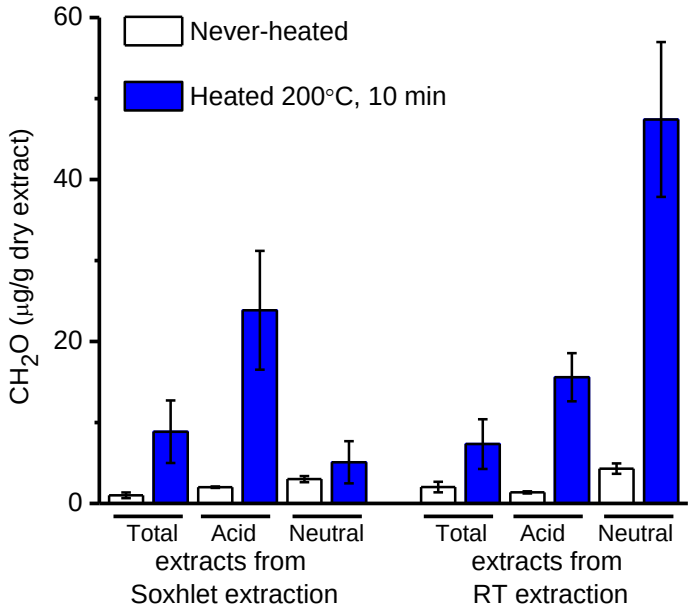

Figure 5.4. CH_2O content and heat generation (200°C, 10 min) total extracts, acid extracts, and neutral extracts obtained from Soxhlet and room temperature (RT) extraction. Number of measurements n ≥ 3. Error bar = ± 1 standard deviation.

Accordingly, a second Virginia pine (tree 2) was harvested and immediately subjected to RT extraction, yielding a fresh total extract (4% on dry wood) with air oxidation minimized. In this case, RT extraction reduced CH_2O generation by 41% (corrected for existing CH_2O in Never-heated specimens), Figure 5.5. Consider the unit mass contribution of extractives to the direct thermochemical generation of CH_2O, where the "CH_2O activity" is defined as µg CH_2O generated per unit mass of heated material (for the total extract in Figure 5.5 this is 6.2 µg CH_2O/g extract). With an extractives content of 4%, and CH_2O activity stated, extractives removal is expected to reduce CH_2O generation by 1%. In other words, extractives removal should reduce CH_2O generation in the extracted wood by 1%, if the extractives only produced CH_2O by direct thermochemical mechanisms. Since the removal of extractives caused a 41% reduction in CH_2O generation, we conclude that pine extractives participate in catalytic interactions that that promote CH_2O generation. This hypothesis was tested by reconstituting the total extract back into the extracted flakes. Dry extractive-free pine flakes were dipped into ethanol solutions of the total extract, dried, and subjected to CH_2O measurement as a function of heating (200°C 10 min), Figure 5.5.

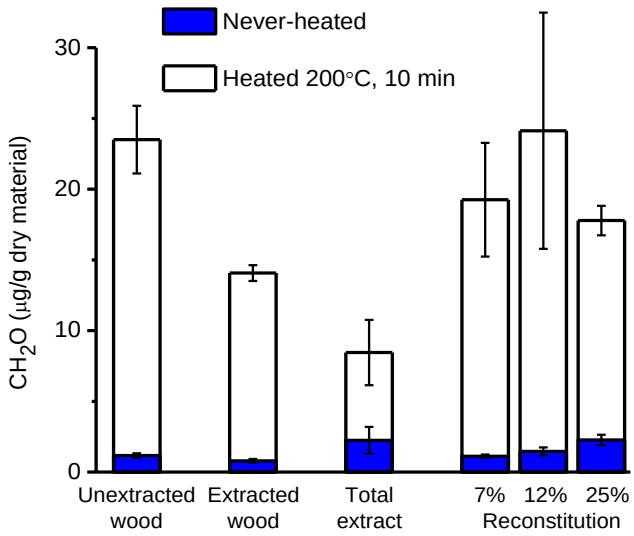

Figure 5.5. CH_2O content and heat generation (200°C, 10 min) from unextracted whole-wood, extracted wood, total extract, and reconstituted Virginia pine flakes. Number of measurement n ≥ 3. Error bars = ± 1 standard deviation.

Notice that 12% reconstitution was required to reach the CH_2O generation observed in the parent, unextracted wood (having only 4% extractives); so the natural state of the wood/extractives interaction was not restored by reconstitution. As reconstitution was increased to 25%, the resulting CH_2O generation was reduced because the total extract has a lower CH_2O activity than the extracted wood.

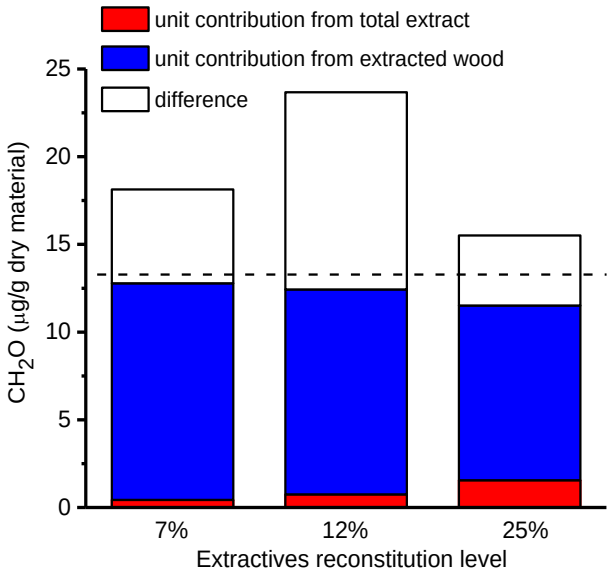

Figure 5.6. CH_2O generation in reconstituted pine flakes, where unit contributions of the total extract (red) and extracted wood (blue) are presented, as calculated from the wood/extract composition and the CH_2O activity (g CH_2O generated/g dry mass) of the total extract and extracted wood. Initial CH_2O levels (Never-heated levels, Figure 5.4) were subtracted. Dash line indicates CH_2O generation of the extracted pine.

The expected unit contributions to CH_2O generation (summing the mass contributions of the total extract and extracted wood) are presented in Figure 5.6. For each level of reconstitution, it was observed that the total CH_2O generation exceeded that which is expected from the combined unit contributions of extract and extracted wood. We conclude that the difference reflects a catalytic interaction between wood and extractives. Schäfer and Roffael reported that solvent extraction of spruce and pine wood removed 2-4% extractives, and that this caused ~50% reduction in CH_2O generation due to heating. [3] They found that resin acids

(i.e. abietic acid) had a large CH_2O activity, but at only 2-4% of dry wood mass, the unit contribution from pure abietic acid does not simply explain a 50% reduction in CH_2O generation due to extractives removal. Pine extractives clearly generate CH_2O, but not enough to simply explain the reduction in CH_2O generation observed in extracted wood. Again we conclude that pine extractives catalyze CH_2O generation in lignin. Also feasible, but perhaps less likely, is that wood polymers catalyze CH_2O generation in pine extractives.

Since lignin is the major source of biogenic CH_2O in lignocellulose, [3, 6, 7] it is feasible that pine extractives catalyze, or otherwise affect, lignin reactions associated with CH_2O generation. Consequently, thioacidolysis was used to monitor lignin changes caused by heating in the presence or absence of wood extractives (Bear in mind that all thioacidolysis reactions were conducted with extractive free wood, as required). Table 5.2 presents CH_2O generation caused by heating (200˚C, 10 or 60 min) Virginia pine and yellow-poplar wood, and the corresponding thioacidolysis yields as a function of extractives removal. When Virginia pine was first heated for 10 minutes and then extracted (H10/E), the thioacidolysis yield was unchanged from that seen in the unheated control. However, when extraction occurred before 10-minute heating (E/H10), the thioacidolysis yield was reduced by 58%, and the corresponding CH_2O generation was reduced by 41%. Note that specimen H10/E produced CH_2O with no loss in thioacidolysis yield. Perhaps incipient CH_2O generation is dominated by reaction of□□-5 linkages (not detected in thioacidolysis); but this is in contradiction to model compound studies, [15] and the anomaly perhaps indicates a deficiency in thioacidolysis sensitivity. When heated for 60 minutes, the Virginia pine thioacidolysis yield was reduced by 52% when extractives were present, but reduced by 66% when extractives were absent. In other words, upon removal of Virginia pine extractives, heating wood results in substantially less CH_2O generation and substantially more lignin degradation. This is in stark contrast to yellow-poplar wood, Table 5.2.

When yellow-poplar extractives were removed, CH_2O generation from wood heating was unchanged, and lignin underwent less degradation. Clearly, Virginia pine extractives (and/or wood extraction processes), significantly affect lignin thermochemistry. Under the catalytic hypothesis, pine extractives appear to promote C2 cleavage (CH_2O generation, Figure 5.1) while somehow limiting the overall extent of lignin degradation.

Table 5.2. CH_2O generation in yellow-poplar (sapwood) and Virginia pine (tree 2, mature tissue) during heating (200˚C, 10 or 60 min), and the corresponding thioacidolysis yield. Number of observations, n ≥ 2 for thioacidolysis, and n ≥ 3 for CH_2O measurements. Standard deviations in parentheses.

		CH_2O generated	Thioacidolysis yield	% thio-yield loss
		μmol/g wood		
Virginia pine (mature)	Control	0.1 (0.1)	314.6 (5.2)	-
	H10/E	4.2 (1.4)	328.2 (14.9)	0
	E/H10	2.5 (0.6)	133.4 (39.4)	58
	H60/E	42.0 (1.8)	152.5 (24.9)	52
	E/H60	30.8 (5.6)	108.2 (2.9)	66
Yellow-poplar (sapwood)	Control	0.1 (0.0)	441.7 (18.5)	-
	H10/E	4.1 (0.3)	388.1 (19.3)	12
	E/H10	3.9 (0.8)	478.3 (28.3)	0
	H60/E	31.4 (4.7)	42.8 (3.2)	90
	E/H60	33.7 (2.1)	52.7 (1.7)	88

However when pine extractives are absent, alternative lignin reactions (like C3 cleavage and others) are strongly promoted, and presumably with less C2 cleavage because CH_2O generation is reduced. In summary, these observations indicate that pine extractives play a major role in lignin thermochemistry, apparently promoting C2 lignin cleavage (CH_2O

generation) to an extent that far exceeds the extractives ability to directly generate CH_2O. Furthermore, Virginia pine extractives appeared to prevent lignin thermochemical change, whereas yellow-poplar extractives promoted lignin reactions. This could have important implications for biorefineries, in that lignin removal could be complicated or even promoted by specific extractive compounds. In the manufacture of wood-based composites, perhaps lignin reactions could be manipulated for some benefit, to reduce or even increase CH_2O generation, or otherwise promote lignin reactions that improve the performance of wood-based composites.

5.5. Conclusions

Wood contains natural, biogenic CH_2O, and heating generates much higher levels. Heat generation of CH_2O in Virginia pine and radiata pine was substantially reduced by extractives removal, but there was no such effect in yellow-poplar wood. Pine extractives directly generated CH_2O, but not enough to simply explain the reduction in CH_2O generation caused by their removal. Results suggested that pine extractives promote CH_2O generation by catalyzing or otherwise promoting C2 cleavage in lignin. Thioacidolysis results were consistent with this hypothesis, where it was observed that pine lignin reactions were strongly dependent upon the presence or absence of the extractives. When present, pine extractives seemed to promote C2 cleavage (CH_2O generation), but otherwise prevented or reduced lignin degradation. When pine extractives were removed, lignin suffered substantial degradation, but apparently less C2 cleavage since CH_2O generation was reduced. In contrast, yellow-poplar extractives appeared to promote lignin degradation (according to thioacidolysis), but they had no detectable impact on CH_2O generation. These results could have implications in biorefinery research because it was shown that lignin reactions can be strongly affected by the wood extractives. Hopefully these findings will lead to new strategies for manipulating lignin reactions during the manufacture of wood-based composites.

5.6. References

1. Meyer, B. and C. Boehme, *Formaldehyde emission from solid wood.* For. Prod. J, 1997. **47**(5): p. 45.
2. Martinez, E. and M.I. Belanche, *Influence of veneer wood species on plywood formaldehyde emission and content.* Holz Als Roh-Und Werkstoff, 2000. **58**(1-2): p. 31-34.
3. Schafer, M. and E. Roffael, *On the formaldehyde release of wood.* Holz Als Roh-Und Werkstoff, 2000. **58**(4): p. 259-264.
4. Tasooji, M. and C.E. Frazier, *Simple Milligram-Scale Extraction of Formaldehyde from Wood.* ACS Sustainable Chemistry & Engineering, 2016. **4**(9): p. 5041-5045.
5. Tasooji, M., G. Wan, G. Lewis, H. Wise, and C.E. Frazier, *Biogenic formaldehyde: Content and heat generation in the wood of three tree species.* **Chapter 3** in this dissertation.
6. Tjeerdsma, B.F., M. Boonstra, A. Pizzi, P. Tekely, and H. Militz, *Characterisation of thermally modified wood: molecular reasons for wood performance improvement.* Holz Als Roh-Und Werkstoff, 1998. **56**(3): p. 149-153.
7. Wan, G. and C.E. Frazier, *Formaldehyde in pine wood forms as predicted by lignin acidolysis.* **Chapter 4** in this dissertation.
8. Lundquist, K. and L. Ericsson, *Acid degradation of lignin III formation of formaldehyde.* Acta Chemica Scandinavica, 1970. **24**: p. 3681-3686.
9. Lundquist, K. and R. Lundgren, *Acid Degradation of Lignin .7. Cleavage of Ether Bonds.* Acta Chemica Scandinavica, 1972. **26**(5): p. 2005-&.
10. Lundquist, K., *Low-molecular weight lignin hydrolysis products.* Applied Polymer Symposia, 1976. **28**: p. 1393-1407.
11. Yasuda, S., K. Adachi, N. Terashima, and K. Ota, *Chemical Structures of Sulfuric-Acid Lignin .8. Reactions of 1,2-Diaryl-1,3-Propanediol and Pinoresinol with Sulfuric-Acid.* Mokuzai Gakkaishi, 1985. **31**(2): p. 125-131.
12. Karlsson, O., K. Lundquist, S. Meuller, and K. Westlid, *On the Acidolytic Cleavage of Arylglycerol Beta-Aryl Ethers.* Acta Chemica Scandinavica Series B-Organic Chemistry and Biochemistry, 1988. **42**(1): p. 48-51.

13. Imai, T., T. Yokoyama, and Y. Matsumoto, *Revisiting the mechanism of beta-O-4 bond cleavage during acidolysis of lignin IV: dependence of acidolysis reaction on the type of acid.* Journal of Wood Science, 2011. **57**(3): p. 219-225.

14. Sturgeon, M.R., S. Kim, K. Lawrence, R.S. Paton, S.C. Chmely, M. Nimlos, T.D. Foust, and G.T. Beckham, *A Mechanistic Investigation of Acid-Catalyzed Cleavage of Aryl-Ether Linkages: Implications for Lignin Depolymerization in Acidic Environments.* Acs Sustainable Chemistry & Engineering, 2014. **2**(3): p. 472-485.

15. Lahive, C.W., P.J. Deuss, C.S. Lancefield, Z.H. Sun, D.B. Cordes, C.M. Young, F. Tran, A.M.Z. Slawin, J.G. de Vries, P.C.J. Kamer, N.J. Westwood, and K. Barta, *Advanced Model Compounds for Understanding Acid-Catalyzed Lignin Depolymerization: Identification of Renewable Aromatics and a Lignin-Derived Solvent.* Journal of the American Chemical Society, 2016. **138**(28): p. 8900-8911.

16. Kalisch, J.H., *Alkali-formaldehyde pretreatment of coniferous woods in sulphite pulping.* Pulp Pap Mag Can, 1969. **21**: p. 55-68.

17. Lelis, R., E. Roffael, and G. Becker, *Zum Verhalten von Splint-und Kernholz der Kiefer bei der Verleimung mit Diisocyanat-Klebstoffen (PMDI).* Holz Zentralblatt, 1992. **134**: p. 2204-2210.

18. H., S. and R. E, *Untersuchungen der Schälfurnier-Eignung von in Deutschland erwachsenem Douglasienholz.* Holz Roh Werkst, 1993. **51**: p. 167-176.

19. Dix, B. and E. Roffael, *Einfluß der Verkernung und des Baumalters auf die Eigenschaften von Spanplatten aus Kiefernholz (Pinus sylvestris) Teil 1: Kernholz und seine Eigenschaften.* Holz als Roh-und Werkstoff, 1997. **55**(1): p. 25-33.

20. Buyuksari, U., N. Ayrilmis, E. Avci, and E. Koc, *Evaluation of the physical, mechanical properties and formaldehyde emission of particleboard manufactured from waste stone pine (Pinus pinea L.) cones.* Bioresource Technology, 2010. **101**(1): p. 255-259.

21. Hoong, Y.B., M.T. Paridah, Y.F. Loh, M.P. Koh, C.A. Luqman, and A. Zaidon, *Acacia mangium Tannin as Formaldehyde Scavenger for Low Molecular Weight Phenol-Formaldehyde Resin in Bonding Tropical Plywood.* Journal of Adhesion Science and Technology, 2010. **24**(8-10): p. 1653-1664.

22. Tasooji, M. and C.E. Frazier, *Simple milligram-scale extraction of formaldehyde from wood.* ACS Sustainable Chemistry & Engineering, 2016. **4**(9): p. 5041-5045.
23. Lapierre, C., B. Monties, and C. Rolando, *Thioacidolysis of Lignin - Comparison with Acidolysis.* Journal of Wood Chemistry and Technology, 1985. **5**(2): p. 277-292.
24. Rolando, C., B. Monties, and C. Lapierre, *Thioacidolysis*, in *Methods in lignin chemistry*. 1992, Springer Berlin Heidelberg. p. 334-349.
25. Wise, L.E. and E.C. Jahn, *Wood Chemistry*. Vol. 1. 1952: Reinhold.
26. Rowe, J.W. and A.H. Conner, *Extractives in Eastern Hardwoods-A Review* 1979: FOREST PRODUCTS LAB MADISON WIS.
27. Burnes, T.A., R.A. Blanchette, and R.L. Farrell, *Bacterial biodegradation of extractives and patterns of bordered pit membrane attack in pine wood.* Appl Environ Microbiol, 2000. **66**(12): p. 5201-5.
28. Ritter, D.C. and A.G. Campbell, *Supercritical carbon dioxide extraction of southern pine and ponderosa pine.* Wood and Fiber Science, 2007. **23**(1): p. 98-113.

Chapter 6 Evidence of in situ lignin crosslinking and repolymerization

Guigui Wan, and Charles E. Frazier

Macromolecular Science & Engineering, Sustainable Biomaterials

Virginia Tech, Blacksburg VA 24061, U.S.A

6.1. Abstract

Two wood species, Virginia pine and yellow-poplar, were carefully studied here to investigate the multiple reaction pathways of in situ lignin, including chain cleavage reactions (C2 and C3) and also crosslinking/repolymerization reactions. A wide array of analytical tools, including CH_2O generation measurement, thioacidolysis, methoxyl content measurement, and also HSQC (2D NMR: Heteronuclear Single Quantum Coherence) were extensively used. We found that extractives have strong impact on CH_2O generation, but also affect other lignin reaction pathways without CH_2O generation, i.e. C3 cleavage and also crosslinking/repolymerization (Figure 6.1, D), and this effect is species dependent. Lignin methoxyl is less likely to be a CH_2O generation source, because the different behavior for Virginia pine and yellow-poplar and also much higher degradation magnitude (Virginia pine) compared to CH_2O generation quantity. However, the degradation of methoxyl introduces more crosslinking/repolymerization, specifically at lignin aromatic position. Compared to thioacidolysis, HSQC provided much more information other than lignin ether-linkage content after heat treatments, but also other lignin substructures, and polysaccharides and also the extent of crosslinking/repolymerization at aromatic ring. HSQC also is a strong tool to search for marker compounds for each lignin reaction pathways, but quantification accuracy is poor. It can serve as a useful tool for comparison among different specimens. DMA (Dynamic Mechanical Analysis) is used here to evaluate the overall performance of lignin cleavage and crosslinking/repolymerization by looking into the Tg (glass transition temperature) and Ea (activation energy associated with glass transition) of wood specimens after heat treatments.

6.2. Introduction

Wood contains natural, biogenic formaldehyde (CH_2O), and heating generates much higher levels that vary according to wood moisture content, tissue type, and tree species. [1-5] All organic wood components are capable of generating CH_2O, but lignin appears to be the major source. [3, 6] Polysaccharides are minor contributors, [3, 7] and extractives can directly generate CH_2O in small quantity, [3, 8] or they may catalyze CH_2O generation depending on wood species, [3, 5, 8] or they react with CH_2O such that emissions are reduced. [9-14]

Most woods naturally acidic and in situ lignin thermochemistry can be described by the classic lignin acidolysis literature. Extensive acidolysis studies on model compounds and isolated lignins indicate that β-aryl ether bonds are readily cleaved via a benzylic carbocation reacting in one of two pathways, C2 cleavage or C3 cleavage, Figure 6.1, A and B. [15-20] The relative occurrence of these pathways depends upon the nature of the acid catalyst. [7, 21, 22] C2 cleavage produces CH_2O, a phenylacetaldehyde derivative (homovanillin), and a free phenol; whereas C3 cleavage produces the Hibbert's ketones and a free phenol. Homovanillin is very reactive and readily react into lignin through electrophilic substitution reaction to form stilbene, Figure 6.1, C. Lahive et al found homovanillin immediately repolymerized after its formation from β-O-4 model compounds, and ethylene glycol prevented the repolymerization by forming a stabilized five-membered ring structure with the aldehyde group. [20] Sharing the same reaction intermediate, benzyl carbocation, lignin also readily self-crosslinks to form condensed C-C bonds through reaction D, Figure 6.1, [23] which also consumes lignin β-O-4 linkages without generating CH_2O and is believed to be able to compete with the other two chain cleavage reactions (A and B). The existence of reaction D provides extra opportunity to manipulate CH_2O generation from wood. Li et al added a benzyl carbocation scavenger, 2-naphthol to suppress further reactions, including reactions A, B and C. [24] Lignin methoxyl may also degrade to form methanol and a free phenol, which possibly leads to more condensation. [25, 26]

In summary, lignin undergoes complex reactions under heat treatments, including cleavage reaction (A and B) and crosslinking/repolymerization reactions (C, D, and E). Those reactions happen simultaneously and compete with each other.

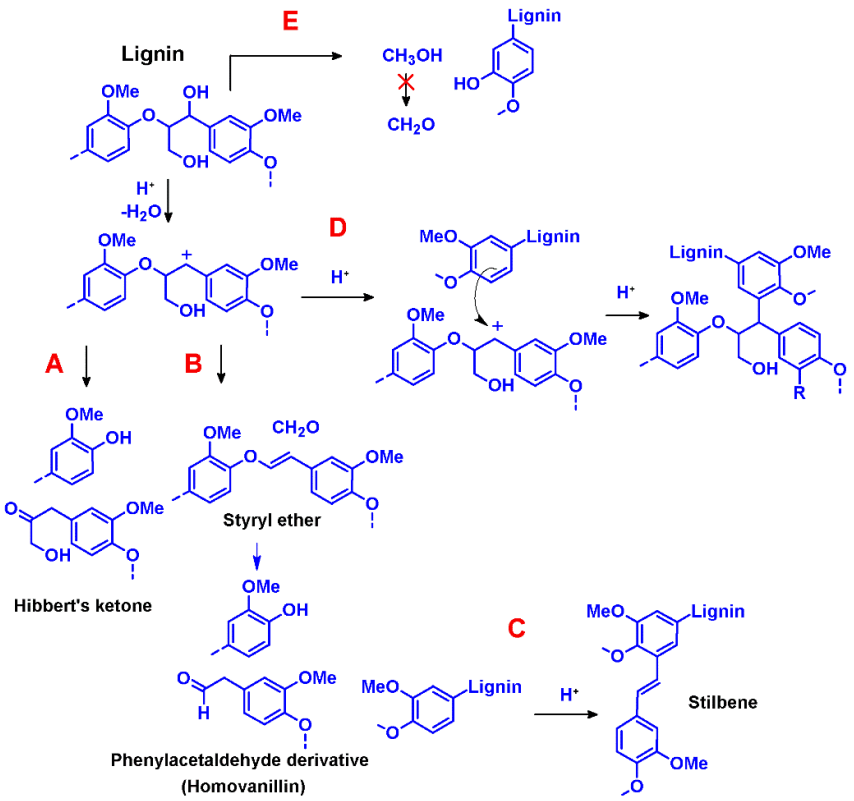

Figure 6.1. Lignin reaction pathways under acid-catalyzed thermal treatment. A: C3 cleavage, B: C2 cleavage, C: repolymerization of homovanillin to form stilbene, D: lignin crosslinking reaction, competing with A and B because these three reactions share the same intermediate, benzyl carbocation, E: demethoxylation, lignin methoxyl cleaved to form methanol, potentially with a very reactive catechol structure.

Here, yellow-poplar (*Liriodendron tulipifera*) and Virginia pine (*Pinus virginiana*) are selected to investigate multiple lignin reaction pathways in Figure 6.1. Thioacidolysis and HSQC are two main analytical tools used here to analyze lignin structural changes after heat treatments. Thioacidolysis is a well-established wet method, which degrades lignin ether linkages and form analyzable monomers or dimers for chromatography analysis. [27, 28] HSQC provides a much wider array of information compared to thioacidolysis, including β-O-4, β-5, and β-β, lignin aromatics, and also polysaccharides. [29] The biggest challenge for HSQC

quantification is to choose proper internal standards. Among many have been done, lignin aromatics signal is the most commonly used. [30-32] Here, lignin methoxyl is used instead, and accurate content is determined using a standard titration method.

Dynamic mechanical analysis (DMA) is also used to characterize rheological properties of heated wood, i.e. glass transition temperature (Tg) and activation energy associate with Tg (Ea) to evaluate the overall competence of cleavage and repolymerization/crosslinking reactions. If repolymerization/crosslinking reactions overwhelm cleavage reactions, polymeric flexibility is expected to decrease, resulting in more restricted chains and increasing Tg and Ea.

6.3. Materials and methods

Two healthy Virginia pine trees, 70-80 years old, were felled in a natural wooded region (~4 ha) east of Blacksburg, VA, U.S.A., (Nellies Cave area). Stem sections (~15 cm thick) were cut from locations that were 1.0-1.3 m above ground.

Tree 1: fresh sections were air dried and stored in the open laboratory at room temperature for ~16 months, then immersed in water for 3 days, debarked, and processed into rectangular wood blocks (4×10×40 mm, thickness×width×length). Three grain orientations were defined as RT, TR and XL; the first letter indicates the smallest wood surfaces of the rectangular block (R-radial, T-tangential, and X-cross-sectional) and the second indicates the grain direction along the length direction (T-tangential, R-radial, and L-longitudinal).

Tree 2: Fresh sections were processed into flakes (70×100×0.5 mm, tan.×long.×rad.), but immediately after felling with no water immersion, and no open-air storage; juvenile and mature tissues were combined and randomized. Specimens were stored at -80°C. Also obtained from tree 2 were six increment cores (5 mm dia) at ~1.4 m above ground from a 100 cm^2 area; they were transported to the laboratory and razor cut into ~1 mm thick disks; juvenile (first 10 rings from pith) and mature (last 60-70 rings) tissue was isolated and stored at -80°C. Sampling, processing, and storage of all specimens was conducted as rapidly as possible in order to minimize atmospheric exposure; from harvest to final storage, 12 hrs elapsed. Prior to aqueous pretreatment/heating, specimens were razor cut into small pieces (~0.5×0.5×0.5 mm).

Increment cores from Yellow-poplar were sampled, razor cut into 1 mm thick sections, and stored as described in a previous publication. [5]

Specimen pretreatments/heating/CH_2O measurements

Specimens were Soxhlet extracted (95% ethanol, 48 hours). Then extracted and unextracted specimens were dried by cycling between vacuum (room temperature, 0.02 kPa; 0.15 mm Hg) and dry N_2, three times, and then stored with dry N_2/molecular sieves until reaching constant weight. Prior to heating, specimens were pretreated as follows: 1) saturated in HPLC water, 2) saturated in 10 mmol TsOH, 3) saturated in 10 mmol sodium NaOH. Saturated specimens were subsequently adjusted to 100% moisture content. Heat treatments were subsequently conducted in sealed 50 ml serum bottles for 10, 20, 30, 60, 90, or 120 min. [4, 5] The CH_2O generated during heating remained sealed in the serum bottle and was determined as in [4, 5]. Specimens were identified with respect extraction (E) history, pretreatments prior to heating (H_2O: H; Acid: A; Base: B), and heating time, i.e. E/H10, H60, A10, etc.

Thioacidolysis

As described above, after heat treatments, specimens (i.e. H60 and A10, etc), and control specimens (no heating), were Soxhlet extracted (95% ethanol, 48 hours). Along with specimens, i.e. E/H10, etc (extracted first, then heated), all were air dried, ground and sieved to retain >40 mesh fraction, then vacuum dried as above, then subjected to thioacidolysis. [27, 28]

Methoxyl Content Determination

Specimens above (**>**40 mesh) were subjected to duplicate analysis as in ASTM D1166-84: standard test method for methoxyl groups in wood and related materials.

2D NMR (HSQC)

Specimens above (>40 mesh) were ball milled followed procedure, [33] then ~90 mg ball-milled powder (mostly <5 µm) were suspended into 1ml DMSO-d6/pyridine-d5 (4:1, v:v) and magnetically stirred until reaching visual homogeneousness (~4 hours), then transferred into 5 mm 600 MHz NMR tubes. NMR spectra were acquired on a 500 MHz Bruker Avance II

instrument, equipped with a cyroprobe for higher sensitivity. An adiabatic HSQC experiment (hsqcedetgpsisp2.3) was performed with following parameters: 12 to -1.65 ppm in F2 (^{1}H) using 2048 data points for an acquisition time of 150 ms; 220 to 0 ppm in F1 (^{13}C), acquisition time 4.6 ms, with a total acquisition time of 5 hours 23 mins. The central solvent (DMSO) peak was used as an internal chemical shift reference point (δC: 40.1, δH: 2.50ppm). Lignin methoxyl content was used an internal reference for quantification. Data processing and contour coloring was done using Bruker Topspin3.5 and Adobe Illustrator CC.

Dynamic mechanic analysis (DMA)

Air dried rectangular wood blocks (Virginia pine tree 1, grain orientations XL, RT and TR) were saturated in HPLC water or 10 mmol TsOH under reduced pressure (room temperature, 2.67 kPa; 20 mm Hg, 10 min), then immersed for another 2 hours under atmospheric pressure. After adjusting to 100%MC, blocks were sealed in pressure tubes (~10 hours), heated at 200°C for 60 min under two conditions: 1) pressure tube open (O), 2) pressure tube closed (C), then saturated in ethylene glycol under reduced pressure (20 mm Hg, 10 min), and immersed for 3 days under atmospheric pressure until complete saturation. Specimens were identified with pretreatments prior to heating (H_2O: H; Acid: A), and heating condition, i.e. H/C or A/O, etc. Control specimens were water saturated, adjusted to 100%MC, and immediately saturated into ethylene glycol as described above without heat treatments.

Ethylene glycol saturated wood blocks were subjected to solvent-submersion tensile-torsion DMA test, described as in [34, 35]. Sequential heating and cooling was applied as follows: 1) 25°C, equilibrate 10 min, 2) 25-120°C, 2°C/min, 1 Hz, 100,000 Pa, 3) 120°C, equilibrate 10 min, 4) 120-25°C, 2°C/min, 1 Hz, 100,000 Pa. Another set of specimens were subjected to Time-Temperature Superposition (TTS) test: 1) rapidly heat to 120°C; equilibrate 5 min, 3) isothermal frequency sweep, 0.1-1 Hz, 100,000 Pa, 120°C, 3) reduce temperature by 5°C; equilibrate 5 min, isothermal frequency sweep, 0.1-1 Hz, 100,000 Pa, 4) repeat step 3 to obtain isothermal frequency sweeps from 110°C to 25°C. All experiments were carried within linear viscoelastic response region (LVR). Data analysis was accomplished using OriginPro8.0 and TA Data Analysis software.

6.4. Results and discussions

Table 6.1 summarized CH_2O generation, thioacidolysis yield, methoxyl content and also partial HSQC quantification data from Virginia pine and yellow-poplar specimens after heat treatments at 200°C (10, 20 or 60 min) under various pretreatment conditions.

As published before and also shown here, impact of extractives on CH_2O generation from wood is highly species dependent, with no influence for yellow-poplar but great catalytic effect on Virginia pine. [8] Thioacidolysis indicates that extractives also have species-dependent influences on other lignin reaction pathways, i.e. C3 cleavage, reflecting at the C9 yield. With the presence of extractives, more lignin degraded for yellow-poplar, but opposite for Virginia pine, i.e. E/H10 vs. H10. For many cases, C8 yield is much lower than the heat-generated CH2O quantity, especially for Virginia pine specimens, i.e. A60, which can be explained by the existence of reaction C, Figure 6.1.

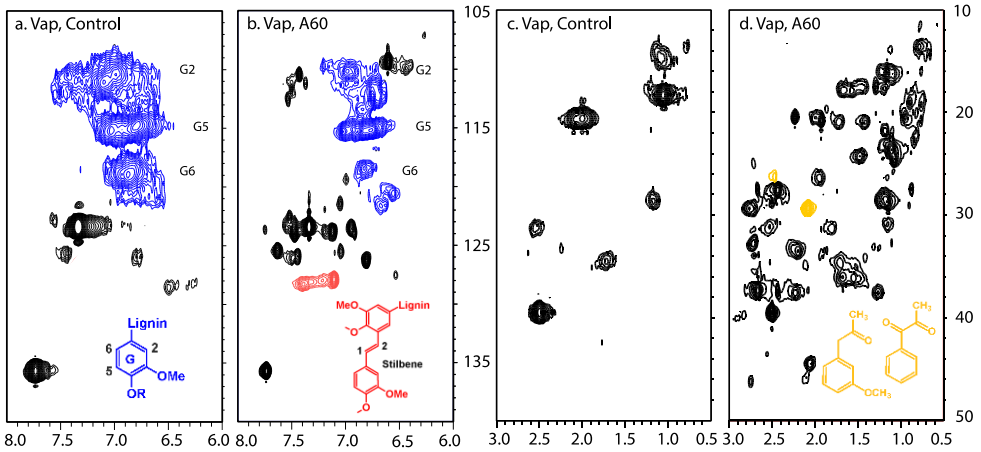

Figure 6.2. Stilbene and possible Hibbert's ketones observed from Virginia pine specimen after heat treatment at 200°C for 60 min with acid pretreatment (A60).

Table 6.1. The extractives effect on lignin degradation and CH_2O generation for yellow-poplar (sapwood tissue) and Virginia pine (tree 2, mature tissue) under heat treatments at 200˚C, 10, 20 or 60 min. Number of measurements n ≥ 2 for thioacidolysis, n ≥ 3 for CH_2O measurements, n = 2 for methoxyl content, n = 1 for HSQC. HSQC calculation based on internal standard methoxyl content. Control: no heating. Standard deviations in parentheses.

µmol/g wood		CH_2O	Thioacidolysis		Methoxyl content	HSQC‡			
			C9	C8		β-O-4 (C-Hα)	β-O-4 (C-Hβ)	Stilbene	Hibbert's ketone
Yellow-poplar (sapwood)	Control	0.1 (0.0)	441.7 (18.5)	59.3 (2.0)	1775.7 (6.8)	390.7	248.6		
	E/H10	3.9 (0.8)	478.3 (28.3)	82.5 (12.3)	1727.4 (34.2)	380.0	276.4		
	H10	4.1 (0.3)	388.1 (19.3)	59.5 (3.2)	1727.4* (34.2)	362.8	224.6		
	A10	4.5 (2.5)	398.4 (19.4)	73.9 (5.4)	1775.7 (182.3)	337.4	248.6	+	
	E/H60	33.7 (2.1)	52.7 (1.7)	15.8 (4.8)	1930.4 (125.3)	96.5	38.6		
	H60	31.4 (4.7)	42.8 (3.2)	16.0 (5.9)	1930.4* (125.3)	135.1	77.2		
	A60	66.7 (15.1)	11.4 (2.9)	17.8 (7.2)	1898.2 (34.2)	Below detection limit		+	+
Virginia pine (mature)	Control	0.1 (0.1)	314.6 (5.2)	20.1 (0.8)	1596.9 (148.4)	382.9	287.2		
	E/H10	2.5 (0.6)	133.4 (39.4)	20.6 (3.66)	1006.5 (48.4)	150.8	100.5		
	H10	4.2 (1.4)	328.2 (14.9)	22.4 (3.0)	1006.5* (48.4)	251.3	221.8	+	
	A10	27.5 (4.2)	101.9 (18.4)	12.3 (1.9)	1032.3 (32.3)	164.9	113.4	+	
	E/H20	3.5 (1.3)	165.8 (9.0)	11.7 (1.1)		NA			
	H20	5.8 (0.9)	272.7 (38.0)	17.5 (4.9)					
	E/H60	30.8 (5.6)	108.2 (2.9)	17.8 (0.7)	874.3 (93.6)	52.4	40.6		
	H60	42.0 (1.8)	152.5 (24.9)	24.9 (5.7)	874.3* (93.6)	104.8	100.8	+	
	A60	80.5 (21.3)	26.3 (7.0)	15.2 (5.7)	735.5 (51.6)	Below detection limit		+	+

* Actual methoxyl content not available. HSQC quantification based on methoxyl content from E/H specimens heated for same time period.
‡ Two individual HSQC experiments were conducted on Virginia pine Control specimens. Variation for contour volume integration ~5%.
+ Analyst above detection limit

Homovanillin endgroups were highly reactive to lignin aromatic rings to form condensed structures, i.e. stilbene. [20] As for C3 pathway (Figure 6.1, A), Hibbert's ketone was formed. To further look into the C2 and C3 cleavage, HSQC was used to search for marker compounds for each pathway. Reference chemical shifts for Hibbert's ketone was obtained from –CH3 signal of propane side chain of model compounds. Signals from stilbene vinylic –CH=CH-groups locate in the range of δC/δH 126-128/7.0-7.4 ppm. [36] Summarized in Table 6.1 also the presence of these two markers with positive sign (+) meaning levels above detection limit. Figure 6.2 showed existence of these markers in specimen Virginia pine (Vap) A60 as an example.

Lignin methoxyl was chosen as internal standard for HSQC quantification. Titration was done to reveal the accurate lignin methoxyl content, and result was shown in Table 6.1. Yellow-poplar remained unchanged after heat treatments, even for the most severe treatment A60, whereas Virginia pine experienced dramatic degradation on lignin methoxyl to form methanol. Wikberg and Maunu also observed no demethoxylation for hardwoods while softwoods experienced significant lignin methoxyl cleavage using ^{13}C CPMAS NMR. [26] Rationalizing from the species-dependent methoxyl degradation and also the much higher degradation magnitude compared to CH_2O generation quantity, methoxyl is less likely to be the CH_2O generation contributor. Methoxyl content was not available for specimens H10 and H60, but E/H10 and E/H60 was used to represent them respectively because heating time and external acid catalyst appear to be main factors causing lignin methoxyl degradation. Overall, HSQC agreed with thioacidolysis in general trend, but confidence was lacking for absolute data accuracy, especially for specimen with lower content, i.e. A60. So in following discussion, HSQC is used only to describe generic trend, not as quantification tool.

Compared to thioacidolysis, HSQC offered much more information, not only restricted at lignin β-O-4, but also β-5, β-β, and also polysaccharides. Its aromatic signals also revealed lignin crosslinking/repolymerization extent. Figure 6.3 listed HSQC spectra for yellow-poplar specimens, aliphatic region and also aromatic region. External acid, longer heating time and also the presence of extractives all promoted lignin degradation, seen from the decrease or even disappearance of lignin substructures signals from aliphatic region. In the aromatic region, Figure 6.3 also showed that acid and extractives promoted more substitution reactions on

aromatic rings, indicating by decreasing aromatic signal intensity, and the substitution reaction more likely happened at 2 and 6 positions, instead of 5. [37] Those substitution reactions included reaction C, D and also post-reaction after reaction E if catechol was formed from phenolic lignin endgroup.

Figure 6.4 summarized HSQC spectra for various Virginia pine specimens, including both aliphatic and aromatic. Apparently, from comparison for aliphatic region signals among specimens, acid promoted the most lignin degradation. Under the most severe case, specimen A60 was altered the most. For aromatic region, extractives did not play a big role, not much as in yellow-poplar (Figure 6.3). As for external acid catalyst, it promoted lignin aromatic substitution, especially under heat treatment for 60 min.

In summary, extractives played complicated role, depending on wood species. They impacted not only the CH_2O generation from wood, but also other cleavage or even crosslinking/repolymerization pathways. Implications are not restricted for wood-based composites industries, but hopefully biomass treatment and biorefinery could also benefit from this.

In Figure 6.1, reactions A and B are lignin cleavage reactions, while reactions C, D and E relate to lignin crosslinking/repolymerization. Lignin cleavage reactions should result in lower lignin Tg while crosslinking/repolymerization reactions should maintain the integrity of polymeric structures and immobilize the chain movement, which should counterpart the decreasing Tg. Table 6.2 summarized Tg, Ea after heat treatments at 200°C (60 min) for water and acid pretreated XL-oriented Virginia specimens. Experimental results for the other two grain orientations, RT and TR are not shown here, and they both followed the same trend of XL specimens after heat treatments.

In Table 6.2, 3 of 4 heating cases exhibited increasing Tg and increasing Ea, meaning crosslinking/repolymerization overwhelmed the cleavage reactions. The only case, H/C, resulted in a decreased Tg, which is probably valuable regarding to biomass pretreatment because lower Tg may relate to lower processing temperature and lower energy consumption.

Table 6.2. Glass transition temperature (Tg), activation energy associated with glass transition (Ea) of XL-grained Virginia pine tree 1 after various heat treatments (200°C), number of repetitions n ≥ 2. Standard deviations in parentheses.

XL	Tg (°C)	Ea (KJ/mol)
Control	78.1 (3.7)	273.9 (2.8)
H/C	69.6 (2.0)	289.7 (13.3)
H/O	80.6 (2.5)	269.9 (5.1)
A/C	85.3 (1.8)	310.5 (2.7)
A/O	92.8 (3.9)	300.5 (9.6)

Base catalyst is also commonly used in industries. Figure 6.5 plotted CH_2O generation from pretreated Virginia pine with acid or base as catalyst. Previous research quantified the alkaline and acid buffering capacity of Virginia pine specimens was respectively 0.05-0.08 mM HCl and 0.03-0.05 mM NaOH, so the wood buff capacity was easily exceeded by all acid and alkaline pretreatments used here. [7] Surprisingly, base didn't promote or even suppressed CH_2O generation compared to water saturated conditions, especially when heated for 60 min. In comparison, acid greatly catalyzed CH_2O generation. So next, 10 min and 60 min heating periods were selected to see if acid and base can do differently to the lignin substructures, shown in Figure 6.6.

Figure 6.6, lignin experienced minor alternation under 200°C for 10 min heat treatments with all three pretreatment conditions, water, acid and base. Once the heating time increased to 60 min, lignin experienced dramatic structural alternation with acid, while water treated specimen had less degradation and base treated specimen remained the least damaged. This observation correlated to the CH_2O generation trend observed in Figure 6.5.

As many literature suggested, most of the heat-generated CH_2O is readily crosslinked with lignin to form guaiacyl-guaiacyl diarylmethylene bridges (5-CH_2-5) structures once it is formed with additional formation of styryl ether (β-O-4) and stilbene structures (β-5) under alkaline condition. [36] However, the methylene moieties in the diarylmethylene structure should exhibit δC 29 ppm and δH 3.8 ppm, which have not been detected in the present work or similar work done by Capanema et al [38] and Balakshin et al. [36] This discrepancy may due to the reason that the minor amount of released CH_2O would not have a chance to condense to form diarylmethanes, or the amount of condensed structure is below the detection limit.

The above discussions indicated that, 1) in-situ lignin experienced different reaction pathways under acid or base catalyst, 2) lignin cleavage reactions and repolymerization/crosslinking reactions competed with each other, 3) there were many other reaction pathways for in-situ lignin under heat treatments except the CH_2O generation pathway, and this provided extra opportunity for us to manipulate the CH_2O generation for wood-based composites industries or even make an impact for other industries, such as biorefinery or bioenergy production, 4) extractives have impact on CH_2O generation, but also other lignin reactions, and this complex interaction is strongly species dependent.

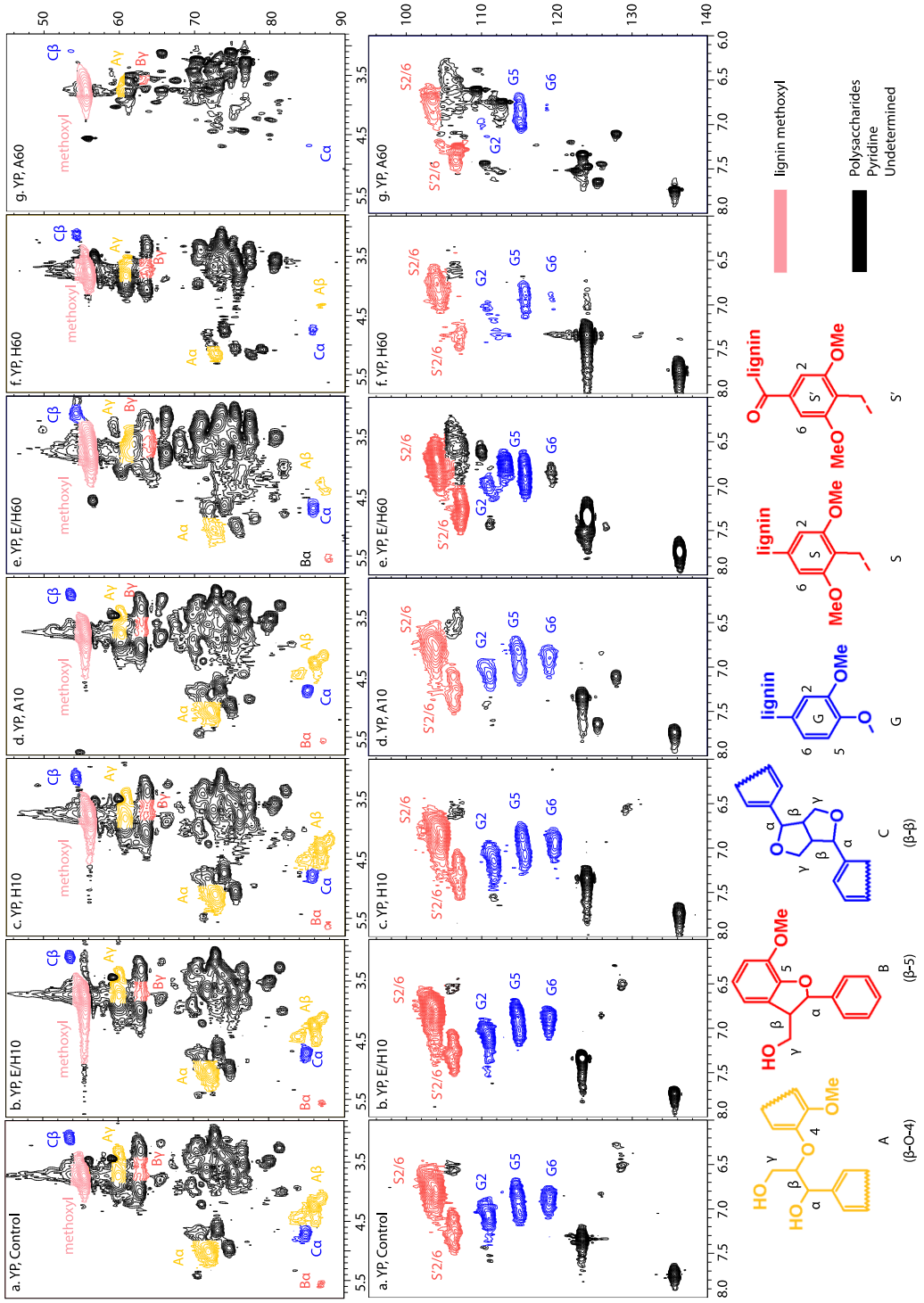

Figure 6.3. HSQC spectra for yellow-poplar (sapwood tissue), changes in the aliphatic and aromatic structures. a: Control, no heating; b: E/H10; c: H10; d: A10, e: E/H60; f: H60; g: A60. Aliphatic region: 90-45 ppm, 5.8-2.8 ppm; aromatic region: 140-95 ppm, 8-6 ppm. Chemical shifts of analyzed structures obtained from [29-31, 36]

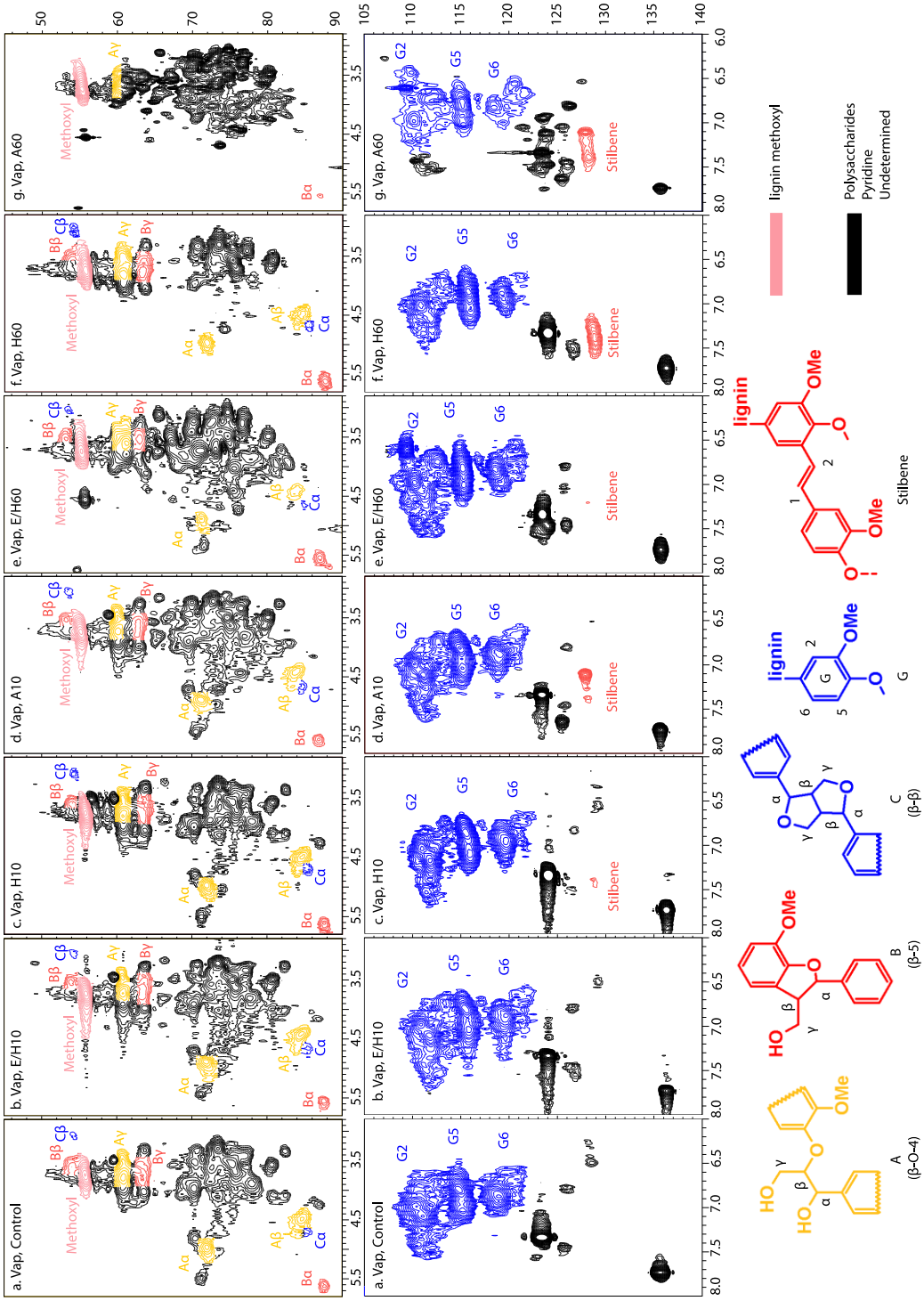

Figure 6.4. HSQC spectra for Virginia pine (tree 2 mature tissue), changes in the aliphatic and aromatic structures. a: Control, no heating; b: E/H10; c: H10; d: A10, e: E/H60; f: H60; g: A60. Aliphatic region: 90-45 ppm, 5.8-2.8 ppm; aromatic region: 140-95 ppm, 8-6 ppm. Chemical shifts of analyzed structures obtained from [29-31, 36]

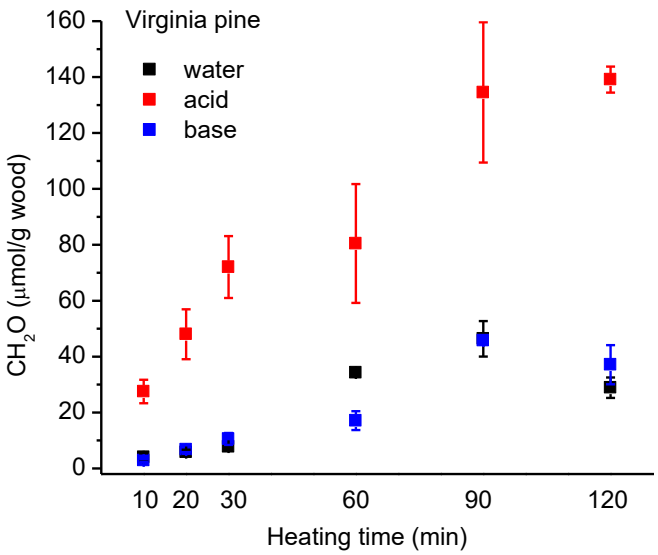

Figure 6.5. CH_2O generation (200°C, 10-120 min) from Virginia pine tree 2 mature tissue, under water, acid and base pretreated condition. Number of measurements n ≥ 3. Error bars = ± 1 standard deviation.

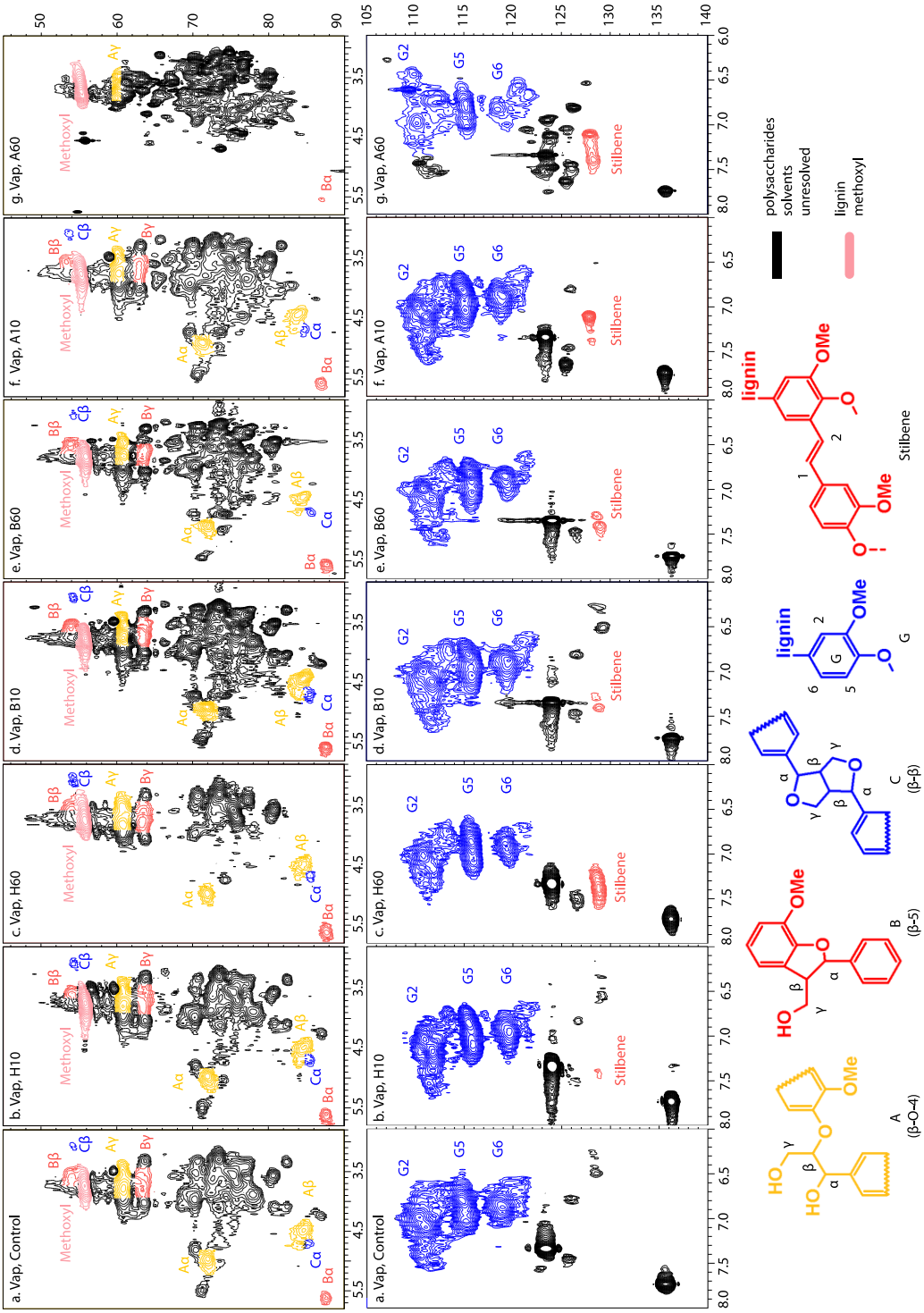

Figure 6.6. HSQC spectra for Virginia pine (tree 2 mature tissue), changes in the aliphatic and aromatic structures. a: Control, no heating; b: H10; c: H60; d: B10, e: B60; f: A10; g: A60. Aliphatic region: 90-45 ppm, 5.8-2.8 ppm; aromatic region: 140-95 ppm, 8-6 ppm. Chemical shifts of analyzed structures obtained from [29-31, 36]

6.5. Conclusions

Extensive evidence from a wide array analytical tools, including CH_2O generation measurement, thioacidolysis, methoxyl content measurement, and also HSQC, proved that in situ lignin undergoes cleavage and repolymerization/crosslinking reaction simultaneously. Extractives have strong impact on CH_2O generation, but also affect other lignin reaction pathways without CH_2O generation, i.e. C3 cleavage and also crosslinking/repolymerization (Figure 6.1, D), and this effect is species dependent. Lignin methoxyl is less likely to be a CH_2O generation source, because the different behavior for Virginia pine and yellow-poplar and also much higher degradation magnitude (Virginia pine) compared to CH_2O generation quantity. However, the degradation of methoxyl introduces more crosslinking/repolymerization, specifically at lignin aromatic position. Compared to thioacidolysis, HSQC provided much more information other than lignin ether-linkage content after heat treatments, but also other lignin substructures, and polysaccharides and also the extent of crosslinking/repolymerization at aromatic ring. HSQC also is a strong tool to search for marker compounds for each lignin reaction pathways, but quantification accuracy is poor. It can serve as a useful tool for comparison among different specimens. DMA is used here to evaluate the overall performance of lignin cleavage and crosslinking/repolymerization by looking into the Tg and Ea of wood specimens after heat treatments.

6.6. References

1. Meyer, B. and C. Boehme, *Formaldehyde emission from solid wood.* For. Prod. J, 1997. **47**(5): p. 45.
2. Martinez, E. and M.I. Belanche, *Influence of veneer wood species on plywood formaldehyde emission and content.* Holz Als Roh-Und Werkstoff, 2000. **58**(1-2): p. 31-34.
3. Schafer, M. and E. Roffael, *On the formaldehyde release of wood.* Holz Als Roh-Und Werkstoff, 2000. **58**(4): p. 259-264.
4. Tasooji, M. and C.E. Frazier, *Simple Milligram-Scale Extraction of Formaldehyde from Wood.* ACS Sustainable Chemistry & Engineering, 2016. **4**(9): p. 5041-5045.

5. Tasooji, M., G. Wan, G. Lewis, H. Wise, and C.E. Frazier, *Biogenic formaldehyde: Content and heat generation in the wood of three tree species.* **Chapter 3** in this dissertation.
6. Tjeerdsma, B.F., M. Boonstra, A. Pizzi, P. Tekely, and H. Militz, *Characterisation of thermally modified wood: molecular reasons for wood performance improvement.* Holz Als Roh-Und Werkstoff, 1998. **56**(3): p. 149-153.
7. Wan, G. and C.E. Frazier, *Formaldehyde in pine wood forms as predicted by lignin acidolysis.* **Chapter 4** in this dissertation.
8. Wan, G. and C.E. Frazier, *Pine extractives control lignin reactions and the formation of biogenic formaldehyde.* **Chapter 5** in this dissertation.
9. Kalisch, J.H., *Alkali-formaldehyde pretreatment of coniferous woods in sulphite pulping.* Pulp Pap Mag Can, 1969. **21**: p. 55-68.
10. Lelis, R., E. Roffael, and G. Becker, *Zum Verhalten von Splint-und Kernholz der Kiefer bei der Verleimung mit Diisocyanat-Klebstoffen (PMDI).* Holz Zentralblatt, 1992. **134**: p. 2204-2210.
11. H, S. and R. E, *Untersuchung der Schälfurnier-Eignung von in Deutschland erwachsenem Douglasienholz.* Holz Roh- Werkst, 1993. **51**: p. 167-176.
12. Dix, B. and E. Roffael, *Einfluß der Verkernung und des Baumalters auf die Eigenschaften von Spanplatten aus Kiefernholz (Pinus sylvestris) Teil 1: Kernholz und seine Eigenschaften.* Holz als Roh-und Werkstoff, 1997. **55**(1): p. 25-33.
13. Buyuksari, U., N. Ayrilmis, E. Avci, and E. Koc, *Evaluation of the physical, mechanical properties and formaldehyde emission of particleboard manufactured from waste stone pine (Pinus pinea L.) cones.* Bioresource Technology, 2010. **101**(1): p. 255-259.
14. Hoong, Y.B., M.T. Paridah, Y.F. Loh, M.P. Koh, C.A. Luqman, and A. Zaidon, *Acacia mangium Tannin as Formaldehyde Scavenger for Low Molecular Weight Phenol-Formaldehyde Resin in Bonding Tropical Plywood.* Journal of Adhesion Science and Technology, 2010. **24**(8-10): p. 1653-1664.
15. Lundquist, K. and L. Ericsson, *Acid degradation of lignin III formation of formaldehyde.* Acta Chemica Scandinavica, 1970. **24**: p. 3681-3686.

16. Lundquist, K. and R. Lundgren, *Acid Degradation of Lignin .7. Cleavage of Ether Bonds.* Acta Chemica Scandinavica, 1972. **26**(5): p. 2005-&.

17. Lundquist, K., *Low-molecular weight lignin hydrolysis products.* Applied Polymer Symposia, 1976. **28**: p. 1393-1407.

18. Imai, T., T. Yokoyama, and Y. Matsumoto, *Revisiting the mechanism of beta-O-4 bond cleavage during acidolysis of lignin IV: dependence of acidolysis reaction on the type of acid.* Journal of Wood Science, 2011. **57**(3): p. 219-225.

19. Sturgeon, M.R., S. Kim, K. Lawrence, R.S. Paton, S.C. Chmely, M. Nimlos, T.D. Foust, and G.T. Beckham, *A Mechanistic Investigation of Acid-Catalyzed Cleavage of Aryl-Ether Linkages: Implications for Lignin Depolymerization in Acidic Environments.* Acs Sustainable Chemistry & Engineering, 2014. **2**(3): p. 472-485.

20. Lahive, C.W., P.J. Deuss, C.S. Lancefield, Z.H. Sun, D.B. Cordes, C.M. Young, F. Tran, A.M.Z. Slawin, J.G. de Vries, P.C.J. Kamer, N.J. Westwood, and K. Barta, *Advanced Model Compounds for Understanding Acid-Catalyzed Lignin Depolymerization: Identification of Renewable Aromatics and a Lignin-Derived Solvent.* Journal of the American Chemical Society, 2016. **138**(28): p. 8900-8911.

21. Yasuda, S., K. Adachi, N. Terashima, and K. Ota, *Chemical Structures of Sulfuric-Acid Lignin .8. Reactions of 1,2-Diaryl-1,3-Propanediol and Pinoresinol with Sulfuric-Acid.* Mokuzai Gakkaishi, 1985. **31**(2): p. 125-131.

22. Karlsson, O., K. Lundquist, S. Meuller, and K. Westlid, *On the Acidolytic Cleavage of Arylglycerol Beta-Aryl Ethers.* Acta Chemica Scandinavica Series B-Organic Chemistry and Biochemistry, 1988. **42**(1): p. 48-51.

23. Sarkanen, K.V. and L.H. Hoo, *Kinetics of Hydrolysis of Erythro-Guaiacylglycerol β-(2-Methoxyphenyl) Ether and Its Veratryl Analogue Using Hc1 and Aluminum Chloride As Catalysts.* Journal of Wood Chemistry and Technology, 1981. **1**(1): p. 11-27.

24. Li, J., G. Henriksson, and G. Gellerstedt, *Lignin depolymerization/repolymerization and its critical role for delignification of aspen wood by steam explosion.* Bioresour Technol, 2007. **98**(16): p. 3061-8.

25. Wacek, A.V., W. Limontschew, and C. Aas, *Stability of Methoxyl Groups in Wood and Lignin.* Industrial & Engineering Chemistry Analytical Edition, 1957. **49**(9): p. 1389-1390.

26. Wikberg, H. and S.L. Maunu, *Characterisation of thermally modified hard-and softwoods by 13 C CPMAS NMR.* Carbohydrate Polymers, 2004. **58**(4): p. 461-466.

27. Lapierre, C., B. Monties, and C. Rolando, *Thioacidolysis of Lignin - Comparison with Acidolysis.* Journal of Wood Chemistry and Technology, 1985. **5**(2): p. 277-292.

28. Rolando, C., B. Monties, and C. Lapierre, *Thioacidolysis*, in *Methods in lignin chemistry*. 1992, Springer Berlin Heidelberg. p. 334-349.

29. Mansfield, S.D., H. Kim, F. Lu, and J. Ralph, *Whole plant cell wall characterization using solution-state 2D NMR.* Nat Protoc, 2012. **7**(9): p. 1579-89.

30. Sette, M., H. Lange, and C. Crestini, *Quantitative HSQC Analyses of Lignin: A Practical Comparison.* Comput Struct Biotechnol J, 2013. **6**: p. e201303016.

31. Heikkinen, H., T. Elder, H. Maaheimo, S. Rovio, J. Rahikainen, K. Kruus, and T. Tamminen, *Impact of steam explosion on the wheat straw lignin structure studied by solution-state nuclear magnetic resonance and density functional methods.* J Agric Food Chem, 2014. **62**(43): p. 10437-44.

32. Yuan, T.Q., S.N. Sun, F. Xu, and R.C. Sun, *Characterization of lignin structures and lignin–carbohydrate complex (LCC) linkages by quantitative 13C and 2D HSQC NMR spectroscopy.* Journal of agricultural and food chemistry, 2011. **59**(19): p. 10604-0614.

33. Mansfield, S.D., H. Kim, F. Lu, and J. Ralph, *Whole plant cell wall characterization using solution-state 2D NMR.* Nature protocols, 2012. **7**(9): p. 1579-1589.

34. Chowdhury, S., J. Fabiyi, and C.E. Frazier, *Advancing the dynamic mechanical analysis of biomass: comparison of tensile-torsion and compressive-torsion wood DMA.* Holzforschung, 2010. **64**(6): p. 747-756.

35. Wan, G., T. Frazier, J. Jorgensen, B.Y. Zhao, and C.E. Frazier, *Rheological analysis of switchgrass stem.* **Appendix A** in this dissertation.

36. Balakshin, M.Y., E.A. Capanema, C.L. Chen, and H.S. Gracz, *Elucidation of the structures of residual and dissolved pine kraft lignins using an HMQC NMR technique.* Journal of agricultural and food chemistry, 2003. **51**(21): p. 6116-6127.

37. Shuai, L., M.T. Amiri, Y.M. Questell-Santiago, F. Héroguel, Y. Li, H. Kim, R. Meilan, C. Chapple, J. Ralph, and J.S. Luterbacher, *Formaldehyde stabilization facilitates lignin monomer production during biomass depolymerization.* Science, 2016. **354**(6310): p. 329-333.

38. Capanema, E.A., M.Y. Balakshin, C.L. Chen, J.S. Gratzl, and H. Gracz, *Structural analysis of residual and technical lignins by 1H-13C correlation 2D NMR-spectroscopy.* Holzforschung, 2001. **55**(5): p. 302-308.

Chapter 7 The effect of lignin esterification on biogenic formaldehyde generation

Guigui Wan, and Charles E. Frazier

Macromolecular Science & Engineering, Sustainable Biomaterials

Virginia Tech, Blacksburg VA 24061, U.S.A

7.1. Abstract

Previous study confirmed that lignin is the main contributor of biogenic formaldehyde (CH_2O) generation from wood. CH_2O is generated from gamma-methylol of lignin propane side chain through C2 cleavage pathway. To further study this reaction mechanism, two different biomass types, Virginia pine and corn stalk were selected in this study. Our compositional analysis proved that those two biomasses differ dramatically in composition, i.e. extractives content, polysaccharides and also lignin content. But what's more intriguing is the lignin structure. Corn stalk is extensively esterified at γ-methylol position by p-coumaric acid, proven by alkaline hydrolysis and also DFRC. DFRC analysis showed ~33% lignin was esterified based on its monomer and dimer product yield, whereas Virginia pine was not. A previous CH_2O generation mechanism predicted higher CH_2O generation potential from Virginia pine compared to corn stalk due to the extensive side chain esterification at γ-methylol position for corn stalk, which was verified in 4 of 6 cases for the CH_2O generation measurements. For unextracted specimens, Virginia pine generated more CH_2O than corn stalk by 84-161% for Dry/10 and Acid/10. After the removal of extractives, Virginia pine still generated more CH_2O than corn stalk, by 166-175% for Dry/10 and H_2O/10.

7.2. Introduction

Our previous research efforts on three different wood species, Virginia pine (*Pinus virginiana*), yellow-poplar (*Liriodendron tulipifera*) and radiata pine (*Pinus radiata),* revealed that wood contains natural, biogenic formaldehyde (CH_2O), and heating generates much higher levels that vary according to wood moisture content, tissue type, and tree species. [1-5] All

organic wood components are capable of generating CH_2O. Polysaccharides are proven to be minor contributors. [3, 6] Extractives can directly generate CH_2O under heat. [3, 7] Some extractives components act as internal catalyst and impact lignin degradation pathways. [3, 5, 7] Lignin is the major source. [3, 6, 8] Extensive acidolysis studies on lignin model compounds and isolated lignins indicate that β-aryl ether bonds are readily cleaved via a benzylic carbocation reacting in one of two pathways, C2 cleavage or C3 cleavage [9-14], but only C2 cleavage generates CH_2O from the γ-methylol group by cleaving the Cγ-Cβ bond of lignin propane side chain, Figure 7.1.

Here, corn stalk is selected to further verify this well-established CH_2O generation theory. Due to extensive esterification at its γ-methylol group of lignin propane side chain by p-coumaric acid, [15-19] we hypothesized that the C2 cleavage pathway should be restricted, therefore, CH_2O generation from corn stalk may be lower than Virginia pine once subjected to same heat treatments, Figure 7.1.

The content of lignin esterification was quantified by two methods: alkaline hydrolysis [20, 21], and DFRC (Derivatization Followed by Reductive Cleavage) [19, 22]. Alkaline hydrolysis breaks the ester linkages and release p-coumaric acid, then the free phenolic acid can be derivatized and quantified by gas chromatography (GC) while DFRC is a method to selectively cleave lignin ether linkage and keep ester group intact, resulting lignin monomers and dimers for the further analysis. In combination of CH_2O generation measurements under various conditions for both Virginia pine and corn stalk, and lignin esterification content quantified by wet chemistry, one hope to understand CH_2O generation mechanism for more biomass types.

7.3. Materials and methods

Fifteen randomly selected healthy corn (*Zea mays L.*) plants, Southern States 65-22 vt2 variety cultivar, were harvested from local Blacksburg area, VA, U.S.A. after being planted for 108 days and reaching to dent (or R5 stage) maturity. Only the 2nd internodes (internode number increases from the groud level with the 1st internode closest to the ground) were used for further experiments after removing surface wax and corn stalk pith. Internodes were cut

along the stem length into long strips, then further reduced to smaller pieces (~4×4×0.5 mm, len.×wid.×thick.), and randomized.

A healthy Virginia pine (*Pinus virginiana*) tree, 70-80 years old, was felled in a natural, wooded region (~4 ha) east of Blacksburg, VA, U.S.A., (Nellies Cave area). Stem sections (~15 cm thick) were cut from locations that were 1.0-1.3 m above ground. Fresh sections were air dried for 7 days, immersed in water for 3 days, debarked, and processed into flakes (~70×100×0.5 mm, tan.×long.×rad.). The first 10 years of juvenile tissue was excluded. Flakes were stored in the open laboratory at room temperature for ~5 months. Prior to solvent extraction or aqueous pretreatment/heating, flakes were razor cut into smaller pieces (~0.5×0.5×0.5 mm).

Specimen solvent extraction

Specimens were dried by cycling between vaccum (0.15 mm Hg) and dry N_2, three times, stored with dry N_2/P_2O_5 until reaching constant weight, then followed by Soxhlet extraction. Corn stalk: a continuous two-step extraction, ~16 hours HPLC water extraction followed by ~23 hours 95% ethanol extraction. Virginia pine: one step ~48 hours 95% ethanol extraction.

Compositional analysis

Soxhlet extracted specimens were ground, sieved to retain the > 40 mesh fraction, vacuum dried, and subjected to duplicate compositional analysis as in NREL/TP-510-42618: Determination of Structural Carbohydrates and Lignin in Biomass. Ion chromatography (IC, Metrohm) was used for sugar analysis.

Alkaline hydrolysis

The extractives-free corn stalk powder (5 g, 40-80 mesh) was immersed into 100 ml 2mol/L NaOH aqueous solution with continuously magnetic stirring under N_2 at room temperature for ~20 hours. The suspension was then acidified by 37wt% HCl until pH < 3, extracted by diethyl ether (3 * 50 ml), organic phase combined, dried over anhydrous $MgSO_4$, rotary evaporated and vacuum dried, and finally redissolved into 3 ml dry diethyl ether. Roughly 0.5 ml ether solution was mixed with 2 ml N,O-Bis(trimethylsilyl)trifluoroacetamine (BSTFA) and 0.5 ml pyridine, then quantified by gas chromatography (GC) using tetracosane as

the internal standard after sitting at room temperature for 2 hours. Known amount of p-coumaric acid was used to determine its relative response factor to tetracosane.

To quantify the content of p-coumaric acid from each extraction step, extractives solutions from solvent extraction step were extracted by diethyl ether, and repeated the above steps.

Derivaization Followed by Reductive Cleavage (DFRC)

The extractives-free corn stalk powder (40-80 mesh) was subjected to DFRC, as described by Lu and Ralph. [22] Tetracosane was used as internal standard for GC analysis. β-aryl ether γ-p-coumarate ester models were synthesized (compound 1, Figure 6.2) for quantification purposes based on established procedure. [23] Structures confirmation using GC-MS and NMR, attached in appendix. P-coumaryl alcohol (H), coniferyl alcohol (G) and sinapyl alcohol (S) were acetylated for confirmation purposes of compound 2 (Figure 6.2).

Specimen pretreatment/heating/CH_2O measurement

Prior to heating, specimens were pretreated as follows: 1) Dry control, no treatment, 2) saturated in HPLC water, 3) saturated in 10 mmol tosyl acid. Saturated specimens were subsequently adjusted to 100% moisture content. Heat treatments were conducted in sealed 50 ml serum bottles at 200°C for 10 min. [4] The CH_2O generated during heating remained sealed in the serum bottle and was determined as in [4]. Specimens were identified with respect pretreatments prior to heating (Dry; H_2O; Acid), i.e. Dry/10, Acid/10, etc.

7.4. Results and discussions

Corn stalk and Virginia pine differ greatly in lignin, polysaccharides and extractives compositions and contents, [6, 24-26]. Speaking of extractives, the first water extraction removed 16.5% water soluble extractives from corn stalk, mainly monosaccharides and disaccharides, [27] while the second ethanol extraction further got rid of 1.1% of waxes, resins, tannins, etc. As for Virginia pine, one single 95% ethanol extraction washed away 7.4% extractives, mainly resin acids, fatty acids, waxes and fats. [3] Despite the fact that corn stalk

contained almost 2-3 times more extractives than Virginia pine did, most of its extractives are sugars, which were proven to be minor CH_2O generator. [3, 6, 27] Detailed discussion about extractives are not included here. Further investigation will be focused on lignin, especially the lignin structural differences between Virginia pine and corn stalk and the impact on CH_2O generation.

Table 7.1 summarizes sugar, lignin, and ash contents for extractives-free never-heated Virginia pine and corn stalk. The relative composition of cellulose, hemicelluloses, lignin and ash agreed well with the literature reported. [6, 24-26]. Virginia pine contained more cellulose and hemicelluloses than corn stalk by ~3% each, but hemicelluloses composition was dramatically different. For example, ~51% mannose was seen from Virginia pine hemicelluloses, but only traces in corn stalk; ~94% xylan in corn stalk hemicelluloses, while only ~27% for Virginia pine. Since acetyl groups are preferentially linked to xylan [28, 29], corn stalk may contain more acetyl groups than Virginia pine due to its much higher xylan content.

Table 7.1. Sugar, lignin and ash contents (based on initial dry mass) for extracted never-heated Virginia pine and corn stalk, number of measurements n ≥ 2. Standard deviations in parentheses.

Specimen	% Sugar						% Lignin			% ash	% total
	glu	xyl	gal	ara	man	total	Sol.	Insol.	total		
Virginia pine	44.4 (0.5)	6.8 (0.0)	4.2 (0.2)	1.1 (0.1)	12.7 (0.0)	69.2 (0.8)	1.5 (0.0)	26.6 (0.0)	28.1 (0.0)	0.1 (0.0)	97.4 (0.3)
Corn stalk	41.5 (0.6)	20.1 (0.1)	0.2 (0.0)	1.1 (0.1)	0.1 (0.0)	63.0 (0.4)	2.3 (0.1)	20.0 (0.1)	22.3 (0.1)	6.8 (0.5)	92.2 (0.4)

While extractive-free Virginia pine contained more lignin than extracted corn stalk by ~6% (Table 7.1), the lignin structure differs more dramatically. Corn stalk lignin is esterified by p-coumaric acid at its γ-methylol position of lignin propane side chain, [15-17, 19] whereas Virginia pine is not. Previous studies and extensive literature research indicated that CH_2O is formed from γ-methylol of lignin propane side chain. Expectation is that corn stalk generates

less CH_2O than Virginia pine under the same heating conditions. But first of all, the degree of esterification for corn stalk lignin should be quantified.

Two different methods were used to quantify the content of lignin esterification in corn stalk: alkaline hydrolysis and DFRC (Derivatization Followed by Reductive Cleavage). Prior to alkaline hydrolysis and DFRC, corn stalk experienced a two-step Soxhlet extraction. Only 0.10 wt% and 0.05 wt% p-coumaric acid (based on Klason lignin content) was detected from each step, probably due to hydrolysis of the p-coumarate ester resulted from extended heating in each Soxhlet extraction.

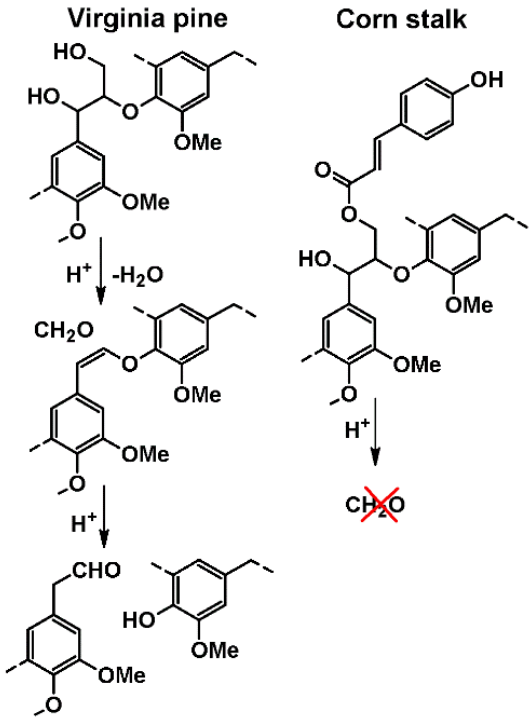

Figure 7.1. CH_2O is generated from γ-methylol of lignin propane side chain through C2 cleavage degradation. Virginia pine lignin: γ-methylol of lignin propane side chain is free without acid esterification. Corn stalk lignin: extensive esterification at γ position by p-coumaric acid.

After Soxhlet extraction, alkaline hydrolysis was performed to completely hydrolyze the p-coumarate ester into free acid form from corn stalk, and the resulting p-coumaric acid was determined to be 7.05 ± 0.82 wt% (based on Klason lignin), which was consistent with literature reported 7.12 wt% (based on Klason lignin). [30]

Another method to quantify p-coumarate ester content in corn stalk lignin is DFRC, reaction scheme shown in Figure 7.2. Developed by Lu and Ralph, this method produces analyzable monomers and dimers by cleaving α- and β-ethers in lignins, which is very similar to another well-established thioacidolysis technique [31, 32]. Although thioacidolysis was reported to result higher lignin monomer yield, [33] one advantage of DFRC is that γ-ester groups on lignins remain largely intact whereas significant ester hydrolysis occurs using thioacidolysis. [19]

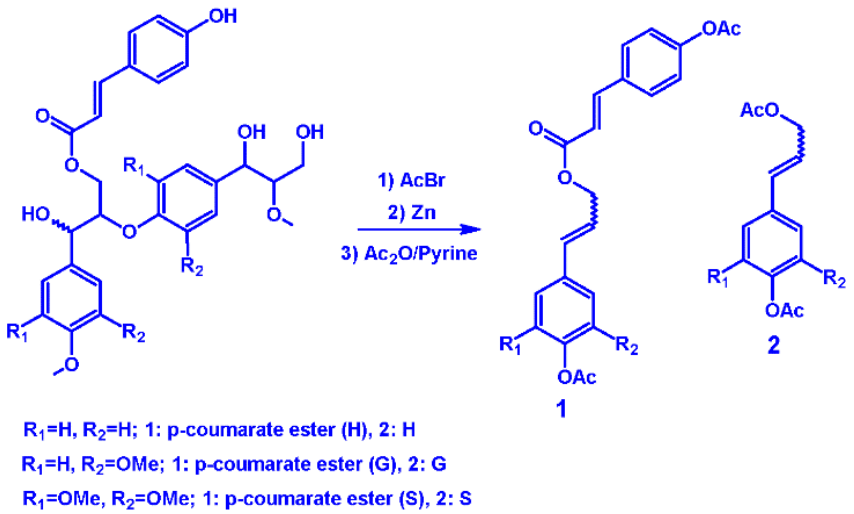

Figure 7.2. DFRC reaction scheme for formation of analyzable ester conjugates and acylated β-aryl ether units in corn stalk lignin. Compounds 1 (p-coumarate ester (G) and p-coumarate ester (S)) derived from esterified lignin unit, and model compounds synthesized for quantification purposes. Compounds 2 (H, G, and S) originated from non-esterified lignin unit.

Table 7.2 summarized averaged DFRC product yield for corn stalk. Compared with literature reported data, the overall monomer and dimer yield was lower by 14-41%, but literature reported 32% p-coumarate ester in corn based on the total monomer and dimer yield, which was comparable to 33.39% obtained here. [19] Here, only sinapyl ester was present in corn stalk, which indicated a strong preference for acylation of syringyl units. DFRC was also conducted on Virginia pine, and only G monomer was detected with yield 400.53 ± 33.13 μmol/g Klason lignin, while p-coumarate ester was not seen in the resulting products.

Table 7.2. DFRC product yield for corn stalk. H, G, S monomers derived from non-esterified lignin β-O-4. p-coumarate ester (S) obtained from ether-linked esterified lignin unit. %p-coumarate ester based on total DFRC product yield. Number of measurements n = 3. Standard deviations in parentheses.

	Yield (µmol/g Klason lignin)					%p-coumarate ester
	H	G	S	p-coumarate ester (S)	total	
Corn stalk	35.0 (11.2)	99.8 (21.3)	106.2 (11.0)	169.4 (18.1)	510.4 (45.5)	33.3 (3.5)

Table 7.3. CH_2O content and generation (200°C 10 min) from unextracted and extracted Virginia pine and corn stalk specimens. Number of measurements n ≥ 3. Initial CH_2O content from never-heated control specimens subtracted. Standard deviations in parentheses. CH_2O reported based on Klason lignin content of never-heated specimens (Table 7.1).

CH_2O detected (µg/g Klason lignin)	Unextracted		Extracted	
	Virginia pine	Corn stalk	Virginia pine	Corn stalk
Control	39.9 (15.0)	10.9 (1.3)	3.1 (0.3)	2.1 (1.3)
Dry/10	144.8 (44.6)	78.6 (26.3)	73.5 (31.9)	27.6 (5.1)
H_2O/10	122.2 (27.0)	126.5 (57.5)	62.7 (30.9)	22.8 (10.5)
Acid/10	3019.0 (720.3)	1156.3 (238.3)	3694.1 (798.3)	3875.8 (1531.4)

Both alkaline hydrolysis and DFRC demonstrated that corn stalk lignin was significantly esterified by p-coumaric acid at γ-methylol position of lignin propane side chain, which predicted lower CH_2O generation potential from corn stalk compared to Virginia pine. Next,

CH_2O generation from corn stalk and Virginia pine under various conditions for both unextracted and extracted specimens are shown in Table 7.3.

Alkaline buffering capacity of Virginia pine was 0.05-0.08 mM HCl, so the wood buff capacity was easily exceeded by the acid pretreatments used here. [6] Although alkaline buffering capacity was not available for corn stalk, literature data from Kargarfard et al [34] showed 0.225 mM H_2SO_4 needed for 1 g corn stalk fiber to decrease pH to 3, meaning the acid pretreatment should be adequate for corn stalk specimen too.

For corn stalk and Virginia pine, Table 7.3 summarized initial CH_2O content and heat-promoted CH_2O generation at 200°C (10 min) with initial content subtracted. Virginia pine contained more CH_2O then corn stalk by ~3.6 times before Soxhlet extraction. Most of the initial CH_2O was removed after extraction, but less than ~10% was still detected, which may be due to lab atmosphere contamination during specimen handling. Once heated, more CH_2O was quantified for all specimen types.

Before extraction, Virginia pine generated more CH_2O than corn stalk by 84-161% for Dry/10 and Acid/10 while CH_2O generation was quite similar for H_2O/10. Corn stalk contained much more xylan than Virginia pine, which probably correlated to higher acetyl content that was able to hydrolyze into acetic acid to catalyze CH_2O generation from the non-esterified lignin in corn stalk, resulting in similar CH_2O generation quantity for unextracted H_2O/10, but this can't explain the higher CH_2O generation quantity for extractives-free Virginia pine under the same treatment (H_2O/10) than extracted corn stalk. For both biomass types, CH_2O generation decreased after the removal of extractives for Dry/10 and H_2O/10 cases, by ~49% for Virginia pine and 65-82% for corn stalk. Extractives removal had bigger impact for corn stalk which may due to its higher extractives content. For Acid/10, extraction had no influence for CH_2O generation from Virginia pine, while removal of extractives increased CH_2O generation by ~235% for corn stalk, which again indicated the complicated roles of extractives for different biomass types.

7.5. Conclusions

Two biomass types, Virginia pine and corn stalk were selected in this study. The compositional analysis showed that corn stalk contained more extractives, and ash, but less polysaccharides and less lignin than Virginia pine by ~3%. Corn stalk is extensively esterified at the γ-methylol position by p-coumaric acid, proven by alkaline hydrolysis. DFRC analysis showed ~33% lignin was esterified based on its monomer and dimer product yield, whereas Virginia pine wasn't. All these structural differences potentially affected CH_2O generation behavior for these two biomasses. Previous study and literature suggested that lignin was the main CH_2O generator compared to other components, including polysaccharides and extractives. Based on many acidolysis studies from literature on isolated lignin and lignin model compounds, lignin-derived CH_2O is generated from γ-methylol of lignin propane side chain. So this CH_2O generation mechanism predicted high CH_2O generation potential from Virginia pine compared to corn stalk due to the extensive side chain esterification at γ-methylol position for corn stalk, which was verified in 4 of 6 cases for the CH_2O generation measurements. For unextracted specimens, Virginia pine generated more CH_2O than corn stalk by 84-161% for Dry/10 and Acid/10. After the removal of extractives, Virginia pine still generated more CH_2O than corn stalk, by 166-175% for Dry/10 and H_2O/10. No certain explanations can be made for the discrepancy from unextracted H_2O/10 and extracted Acid/10 cases.

7.6. References

1. Meyer, B. and C. Boehme, *Formaldehyde emission from solid wood.* For. Prod. J, 1997. **47**(5): p. 45.
2. Martinez, E. and M.I. Belanche, *Influence of veneer wood species on plywood formaldehyde emission and content.* Holz Als Roh-Und Werkstoff, 2000. **58**(1-2): p. 31-34.
3. Schafer, M. and E. Roffael, *On the formaldehyde release of wood.* Holz Als Roh-Und Werkstoff, 2000. **58**(4): p. 259-264.
4. Tasooji, M. and C.E. Frazier, *Simple Milligram-Scale Extraction of Formaldehyde from Wood.* ACS Sustainable Chemistry & Engineering, 2016. **4**(9): p. 5041-5045.

5. Tasooji, M., G. Wan, G. Lewis, H. Wise, and C.E. Frazier, *Biogenic formaldehyde: Content and heat generation in the wood of three tree species.* **Chapter 3** in this dissertation.
6. Wan, G. and C.E. Frazier, *Formaldehyde in pine wood forms as predicted by lignin acidolysis.* **Chapter 4** in this dissertation.
7. Wan, G. and C.E. Frazier, *Pine extractives control lignin reactions and the formation of biogenic formaldehyde.* **Chapter 5** in this dissertation.
8. Tjeerdsma, B.F., M. Boonstra, A. Pizzi, P. Tekely, and H. Militz, *Characterisation of thermally modified wood: molecular reasons for wood performance improvement.* Holz Als Roh-Und Werkstoff, 1998. **56**(3): p. 149-153.
9. Lundquist, K. and L. Ericsson, *Acid degradation of lignin III formation of formaldehyde.* Acta Chemica Scandinavica, 1970. **24**: p. 3681-3686.
10. Lundquist, K. and R. Lundgren, *Acid Degradation of Lignin .7. Cleavage of Ether Bonds.* Acta Chemica Scandinavica, 1972. **26**(5): p. 2005-&.
11. Lundquist, K., *Low-molecular weight lignin hydrolysis products.* Applied Polymer Symposia, 1976. **28**: p. 1393-1407.
12. Imai, T., T. Yokoyama, and Y. Matsumoto, *Revisiting the mechanism of beta-O-4 bond cleavage during acidolysis of lignin IV: dependence of acidolysis reaction on the type of acid.* Journal of Wood Science, 2011. **57**(3): p. 219-225.
13. Sturgeon, M.R., S. Kim, K. Lawrence, R.S. Paton, S.C. Chmely, M. Nimlos, T.D. Foust, and G.T. Beckham, *A Mechanistic Investigation of Acid-Catalyzed Cleavage of Aryl-Ether Linkages: Implications for Lignin Depolymerization in Acidic Environments.* Acs Sustainable Chemistry & Engineering, 2014. **2**(3): p. 472-485.
14. Lahive, C.W., P.J. Deuss, C.S. Lancefield, Z.H. Sun, D.B. Cordes, C.M. Young, F. Tran, A.M.Z. Slawin, J.G. de Vries, P.C.J. Kamer, N.J. Westwood, and K. Barta, *Advanced Model Compounds for Understanding Acid-Catalyzed Lignin Depolymerization: Identification of Renewable Aromatics and a Lignin-Derived Solvent.* Journal of the American Chemical Society, 2016. **138**(28): p. 8900-8911.
15. Smith, D.C.C., *Ester Groups in Lignin.* Nature, 1955. **176**(4475): p. 267-268.

16. Nakamura, Y. and T. Higuchi, *Ester Linkage of P-Coumaric Acid in Bamboo Lignin.* Holzforschung, 1976. **30**(6): p. 187-191.

17. Ralph, J. and R.F. Helm, *Lignin Hydroxycinnamic Acid Polysaccharide Complexes - Synthetic Models for Regiochemical Characterization.* Forage Cell Wall Structure and Digestibility, 1993: p. 201-246.

18. Ralph, J., R.D. Hatfield, S. Quideau, R.F. Helm, J.H. Grabber, and H.J.G. Jung, *Pathway of p-coumaric acid incorporation into maize lignin as revealed by NMR.* Journal of the American Chemical Society, 1994. **116**(21): p. 9448-9456.

19. Lu, F.C. and J. Ralph, *Detection and determination of p-coumaroylated units in lignins.* Journal of Agricultural and Food Chemistry, 1999. **47**(5): p. 1988-1992.

20. Sun, R.C., X.F. Sun, and S.H. Zhang, *Quantitative determination of hydroxycinnamic acids in wheat, rice, rye, and barley straws, maize stems, oil palm frond fiber, and fast-growing poplar wood.* Journal of Agricultural and Food Chemistry, 2001. **49**(11): p. 5122-5129.

21. Torre, P., B. Aliakbarian, B. Rivas, J.M. Domingue, and A. Converti, *Release of ferulic acid from corn cobs by alkaline hydrolysis.* Biochemical Engineering Journal, 2008. **40**(3): p. 500-506.

22. Lu, F.C. and J. Ralph, *Derivatization followed by reductive cleavage (DFRC method), a new method for lignin analysis: Protocol for analysis of DFRC monomers.* Journal of Agricultural and Food Chemistry, 1997. **45**(7): p. 2590-2592.

23. Lu, F. and J. Ralph, *Facile synthesis of 4-hydroxycinnamyl p-coumarates.* Journal of Agricultural and Food Chemistry, 1998. **46**(8): p. 2911-2913.

24. Chundawat, S.P.S., B. Venkatesh, and B.E. Dale, *Effect of particle size based separation of milled corn stover on AFEX pretreatment and enzymatic digestibility.* Biotechnology and Bioengineering, 2007. **96**(2): p. 219-231.

25. Lv, G.J., S.B. Wu, and R. Lou, *Kinetic study for the thermal decomposition of hemicellulose isolated from corn stalk.* BioResources, 2010. **5**(2): p. 1281-1291.

26. Theerarattananoon, K., F. Xu, J. Wilson, S. Staggenborg, L. Mckinney, P. Vadlani, Z.J. Pei, and D.H. Wang, *Effects of the pelleting conditions on chemical composition and sugar*

yield of corn stover, big bluestem, wheat straw, and sorghum stalk pellets. Bioprocess and Biosystems Engineering, 2012. **35**(4): p. 615-623.

27. Chen, S.F., R.A. Mowery, C.J. Scarlata, and C.K. Chambliss, *Compositional analysis of water-soluble materials in corn stover.* Journal of Agricultural and Food Chemistry, 2007. **55**(15): p. 5912-5918.
28. Bouveng, H.O., P.J. Garegg, and B. Lindberg, *Position of the O-Acetyl Groups in Birch Xylan.* Chemistry & Industry, 1958(52): p. 1727-1727.
29. Maloney, M.T., T.W. Chapman, and A.J. Baker, *Dilute Acid-Hydrolysis of Paper Birch - Kinetics Studies of Xylan and Acetyl-Group Hydrolysis.* Biotechnology and Bioengineering, 1985. **27**(3): p. 355-361.
30. Min, D.Y., H.M. Chang, H. Jameel, L. Lucia, Z.G. Wang, and Y.C. Jin, *The structure of lignin of corn stover and its changes induced by mild sodium hydroxide treatment.* BioResources, 2014. **9**(2): p. 2405-2414.
31. Lapierre, C., B. Monties, and C. Rolando, *Thioacidolysis of Lignin - Comparison with Acidolysis.* Journal of Wood Chemistry and Technology, 1985. **5**(2): p. 277-292.

32 Rolando, C., B. Monties, and C. Lapierre, *Thioacidolysis*, in *Methods in lignin chemistry*. 1992, Springer Berlin Heidelberg. p. 334-349.

33. Holtman, K.M., H.M. Chang, H. Jameel, and J.F. Kadla, *Elucidation of lignin structure through degradative methods: Comparison of modified DFRC and thioacidolysis.* Journal of Agricultural and Food Chemistry, 2003. **51**(12): p. 3535-3540.
34. Kargarfard, A. and A. Jahan-Latibari, *The Performance of Corn and Cotton Stalks for Medium Density Fiberboard Production.* Bioresources, 2011. **6**(2): p. 1147-1157.

Chapter 8 Conclusions and future work

In order to respond to the stringent formaldehyde emission regulation and promote a thorough understanding about formaldehyde generation in wood-based composites industries, this study utilized a wide array of analytical/synthetic tools to reveal the in-situ biogenic formaldehyde generation mechanism from wood, therefore, propose practical recommendations to manipulate/reduce CH_2O generation and later on impact emission from end-products.

Chapter 2 introduced a custom-designed small chamber for measuring CH_2O emission from wood under well-controlled conditions (i.e. gas flow rate, and relative humidity). A fixed rate of carrier gas (N_2) flew through the system, carrying out CH_2O emitted from wood and bubbling into two water-containing impingers to absorb CH_2O completely. Thin wood flakes were sat in a slotted flake holder, which offered great flexibility for specimen pretreatment (i.e. acid immerse) and following heat treatments, and convenience for specimen loading/unloading. Background CH_2O from the carrier gas was quantified and subtracted correspondingly to guarantee experimental rigorousness. Our observations showed that CH_2O emission varied among different trees for the same wood species; heat treatment (120°C or 200°C, 1hour) increased CH_2O emission, however, sequential heating decreased emission; external acid pretreatment increase emission after heat treatment; the predicted long-term emission fitted into an exponential decay model.

Chapter 3 adopted a simple milligram-scale water extraction method to quantify CH_2O content/generation from fresh or dried wood core specimens. Three wood species were focused in this study, Virginia pine (*Pinus virginiana*), yellow-poplar (*Liriodendron tulipifera*), and radiata pine (*Pinus radiata*). Heating increased CH_2O levels by 3-60 fold. The presence of moisture also led to higher CH_2O generation than dry specimen. Significant variations within and between trees of the same species were observed. Tissue types (juvenile/mature, heartwood/sapwood) didn't correlate to a uniform CH_2O content/generation trend. Radiata pine generated extraordinarily high CH_2O levels when heated compared the other two species, which indicated the possible catalytic influences from its extractives. The goal of this study was

to quantify and understand CH_2O generation from wood itself, and correlated to hot-press scenario. If we could reveal the precise mechanisms of CH_2O biogenesis in wood, we could perhaps manipulate these mechanisms for beneficial purposes.

Chapter 4 extended the discussion about biogenic CH_2O generation from Virginia pine (*Pinus virginiana*), but focused in chemical mechanisms. Adequate literature evidence pointed that the main contributor should be lignin. As for polysaccharides, they played minor or neglectable roles. The effect of extractives were complex and carefully discussed in the following chapter. Due to the acidic nature of most woods, the generation mechanism was predicted by classic acidolysis of isolated lignin or lignin model compounds. Two pathways, C2 cleavage and C3 cleavage, were responsible for in-situ lignin degradation, but only C2 cleavage pathway generated CH_2O. The selection of external acid catalyst manipulated lignin cleavage pathways, resulting in different amount of heat-generated CH_2O. External alkaline pretreatment suppressed CH_2O generation under heat treatments. The benefits of this study were not only limited to understand CH_2O generation mechanism from wood in order to impact wood-based composites industries, but also this fundamental lignin chemistry study was able to promote lignin crosslinking/repolymerization understanding in biorefinery industries.

Chapter 5 emphasized the catalytic interaction between extractives and lignin Two wood species were selected, Virginia pine and yellow-poplar. First of all, isolated extractives generated CH_2O under heat, but in an extremely low level. Extractives removal resulted in lower CH_2O generation from Virginia pine, but no impact on yellow-poplar. Extractives reconstitution recovered original CH_2O generation behavior from unextracted wood for some cases. A simple weight addition of the constituted components, extracted wood and extractives, can't make up the total CH_2O generation, which indicated the presence of catalytic interaction between these two components. Furthermore thioacidolysis indicated that the presence of extractives affect lignin degradation pathways, and this influence depended on wood species. This chapter provided additional information on biogenic CH_2O generation from wood, and also offered alternatives for controlling CH_2O generation.

Chapter 6 discussed additional lignin crosslinking/repolymerization reactions under heat treatments. One particular crosslinking reaction shared the same intermediate (benzyl carbocation) as the other two pathways, C2 and C3 cleavage, which can potentially compete with the CH_2O generation. The finding of this pathway provided extra opportunity to manipulate CH_2O generation, but implications of additional crosslinking/repolymerization still remained unknown. After lignin chain cleavage, the degraded fragments were also subjected to repolymerization, i.e. homovanillin endgroup from C2 cleavage cross linked with lignin aromatic rings. 2D NMR (HSQC) was used to monitor the changes of in-situ lignin after heat treatments, including various lignin linkages (β-O-4, β-5, β-β) and aromatic signals. Dynamic mechanical analysis (DMA) detected rheological properties of heated wood, including glass transition temperature (Tg) and activation energy associate with Tg (Ea). Results from DMA showed an increase of Tg even after heat treatment at 200°C for 1 hour with the presence of acid catalyst, which was a strong evidence to prove lignin crosslinking/repolymerization.

Chapter 7 compared CH_2O generation from two different biomass types, Virginia pine wood and corn stalk. Lignin structures in these two biomasses differed greatly, especially on γ-methylol group of propane side chain, what was believed to be the CH_2O generation source. In corn stalk, γ-methylol was extensively esterified by p-coumaric acid, in contrast, no esterification for Virginia pine lignin. So it was hypothesized that corn stalk should generate less CH_2O than Virginia pine under same heating conditions. To quantify the esterification content, alkaline hydrolysis and DFRC were used, then CH_2O generation from both biomasses was quantified. Results showed that corn stalk generated less CH_2O than Virginia pine under more cases. This study provided a nice supplementary information for proving the CH_2O generation pathways provided in Chapter 3.

Overall, the entire study covered the following aspects: 1) how much CH_2O can be generated from wood; 2) relative contribution from each wood component; 3) CH_2O generation mechanism from lignin and methods to manipulate CH_2O generation from wood; 4) other lignin reactions and implications to biorefinery industries besides wood-based composites industries.

There are still many remaining tasks, and hopefully someone else could address them in future: 1) significance of biogenic CH_2O compared to synthetic CH_2O contribution from resin (unreacted and urea-formaldehyde resin hydrolysis); 2) CH_2O content and generation from other economy significant species; 3) CH_2O generation mechanism with the presence of base catalyst, and the implications to wood-based industries and beyond.

As for the appendix, it contains a fair amount of rheological data for a bioenergy crop, switchgrass. Our goal was to make a connection between its chemical/structural changes resulting from transgenic modification and rheological properties, including glass transition temperature (Tg), dynamic modulus (G' and G''), and activation energy associated with the Tg (Ea), and finally provide supplementary information to evaluate if certain transgenic switchgrass is suitable for bioenergy production. The rest of the appendix included CH_2O generation measurement from three wood species, Virginia pine, yellow-poplar and radiata pine, under 200°C for extended heating period up to 120 min. The goal was to reveal maximum CH_2O generation potential and species-dependent generation kinetics. A thorough study about rheological properties of heated wood (Virginia pine) was also presented, i.e. Tg, G', G'' and Ea. We hoped to correlate the mentioned parameters to chemical changes of the heated wood, such as lignin degradation and crosslinking/repolymerization. Some supplementary ^{1}HNMR, ^{13}CNMR and GC/MS data was also presented to support the synthesis work mentioned in following chapter.

Appendix A Rheological analysis of switchgrass stem

Guigui Wan, Taylor Frazier, Julianne Jorgensen, Bingyu Zhao, and Charles E. Frazier

Department of Horticulture

Macromolecular Science & Engineering, Department of Sustainable Biomaterials

Virginia Tech, Blacksburg VA 24061, USA

Attribution

In this paper, genetically engineered Switchgrass specimens were provided by Dr. Taylor Frazier and Dr. Bingyu Zhao from the Department of Horticulture at Virginia Tech. Guigui Wan developed all rheological procedures. Supervised by Guigui Wan, Julianne Jorgensen was a summer REU student, and she collected about 30% of the data described herein.

A.1. Abstract

A solvent submersion tensile-torsion dynamic mechanical analysis method was carefully developed to evaluate rheological properties of two groups of transgenic switchgrass plants (4CL-7 + and 4CL-7 -), including storage modulus (G'), glass transition temperature (Tg), activation energy associated with Tg (Ea) and also torsional strength. The goal was to reveal how the transgenic modification affected rheological behavior, and ultimately evaluated the viability of the plants as well as the practical aspects of biomass handling and processing. Overall, positive group contained less lignin than negative group by ~22%. Stress sweeps at 25°C and 120°C indicated that positive specimens are overall less stiff than those negative specimens. The positive group exhibited lower Tg by 10°C than the negative group. 40 + and 18 – were chosen to represent each group. Lower Ea and lower torsional strength was seen from 40 +, which possibly could represent the general trend if compared other specimens across two groups. These information is highly valuable regarding to bioenergy production, and may serve as critical criterions for selecting proper transgenic modifications to obtain modified energy crops with preferable traits.

A.2. Introduction

Switchgrass (*Panicum virgatum*), a perennial warm season grass native to North America, has been identified as important for development into an herbaceous biomass fuel crop. [1-3] Such crops should efficiently release sugars from the cell wall polysaccharides through (bio) chemical conversion. Lignin has complex associations with polysaccharides, and its presence limits the accessibility of plant cell wall polysaccharides to chemical, enzymatic and microbial digestion. [1-3] The lignin content of feedstocks has been proposed as one key agronomic trait impacting biofuel production from lignocellulosic biomass. To improve biomass fermentability, genetic modifications aiming to lower lignin content and modify lignin structure have been extensively developed. Besides sugar accessibility, such modifications could impact plant viability as well as the practical aspects of biomass handling and processing. In light of these issues it is appropriate to develop rheological methods that could help reveal how plant tissue mechanical properties are impacted through the development of biomass fuel crops.

Rheology is the study of deformation and flow in materials, both liquids and solids. Carefully measured deformations reveal insights about molecular structure, hierarchical organization, and aspects of material processing. Dynamic mechanical analysis, DMA, is one common rheological methodology. It involves the application of an oscillating stress or strain, and the resulting strain or stress is measured. The DMA response in polymeric materials is viscoelastic; it is simultaneously elastic like a spring, and also viscous like flowing water. However in viscoelastic solids, the viscous response is not macroscopic liquid flow, but rather localized flow as when two lignin segments rub and slip past one another when mechanical energy is dissipated. When carefully conducted, the DMA of viscoelastic lignocellulose may be used to reveal insights about the structure and organization of cellulose, hemicelluloses, and lignin. Most of this type of research has been devoted to wood, with examples such as [4-8]. Given the variety of polymers and the complexity of their organization in lignocellulose, it is interesting to note that lignocellulose exhibits only one major thermo-mechanical softening transition, a glass-to-rubber transition attributed to lignin. [9, 10] The in situ lignin glass transition is quite sensitive to moisture levels, meaning that moisture control is a very practical

experimental concern. [4, 11] In the present work switchgrass specimens were analyzed while immersed in ethylene glycol. This approach provides a crude approximation of natural hydration in the living plant, but with a wider analytical temperature range as compared to water. [6] Chowdhury et al. [6] demonstrated that the thermo-rheological response of switchgrass stem is quite similar to that of wood, and tissue maturity effects are easily detected in switchgrass. The objective of this paper is to demonstrate solvent submersion rheological methods that may be used to reveal the impact of genetic modifications on switchgrass lignin. Furthermore, the intention is to address practical experimental challenges that should assist others interested in biomass rheology. The analytical stress mode was torsion, with the torsional axis parallel to the plant stem, and with the specimen clamped under a minor tensile stress. This so-called tensile-torsion analysis was discussed by Chowdhury et al. [6] In the work described here, switchgrass specimens were subjected to DMA that was carefully restricted to the linear response regime. Additionally, a novel continuous stress-ramp (nonlinear) analysis was imposed such that switchgrass stem sections underwent yielding and failure.

A.3. Materials and methods

Selection of RNAi:4CL over-expressing transgenic switchgrass plants

In a previous study, T_0 transgenic switchgrass plants over-expressing an *RNAi:Pv4CL1* construct were characterized and crossed with wild-type HR8 switchgrass plants. [12] One segregating population, designated as Pv4Cl-7, was used for further analysis. The plants of this T_1 population were phenotyped based on stem color for the presence (brown) or absence (green) of the transgene (Figure A.1). Seven T_1 Pv4CL-7 plants were selected for this study: three plants (10 -, 18 -, 25 -) where the transgene was absent (green stem), indicated by the negative sign (-), and four plants (5 +, 7 +, 34 +, 40 +) where the transgene was present (brown stem), indicated by the positive sign (+). The plants were maintained in a greenhouse under a 16 hour day/8 hour night photoperiod. The lignin in these specimens was not analyzed, but it is assumed to be similar to the related transgenic lines described in [12]. Consequently, the transgene negative plants in this study are similar to wild type plants (H/G/S monomer ratio =

0.04/1.05/1.00); whereas the transgene positive plants have about 22% less lignin, with an altered H/G/S monomer ratio = 0.07/0.56/1.00.

E4 stage tillers were freshly harvested from all switchgrass plants at soil level and then divided into different parts according to the location of the internodes. The internode closest to the soil was labeled as the first internode. The second internode, which is positioned adjacent to the first one and second from soil level, was selected for analysis. Within the second internode, the stem was sectioned into small pieces with lengths of 2 to 3 cm. The 2-3 cm long sections (hollow cylinders) were cut along the stem length and subsequently cut into rectangular shapes with widths between 3-5 mm. The thicknesses of the specimens ranged from 0.7-1.0 mm. For each plant specimen, at least three tillers (second internode) were obtained from three individual plants, and rectangular sections from a single plant were randomized into one batch. After rectangular sections were prepared, they were immediately transferred into ethylene glycol (Fisher Scientific, Certified), vacuum-treated (20 Torr) for 30 min, followed by vacuum release and solvent immersion at atmospheric pressure for at least 48 hours. After this solvent saturation, all specimens were stored at 12°C.

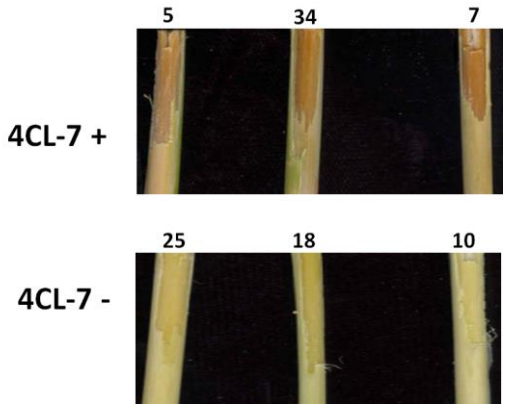

Figure A.1. Stem color phenotype in 4CL-7 + (top) and 4CL-7 – (bottom) specimens. The presence of the transgene correlated with brown stem color, while transgene absence correlated with green stem color.

Tension-torsional submersion DMA

Specimens were subjected to solvent-submersion rheological analysis in torsional stress mode using a TA Instruments AR-G2 rheometer (New Castle, Delaware, USA) with a concentric cylinder attachment containing a fluid-cooled jacket. Specimens were secured in tension clamps using 40 cN×m torque, where the specimen long axis was parallel to the torsional axis, Figure A.2. During all rheological tests, specimens were subjected to a 1 N static tensile force and immersed in ethylene glycol. Specimen length between the clamps was 0.8-1.5 cm.

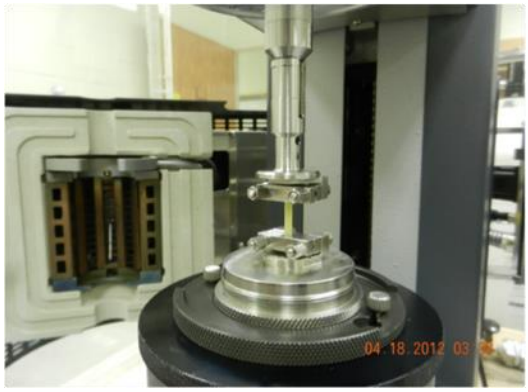

Figure A.2. Specimen clamping system assembled without the surrounding solvent-submersion hardware.

LVR determination

Great care was exerted to ensure that dynamic (oscillatory) experiments were conducted within the linear viscoelastic response (LVR). This typically involved numerous frequency sweep and stress sweep experiments conducted (on sacrificial specimens) at the temperature extremes used in this study, 25°C and 120°C. Frequency sweeps were typically conducted from 0.01 Hz to 10 Hz; stress sweeps were typically conducted from 5,000 Pa to 60,000 Pa. Dynamic stress/strain plots were fitted to a line and the LVR stress limit was defined as the stress beyond which the correlation coefficient (r^2 for the least squares fit) was less than 0.99995.

Temperature ramps

Once typical LVR behavior was established, separate specimens were subjected to temperature ramp experiments as follows: 1) equilibrate, 25°C, 5 min, 2) stress sweep, 5,000Pa - 50,000 Pa, 0.5 Hz, 3) heat, 25°C-120°C, 2°C/min, 0.5 Hz, 50,000 Pa, 4) equilibrate, 120°C, 5 min,

5) stress sweep, 5,000 Pa - 50,000 Pa, 0.5 Hz, 6) cool, 120°C-25°C, 2°C/min, 0.5 Hz, 50,000 Pa. For these temperature ramp experiments, note that stress sweeps were conducted at the temperature extremes to further verify that all analyses were conducted within the LVR.

Time-Temperature Superposition

Time-Temperature Superposition experiments were conducted as a series of isothermal frequency sweeps as follows: 1) rapidly heat to 120°C; equilibrate 5 min, 2) cool, 120°C-25°C, 2°C/min, 50,000 Pa, 0.5 Hz, 3) rapidly heat to 120°C; equilibrate 5 min, 4) isothermal frequency sweep, 0.05 Hz - 0.5 Hz, 50,000 Pa, 120°C, 5) reduce temperature by 5°C; equilibrate 5min, ; isothermal frequency sweep, 0.05 Hz - 0.5 Hz, 50,000 Pa, 6) repeat step 5 to obtain isothermal frequency sweeps from 110°C to 25°C, 7) rapidly heat to 120°C; equilibrate 5 min, 8) cool, 120°C-25°C, 2°C/min, 50,000 Pa, 0.5 Hz. Note that cooling temperature ramps were conducted before and after the sequential isothermal frequency sweeps as a means to determine if any substantial thermal degradation occurred during this analysis.

Torsional strength

Unidirectional torsional stress ramps were conducted until specimen failure. Otherwise specimen preparation, clamping, and submersion in ethylene glycol were as described above. The AR-G2 rheometer was operated in continuous flow with a shear stress increasing from 100,000 Pa to 100,000,000 Pa, using linear mode data acquisition over a 33 min maximum period collecting 300 data points.

Statistical analysis

JMP software was employed to conduct statistical analysis. Comparisons were based upon a 95% confidence level pair-wise non-parametric Wilcoxon analysis.

A.4. Results and discussions

A principal concern in dynamic mechanical analysis (DMA) is verified operation within the linear viscoelastic response (LVR). Within the LVR, observations are independent of input levels (stress or strain), and mathematical descriptions and manipulations of the raw data are

well understood. [13-15] A related concern is the determination of valid oscillation frequencies. When using small, low stiffness specimens with a stress-control rheometer, as in this work, caution is required to avoid inertia effects, where the specimen stiffness is overwhelmed by the momentum of the specimen clamping system. For instance, Figure A.3 displays typical frequency sweep data for specimens in this work. At oscillation frequencies above 2 Hz, the storage moduli exhibit a sharp decline, and the raw phase angles (phase lag between input stress and measured strain) show a correspondingly abrupt increase to values that exceed the theoretical maximum of 90°. Figure A.3 indicates that inertia effects prevent operation at oscillation frequencies above 2 Hz, for the specimen presented here. However considering the familiar variability of biomass, the maximum oscillation frequency in this work was limited to 0.5 Hz. Having established the maximum oscillation frequency, the maximum stress levels were determined with a stress sweep at the frequency maximum, as shown in Figure A.4.

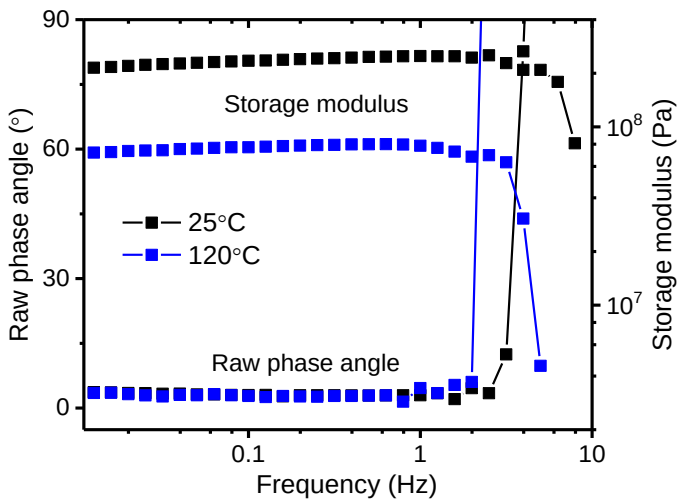

Figure A.3. Example frequency sweep data at temperature extremes for a specimen (4LC-7 40 +) immersed in ethylene glycol; oscillation stress = 50,000 Pa.

The LVR limit was arbitrarily defined as the maximum stress in which a linear fit to the stress/strain plot provided a correlation coefficient (R^2) not less than 0.99995. Figure A.4 demonstrates that this criterion was very conservative; in other words for the specimen in Figure A.4, a safely linear response extends beyond the LVR limit defined here. As

demonstrated, the maximum oscillation frequency and maximum oscillation stress settings used in this work were conservatively restricted so as to optimize data quality and simplify data interpretation. Other investigators might select less conservative restrictions on DMA acquisition parameters. As a practical matter, DMA signal-to-noise tends to increase with increasing stress levels. Consequently, one would wish to operate at the highest possible stress level that remains within the LVR. However the LVR behavior of biomass can be highly variable as demonstrated by Chowdhury and Frazier using wood from *Liriodendron tulipifera*. [7] Consequently we elected to remain conservatively within the LVR and at times this resulted in poor signal-to-noise, as will be discussed.

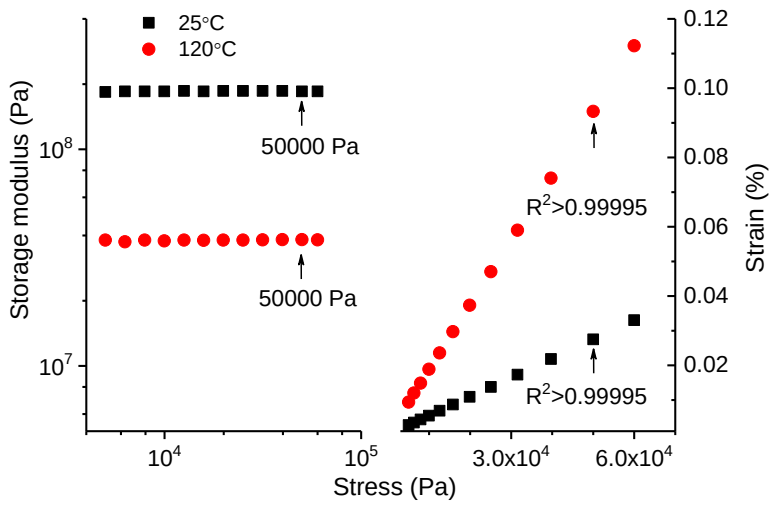

Figure A.4. Typical stress sweep data used to establish the LVR limit at the analytical temperature extremes, (specimen: 4LC-7 5 +; 0.5 Hz). Arrows indicate the maximum stress used in the linear stress/strain fit; stresses above this level result in correlation coefficients (R^2) below 0.99995.

Figure A.5 compares the storage moduli of all specimens at the temperature extremes used in this work. Note that these storage moduli were obtained from stress sweeps immediately before and after the temperature ramps discussed below. The temperature induced softening represented here is attributed to the lignin glass transition. However it is not entirely clear if and how hemicelluloses impact this transition. [8] As measured in ethylene

glycol, this softening behavior is similar in appearance to that observed in water, but that a more nearly complete softening transition is observed in the higher boiling ethylene glycol. [8] The magnitude of softening shown is less than one decade of storage modulus, and this is within the typical range for liquid-saturated lignocellulose (~ 0.6 – 1 decade). Relative to non-filled thermoplastic polymers, this is a minor degree of softening, reflective of a low volume fraction matrix dispersed among highly oriented cellulose fibrils.

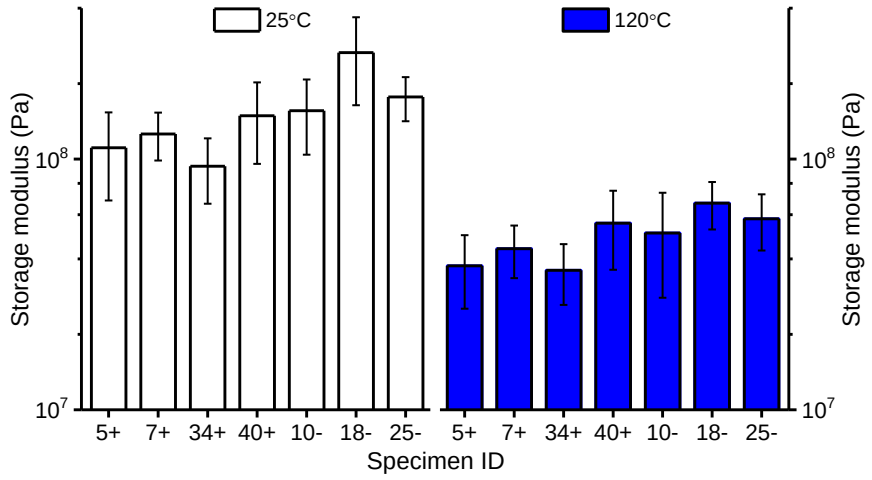

Figure A.5. Average storage moduli of all switchgrass specimens at 25˚C and 120˚C. Obtained from stress sweep experiments; number of observations, n = 5-6; error bars = ± 1 standard deviation.

Table A.1. Probability values (p-values) from the intragroup comparison of average storage moduli at the experimental temperature extremes (25˚C and 120˚C) using the nonparametric Wilcoxon method; number of measurements n = 5-6.

	5 +	**5 +**	**5 +**	**7 +**	**7 +**	**34 +**	**10 -**	**10 -**	**18 -**
	7 +	34 +	40 +	34 +	40 +	40 +	18 -	25 -	25 -
25˚C	0.33	0.56	0.18	0.09	0.47	0.07	0.07	0.65	0.03
120˚C	0.48	0.75	0.15	0.13	0.23	0.13	0.17	0.48	0.24

Within transgene groupings the specimens were nearly all of the same stiffness at the respective temperatures, Table A.1. Generally speaking, specimens containing the expressed transgene (positive specimens) were less stiff than those with the silent transgene (negative specimens), but not in all cases, Table A.2. These comparisons are based upon a 95% confidence level using the pair-wise non-parametric Wilcoxon analysis. Considering the 25°C data, this implies that on average the specimens expressing the transgene might be less resistant to wind loading; on the other hand they may require less energy for milling and other physical pretreatments. Between transgene groupings and at the higher temperature, the reduced stiffness of transgene positive specimens is very possibly associated with easier access to, and removal of lignin, as discussed later.

Table A.2. Probability values (p-values) from the intergroup comparison of average storage moduli at the experimental temperature extremes (25˚C and 120˚C) using the nonparametric Wilcoxon method; number of measurements n = 5-6.

	5 +			**7 +**			**34 +**			**40 +**		
	10 -	18 -	25 -	10 -	18 -	25 -	10 -	18 -	25 -	10 -	18 -	25 -
25˚C	0.08	0.01	0.02	0.3	0.01	0.01	0.03	0.01	0.00	0.94	0.01	0.15
120˚C	0.48	0.01	0.01	0.94	0.01	0.11	0.17	0.01	0.01	0.94	0.38	0.95

Figure A.6 presents typical first heat and first cool scans of a switchgrass specimen (10 -) immersed in ethylene glycol. First heat scans were characteristically noisy in the loss modulus signal, which is magnified in the tan δ (loss modulus/storage modulus). The noisy response is attributed to the low stress settings that were selected to assure that analysis remained within the LVR. Characteristically for these specimens, the subsequent first cool presented much less noise. Since the first heat and first cool acquisition parameters were identical, the improved signal quality in the first cool perhaps reflects specimen stress relaxation (mechanical conditioning) within the specimen clamping mechanism, leading to an improved signal. Note that first cool scans were not always ideal; for instance, best and worst case examples are presented in Figure A.7. Because of the signal noise demonstrated, first heat glass transition

temperature (Tg) data is omitted here, and all first cool Tg's (temperature at tan δ maximum) were identified using non-linear curve fitting of the first cool tan δ curve. This curve fitting procedure often increases the precision of Tg determination, while also improving estimates of the tan δ maximum, and the width of the tan δ signal at half maximum. Table A.3 demonstrates that transgene positive specimens exhibited Tg's in the range of 65-70°C, and this was about 10°C lower than for the transgene negative specimens. The lignin in these specimens was not analyzed, but it is assumed to be similar to the related transgenic lines described in [12]. Consequently, the transgene negative plants in this study are similar to wild type plants (H/G/S monomer ratio = 0.04/1.05/1.00); whereas the transgene positive plants have about 22% less lignin, with an altered H/G/S monomer ratio = 0.07/0.56/1.00. Having a substantially reduced quantity of G-monomers, the lignin in the transgene positive plants is more flexible, either because of less lignin crosslinking, and/or because of the greater free volume associated with the dominant S-monomers [9]. On the other hand, it is not entirely clear why the tan δ maxima and width of the tan δ signal at half maximum (Width), were not significantly different between the transgene groupings, Table A.3. Roughly speaking, these parameters reflect the quantity of relaxing polymer (tan δ maxima) and the heterogeneity of lignin relaxation (Width). Given a 22% difference in lignin content, one might expect the tan δmaxima and Width parameters to differ between the transgene groupings. Perhaps this indicates that the tan δ maxima and Width parameters reveal more about the lignin/polysaccharide interaction, and less about lignin relaxation. A general comparison of the transgene groups is provided in Figure A.8, where the 40 + and 18 - specimens are compared.

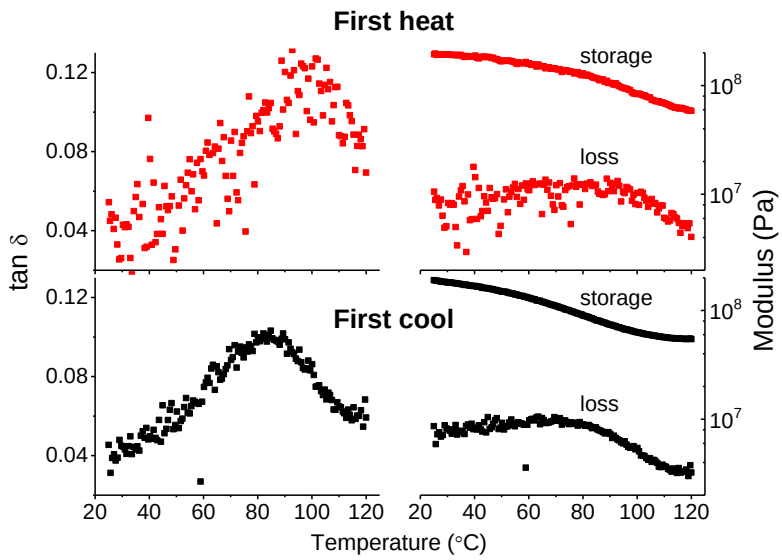

Figure A.6. Example of first heating scan (red trace) and first cooling scan (black trace) of a switchgrass specimen (10 -) immersed in ethylene glycol.

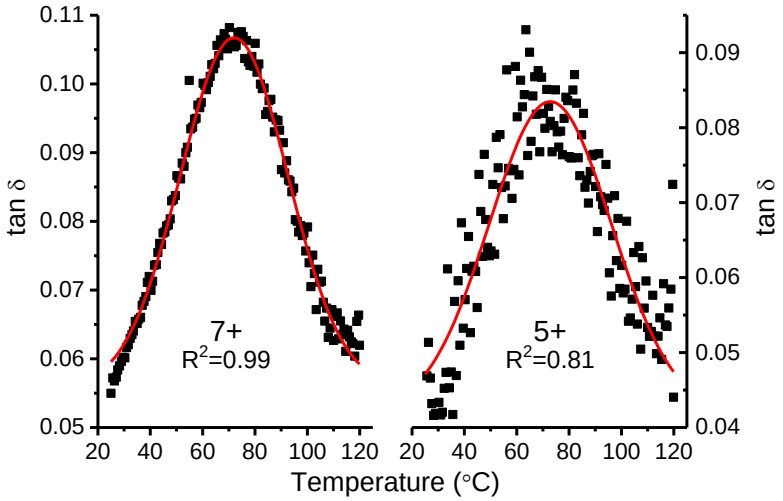

Figure A.7. Examples of good (left) and poor (right) first cool tan δ curves, and the non-linear fitting used to improve precision in the Tg (temperature at tan δ maxima) determination.

A more detailed analysis of the lignin glass transition is available through time-temperature superposition (TTS) where isothermal frequency sweeps are shifted on the

frequency axis to simulate the rheological response over a much broader frequency range. [8] The shifting procedure results in master curves, like the examples shown in Figure A.9.

Table A.3. Average glass transition temperature (Tg), tan δ maxima, and width of the tan δ signal at half maximum (Width) for 4CL-7 specimens; Number of measurements n = 3, standard deviations in parentheses.

4CL-7	5 +	7 +	34 +	40 +	10 -	18 -	25 -
Tg (°C)	69.2 (3.8)	70.3 (1.7)	64.8 (1.4)	66.7 (1.1)	77.2 (0.7)	82.2 (1.0)	77.2 (1.7)
tan δ max	0.086 (0.003)	0.094 (0.011)	0.095 (0.005)	0.093 (0.004)	0.092 (0.011)	0.105 (0.021)	0.095 (0.011)
Width (°C)	22.0 (3.2)	19.9 (0.8)	20.8 (1.0)	22.9 (1.7)	20.7 (1.6)	22.1 (2.0)	20.6 (0.9)

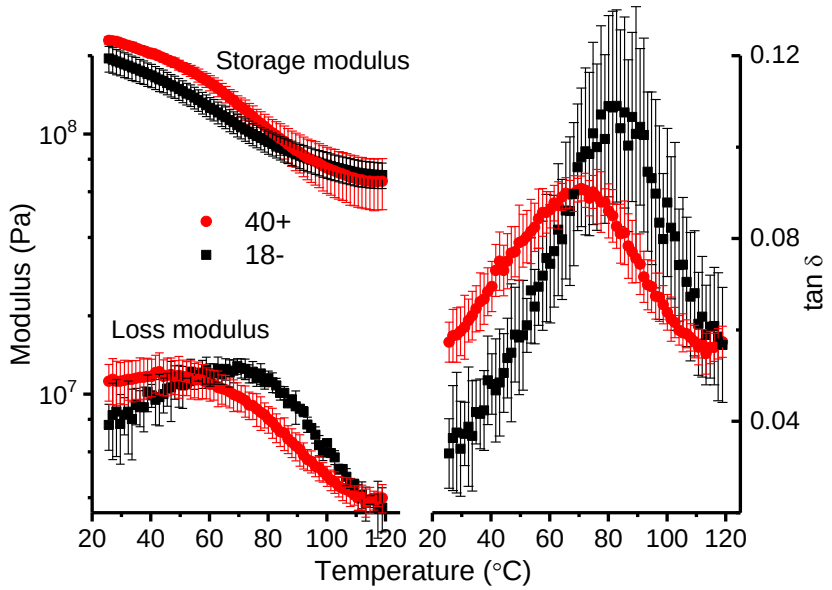

Figure A.8. Comparison of first cool scans for 40 + (red trace) and 18 - (black trace) specimens; number of measurements, n = 3. Error bars = ± 1 standard deviation.

Notable here is that the master curves were generally smooth for all three DMA parameters (storage, loss, and tan δ), and this is atypical for lignocellulose- typically the loss

and tan δ master curves are storage are much more imperfect than those shown in Figure A.9. The smoothness, or lack thereof, in lignocellulose master curves might reflect the state of thermorheological complexity in lignocellulose [8]. When creating the master curves, the so-called "shift factor" records the magnitude of the frequency shift and thus reflects the temperature dependence of the lignin relaxation, Figure A.10. The shift factor plot allows for determination of the activation energy associated with the glass transition using equation [13] below:

$$\log a_T = \frac{E_a}{2.303 \times R}\left(\frac{1}{T} - \frac{1}{T_o}\right)$$

Where Ea is activation energy, R is gas constant, T is measurement temperature and To is reference temperature. Ea for 40 + and 18 – was calculated and and shown in Table A.4. 40 + exhibited significantly lower Ea than 18 -, and this possibly could represent the overall trend if compared specimens across the two groups.

Table A.4. Activation energy (Ea) calculated for 40 + (n = 6) and 18 – (n = 4) according to the equation above. n = number of measurements, standard deviations in parentheses.

Specimen	Activation energy Ea (kJ/mol)
40 +	310.7 (14.9)
18 -	261.3 (15.1)

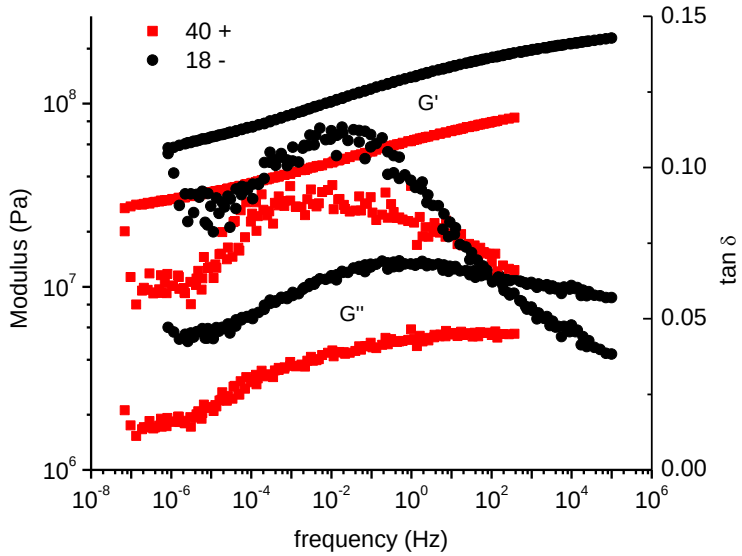

Figure A.9. Example of storage modulus, loss modulus, and tan δ master curves for 40 + (red) and 18 - (black) specimens.

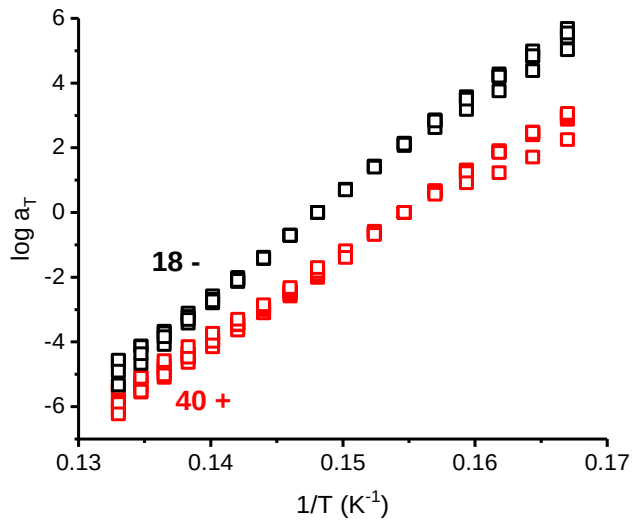

Figure A.10. Shift factor log a_T against 1/T (K^{-1}) for 18 – (n = 4) and 40 + (n = 6), n is number of measurements, slope is the activation energy Ea. 18 – : 310.7 ± 14.9 kJ/mol, 40 + : 261.3 ± 15.1 kJ/mol.

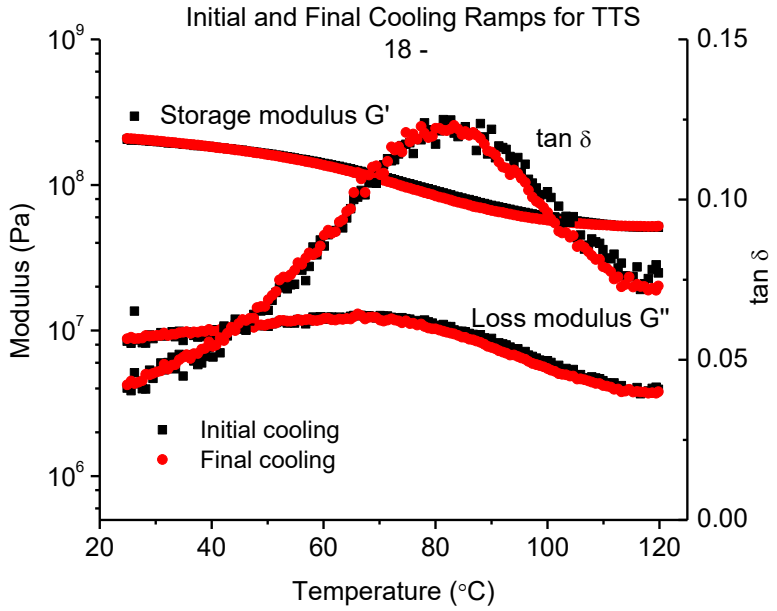

Figure A.11. Initial cooling (before isothermal frequency scans, black trace) and final cooling ramp (after isothermal frequency scans, red trace) overlay for 18 -.

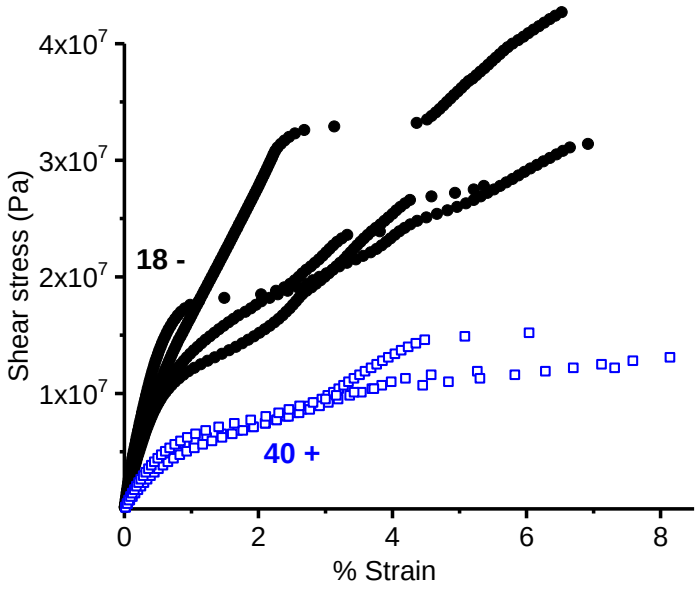

Figure A.12. Examples of % strain response for unidirectional continuous shear stress on specimen 40 + and 18 -.

TTS procedures place the experimental specimens under prolonged heating, and the extent of possible thermal degradation may be determined by comparing simple temperature ramp scans acquired before and after the TTS procedure. Figure A.11 demonstrates that the TTS procedure caused little or no thermal degradation in the switchgrass specimens.

To have a direct comparison of specimen mechanical behavior under extreme torsional stress, i.e. wind load. A continuously increasing shear stress was applied on specimen 18 – and 40 + until specimen failure, and specimen response (% Strain) is shown in Figure A.12.

Table A.5. Ultimate strength comparison between 18 - and 40 +. Number of measurements n = 4, standard deviations in parentheses.

4CL specimen	E' (Pa)	X (Pa)
40 +	9.2×10^{6} (2.9×10^{6})	1.3×10^{7} (1.9×10^{6})
18 -	3.0×10^{7} (7.4×10^{6})	3.1×10^{7} (8.1×10^{6})

Two characteristic parameters were derived from Figure A.12, and were used to reflect the mechanical strength of the sample. One is the slope of the initial linear region (defined as stress beyond which $R^2 < 0.995$), denoted as E'. The other one is the shear stress corresponding to the ultimate breaking point, denoted as X. For both E' and X, 18 - is significantly higher than 40 +, meaning 18 – is stronger than 40 +, Table A.5.

A.5. Conclusions

The goal of this study was to reveal how the transgenic modification affected rheological behaviors, and ultimately evaluated the viability of the plants as well as the practical aspects of biomass handling and processing. This carefully developed solvent submersion tensile-torsion DMA method was intended to compare rheological properties between two group of

transgenic modified switchgrass specimens, including Tg, Ea, torsional strength, et al. Overall, positive group contained less lignin than negative group by ~22%. Stress sweeps at 25°C and 120°C indicated that positive specimens are overall less stiff than those negative specimens. The positive group exhibited lower Tg by 10°C than the negative group. 40 + and 18 – were chosen to represent each group. Lower Ea and lower torsional strength was seen from 40 +, which possibly could represent the general trend if compared other specimens across two groups. These information is highly valuable regarding to bioenergy production, and may serve as critical criterions for selecting proper transgenic modifications to obtain modified energy crops with preferable traits.

A.6 References

1. Vogel, K.P. and H.J.G. Jung, *Genetic modification of herbaceous plants for feed and fuel.* Critical Reviews in Plant Sciences, 2001. **20**(1): p. 15-49.
2. Schmer, M.R., K.P. Vogel, R.B. Mitchell, and R.K. Perrin, *Net energy of cellulosic ethanol from switchgrass.* Proc Natl Acad Sci U S A, 2008. **105**(2): p. 464-9.
3. David, K. and A.J. Ragauskas, *Switchgrass as an energy crop for biofuel production: a review of its ligno-cellulosic chemical properties.* Energy & Environmental Science, 2010. **3**(9): p. 1182-1190.
4. L., S., *Viscoelastic properties of in situ lignin under water-saturated conditions.* J. Mater. Sci., 1984. **19**: p. 3090-3096.
5. Placet, V., J. Passard, and P. Perré, *Viscoelastic properties of green wood across the grain measured by harmonic tests in the range 0-95C : hardwood vs. softwood and normal wood vs. reaction wood.* Holzforschung, 2007. **61**(5): p. 548-557.
6. Chowdhury, S., J. Fabiyi, and C.E. Frazier, *Advancing the dynamic mechanical analysis of biomass: comparison of tensile-torsion and compressive-torsion wood DMA.* Holzforschung, 2010. **64**(6): p. 747-756.
7. Chowdhury, S. and C.E. Frazier, *Compressive-torsion DMA of yellow-poplar wood in organic media.* Holzforschung, 2013. **67**(2): p. 161-168.

8. Chowdhury, S. and C.E. Frazier, *Thermorheological complexity and fragility in plasticized lignocellulose.* Biomacromolecules, 2013. **14**(4): p. 1166-1173.

9. Olsson, A.M. and L. Salmén, *The effect of lignin composition on the viscoelastic properties of wood.* Nordic Pulp and Paper Research Journal, 1997. **12**(3): p. 140-144.

10. Stelte, W., C. Clemons, J.K. Holm, J. Ahrenfeldt, U.B. Henriksen, and A.R. Sanadi, *Fuel pellets from wheat straw: The effect of lignin glass transition and surface waxes on pelletizing properties.* BioEnergy Research, 2012. **5**(2): p. 450-458.

11. Kelley, S.S., T.G. Rials, and W.G. Glasser, *Relaxation behaviour of the amorphous components of wood.* Journal of materials science, 1987. **22**(2): p. 617-624.

12. Xu, B., L.L. Escamilla-Trevino, N. Sathitsuksanoh, Z.X. Shen, H. Shen, Y.H.P. Zhang, R.A. Dixon, and B.Y. Zhao, *Silencing of 4-coumarate:coenzyme A ligase in switchgrass leads to reduced lignin content and improved fermentable sugar yields for biofuel production.* New Phytologist, 2011. **192**(3): p. 611-625.

13. Ferry, J.D., *Viscoelastic properties of polymers*. 2 ed. 1970, New York: John Wiley Interscience.

14. Jiang, J. and J. Lu, *Impact of temperature on the linear viscoelastic region of wood.* Canadian journal of forest research, 2009. **39**(11): p. 2092-2099.

15. Kaboorani, A. and P. Blanchet, *Determining the linear viscoelastic region of sugar maple wood by dynamic mechanical analysis.* BioResources, 2014. **9**(3): p. 4392-4409.

Appendix B Biogenic formaldehyde generation potential from three wood species

Guigui Wan, Charles E. Frazier

Macromolecular Science & Engineering, Sustainable Biomaterials

Virginia Tech, Blacksburg VA 24061, U.S.A

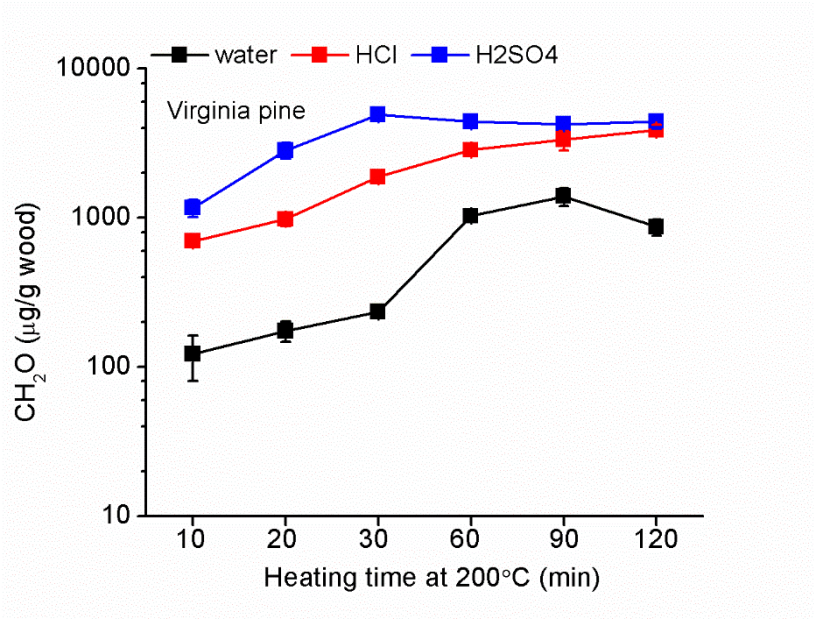

Figure B.1. Acid-catalyzed (HCl or H_2SO_4) CH_2O generation from Virginia pine (tree 1 flakes), heated at 200°C from 10 min up to 120 min. Number of measurements n ≥ 3. Y axis is in log scale.

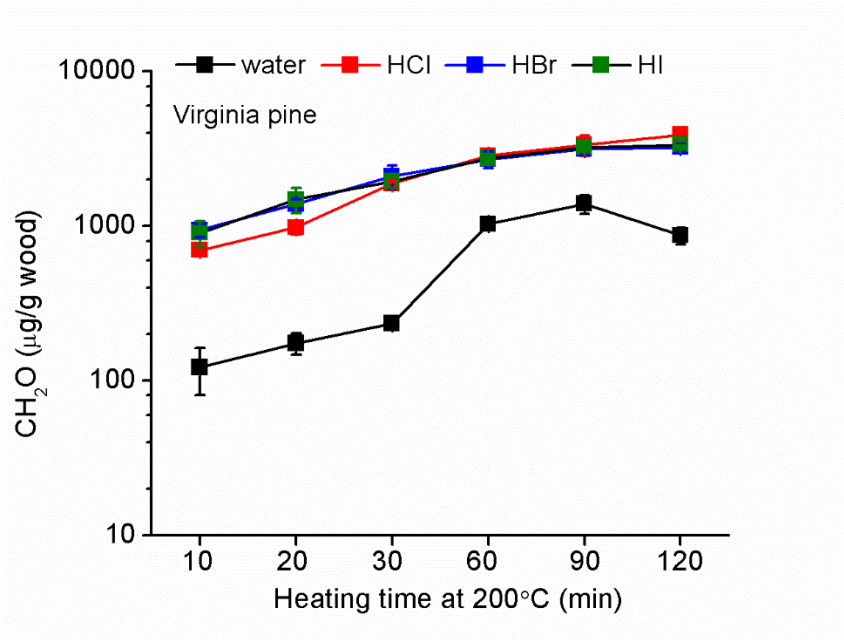

Figure B.2. Acid-catalyzed (HCl, HBr, and HI) CH_2O generation from Virginia pine (tree 1 flakes), heated at 200°C from 10 min up to 120 min. Number of measurements n ≥ 3. Y axis is in log scale.

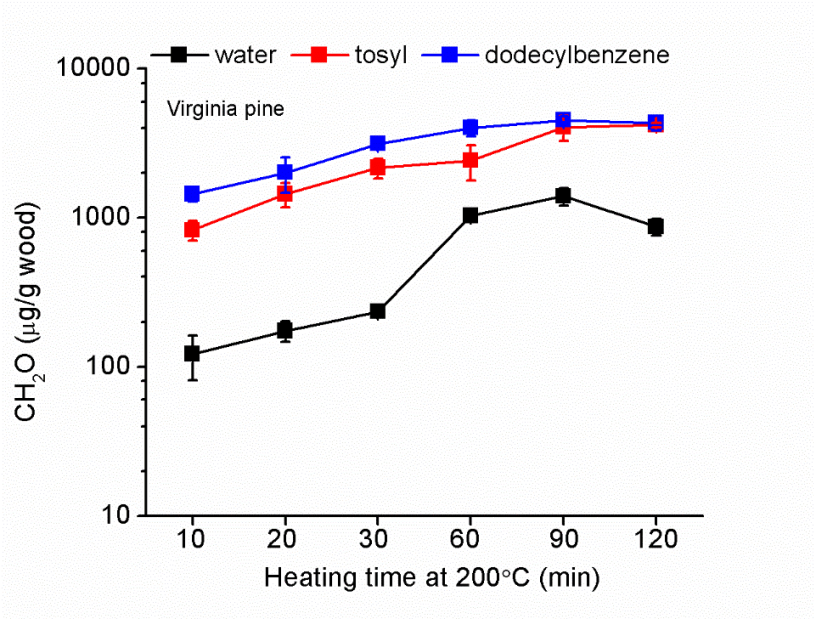

Figure B.3. Acid-catalyzed (tosyl acid and dodecylbenzene sulfonic acids) CH_2O generation from Virginia pine (tree 1 flakes), heated at 200°C from 10 min up to 120 min. Number of measurements n ≥ 3. Y axis is in log scale.

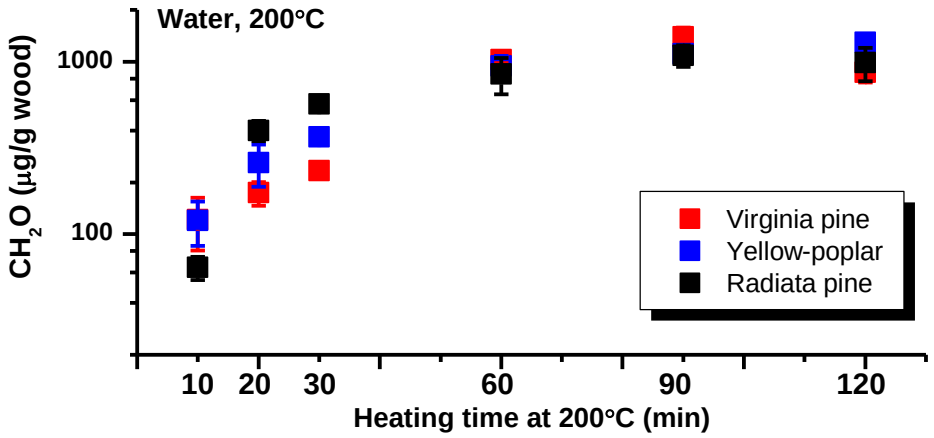

Figure B.4. Formaldehyde generation potential from three wood species, heated at 200°C from 10 min up to 120 min without catalysts. Number of measurements n ≥ 3. Y axis in log scale.

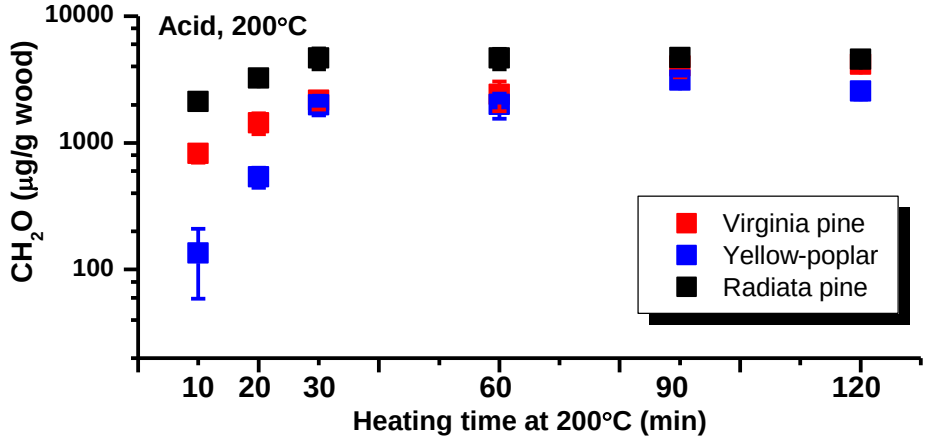

Figure B.5. Formaldehyde generation potential from three wood species, heated at 200°C from 10 min up to 120 min, catalyzed by TsOH (tosyl acid). Number of measurements n = 3. Y axis in log scale.

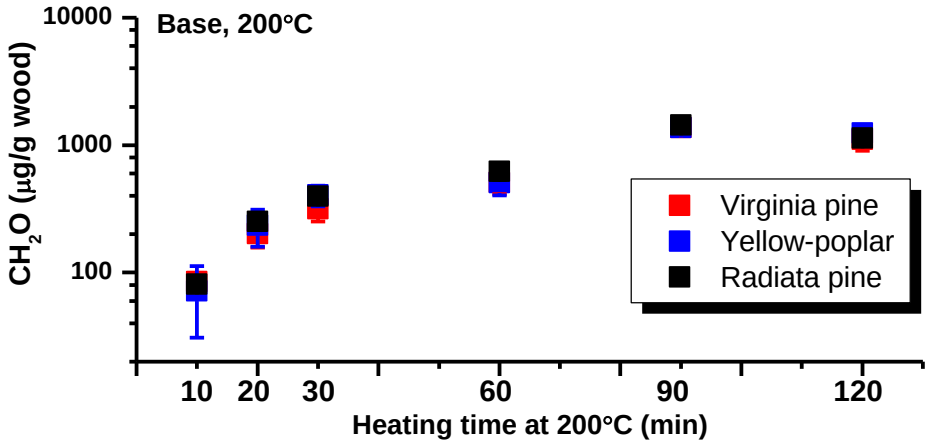

Figure B.6. Formaldehyde generation potential from three wood species, heated at 200°C from 10 min up to 120 min, catalyzed by NaOH (sodium hydroxide). Number of measurements n = 3. Y axis in log scale.

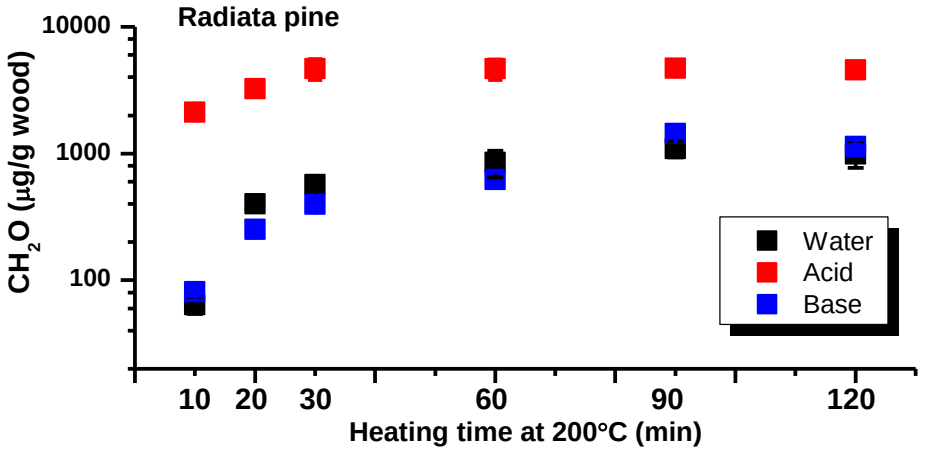

Figure B.7. Formaldehyde generation potential from radiata pine, heated at 200°C from 10 min up to 120 min, catalyzed by NaOH (sodium hydroxide) or TsOH (tosyl acid). Number of measurements n = 3. Y axis in log scale.

Appendix C Rheology of heated Virginia pine wood

C.1. Material and methods

A healthy Virginia pine tree, 70-80 years old, was felled in a natural wooded region (~4 ha) east of Blacksburg, VA, U.S.A., (Nellies Cave area). Stem sections (~15 cm thick) were cut from locations that were 1.0-1.3 m above ground. Fresh sections were air dried and stored in the open laboratory at room temperature for ~16 months, then immersed in water for 3 days, debarked, and processed into rectangular wood blocks (4×10×40 mm, thickness×width×length). Three grain orientations were defined as RT, TR and XL; the first letter indicates the smallest wood surfaces of the rectangular block (R-radial, T-tangential, and X-cross-sectional) and the second indicates the grain direction along the length direction (T-tangential, R-radial, and L-longitudinal).

Air dried rectangular wood blocks (grain orientations XL, RT and TR) were saturated in HPLC water or 10 mmol TsOH under reduced pressure (room temperature, 2.67 kPa; 20 mm Hg, 10 min), then immersed for another 2 hours under atmospheric pressure. After adjusting to 100%MC, blocks were sealed in pressure tubes (~10 hours), heated at 200°C for 25 or 60 min under two conditions: 1) pressure tube open (O), 2) pressure tube closed (C), then saturated in ethylene glycol under reduced pressure (20 mm Hg, 10 min), and immersed for 3 days under atmospheric pressure until complete saturation. Specimens were identified with pretreatments prior to heating (H_2O: H; Acid: A), and heating condition, i.e. H/O60 or A/C26, etc. Control specimens were water saturated, adjusted to 100%MC, and immediately saturated into ethylene glycol as described above without heat treatments.

Control100: a set of water-saturated blocks (100%MC) were saturated in ethylene glycol, repeated above steps before analysis. Control5: without water saturation, the air-dried wood blocks (5%MC) were saturated in ethylene glycol and repeated above steps before analysis.

Frequency selection and LVR determination

Proper frequency should be selected for all the steps. Two frequency sweeps were conducted from 0.01 Hz to 10 Hz under two temperature extremes, 25°C and 120°C. 1 Hz was chosen with figures shown below.

All of our testing steps should be operated within linear viscoelastic response (LVR) region, which was determined using stress sweeps from 1,000 Pa to 400,000 Pa at frequency 1Hz, with at least five observations for each sample type. Measurements were conducted at temperature extremes (25°C and 120°C) in heating and then cooling as follows: 1) equilibrate at 25°C for 5 min; run stress sweep, 2) directly heat to 120°C, equilibrium for 5 min; run stress sweep. The LVR stress limit was identified at the stress beyond which the coefficient of determination (R^2) was less than 0.99995. Note: this 0.99995 was determined arbitrarily. Stress 100,000 Pa was chosen for the following tests after the LVR determination, which was shown later.

Stress sweeps and Temperature ramps

A separate collection of specimens was subjected to a sequential stress sweep/heat/stress sweep/cool treatment as follows: 1) equilibrate at 25°C for 5 min, 2) stress sweep at 25°C from 1,000 Pa to 400,000 Pa, 1 Hz, 2) heat from 25°C to 120°C, 2°C/min, 1 Hz, 100,000 Pa; hold for 5 min, 3) stress sweep at 120°C from 1,000 Pa to 400,000 Pa, 1 Hz, 4) cool from 120°C to 25°C, 2°C/min, 1 Hz, 100,000 Pa.

Thermal reversibility and Time-Temperature Superposition (TTS)

The Time-Temperature Superposition (TTS) tests were also performed in solvent-submersion tensile-torsion mode, using a different set of specimens. All experiments were carried out within the linear viscoelastic response (LVR) limit of solvent plasticized switchgrass. Specimens were subjected to a serial isothermal frequency sweeps and two cooling ramps as follows: 1) rapidly heat to maximum temperature 120°C, hold it for 5 min, 2) cool from 120°C to 25°C, 2°C/min, 100,000 Pa, 1 Hz, 3) rapidly heat to 120°C, hold it for 5 min, 4) isothermal frequency sweep from 0.1 Hz to 1 Hz, 100,000 Pa, 120°C, 5) cool it down by 5°C and condition for 5 min, perform another isothermal frequency

sweep in the same range, 6) repeat step 5 every 5°C till isothermal frequency sweep reaches to 25°C, 7) rapidly heat to 120°C, hold it for 5 min, 8) cooling ramp from 120°C to 25°C, 2°C/min, 100,000 Pa, 1 Hz.

C.2. Results and discussions

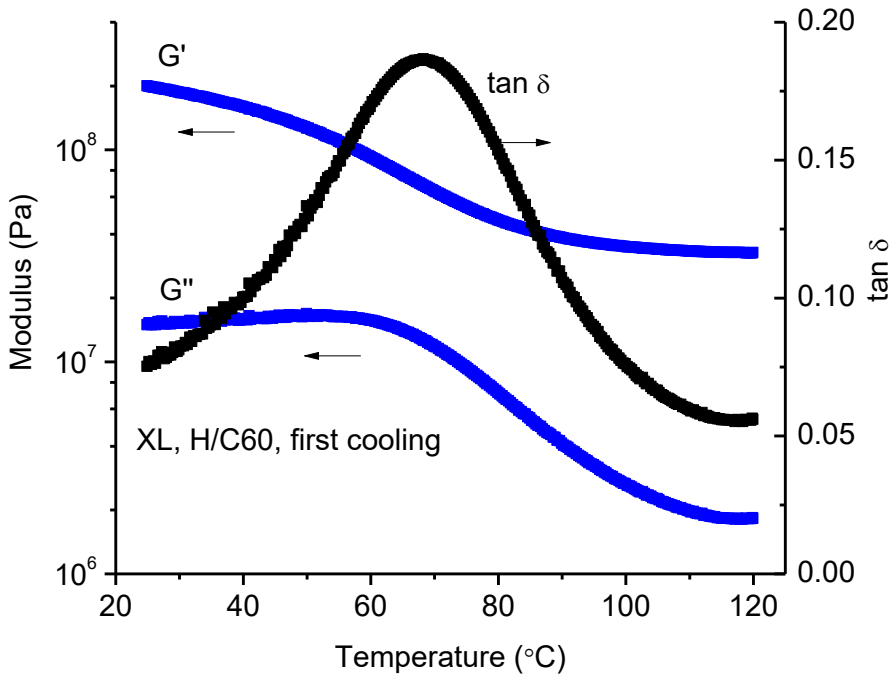

Figure C.1. Example curve of first cooling for XL grain oriented specimen (H/C60).

Table C.1. Summary of storage modulus (G'), glass transition temperature (Tg), max tan delta, activation energy associated with glass transition (Ea) for rectangular specimens with three grain orientations after various heat treatments. Number of measurements n ≥ 2 for stress sweeps and temperature ramps, number of measurements n ≥ 1 for Time-Temperature Superposition (TTS), standard deviations in parentheses.

First cool		Stress sweep (G')		Temperature ramp		TTS
		25C (Pa)	120°C (Pa)	Tg (°C)	Max tan δ	Ea (KJ/mol)
Control100	RT	1.7×10^{8} (3.2×10^{6})	2.7×10^{7} (1.2×10^{6})	75.5 (0.6)	0.168 (0.002)	241.5
	TR	1.7×10^{8} (1.7×10^{7})	2.5×10^{7} (1.6×10^{6})	75.2 (1.1)	0.169 (0.001)	254.1
	XL	5.9×10^{8} (8.510^{7})	1.2×10^{8} (4.4×10^{6})	78.1 (3.7)	0.123 (0.004)	273.9 (2.8)
Control5	RT	3.1×10^{8} (1.6×10^{7})	4.4×10^{7} (4.1×10^{6})	78.2 (1.9)	/	
	TR	2.5×10^{8} (2.710^{7})	3.6×10^{7} (2.8×10^{6})	78.2 (0.6)	/	
	XL	7.8×10^{8} (1.2×10^{8})	1.9×10^{8} (2.3×10^{7})	80.4 (1.7)	/	
H/C60	RT	6.5×10^{7} (6.4×10^{5})	6.6×10^{6} (1.2×10^{5})	69.0 (3.4)	0.226 (0.004)	258.2
	TR	5.1×10^{7} (9.3×10^{6})	5.5×10^{6} (1.0×10^{6})	68.7 (4.0)	0.232 (0.006)	288.3
	XL	2.4×10^{8} (2.8×10^{7})	3.5×10^{7} (7.2×10^{5})	69.6 (2.0)	0.180 (0.007)	289.7 (13.3)
A/C60	RT	2.4×10^{7} (1.7×10^{6})	2.0×10^{6} (1.7×10^{5})	88.8 (0.7)	0.228 (0.005)	/
	TR	2.8×10^{7} (2.0×10^{6})	2.4×10^{6} (1.9×10^{5})	85.0 (0.7)	0.231 (0.002)	313.7
	XL	1.5×10^{8} (2.1×10^{7})	1.8×10^{7} (2.9×10^{6})	85.3 (1.8)	0.206 (0.007)	310.5 (2.7)

Table C.1 (continued). Summary of G', Tg, max tan delta, Ea for rectangular specimens with three grain orientations after various heat treatments. Number of measurements n ≥ 2 for stress sweeps and temperature ramps, number of measurements n ≥ 1 for Time-Temperature Superposition (TTS), standard deviations in parentheses.

First cool		Stress sweep (G')		Temperature ramp		TTS
		25°C (Pa)	120°C (Pa)	Tg (°C)	Max tan δ	Ea (KJ/mol)
A/C25	RT	8.3×10^{7} (9.4×10^{6})	1.3×10^{7} (2.0×10^{6})	78.9 (4.9)	0.165 (0.006)	/
	TR	6.8×10^{7} (6.6×10^{6})	1.0×10^{7} (2.8×10^{5})	81.0 (0.6)	0.167 (0.001)	/
	XL	2.8×10^{8} (5.8×10^{7})	5.6×10^{7} (1.0×10^{7})	81.7 (1.1)	0.131 (0.001)	/
H/O60	RT	2.8×10^{8} (4.0×10^{7})	4.1×10^{7} (5.1×10^{6})	79.3 (2.5)	0.164 (0.003)	256.3
	TR	2.9×10^{8} (2.5×10^{7})	4.2×10^{7} (1.7×10^{6})	79.8 (1.8)	0.161 (0.002)	258.7
	XL	7.9×10^{8} (1.1×10^{8})	1.8×10^{8} (5.7×10^{6})	80.6 (2.5)	0.117 (0.008)	275.0 (7.1)
A/O60	RT	2.4×10^{8} (2.3×10^{7})	4.4×10^{7} (1.0×10^{7})	100.5 (2.0)	0.164 (0.002)	
	TR	2.6×10^{8} (5.8×10^{7})	4.6×10^{7} (7.4×10^{6})	101.3 (4.6)	0.162 (0.003)	290.8
	XL	9.0×10^{8} (1.4×10^{8})	1.8×10^{8} (2.2×10^{7})	92.8 (3.9)	0.125 (0.007)	300.5 (9.6)

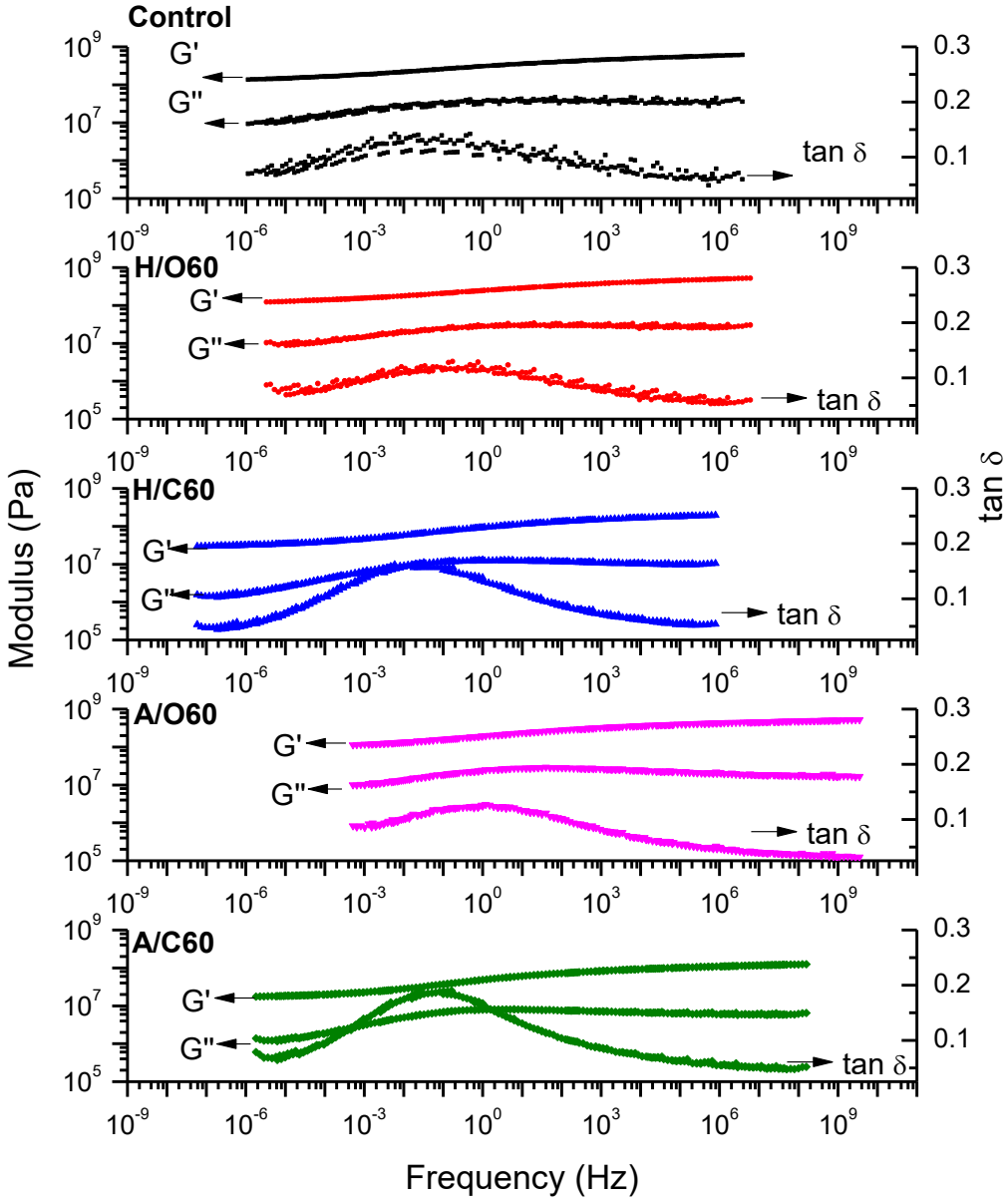

Figure C.2. Example of TTS (Time-Temperature Superposition) master curves for XL grain oriented specimens.

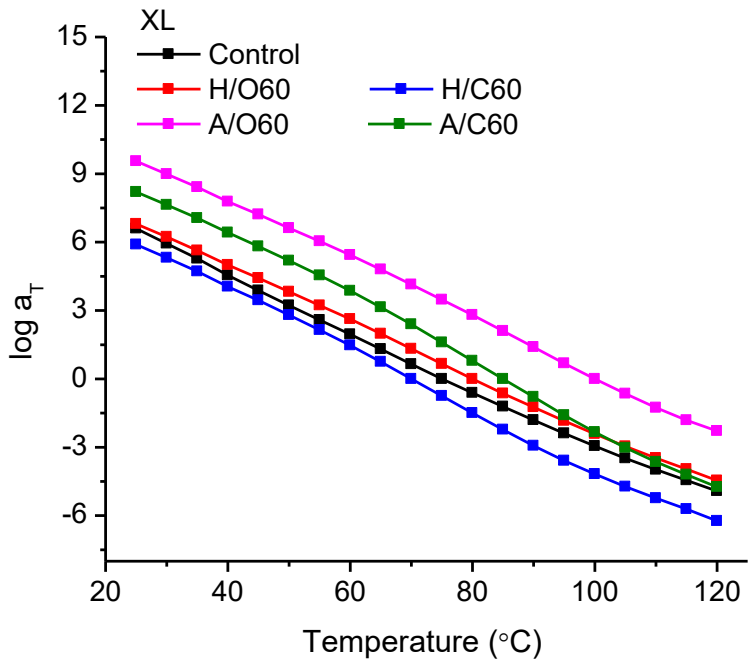

Figure C.3. Shift factors (TTS) for XL-grain oriented specimens.

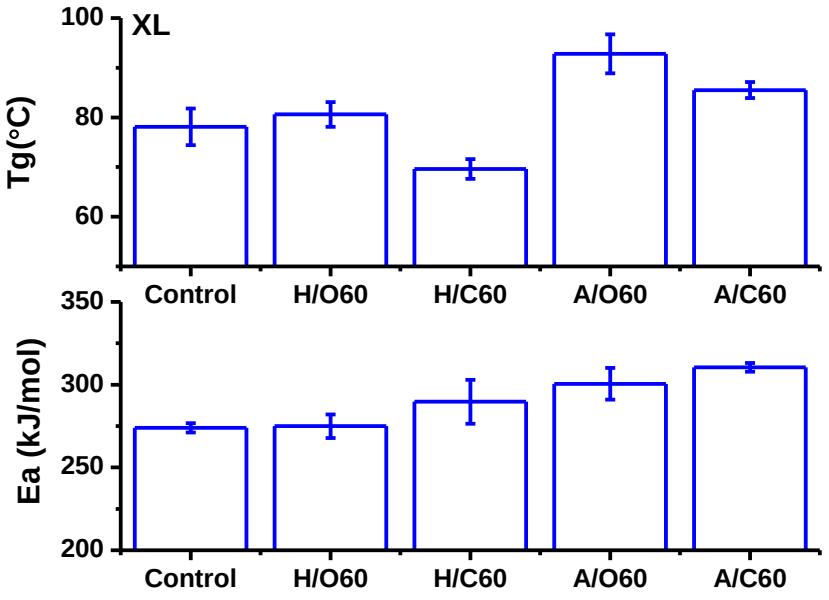

Figure C.4. Tg (glass transition temperature) and Ea (activation energy associated with Tg) summary for XL-grain oriented specimens.

Appendix D NMR spectra for synthesized lignin model compounds

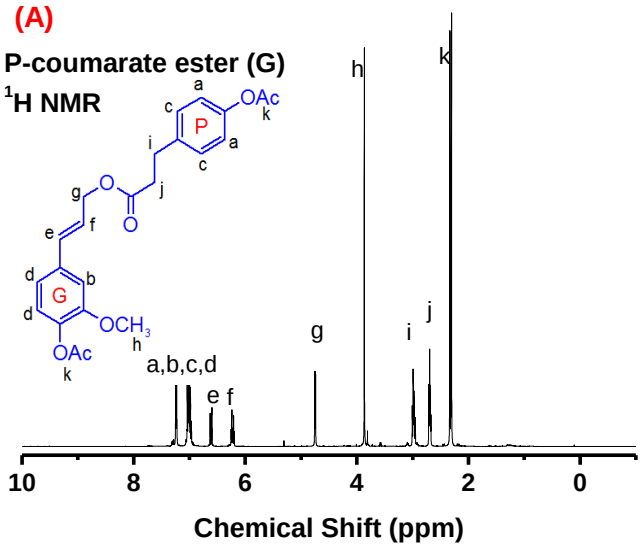

Figure D.1. ^{1}HNMR spectrum for p-coumarate ester (G) derived from esterified lignin unit after the DFRC (Derivatization Followed by Reductive Cleavage) reaction.

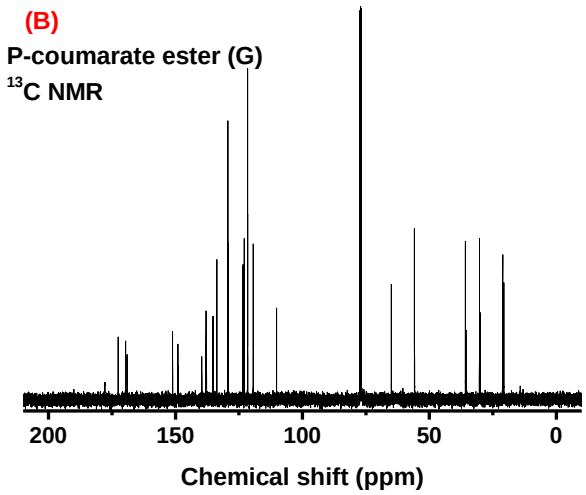

Figure D.2. ^{13}CNMR spectrum for p-coumarate ester (G) derived from esterified lignin unit after DFRC reaction.

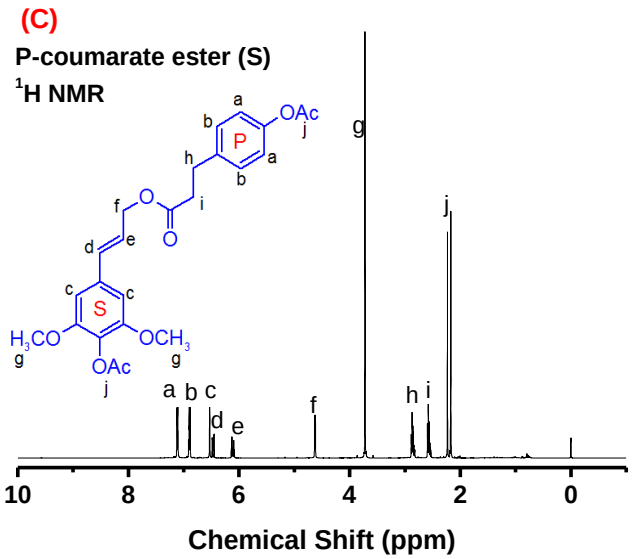

Figure D.3. ^{1}HNMR spectrum for p-coumarate ester (S) derived from esterified lignin unit after DFRC reaction.

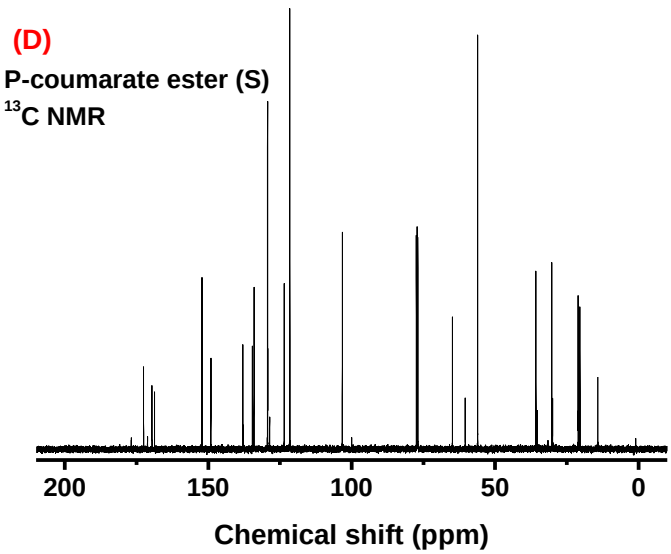

Figure D.4. ^{13}CNMR spectrum for p-coumarate ester (S) derived from esterified lignin unit after DFRC reaction.

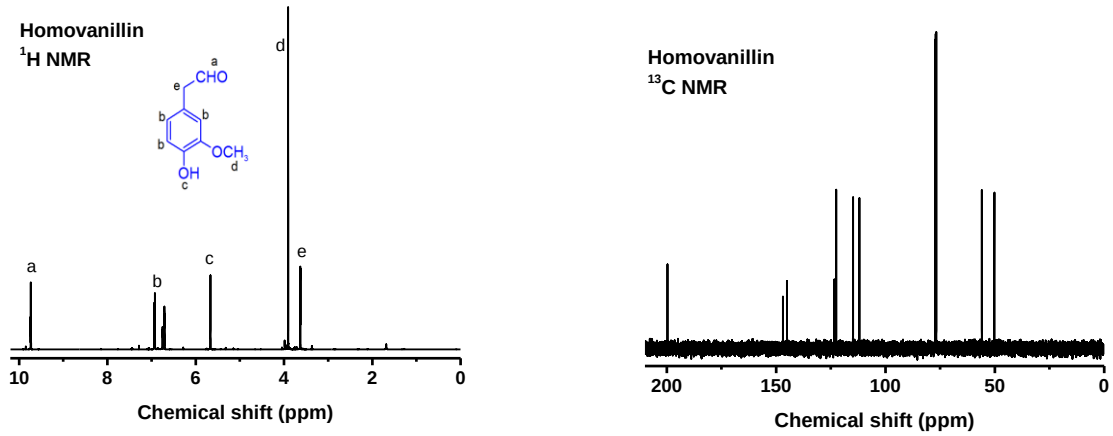

Figure D.5. ^{1}HNMR (left) and ^{13}CNMR (right) spectra for purified homovanillin.

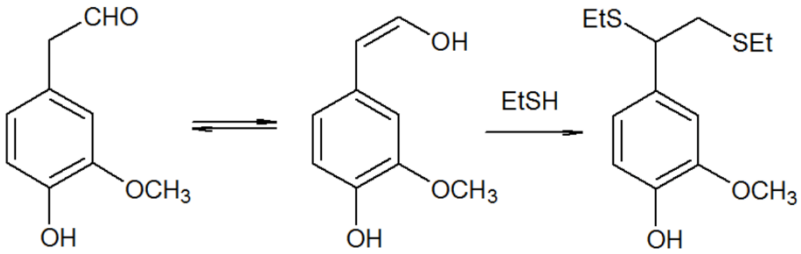

Figure D.6. Model compound (HA-THIO) of homovanillin after thioacidolysis.

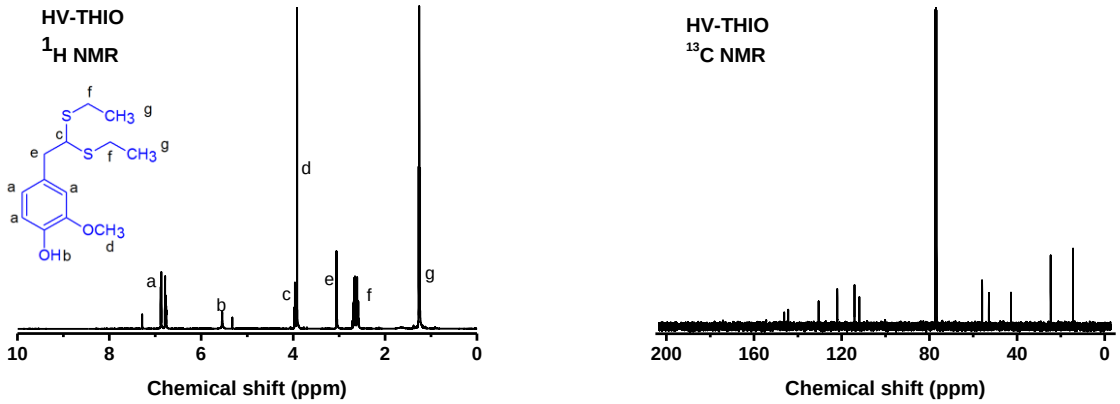

Figure D.7. ^{1}HNMR (left) and ^{13}CNMR (right) spectra for purified HA-THIO.